The genetic and functional basis of three inherited cutaneous and gastro-intestinal diseases in humans

Matthew A. Brooke

Supervisor: Professor David Kelsell

A Thesis submitted for the degree of PhD

Centre for Cutaneous Research, Blizard Institute

Barts & The London School of Medicine & Dentistry,

Queen Mary, University of London

I, Matthew Alexander Brooke, hereby declare that the work presented in this thesis is my own, unless otherwise stated, and is in accordance with the University of London's regulations for the degree of PhD

Matthew Alexander Brooke

Abstract

This thesis describes investigations into the genetic basis and pathophysiology of three distinct inherited diseases in humans, two of which are strongly associated to the function of the ectodomain sheddase enzyme ADAM17.

The first of these is a novel inherited syndrome of neonatal onset inflammatory skin and bowel disease, which is associated in a consanguineous family with homozygous loss-of-function mutations in *ADAM17.* This thesis describes investigations of the expression and function of ADAM17 – and downstream proteins it regulates – in an individual affected by this disease. This is accompanied by genetic investigations into other individuals suspected of suffering from the same syndrome.

The second investigated disease is Tylosis with Oesophageal Cancer (TOC), an inherited cutaneous disease which represents the only known syndrome of familial oesophageal cancer susceptibility. This disease was associated to dominantly inherited mutations in the Rhomboid protein iRHOM2. This work describes investigations of immortalised keratinocyte cell lines and tissues derived from TOC-affected individuals, and illustrates that the pathogenesis of TOC is characterised by increased iRHOM2-dependent activation and activity of ADAM17, and upregulation of the shedding of ADAM17 substrates, particularly in the EGFR ligand family, accompanied by increased desmosome turnover and transglutaminase 1 activity. This pattern of upregulation results in attendant increases in growth factor signalling, proliferation and motility in TOC keratinocytes, dependent on ADAM17.

The third focus of this thesis is a life-threatening inherited gastrointestinal disease (accompanied by severe extraintestinal complications) whose symptoms correspond to Cryptogenic Multifocal Ulcerative Stenosing Enteritis. This work describes the identification of mutations in cytosolic phospholipase A2-α ($cPLA_2\alpha$) – an enzyme responsible for arachidonic acid production, the first step in the eicosanoid synthesis pathway – as associated with this condition in a single affected family. The expression and function of $cPLA_2\alpha$ in this disease was investigated, using platelet aggregation stimulated by a downstream product of $cPLA_2\alpha$ (Thromboxane A_2) as a model.

Contents

Formatted: Font: 12 pt

Formatted: Font: 12 pt

List of Figures

List of Tables

Formatted: Font: Italic

List of Abbreviations

AA	Arachidonic acid	**EGFR**	Epidermal growth factor receptor
ADAM	A Disintegrin And Metalloprotease (e.g. ADAM17, ADAM10)	**ELISA**	Enzyme-linked immunosorbent assay
ANOVA	Analysis of variance	**ER**	Endoplasmic reticulum
APP	Amyloid precursor protein	**ERAD**	ER-associated degradation
AREG	Amphiregulin	**ERK**	Extracellular signal-regulated kinase
ARVC	Arrhythmogenic right ventricular cardiomyopathy	**FAM**	6-carboxyfluorescein
Ca^{2+}	Calcium	**FBS**	Foetal bovine serum
CMUSE	Cryptogenic multifocal ulcerative stenosing enteritis	**FGF**	Fibroblast growth factor
COX	Cyclooxygenase	**GAPDH**	Glyceraldehyde-3-phosphate dehydrogenase
cPLA$_2$α	Cytosolic phospholipase A2 alpha	**GI**	Gastrointestinal
CSTA	Cystatin A	**GPCR**	G-protein-coupled receptor
DAG	Di-acyl glycerol	**GW**	GW280264X (an ADAM17 inhibitor)
DAPI	4',6-diamidino-2-phenylindole	**H & E**	Haematoxylin and eosin
DNA	Deoxyribonucleic acid	**HB-EGF**	Heparin-binding epidermal growth factor
DMEM	Dulbecco's Modified Eagle's Medium	**HPV**	Human papilloma virus
DMSO	Dimethyl sulphoxide	**HRP**	Horseradish peroxidase
dNTPs	Deoxyribonucleotide triphosphates	**IFNγ**	Interferon-gamma
DSG	Desmoglein	**IL**	Interleukin
EGF	Epidermal growth factor	**IL-1/6/8R**	Interleukin-1/6/8 receptor

Ig	Immunoglobulin	**PIP_2**	Phosphatidylinositol 4,5-bisphosphate
IP_3	Inositol triphosphate	**PL**	Phospholipase (e.g. PLA_2, PLC)
kDa	Kilodalton	**PMA**	Phorbol myristate acetate
LOD	Logarithm of odds	**PPK**	Palmoplantar keratoderma
LOX	Lipoxygenase	**RPMI**	Roswell Park Memorial Institute (cell culture medium)
LPS	Lipopolysaccharide	**SDS-PAGE**	Sodium dodecyl sulphate polyacrylamide gel electrophoresis
M	Molar	**siRNA**	Small interfering ribonucleic acid
MAPK	Mitogen-activated protein kinase	**SNP**	Single nucleotide polymorphism
MDC	Monodansylcadaverine	**TACE**	Tumour necrosis factor alpha converting enzyme
MMP	Matrix metalloprotease	**TBS(-T)**	Tris-buffered saline (with Tween)
mRNA	Messenger ribonucleic acid	**TGFα**	Transforming growth factor alpha
NSAID	Non-steroidal anti-inflammatory drug	**TGM**	Transglutaminase (e.g. TGM1)
NSCLC	Non-small-cell lung cancer	**T_h**	Helper T cell
NTP	Non-targeting pool	**TNFα**	Tumour necrosis factor alpha
OSCC	Oesophageal squamous cell carcinoma	**TNFR**	Tumour necrosis factor alpha receptor
(q)PCR	(Quantitative) polymerase chain reaction	**TOC**	Tylosis with oesophageal cancer
PBMC	Peripheral blood mononuclear cell	**TPA**	Tetradecanoyl phorbol acetate
PBS	Phosphate-buffered saline	**PIP_2**	Phosphatidylinositol 4,5-bisphosphate
PFA	Paraformaldehyde	**TRAPS**	~~Tumour necrosis factor~~TNFα receptor-associated periodic febrile syndrome
PG	Prostaglandin (e.g. PGE_2, PGI_2)	**TxA_2**	Thromboxane A_2

PI3K Phosphoinositide 3-kinase **VEGF** Vascular endothelial growth factor

Publications and presentations arising from this thesis

Publications

MA Brooke, SL Etheridge, N Kaplan, C Simpson, EA O'Toole, A Ishida-Yamamoto, O Marchés, S Getsios, DP Kelsell
iRHOM2-dependent regulation of ADAM1~~2~~7 in cutaneous disease and epidermal barrier function
Human Molecular Genetics, 2014, in press, doi: 10.1093/hmg/ddu120

MA Brooke, HJ Longhurst, V Plagnol, NS Kirkby, JA Mitchell, F Rüschendorf, TD Warner, DP Kelsell, TT MacDonald
Cyrptogenic multifocal ulcerating stenosing enteritis associated with homozygous deletion mutations in cytosolic phospholipase A2-α
Gut, 2014, 63(1): 96-104

SL Etheridge, MA Brooke, DP Kelsell, DC Blaydon
Rhomboid proteins: a role in keratinocyte proliferation and cancer
Cell & Tissue Research, 2013, 351(2):301-07

DC Blaydon, P Biancheri, WL Di, V Plagnol, RM Cabral, MA Brooke, DA van Heel, F Rüschendorf, M Toynbee, A Walne, EA O'Toole, JE Martin, K Lindley, T Vulliamy, DJ Abrams, TT MacDonald, JI Harper, DP Kelsell
Inflammatory skin and bowel disease linked to ADAM17 deletion
New England Journal of Medicine, 2011, 365(16):1502-08

Presentations

Oral Presentation at the British Society for Investigative Dermatology (BSID) annual meeting (Exeter, UK; April 2012)
A genetic and functional link between iRHOM2 and ADAM17 in tylosis with oesophageal cancer

Oral (and poster) presentation at the European Society for Dermatological Research (ESDR) annual meeting
(Venice, Italy; September 2012)
A genetic and functional link between iRHOM2 and ADAM17 in tylosis with oesophageal cancer

Oral presentation at Blizard Institute Research Themes Symposium
(London, UK; February 2013)
Cytosolic phospholipase A2-α mutations in a severe inherited gut disease

Poster presentation at the International Investigative Dermatology (IID) meeting

(Edinburgh, UK; May 2013)
iRHOM2 mutations dysregulate ADAM17 in Tylosis with oesophageal cancer, affecting Ephrin- and EGF-family-mediated keratinocyte adhesion

Acknowledgements

Firstly, I would like to thank my supervisor, Professor David Kelsell, who provided me with the opportunity to work on and write this thesis, and without whose knowledge, ideas, motivational style and patience it would never have been completed.

I would also like to express my thanks to many other individuals who have helped me significantly with the work presented here. Specifically, Prof. Tom MacDonald (Blizard Institute, London), who supervised much of the work presented in the fifth chapter of this thesis; Prof. Spiro Getsios and Dr. Nihal Kaplan (Northwestern Feinberg School of Medicine, Chicago, USA) for their extensive work on three-dimensional cultures of tylosis keratinocytes shown in chapter 4; Dr. Claus-Werner Franzke and Cristina Cobzaru (University of Freiburg, Germany), for their help with transglutaminase activity assays; the lab group of Prof. Tim Warner (William Harvey Research Institute, London), for help with cPLA$_2$α activity assays; and My Mahoney (Jefferson Institute, Philadelphia, USA), for the gift of a desmoglein 2 antibody.

Next, it is impossible to overstate the contribution of my colleagues in the lab, in terms of ~~terms of~~ educating me in the variety of techniques on display through this thesis, keeping me company throughout the long days in the lab, and in the close collaborations that have made ~~much of~~ this work possible. I would like to thank Dr. Diana Blaydon, Dr. Claire Scott, Dr. Dan Tattersall, Dr. Charlotte Simpson, Dr. Anissa Chikh, Daniela Niţoiu, Phil Bland, Ben Fell, and Thivi Maruthappu, for these reasons and more. ~~In particular,~~ I would especially like to offer thanks to Sarah Etheridge, with whom I have worked closely and productively on a number of projects, and whose work has done much to inform mine. As well as my lab group, I am indebted to other members of the Blizard Institute for their help with particular experiments. In particular, Dr. Paolo Biancheri and Renata Curciarello were a great help with cell culture and ELISA experiments.

However, I would ~~especially~~ like to dedicate this thesis to all of the friends and family, both inside and outside the Institute, that have made it possible by putting up with me for the last three and a bit years. As well as those I have already mentioned, I would like to thank (in no particular order) my mum, my dad, my brother Thomas and sister ~~Thomas and~~ Lucy, housemates past and present: Thomas Banks, Marc Cranage, James Selkirk, Adam Lewis, Charlotte Overton and Krishan Pau; Dr. Jamie Upton, Ruth Angus, Louise Adams, Rob Abrehart, Zoe Drymoussi, Dr. Emily Ruban, Dr. Ros Hannen, Joe Queening, the Holmfirth girls,

Gordon and Sam, and anyone else that takes the time to read the work I present to you here. You've made it all worthwhile.

Chapter 1

Introduction

1. Introduction

This thesis will focus on understanding the pathophysiology of three distinct, rare, inherited conditions, which affect the skin and the epithelium of the gastrointestinal tract. The genes affected in each of these three conditions encode proteins involved either directly or indirectly in the generation of soluble mediators that play key roles in intercellular communication.

Intercellular communication is a hallmark of and requirement for the maintenance of multicellular life. In addition to nervous transmission over long distances, and direct cell-cell interactions mediated by intercellular junction complexes, much intercellular communication is facilitated by the release, detection of, and response to a vast array of cell-derived soluble mediators. These include broad families of molecules such as growth factors, cytokines, chemokines and hormones, which can be small-molecular, peptide, lipid or phospholipid in nature, and have been shown to regulate vast numbers of diverse processes required for multicellular life. Due to the importance of these various intercellular mediators, regulation of their release can be considered to be of the utmost importance to the control of metabolism. As illustrated by the three conditions examined in this thesis, perturbation of physiological processes involved in the synthesis and release of these extracellular mediators can have wide-ranging effects on human health.

To provide the necessary background for the results that will be presented in later chapters, this introduction will describe the structure of the skin and gastrointestinal epithelium, the importance of intercellular signalling pathways, the structures and functions of proteins involved in the regulation of various relevant intercellular signalling pathways, the importance of these pathways in epithelial development and homeostasis, and genetic techniques for investigating inherited diseases of the skin and gastrointestinal tract.

1.1 The skin and gastrointestinal tract, and EGFR signalling

1.1.1 The epidermis

The skin is the largest organ in the body; covering almost the entirety of the outer surface of the human body, it provides an essential defensive layer, protecting against physical and chemical damage, infectious agents and allergens. Beyond its protective role, the skin has other important functions in preventing water loss and regulating body temperature. On a gross scale, the skin is made up of three broad layers: the outermost is the epidermis, below which lies the dermis, with subcutaneous tissue (the hypodermis) below that.

The epidermis represents the outermost layer of the skin, and consists of a specialised, multi-layered stratified epithelium. It is made up primarily of specialised epidermal cells called keratinocytes, which are organised into defined basal, spinous and granular layers, topped by an outermost cornified layer (the stratum corneum), which provides the specific epidermal barrier function (Madison, 2003). The general structure of the epidermis is illustrated in figure 1.1. Keratinocytes in the epidermis are accompanied by three other cells types: pigment-producing melanocytes; Merkel cells, which have a role in mechanoreception; and Langerhans cells, which have an immune function and act as antigen-presenting cells.

Proliferation of keratinocytes in the epidermis occurs ~~exclusively~~ predominantly in the basal layer, where epidermal stem cells reside. Here, stem cells give rise to a population known as transit-amplifying cells, which can in turn proliferate to give rise to daughter cells that can exit the cell cycle and begin the process of terminal differentiation (Jensen ~~et al~~*et al*., 1999). Keratinocytes differentiate following a set pattern as they rise through the different epidermal layers, maturing eventually into corneocytes – the flattened, dead cells of the stratum corneum, whose plasma membrane has been entirely replaced by an insoluble cornified envelope (Proksch ~~et al~~*et al*., 2008). In the uppermost skin layer, corneocytes are surrounded by an extracellular lipid matrix – roughly comprised (by weight) of around 45-50% ceramides, 25% cholesterol, 10-15% free fatty acids and 5% other lipids (Madison, 2003) – which form the permeability barrier that characterises the stratum corneum. The lipids that make up the permeability barrier originate from lamellar granules, tiny membrane-bound organelles (visible only through electron microscopy) that are prominent

in the granular layer of the epidermis. These fuse with the plasma membrane of keratinocytes late in the process of terminal differentiation, discharging their lipid contents into the extracellular space (Madison, 2003).

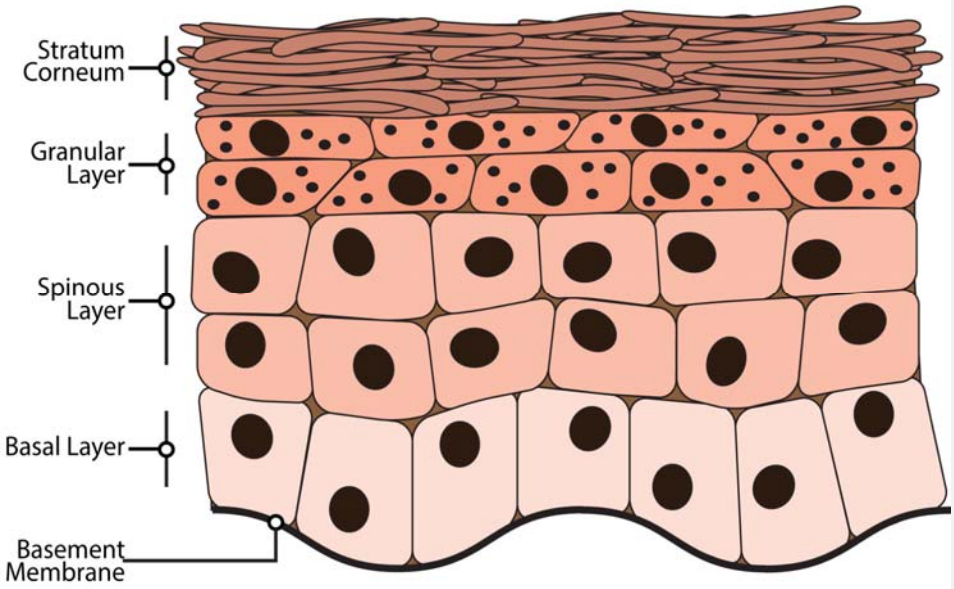

Figure 1.1: The structure of the epidermis. An illustration of the organisation of the interfollicular epidermis, showing the major keratinocyte layers.

The formation of the stratum corneum represents perhaps the most important stage in the formation of an effective epidermal barrier. Key to this process is the formation of the cornified envelope, an insoluble protein structure which replaces the plasma membrane of terminally differentiating keratinocytes, and facilitates the attachment of insoluble lipids during stratum corneum formation. Important in this process are the transglutaminase (TGM) enzymes TGM1 and TGM3, which function to cross-link structural component proteins of the cornified envelope (Franzke ~~et al~~*et al*., 2012), such as, involucrin, loricrin, small proline-rich proteins and filaggrin (Hitomi, 2005), the last of which is also involved in aggregating keratinocytes' keratin filaments into bundles, facilitating the collapse of the cell into its flattened corneocyte shape (Palmer ~~et al~~*et al*., 2006). TGM1 has also been shown to be important in forming an ester link between involucrin (present in the cornified envelope)

and extracellular long-chain hydroxyceramides that make up part of the extracellular lipid matrix of the stratum corneum (Nemes ~~et al~~*et al*., 1999).

1.1.2 The small intestinal epithelium

In contrast to the highly stratified nature of the epidermis, the lumen of the gastrointestinal tract is lined by a specialised simple columnar epithelium only one cell thick, whose primary role is the absorption and digestion of nutrients, as well as in protection from intestinal pathogens. This epithelium is characterised by a very high level of turnover, and has been described as the most vigorously self-renewing tissue in the adult human body (van der Flier and Clevers, 2009).

As it is not stratified, proliferation and migration of cells in the gut epithelium is fundamentally different from that seen in the skin. The luminal surface of the intestine is organised into large tubular structures known as villi, a pattern of organisation which serves to vastly increase the surface area of the gastrointestinal tract available for nutrient absorption. At the base of the villi are specialised structures known as crypts of Lieberkühn, epithelial invasions into the underlying connective tissue, in which intestinal stem cells reside, and where all cell proliferation takes place (van der Flier and Clevers, 2009). The structure of the intestinal epithelium is illustrated in figure 1.3. In the crypts, intestinal stem cells generate transit amplifying cells, which divide 4-5 times before terminally differentiating into one of four specialised intestinal epithelial cell types. Differentiated epithelial cells then migrate upward along the luminal surface of a villus until they reach the tip, whereupon they undergo apoptosis and are shed into the intestinal lumen (Hall ~~et al~~*et al*., 1994). Of the four cell types that make up the epithelium, over 80% are enterocytes, highly polarised cells which express a 'brush border' of microvilli at their apical surface, and are responsible for water and nutrient absorption (van der Flier and Clevers, 2009). Goblet cells are responsible for the secretion of intestinal mucus (important in physical and chemical defence of the intestinal epithelium, and the effective movement of gut contents) in response to a variety of stimuli. The proportion of goblet cells in the intestinal epithelium increases over the length of the gastrointestinal tract, from around 4% in the duodenum, to 16% in the descending colon (van der Flier and Clevers, 2009). Enteroendocrine cells represent a diverse class of cells (up to 15 sub-types have been described) which coordinate gut function through the secretion of

specific peptide hormones (Rehfeld, 2004). Lastly, Paneth cells play a role in the innate immune system of the intestine; they are unique both in their relative longevity (at least three weeks, much longer than any other intestinal epithelial cell type) and in that they do not migrate out of the crypt of Lieberkühn, instead residing in the base of the crypt, where they secrete antimicrobial peptides, defensins and lysozymes (Crosnier ~~et al~~*et al.*, 2006).

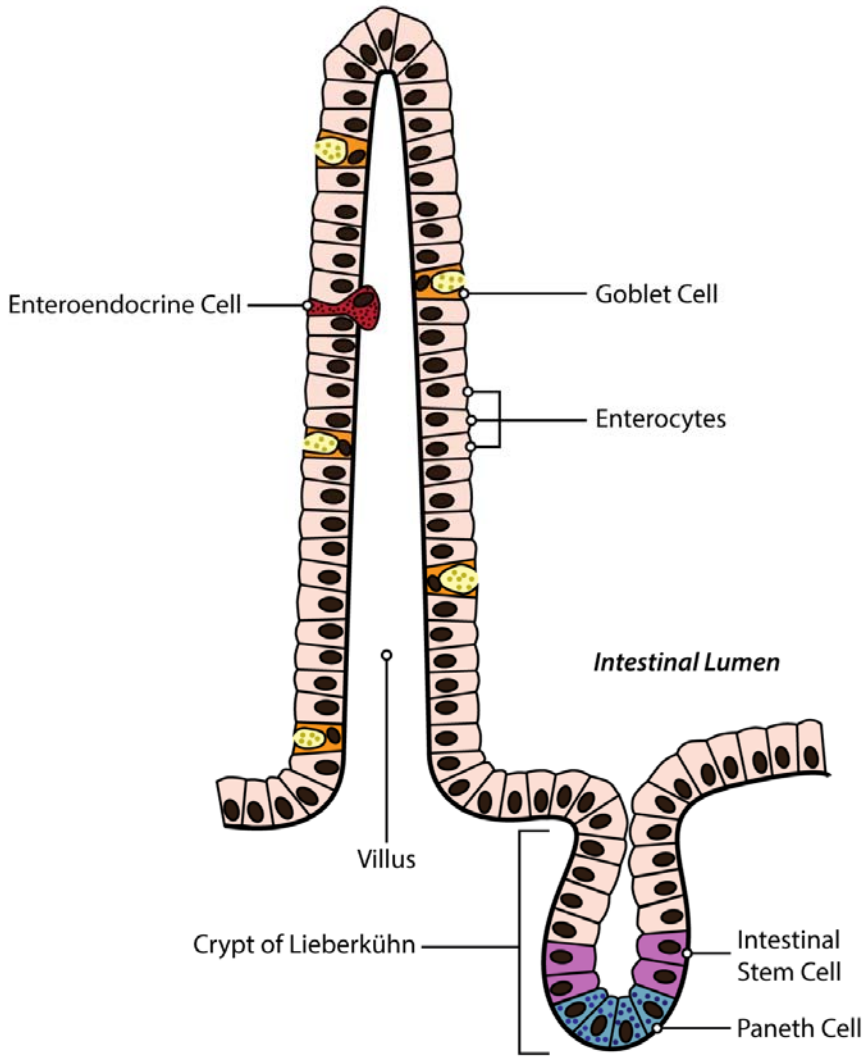

Figure 1.2: The structure of the intestinal epithelium. An illustration (not to scale) of the general structure of the intestinal epithelium, showing a single villus and a crypt of Lieberkühn. The four

major cell types of the epithelium are shown, as well as a representation of the location of intestinal stem cells.

1.1.3 The Epidermal Growth Factor Receptor (EGFR) family, and its ligands

Due to their protective functions and near-constant exposure to potential damage, a high rate of cell turnover is a feature of many epithelial tissues, and is especially prominent in both the skin and the gastrointestinal epithelium. Among the numerous signalling pathways involved in the growth and homeostasis of these tissues, signalling through the epidermal growth factor receptor (EGFR) plays a particularly prominent role.

The EGFR is a member of the closely related, four-member family of receptor tyrosine kinases (RTKs) known as the ErbB family. The ErbB RTKs are a group of receptors which are activated by the binding of specific peptide ligands, with the exception of ErbB2, which has no specific ligand but functions as the preferred dimerisation partner of the of the other three members of the family (Agus ~~et al~~*et al*., 2002). The peptide ErbB ligands are a seven-member family (henceforth referred to as the EGFR ligand family), that consists of epidermal growth factor (EGF), heparin-binding EGF (HB-EGF), transforming growth factor-α (TGFα), amphiregulin, betacellulin, epigen and epiregulin – all of which can bind to the EGFR (ErbB1) (Hynes and Lane, 2005) with varying degrees of specificity. In addition, there exist four members of the neuregulin family, which bind to the ErbB3 and ErbB4 receptors to varying degrees (Chang ~~et al~~*et al*., 1997, Carraway ~~et al~~*et al*., 1997, Zhang ~~et al~~*et al*., 1997, Harari ~~et al~~*et al*., 1999). EGF, TGFα and amphiregulin have been shown to bind exclusively to the EGFR (ErbB1), whilst HB-EGF, betacellulin and epiregulin show dual specificity for the EGFR and the closely related ErbB4 (Hynes and Lane, 2005). Ligand binding to the EGFR and its related ErbB-family receptor tyrosine kinases results in receptor homo- or heterodimerisation, autophosphorylation, and downstream activation of a variety of diverse signalling pathways, prominently including the mitogen-activated protein kinase (MAPK) and phosphatidylinositol 3-kinase (PI3K)-AKT pathways (Yarden and Sliwkowski, 2001), making signalling through the EGFR among the most important signalling pathways in vertebrates. As well as multiple roles in development, responses to EGFR signalling in normal physiology include cell division, differentiation, motility, adhesion and death (Yarden and Sliwkowski, 2001), whilst

dysregulation of the pathway is unsurprisingly associated with dysplasia and cancer (Salomon ~~et al~~*et al*., 1995).

As activation of the EGFR ~~in~~ requires ligand binding, the release of EGFR ligands from synthesising cells is of crucial importance in the signalling pathway, and represents a significant opportunity for the regulation of EGFR signalling. All members of the EGFR ligand family of growth factors are synthesised as membrane bound pro-ligands, which require proteolytic cleavage in a juxtamembrane region to release their extracellular 'ectodomain', which can then function as an active ErbB ligand. This process is known as ectodomain shedding, with the enzymes responsible for pro-ligand cleavage referred to as ectodomain sheddases. The importance of ectodomain shedding will be discussed in section 1.2.

1.1.4 EGFR signalling in the epidermis and small intestinal epithelium

Signalling through the EGFR represents a particularly important pathway in the development and maintenance of the skin. In the epidermis, the EGFR is expressed most prominently in proliferating basal keratinocytes, and to a lesser degree in suprabasal cells undergoing differentiation. EGFR ligands are autocrine and paracrine growth factors for keratinocytes, and play a central role in the regulation of keratinocyte proliferation, survival and differentiation (Schneider ~~et al~~*et al*., 2008, Coffey ~~et al~~*et al*., 1987, Cook ~~et al~~*et al*., 1991, Stoll ~~et al~~*et al*., 1997, Piepkorn ~~et al~~*et al*., 1998). Signalling through the EGFR is essential for normal epidermal development and morphogenesis, as illustrated by the phenotype observed in *Egfr* knockout mice, which die perinatally, and display severe epithelial defects (Sibilia and Wagner, 1995, Miettinen ~~et al~~*et al*., 1995). *In vitro,* keratinocytes express significant levels of amphiregulin, as well as much lower levels of TGFα and HB-EGF (Pastore ~~et al~~*et al*., 2008), illustrating the relevance of EGFR ligand shedding in keratinocyte growth. Analysis of mice ~~who~~ which lack expression of the key ectodomain sheddase ADAM17 (responsible for the shedding of multiple EGFR ligands, to be discussed in detail in section 1.2) in their keratinocytes has suggested that EGFR-ligand dependent signalling is required for normal epidermal differentiation and barrier maintenance, meaning that any disruption of EGFR ligand shedding in the epidermis could be expected to adversely affect normal skin barrier function.

Signalling through the EGFR is also known to play an important role in epithelial wound healing – particularly in the early phase response to wounding – by increasing keratinocyte

proliferation and migration (Barrientos ~~et al~~*et al*., 2008). The importance of this response is illustrated in *Egfr*-null mouse skin grafts, where lesions heal at a slower rate compared to controls (Repertinger ~~et al~~*et al*., 2004). Shedding of EGFR ligands is required for keratinocyte migration during wound healing and is immediately induced upon wounding (Tokumaru ~~et al~~*et al*., 2000), with factors upregulated in wounded skin including amphiregulin, TGFα and HB-EGF; but not EGF or betacellulin (Barrientos ~~et al~~*et al*., 2008). In particular, TGFα is responsible for approximately 80% of keratinocyte migration activity during wound healing (Li ~~et al~~*et al*., 2006) and also promotes proliferation (Cha ~~et al~~*et al*., 1996); whilst HB-EGF promotes re-epithelialisation (Hashimoto ~~et al~~*et al*., 1994) and accelerates cutaneous wound healing when applied topically (Tolino ~~et al~~*et al*., 2011, Shirakata ~~et al~~*et al*., 2005).

Bearing these factors in mind, EGFR signalling would be expected to have a significant function in skin homeostasis, a role which is well illustrated by the epidermal side effects that are a common consequence of treatment with EGFR-inhibiting chemotherapeutics in cancer patients. These side effects include papulopustular rashes of the face and trunk, periungual inflammation, and xerotic (dry), scaly skin (Lacouture, 2006). Although the effect of EGFR inhibition is well described, relatively little is understood of the precise contribution of EGFR signalling to epidermal homeostasis; however, shedding of EGFR ligands by ectodomain sheddases would be expected to be a key regulatory step in this process in the skin. Recently, the first example of an inherited human disease associated with loss-of-function missense mutations in the *EGFR* gene has been identified, which was characterised by inflammatory skin disease that resembled that seen in patients treated with EGFR-inhibiting drugs, as well as bowel and lung inflammation (Campbell ~~et al~~*et al*., 2014).

Within the crypts of the intestinal epithelium, the primary driver of proliferation is considered to be the highly conserved Wnt-β-catenin signalling pathway, activity of which has been shown to be necessary for the maintenance of progenitor cell compartments in the crypt (Ireland ~~et al~~*et al*., 2004). However, EGFR signalling has also been shown to be of key importance in both the development and repair of the gut epithelium. Mouse knockouts of *Egfr* have severely deleterious effects on the development of numerous epithelial tissues, with the intestinal epithelium particularly affected, showing fewer, shorter villi and reduced proliferation, though all cell types do develop (Miettinen ~~et al~~*et al*., 1995). The intestines of *Egfr*-null mice are fragile and strongly susceptible to damage, with numerous intestinal haemorrhages and disintegration of the villi becoming apparent a few days after birth. This is consistent with a particular role for EGFR signalling in the response to damage, and in

regeneration of the intestinal epithelium after injury. The EGFR is expressed on enterocytes, where its activation following intestinal mucosal injury induces repair mechanisms, reduces inflammation and promotes cell survival (McElroy ~~et al~~*et al*., 2012, Dvorak ~~et al~~*et al*., 2002). Similarly, enterocyte proliferation is stimulated via the EGFR following resection of the small intestine, one of the most potent stimuli for enterocyte proliferation (Sheng ~~et al~~*et al*., 2006). So-called 'transactivation' of the EGFR (to be discussed in detail in section 1.2.6) also underlies the gastro-protective effects of prostaglandins, lipid mediators known to play key roles in gastro-intestinal defence and regeneration (Pai ~~et al~~*et al*., 2002). A requirement for EGFR signalling in response to gastrointestinal injury is highly conserved, with EGFR pathway activation required for enterocyte proliferation and gut remodelling following infection in *Drosophila* (Buchon ~~et al~~*et al*., 2010).

1.2 Ectodomain Shedding and ADAM17

1.2.1 Ectodomain shedding in intercellular signalling

As described previously, the release of peptide intercellular mediators (such as EGFR ligands) in vertebrates is frequently accomplished through the process of ectodomain shedding, in which the membrane bound precursor of an intercellular mediator (such as a pro-cytokine) undergoes proteolytic cleavage in a juxtamembrane region by one or more specific enzymes, resulting in the release of a soluble extracellular domain (Blobel, 2005); this is illustrated simply in figure 1.3, A.

Most prominent among the enzymes involved in this process are members of the membrane-anchored ADAM (A Disintegrin And Metalloprotease) family, which appear to be responsible for the majority of known ectodomain shedding events (Huovila ~~et al~~*et al*., 2005). The prototype ADAM protease involved in ectodomain shedding – and the first to be discovered to be involved in this process – is known as ADAM17 (Edwards ~~et al~~*et al*., 2008). Much of the research described in this report concerns the activity of this protein, and thus it will be discussed in greater detail than the other members of its family in the following sections.

1.2.2 The structure of the ADAM ectodomain sheddases

The ADAMs are multi-domain transmembrane proteins, and constitute one major family within a larger super-family of zinc-based metalloproteases ('metzincins')(Stocker and Bode, 1995), whose members also include the well-known family of matrix metalloproteases (MMPs) and lesser studied protease groups such as reprolysins and astacins (Edwards ~~et al~~*et al*., 2008). Active members of the metzincin super-family contain a highly conserved HEXXHXXGXXH…M motif (Bode ~~et al~~*et al*., 1993), in which three histidine residues bind a zinc

ion, accompanied by an invariant methionine residue in the active site, and a catalytic glutamate residue. Though much research has focussed on the function of the ADAM's catalytically active metalloprotease domain, full length ADAM proteins contain several more distinct domains (illustrated in Figure 1.3, B), including a cytoplasmic tail, a cysteine-rich domain, a disintegrin domain, and at their N-terminus an inhibitory pro-peptide, which blocks access to the active metalloprotease in inactive pro-ADAMs. Each of these domains has distinct functions to regulate an ADAM's activity.

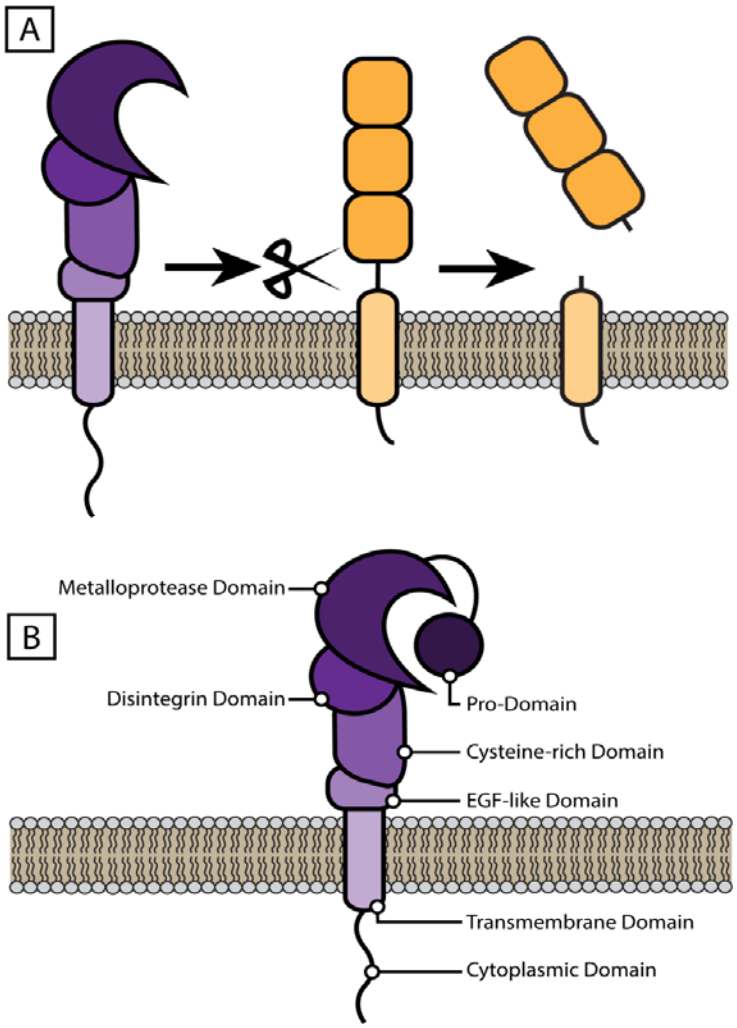

Figure 1.3: Ectodomain shedding and the structure of an ADAM. **A:** A simplified illustration of ectodomain shedding. A membrane tethered precursor (yellow) is cleaved in a juxtamembrane region by the actions of a protease (purple). **B:** The structure of a typical ADAM metallopotease, illustrating the major domains. Note that the EGF-like domain is absent in both of the broad spectrum sheddases ADAM17 and ADAM10. ADAM structure inspired in part by Murphy (~~Murphy,~~ 2008)

Intracellularly, the length and complexity of an ADAM's cytoplasmic domain varies greatly between different members of the family, ranging from 11 (ADAM11) up to 291 (ADAM19) residues (Seals and Courtneidge, 2003); these domains mediate interactions of the ADAM with specific intracellular partners to control trafficking of the protein and modulation of its activity. For example, a region of ADAM10's cytoplasmic domain rich in proline has been found to be important for the correct basolateral localisation of this protease in polarised epithelium, allowing for the cleavage of the ADAM10 substrate E-Cadherin to promote cell migration (Wild-Bode ~~et al~~*et al*., 2006). Several ADAM cytoplasmic domains contain putative binding sites for proteins containing SH3 domains – such as for example the endocytosis-associated, SH3-carrying protein PACSIN3, which has been shown to interact with several ADAMs (though not ADAM17) (Mori ~~et al~~*et al*., 2003), and may regulate their sub-cellular localisation. Additionally, the cytoplasmic regions can contain potential sites for kinase phosphorylation (serine, threonine or tyrosine residues), allowing for kinase-based control of their activity; for example, ADAM17 is able to be phosphorylated by the MAP kinase ERK on Threonine (Thr)-735, with this phosphorylation required for successful trafficking of Pro-ADAM17 from the endoplasmic reticulum (Soond ~~et al~~*et al*., 2005).

At the immediate extracellular side of several ADAM's transmembrane domain lies an epithelial growth factor (EGF)-like repeat region (though this is absent in the key sheddases ADAM10 and ADAM17), followed by a cysteine-rich domain. This cysteine-rich region is thought to influence interactions of an ADAM its substrates (and other proteins). For example, the ADAM10 cysteine-rich domain has been shown to regulate of the availability of Ephrin-A5 (an ADAM10 substrate) to its active site (Janes ~~et al~~*et al*., 2005), whilst the cysteine-rich domain of ADAM17 is required for the shedding of the IL-1 receptor, but not of TNFα (Reddy ~~et al~~*et al*., 2000).

The ADAM disintegrin domain is named due to its resemblance to true disintegrin proteins, snake venom constituents that prevent blood clotting by direct binding to integrins, and inhibition of integrin-mediated platelet-fibrinogen adhesion (Gould ~~et al~~*et al*., 1990). As suggested by their close resemblance to true disintegrins, studies using both recombinant ADAM disintegrin domains and full length ADAMs have shown that these domains can interact directly with integrins, and can thereby influence cell adhesion either positively or negatively (Edwards ~~et al~~*et al*., 2008). These interactions have been found to be important in fertility (reviewed by Evans [~~{Evans, 2001}~~]), and may have a role to play in promoting

migration or metastasis in cancer (to be discussed below, but also reviewed by Arribas ~~{~~[~~Arribas et al~~*et al*~~.,~~ 2006~~}~~]).

Key to the functioning of the ADAMs is their N-terminal pro-domain, a structure present in inactive pro-ADAMs, which inhibits the function of the metalloprotease domain until it is removed as part of an ADAM's maturation. The pro-domain functions by means of a 'cysteine-switch' mechanism (Loechel ~~et al~~*et al*., 2000), a feature shared in common with the inhibitory pro-domains of the MMPs (Roghani ~~et al~~*et al*., 1999). This system is dependent on the binding of a cysteine residue in the pro-domain to the catalytic zinc ion in the active site of the metalloprotease domain (Becherer and Blobel, 2003). This serves not only to prevent catalytic activity, but positions the pro-domain so as to completely block the entrance to the active site. Removal of the pro-domain during ADAM maturation is accomplished by the actions of pro-protein convertase enzymes such as furin (Schlondorff ~~et al~~*et al*., 2000), and takes place intracellularly in the secretory pathway following the transit of the pro-protein from the ER into the Golgi apparatus (Murphy, 2008). Regulation of pro-domain removal from an ADAM is therefore expected to play an important role in regulating the activity of the protease.

1.2.3 The functions and substrates of the ADAM ectodomain sheddases

Although their roles in ectodomain shedding are far better known, the first ADAMs to be discovered in mammals (*Adam1* and *2*) are the constituents of the heterodimeric, testis-restricted mouse sperm protein fertilin, (and are thus alternatively named fertilin-α and -β). As such, the first role uncovered for mammalian ADAMs was their involvement in fertility, specifically in the correct function of sperm. The precise contributions of various ADAMs in sperm function remain relatively unclear; however, they are thought to be involved in the binding of the sperm to the zona pellucida (the outermost layer of an unfertilised oocyte) (Ikawa ~~et al~~*et al*., 2010, Linder and Heinlein, 1997). As such, fertilin-β knockout mice are infertile (Cho ~~et al~~*et al*., 1998). While much of the study of the ADAMs' role in fertility has been carried out in mice (and is reviewed as part of a general examination of fertilisation by Ikawa ~~et al~~*et al.* ~~{~~[~~Ikawa et al~~*et al*~~.,~~ 2010~~}~~]), ADAMs are also expected to play important roles in fertility in humans. A significant number of the numerous ADAMs expressed in humans (3 catalytically active and 4 inactive) are expressed only in the testis, and have involvement in spermatogenesis, sperm function and fertility, as in mice. However, how the situation in

Formatted: Font: Not Italic

rodents with regard to ADAM function in fertility reflects that in humans remains confusing, as many important, testis-specific rodent ADAM genes (including *Adam1* and *Adam3*) are represented only as pseudogenes in humans (Jury ~~et al~~*et al*., 1997, Frayne and Hall, 1998, Puente and Lopez-Otin, 2004).

Humans encode 21 distinct ADAMs, of which 13 contain the intact metalloprotease domain and active site required for proteolytic activity (Edwards ~~et al~~*et al*., 2008). Aside from the testis-related members of the family, two further active ADAMs (8 and 28) are expressed primarily in haematopoietic cells, and one more (33) shows a very restricted tissue expression, meaning only six catalytically active ADAMs (ADAM9, 10, 12, 15, 17, and 19) are broadly expressed in somatic tissue (Edwards ~~et al~~*et al*., 2008). Despite ADAMs' role in fertility being the first elucidated, their best-known function remains their key involvement in in ectodomain shedding. Though some catalytically active members of the family have only a single (or indeed no known) substrate, the majority of the ADAM proteases have been shown to cleave a wide variety of substrates *in vitro,* with ADAM10 and ADAM17 notable for the high number and variety of their targets. Even when restricting a list to notable examples, ADAM17 – the first of the ADAMs to be implicated as an ectodomain sheddase – is still known to cleave multiple cytokines, receptors, growth factors, intracellular signalling molecules and cell adhesion molecules, among others. A by-no-means comprehensive list of selected significant ADAM substrates can be found in Table 1.1, whilst a much more complete list is given by Edwards ~~et al~~*et al* (~~Edwards et al.,~~ 2008). In particular, the wide range of substrates proteolytically cleaved by ADAM10 and ADAM17 make these enzymes pivotal in controlling a wide range of cellular processes, including inflammation, cell adhesion, growth and wound repair, among many more.

Formatted: Font: Not Italic

ADAM	Substrates
ADAM9	Amyloid precursor protein (APP) (Koike et al. et al., 1999); EGF (Peduto et al. et al., 2005); Heparin Binding-Epidermal Growth Factor (HB-EGF) (Izumi et al. et al., 1998); Delta-like ligand 1 (Dyczynska et al. et al., 2007); Laminin (Mazzocca et al. et al., 2005)
ADAM10	EGF (Sahin et al. et al., 2004); Betacellulin (Sahin et al. et al., 2004); APP (Slack et al. et al., 2001); Notch-1 (Pan and Rubin, 1997); E-, N- and VE-Cadherins (Reiss et al. et al., 2006, Maretzky et al. et al., 2005, Schulz et al. et al., 2008); Desmoglein 2 (Bech-Serra et al. et al., 2006); RANKL (Hikita et al. et al., 2006); Delta-like ligand 1 (Six et al. et al., 2003); Collagen XVII (Franzke et al. et al., 2004); ErbB2 (Liu et al. et al., 2006); Ephrin A5 (Janes et al. et al., 2005); CD23 (Moss and Rasmussen, 2007); CD44 (Nagano and Saya, 2004)
ADAM12	HB-EGF (Asakura et al. et al., 2002); Fibronectin (Roy et al. et al., 2004); Delta-like ligand 1 (Dyczynska et al. et al., 2007)
ADAM15	HB-EGF (Hart et al. et al., 2005); Amphiregulin (Schafer et al. et al., 2004); E-Cadherin (Najy et al. et al., 2008)
ADAM17	Tumour Necrosis Factor-α (TNFα) (Black et al. et al., 1997, Moss et al. et al., 1997); Transforming Growth Factor-α (TGFα) (Peschon et al. et al., 1998, Sahin et al. et al., 2004); Amphiregulin (Gschwind et al. et al., 2003, Sahin et al. et al., 2004); HB-EGF (Sahin et al. et al., 2004); Neuregulin (Yokozeki et al. et al., 2007); Epigen (Sahin and Blobel, 2007); TNF receptors I and II (Reddy et al. et al., 2000); IL-6 receptor (Chalaris et al. et al., 2007); IL-1 receptor II (Reddy et al. et al., 2000); ErbB4 (Rio et al. et al., 2000, Maatta et al. et al., 2006); Notch1 (Brou et al. et al., 2000); L-selectin (Peschon et al. et al., 1998); VCAM1 (Garton et al. et al., 2003, Singh et al. et al., 2005); Desmoglein 2 (Bech-Serra et al. et al., 2006); CD40 (Contin et al. et al., 2003); CD44 (Nagano and Saya, 2004); VEGF receptor 2 (Swendeman et al. et al., 2008)
ADAM19	Neuregulin (Yokozeki et al. et al., 2007); RANKL (Chesneau et al. et al., 2003) HB-EGF (Horiuchi et al. et al., 2005)

Table 1.1: Selected substrates of the widely expressed, catalytically active ADAMs

It is particularly notable that, among its wide variety of substrates, ADAM17 is responsible for the shedding of numerous members of the EGFR ligand family, making ADAM17 (alongside ADAM10) a key upstream regulator of the EGFR signalling pathway. Of the known ligands of the ErbB receptor family, two (betacellulin and EGF) are shed primarily by ADAM10, whilst the remaining five (HB-EGF, TGFα, amphiregulin, epiregulin and epigen) are

shed primarily by ADAM17 (Sahin and Blobel, 2007, Sahin et al et al., 2004). Though other ADAMs share the ability to cleave some EGFR ligands in vitro, it appears that ADAM10 and 17 are responsible for the majority of their shedding in vivo, as demonstrated by the severe phenotypes seen in *Adam10* and *Adam17* knockout mice (to be discussed in detail in section 1.2.7).

1.2.4 ADAM17 in inflammatory processes

The ectodomain sheddase function of ADAM17 was first discovered due to ability of the enzyme to cleave and release the pro-inflammatory cytokine TNFα (Black et al *et al*., 1997, Moss et al *et al*., 1997). Not only was this discovery pivotal in the understanding of the regulation of the release of TNFα – a cytokine whose paracrine signalling effects make it a key component of the inflammatory and innate immune responses – but it also represented the first association of an ADAM protein with ectodomain shedding events. Increased TNFα shedding has been implicated in the pathogenesis of a large number of inflammatory conditions, including (but not limited to): rheumatoid arthritis (Vinay and Kwon, 2011, Aggarwal et al *et al*., 2012); cardiovascular disease (Feldman et al *et al*., 2000); Alzheimer's disease (Swardfager et al *et al*., 2010); Parkinson's disease (Nagatsu and Sawada, 2005); a variety of lung diseases including chronic obstructive pulmonary disease (COPD)(Lundblad et al *et al*., 2005); and numerous types of cancer (to be discussed in greater detail in section 1.2.8), making the regulation of its shedding of fundamental importance to the understanding a large number of well-known and prevalent conditions. TNFα cleavage remains the best known function of ADAM17, and as such the enzyme is still frequently referred to in literature as TACE (TNFα Converting Enzyme). Subsequent to its discovery as the sheddase for this well-known cytokine, ADAM17 has emerged as an enzyme with an unusually broad and varied range of substrates, as illustrated in Table 1.1.

Even bearing its well-known function as the TNFα sheddase in mind, ADAM17 cannot be considered to be an exclusively pro-inflammatory enzyme. For example, in the regulation of inflammation, it is interesting to note that not only does ADAM17 regulate shedding of TNFα, but also of its receptors TNFR-I and –II (Reddy et al *et al*., 2000). ADAM17-mediated shedding of TNFRs serves to reduce the susceptibility of a given cell to TNFα stimulation, both by directly reducing cell surface TNFR numbers and by producing soluble forms of the receptors that can compete antagonistically with membrane bound receptors to reduce local TNFα signalling. The importance of this process in controlling inflammation is pointedly illustrated by the inherited disease TRAPS (TNFα-receptor-associated periodic febrile syndrome), in

which mutations in the ADAM17 cleavage site of TNFR-I prevent its shedding (and therefore its cell surface downregulation), thereby increasing cells' susceptibility to TNFα, and resulting in recurring episodic high fevers due to an increased inflammatory response (McDermott ~~et al~~*et al*., 1999).

Similarly, ADAM17 is responsible for the shedding of the IL-6 receptor and IL-1 receptor II, and thus also represents an important level of regulation of inflammatory processes mediated by these two cytokines. IL-1 binds to two distinct receptors: IL-1RI and IL-1RII; of these, only IL-1RI is capable of transducing a signal, whilst IL-1RII acts as a decoy receptor (Mullberg ~~et al~~*et al*., 2000). Of the two, only IL-1RII can be shed by ADAM17 (Orlando ~~et al~~*et al*., 1997, Reddy ~~et al~~*et al*., 2000) (whilst IL-1RI cannot be shed at all) to produce a soluble receptor (sIL-1RII) that acts as a competitive inhibitor of IL-1 signalling, binding soluble IL-1, but not the naturally occurring IL-1 antagonist IL-1RA (Symons ~~et al~~*et al*., 1995). Thus, IL-1RII shedding acts as a negative regulator of IL-1-dependent inflammatory processes, in a fashion analogous to shedding of the TNFα receptors. Conversely however, IL-6 receptor (IL-6R) shedding appears to act in an agonistic way, through a process known as IL-6 trans-signalling. This is a mechanism by which shed, soluble IL-6R, in complex with IL-6, is capable of stimulating cells via interaction with the ubiquitously expressed signal transducing protein gp130, without the involvement of membrane bound IL-6R (Rose-John ~~et al~~*et al*., 2006). In this way, shedding of the IL-6 receptor allows for the activation of numerous cell types which are unresponsive to IL-6 alone (due to their not expressing cell surface IL-6R). This process of trans-signalling has been shown to be involved in the pathogenesis of numerous chronic inflammatory diseases, including inflammatory bowel disease, rheumatoid arthritis and asthma (Rose-John ~~et al~~*et al*., 2006), among others, and illustrates the multi-faceted and often paradoxical role of ADAM17 in inflammatory processes.

1.2.5 ADAM17 regulation and activation

Considering its particularly broad range of substrates and the importance of the pathways affected by them, tight regulation of the activity of ADAM17 by cells is to be expected. As previously described, the removal of ADAM17's pro-domain is a prerequisite for ADAM17 activity, and therefore presumably represents an important step in the regulation of its sheddase activity. However, ADAM17 activity can also be rapidly upregulated in response to a variety of stimuli (Doedens ~~et al~~*et al*., 2003), including by bacterial lipopolysaccharide

(Horiuchi ~~et al~~*et al*., 2007a), phorbol esters (~~including~~ such as phorbol myristate acetate – PMA~~; and tetradecanoyl phorbol acetate – TPA~~) (Horiuchi ~~et al~~*et al*., 2007b), G-protein coupled receptor stimulation (to be discussed in 1.2.6), and activation of Src. The mechanism by which such stimuli result in the rapid upregulation of ADAM17 activity remains unresolved; reports have directly contradicted one another on the question of whether or not simulation with PMA results in increased levels of ADAM17 pro-domain removal, and transport of mature ADAM17 to the plasma membrane (Horiuchi ~~et al~~*et al*., 2007b, Nagano ~~et al~~*et al*., 2004). Similarly, the requirement for phosphorylation of ADAM17's cytoplasmic domain for protease activity remains unclear. The cytoplasmic domain of ADAM17 can be phosphorylated at threonine-735 (Diaz-Rodriguez ~~et al~~*et al*., 2002), in a process mediated by extracellular signal-regulated kinase (ERK), and this phosphorylation has been described as being required for the trafficking of ADAM17 to the cell surface (Soond ~~et al~~*et al*., 2005). However, the cytoplasmic domain of ADAM17 has also been shown to be dispensable for stimulated shedding of TNFα (Reddy ~~et al~~*et al*., 2000, Doedens ~~et al~~*et al*., 2003). The exact mechanisms that underlie rapid activation of ADAM17 by external stimuli are therefore still to be resolved. However, one recent report has suggested that phorbol ester-stimulated upregulation of ADAM17 shedding may not in fact require any upregulation of ADAM17 activity at all, and that this upregulation is due to a substrate-selecting signalling pathway dependent on members of the protein kinase C family, which regulates the availability of some, but not all, ADAM17 substrates (including members of the EGFR ligand family) for shedding (Dang ~~et al~~*et al*., 2013).

1.2.6 ~~G-protein coupled receptor (GPCR) and EGFR cross-talk (~~EGFR transactivation~~)~~ and the importance of ADAM17

Interestingly, ADAM17 plays an important role not only in signalling by EGFR ligands, for which it acts directly as a sheddase, but also in signalling by receptors whose ligands it does not directly cleave. Whilst shedding of EGFR ligands influences cell signalling in paracrine and juxtacrine manners, ADAM17 is also involved in the activation of EGFR signalling in response to activation of a number of G-protein coupled receptors (GPCRs) by, for example, ligands such as angiotensin, thrombin and 5-HT. In this process, GPCR activation activates ADAM17 in a process dependent on either the kinases Src (Maretzky ~~et al~~*et al*., 2011b) or ERK (Swendeman ~~et al~~*et al*., 2008). ADAM17 activation in these circumstances results in the shedding of one or more EGFR ligands (the shed ligand is primarily HB-EGF (Prenzel ~~et al~~*et*

al., 1999), though amphiregulin and TGFα are also involved), which can then activate the EGFR in an autocrine fashion (Edwards et al et al., 2008). Thus, EGFR signalling is activated by GPCR ligands, in a process known as 'triple membrane pass signalling', and is also referred to as EGFR transactivation. This function is limited not only to stimulation of GPCRs, but is also involved in activation of EGFR signalling by non-EGFR ligands via other tyrosine kinase receptors. For example, keratinocyte migration in response to keratinocyte growth factor (FGF7) or vascular endothelial growth factor A (VEGF-A) – which signal via the RTKs fibroblast growth factor receptor 2-IIIb (FGFR2b) and VEGF receptor 2 respectively – requires Src-dependent activation of ADAM17 and HB-EGF release (Maretzky et al et al., 2011a). This illustrates the central role of ADAM17 in EGFR signalling, demonstrating that not only can it directly promote EGFR signalling via EGFR ligand release, but also control the cellular response to factors which are not among its substrates.

1.2.7 ADAM mutations and knockouts in mice

Striking examples of the importance of ADAM17-dependent EGFR-ligand shedding can be seen in *Adam17*-knockout (*Adam17*$^{-/-}$) mice. These knockouts produce mice that die around the time of birth (perinatal lethality), aspects of whose phenotype closely resemble those seen in mice lacking various EGFR ligands. Examples of this include defects in epithelial structure maturation and morphogenesis (including un-fused eyelids and serious defects in skin and gastrointestinal structure and function) – resembling TGFα deficient mice (Peschon et al et al., 1998); defects in branching morphogenesis of the mammary gland (similar to that seen in Amphiregulin-deficient mice) and the lung (Zhao et al et al., 2001); and, fatally, defects in heart development such as cardiac muscle hyperplasia and thickened, misshapen heart valves, with both heart and lung phenotypes resembling mice lacking HB-EGF (Jackson et al et al., 2003, Shi et al et al., 2003). Meanwhile, *Adam10*$^{-/-}$ mice die even earlier, for reasons also likely related to impaired angiogenesis, and display phenotypes resembling those of mice with knockouts of the ADAM10 substrates EGF and Notch1 (Hartmann et al et al., 2002).

Whilst mouse *Adam17* knockouts are not viable, hypomorphic *Adam17* mice, expressing around 5% of a normal physiological level of the protein, have been successfully generated. Although viable, these mice develop eye, hair, skin and milk duct defects resembling those of mice lacking TGFα and amphiregulin (Chalaris et al et al., 2010), though these were less

severe than completely *Adam17*- or *Egfr*-null mice. Also in contrast to *Egfr* knockout mice, development of the gastrointestinal tract appeared to be superficially normal. However, these mice were strongly susceptible to inflammatory colitis following challenge with dextran sulphate, a phenotype which resulted from defective regeneration of intestinal epithelium due to an inability to shed EGFR ligands (Chalaris ~~et al~~*et al*., 2010). High levels of EGFR ligands, in particular TGFα, were generated in the enterocytes of these mice after dextran sulphate challenge, but remained at the plasma membrane due to the inability to effectively shed them. Treatment with soluble TGFα was sufficient to restore normal intestinal epithelial function, demonstrating that EGFR signalling pathway dysfunction was responsible for the phenotype observed, and illustrating the importance of the ADAM17-EGFR axis in intestinal epithelial repair and remodelling.

Tissue-restricted *Adam17* mouse knockouts have also been performed, yielding useful information on the role of ADAM17 in specific tissues. Keratinocyte-restricted *Adam17* knockouts result in a phenotype of inflammatory dermatitis and pronounced defects in the integrity of the epidermal barrier, which develop soon after birth. These defects were found to be the consequence of a marked reduction in epidermal transglutaminase activity, resulting from reduced EGFR signalling due to absent EGFR ligand shedding. Indeed, the phenotype of keratinocyte-restricted *Egfr* knockout mice closely resembled this phenotype, and the topical application of TGFα was found both to significantly increase transglutaminase activity, and reduce skin inflammation in the epidermal *Adam17*-knockout mice (Franzke ~~et al~~*et al*., 2012).

1.2.8 ADAM17 and its substrates in cancer

In its role as the sheddase enzyme for a wide variety of substrates, many of which (such as the EGFR ligand family described previously) are able to profoundly affect cellular growth, metabolism and motility, it is perhaps predictable that upregulation of various ADAMs, notably including ADAM17, has been observed in several cancer types. Several notable substrates of ADAM17 have also been shown to play key roles in cancer development, offering a rationale for a function for ADAM17 in oncogenesis.

As its name suggests, TNFα was first discovered as a cytokine responsible for the haemorrhagic necrosis of tumours (Carswell ~~et al~~*et al*., 1975). And whilst large doses of recombinant TNFα have been shown to promote tumour necrosis in rodent models (Balkwill,

2009), it has also been shown to have a paradoxical tumour-promoting activity in many circumstances (Balkwill, 2006), to be expressed constitutively in many tumour types (Suganuma ~~et al~~*et al*., 1999) and may be associated with poorer prognosis *in vivo*. For example, *Tnfa*-knockout mice treated with skin carcinogens develop fewer tumours than controls (Moore ~~et al~~*et al*., 1999), whilst serum TNFα levels in prostate cancer patients increase with advanced disease (Pfitzenmaier ~~et al~~*et al*., 2003), and correlate with disease extent (Michalaki ~~et al~~*et al*., 2004). Indeed, animal models have shown that constitutively expressed TNFα produced by many malignant cells enhances the growth and spread of skin, ovarian, pancreatic and bowel tumours (Balkwill, 2009). Much of the pro-tumour activity of TNFα is thought to derive from its potent pro-inflammatory effects, with inflammation in the tumour microenvironment associated with malignant cell survival, angiogenesis and metastasis, and in altering cellular responses to hormones and chemotherapeutics (Mantovani ~~et al~~*et al*., 2008). Much of this activity derives from the interaction of TNFα with TNFR-I, (TNFR-I knockout mice demonstrate resistance to carcinogenesis ~~(Arnott et al *et al*., 2004)~~[Arnott *et al*., 2004]); the fact that both TNFα and its receptor are ADAM17 substrates therefore illustrates ADAM17's central role in cancer pathogenesis under these circumstances.

The role of ADAM17 in the shedding of the IL-6 receptor has also been implicated in the development and progression of cancer, most prominently in the colon. As described in section 1.2.4, soluble IL-6R (shed by ADAM17) is responsible for stimulation of numerous otherwise IL-6-insensitive cell types, via interaction with the membrane protein gp130. Increased expression of ADAM17 has been observed at the cell surface of epithelial cells in colon tumour lesions, accompanied by a loss of membrane-bound IL-6R (Rose-John ~~et al~~*et al*., 2006, Becker ~~et al~~*et al*., 2005). Furthermore, growth of colonic tumours could be inhibited using neutralising antibodies against soluble IL-6R, and by a soluble IL-6R antagonist made from a soluble gp130 Fc (immunoglobulin-like) domain (Becker ~~et al~~*et al*., 2004), suggesting that IL-6R trans-signalling plays an important role in colon tumour progression.

In addition, dysregulation or hyperactivation, at a number of different levels, of the EGFR pathway has been well studied in terms of cancer development and progression (Hynes and Lane, 2005), with cancer patients with altered EGFR activity tending to have more aggressive disease and poorer clinical outcomes (Zandi ~~et al~~*et al*., 2007). Often, such dysregulation takes the form of ErbB receptor overexpression – such as following gene amplification in glioblastoma (Ohgaki ~~et al~~*et al*., 2004), oesophageal squamous cell carcinoma (OSCC)

(Sunpaweravong ~~et al~~*et al*., 2005) and many others (reviewed by Krause and van Etten (~~Krause and Van Etten, 2005~~)]) – or constitutive activation as a result of mutations, as in the well-studied example of *EGFR* tyrosine kinase domain mutations in non-small cell lung cancer (NSCLC) (Sharma ~~et al~~*et al*., 2007). Considering its previously described importance in the skin, it is unsurprising that EGFR signalling is also a major component in the pathogensis of skin tumours (Schneider ~~et al~~*et al*., 2008), in which it has been found to be activated by UV light to induce epidermal hyperplasia (El-Abaseri ~~et al~~*et al*., 2006), and to maintain the proliferative potential of basal keratinocytes in epidermal tumours (Hansen ~~et al~~*et al*., 2000).

Moreover, overexpression and increased secretion of EGFR ligands has also been reported in various cancer types, with one prime example among others being TGFα upregulation in NSCLC, which can in turn establish a so-called 'autocrine loop' (in which TGFα activation of the EGFR stimulates the production of more TGFα) and lead to receptor hyperactivity (Putnam ~~et al~~*et al*., 1992). Additionally, transgenic overexpression of TGFα in mice leads to the development of ~~breast~~ mammary carcinoma, as well as epithelial and pancreatic hyperplasia (Sandgren ~~et al~~*et al*., 1990). Given the pivotal role of ADAM17 in EGFR signalling, its overexpression concurrent with increased ligand shedding in various cancer types may be relatively unsurprising; indeed, ADAM17 upregulation has been described in breast (Borrell-Pages ~~et al~~*et al*., 2003), colon (Blanchot-Jossic ~~et al~~*et al*., 2005), kidney (Roemer ~~et al~~*et al*., 2004), liver (Ding ~~et al~~*et al*., 2004), ovarian (Tanaka ~~et al~~*et al*., 2005), pancreatic (Mochizuki and Okada, 2007) and prostate (Karan ~~et al~~*et al*., 2003) cancers, and is often correlated with adverse outcomes in patients (McGowan ~~et al~~*et al*., 2008). ~~Despite this, to date no somatic mutations in ADAM17 (or any ADAM) have been linked with any type of tumour.~~ Somatic mutations in numerous members of the ADAM family, including 56 coding mutations in ADAM17 and 57 in ADAM10, have been described to be associated with a wide variety of tumour types (Forbes ~~et al~~*et al*., 2011), underscoring the potential for the involvement of both ADAMs and the pathways they regulate, in oncogenesis.

1.2.9 The desmosome

In addition to the ectodomain shedding of membrane tethered substrates, ADAM17 plays a role in the regulation of intracellular junction complexes, particularly desmosomes. Desmosomes are intracellular junction complexes that serve to form strong adhesions

between two neighbouring cells, providing mechanical stability to tissues via the anchoring of intermediate filaments. Desmosome-type structures have been observed in numerous tissues that experience mechanical stress, including the intestinal mucosa, gallbladder, uterus and oviduct, liver, pancreas, stomach, salivary and thyroid glands and the epithelial cells of the nephron, but are most abundant in the skin and myocardium (Farquhar and Palade, 1963, Kelly, 1966, Staehelin, 1974, Holthofer ~~et al~~*et al*., 2007), where they anchor cytoskeletal keratin intermediate filaments and desmin intermediate filaments respectively (Green and Gaudry, 2000). In brief, desmosomes consist of desmosomal cadherins (desmogleins and desmocollins), which constitute the extracellular portion of the structure, and bind in homo-and heterodimers to the cadherins of desmosomes on neighbouring cells. The intracellular portions of desmosomal cadherins bind to the armadillo-family proteins plakoglobin and the plakophilins, which in turn link to desmoplakin, which tethers the desmosome to the intermediate filament network (Brooke ~~et al~~*et al*., 2012). Patterns of expression of the desmosomal cadherins and plakophilins differ significantly both between tissues and within stratified epithelia – displaying radical changes in different layers of the epidermis, for example – implying a functional distinction between desmosomes in different tissue types and epithelial layers.

Considering their important role in resistance to mechanical stress, it is unsurprising that mutations in various desmosomal components are often associated with severe inherited diseases, commonly affecting the skin, hair and heart. Mutations in different desmosomal proteins have been found to be associated with palmoplantar keratoderma, woolly hair, alopecia, ectodermal dysplasia, skin fragility, and arrhythmogenic right ventricular cardiomyopathy (ARVC; a common cause of sudden cardiac death associated with exercise), in various combinations (see section 1.3, and Brooke ~~et al~~*et al* [~~{Brooke et al~~*et al*~~.,~~ ~~2012}~~] for an overview).

Formatted: Font: Not Italic

1.2.10 The role of ADAM17 in desmosomal dynamics and turnover

ADAM17 is capable of regulating the formation and turnover of desmosomes both directly and indirectly. Signalling through the EGFR has been shown to promote desmosome disassembly, a function presumably related to facilitating cell motility during wound healing and tissue remodelling (Lorch ~~et al~~*et al*., 2004). Conversely, EGFR inhibition promotes desmosome assembly, and strengthens intercellular adhesion mediated by desmosomes. In

its capacity as a primary EGFR ligand sheddase, ADAM17 can therefore regulate desmosome assembly indirectly. However, ADAM17 is also capable of directly cleaving the desmosomal cadherin desmoglein 2 (DSG2) (Bech-Serra ~~et al~~*et al.*, 2006), to produce both a shed ectodomain and an intracellular product (Brennan ~~et al~~*et al.*, 2012). Upregulation of ADAM17-dependent DSG2 shedding has found to be the mechanism by which EGFR signalling promotes desmosome disassembly (Klessner ~~et al~~*et al.*, 2009). Any modulation of ADAM17 activity can therefore be expected to affect desmosome structure and stability.

1.3 Gene discovery in inherited skin diseases

1.3.1 Genetic techniques in inherited skin disease

Numerous strategies are used in the investigation of the genetic causes of disease, several of which have been key to the identification of disease-associated gene variants associated to the diseases described in forthcoming results chapters.

Until relatively recently, the most commonly used method of identifying regions of the genome associated with inherited monogenic disease relied upon linkage analysis. This process involves the genotyping of DNA polymorphisms, such as single nucleotide polymorphisms (SNPs) and repetitive elements such as microsatellites, and comparing the presence of these polymorphisms in the genomes of disease-affected and unaffected individuals in a family, to identify genomic regions that segregate with the disease (Altshuler ~~et al~~*et al.*, 2008).

Modern SNP array techniques can map the presence of millions of SNPs in a single human genome – for example, the methodology described in section 5.2.2 involves the use of a SNP array mapping 2.44 million SNP loci – allowing for the very close definition of a disease linked region, which can then be investigated in detail to identify disease-associated variants or mutations. This technique was used successfully to identify the mutations described in

chapter 5, and in numerous other disease mapping studies. SNP array and linkage analysis techniques are particularly useful for identifying regions of homozygosity shared between individuals affected by inherited diseases in consanguineous families (or families where consanguinity is predicted to exist). For example, SNP arrays were used to identify the presence of three large stretches of homozygosity (on chromosomes 2, 5, and 21) shared by two individuals affected by the neonatal onset inflammatory skin and bowel disease described in chapter 3 (Blaydon ~~et al~~*et al*., 2011a).

Identifying a region of the genome linked to a particular disease then allows for the identification of the causative genetic mutation within the linked region. For example, in the investigation of a genetic cause for exfoliative ichthyosis, SNP arrays were used to identify a number of genomic regions linked to the disease in a large North African family. When analysed for potential candidate genes, the keratinocyte-expressed *CSTA* (cystatin A) gene could be identified as a likely candidate due to its presence in the linked regions, and known function as an inhibitor of proteases in the epidermis. This allowed for the specific sequencing of that gene, in which the disease associated mutation was then identified (Blaydon ~~et al~~*et al*., 2011b).

In recent years, next generation sequencing techniques have revolutionised genetic diagnosis of skin disease, by allowing particular, targeted portions of the genome to be specifically sequenced with high fidelity. This can be used, for example, to specifically capture and sequence exons (with or without non-coding regions of the genome) within a region specifically linked to disease; such as in the example of the neonatal onset inflammatory skin and bowel disease described above. In this case, a targeted capture array was used to specifically amplify all exons within the three stretches of homozygosity identified by SNP array as being shared between disease-affected individuals, allowing for the sequencing only of those regions already known to be linked to disease (Blaydon ~~et al~~*et al*., 2011a). This resulted in the identification of a causative mutation that segregated with disease. A second practical example of a next generation sequencing technique is in the specific targeting of multiple genes known to be involved in disease pathogenesis, such as in the use of a targeted sequence capture method in the diagnosis of ichthyoses, a large and heterogeneous group of conditions characterised by scaling and/or hyperkeratosis over the majority of the skin. This technique featured the targeted capture and high-throughput sequencing of the exons of 24 genes that had all been previously linked to varying forms of syndromic and non-syndromic ichthyosis, as well as striate palmoplantar keratoderma and peeling skin syndromes, by Scott

~~et al~~*et al* (~~Scott et al.,~~ 2013). The specific targeting of known ichthyosis genes therefore allowed for the genetic diagnosis of specific forms of ichthyosis in affected individuals.

Formatted: Font: Not Italic

Next generation sequencing can also be used at a genome-wide level, to specifically capture every exon in the genome to the exclusion of all non-coding genomic regions. This technique is known as whole exome sequencing, and represents an efficient strategy for the detection of causal variants in rare inherited diseases. Only around 1% of the total human genome is made up of protein coding regions (split across approximately 180,000 exons), but this 1% harbours 85% of the mutations associated to inherited disease (Choi ~~et al~~*et al*., 2009); as a result, exome sequencing allows for the efficient detection of rare variants in an individual's genome, without the time, expense and resources required to sequence the entirety of that genome. Through bioinformatic analysis of exome data it is possible to identify rare and non-synonymous coding variants in an individual exome, and to use these as the basis for further investigation into the genetic causes of Mendelian disease. In concert with SNP array analysis, this technique was used successfully to identify causative mutations in individuals affected by cryptogenic multifocal ulcerative stenosing enteritis, as described in chapter 5.

By the nature of capturing only protein-coding portions of the genome, exome sequencing can however suffer from the limitation of not being able to detect disease-associated variants present in non-coding DNA. Examples of this include disease-associated mutations in gene promoter sequences, such as *PTEN* promoter mutations in Cowden or Bannayan-Riley-Ruvalcaba syndromes (Zhou ~~et al~~*et al*., 2003), *TERT* promoter mutations in familial melanoma (Horn ~~et al~~*et al*., 2013), and *APOE* promoter polymorphisms associated with Alzheimer's disease risk (Lambert ~~et al~~*et al*., 1998). In these cases, sequencing of the whole genome may represent a more efficient strategy.

1.3.2 Genetic disease of the epidermis

Large numbers of genes are involved in the correct differentiation and functioning of the epidermis, and as such numerous pathogenic mutations have been associated with diseases of the epidermis in humans. Although heterogeneous, many of these diseases share common features, such as palmoplantar keratoderma, a characteristic thickening of the skin on the palms and soles of the feet, which can be diffuse, focal or punctate in nature, and may or may not be accompanied by epidermolysis (Patel ~~et al~~*et al*., 2007). Another major group of skin diseases are the ichthyoses, conditions characterised by scaling and/or hyperkeratosis

over the majority of the skin. The ichthyoses are separated into two major groups: the keratinolytic ichthyoses and the autosomal recessive congenital ichthyoses, the latter of which encompasses lamellar ichthyosis, congenital ichthyosiform erythroderma, and harlequin ichthyosis (the most severe known form) (Oji ~~et al~~*et al*., 2010).

The complex interactions required for the proper development and differentiation of skin mean that different mutations in the same gene can be associated with numerous different skin conditions (such as the multiple diseases arising from different *KRT1* mutations), whilst in some cases the same disease can arise due to mutations in several distinct genes (for example, the multiple mutations causing lamellar ichthyosis and congenital ichthyosiform erythyroderma). Table 1.2 displays a selection of genes implicated in the development of numerous conditions which affect the epidermis.

Gene	Common Protein Name (if different)	OMIM Number	Associated Disease(s)
AAGAB		614888	Punctate PPK
ABCA12		607800	Harlequin ichthyosis Lamellar ichthyosis Congenital ichthyosiform erythroderma
ABHD5		604780	Chanarin-Dorfman syndrome
AP1S1		603531	MEDNIK syndrome
ALOXE3	Arachidonate lipoxygenase 3	607206	Congenital ichthyosiform erythroderma
ALOX12B	Arachidonate 12-lipoxygenase, 12R	603741	Congenital ichthyosiform erythroderma
AQP5	Aquaporin 5	600442	Non-epidermolytic PPK
CDSN	Corneodesmosin	602593	Hypotrichosis Peeling skin syndrome
CSTA	Cystatin A	184600	Autosomal recessive exfoliative ichthyosis
CYP4F22		611495	Lamellar ichthyosis
DSG1	Desmoglein 1	125670	Striate PPK
DSP	Desmoplakin	125647	Striate PPK PPK and woolly hair (with or without ARVC) ARVC alone Lethal acantholytic epidermolysis bullosa
FLG	Filaggrin	135940	Ichthyosis vulgaris Atopic eczema
GJB2	Connexin 26	121011	Bart-Pumphrey syndrome Histrix-like ichthyosis with deafness Keratitis-ichthyosis-deafness syndrome PPK with deafness Deafness alone
GJB3	Connexin 31	603324	Erythrokeratoderma variablis
GJB4	Connexin 30.3	605425	Erythrokeratoderma variablis

JUP	Plakoglobin	173325	PPK with ARVC and woolly hair (Naxos disease)
KRT1	Keratin 1	139350	Annular epidermolytic ichthyosis Epidermolytic ichthyosis Epidermolytic PPK Ichthyosis histrix Non-epidermolytic PPK Striate PPK
KRT2	Keratin 2	600194	Superficial epidermolytic PPK
KRT9	Keratin 9	607606	Epidermolytic PPK
KRT10	Keratin 10	148080	Epidermolytic hyperkeratosis Ichthyosis with confetti Cyclic Ichthyosis with epidermolytic hyperkeratosis
KRT16	Keratin 16	148067	Non-epidermolytic focal PPK

Table 1.2: Genes associated to selected diseases affecting the epidermis. Abbreviations: PPK – palmoplantar keratoderma; MEDNIK – mental retardation, enteropathy, deafness, neuropathy, ichthyosis and keratoderma; ARVC – arrhythmogenic right ventricular cardiomyopathy. More information on diseases associated to each gene can be found using the OMIM number provided.

Gene	Common Protein Name (if different)	OMIM Number	Associated Disease(s)
LOR	Loricrin	152445	Loricrin keratoderma
NIPAL4		609383	Congenital ichthyosiform erythroderma
POMP	Proteasome Maturation Protein	613386	Keratosis linearis-ichthyosis congenita-keratoderma
SERPINB7		603357	Nagashima-type PPK
SLC27A4		604194	Ichthyosis prematurity syndrome
SLURP1		606119	Meleda disease (palmoplantar hyperkeratosis)
SNAP29		604202	CEDNIK Syndrome
SPINK5	Lympho-epithelial Kazal-type-related inhibitor (LEKTI)	605010	Netherton syndrome (ichthyosis with hair shaft defects and skin barrier dysfunction)
STS	Steroid Sulphatase	308100	Recessive X-linked Ichthyosis
TGM1	Transglutaminase 1	190195	Lamellar ichthyosis Congenital ichthyosiform erythroderma
TGM5	Transglutaminase 5	603805	Acral peeling skin syndrome

Table 1.2 (continued): Genes associated to selected diseases affecting the epidermis. Abbreviations: PPK – palmoplantar keratoderma; CEDNIK – cerebral dysgenesis, neuropathy, ichthyosis and keratoderma; More information on diseases associated to each gene can be found using the OMIM number provided.

The genes involved play a wide variety of roles in the epidermis; however, numerous genes identified as causing epidermal disease belong to closely related families, or contribute to similar processes in the epidermis, such as involvement in keratinocyte structure (keratins 1, 2, 9, 10 and 16), stratum corneum formation (filaggrin, loricrin, TGM1 and TGM5),

desquamation (cystatin A, LEKTI), the packaging of lamellar granules (ABCA12), and the structure of intercellular junction complexes, including desmosomes (desmoplakin, desmoglein 1, plakoglobin, corneodesmosin) and gap junctions (connexins 26, 30.3 and 31).

It is notable that many of these inherited skin conditions are syndromic in nature. That is, although skin manifestations may in many cases be a prominent feature, they are accompanied by disease affecting numerous other tissues. Examples of this include mutations in desmosomal components (such as desmoplakin or plakoglobin), which may also cause disorders such as (among others) woolly hair, alopecia, and arrhythmogenic right ventricular cardiomyopathy, in addition to skin manifestations of palmoplantar keratoderma or epidermolysis bullosa (Brooke ~~et al~~*et al*., 2012). Next, mutations in the connexin 26 gene (*GJB2*) may variously cause ichthyosis, keratitis or palmoplantar keratoderma, which may or may not be accompanied by inherited deafness (which can also be the sole symptom of *GJB2* mutation) (Scott ~~et al~~*et al*., 2012). Lastly, a skin phenotype may represent only one of numerous symptoms of wide-ranging developmental disorders, examples of which include MEDNIK (mental retardation, enteropathy, deafness, neuropathy, ichthyosis and keratoderma) (Montpetit ~~et al~~*et al*., 2008) and CEDNIK (cerebral dysgenesis, neuropathy, ichthyosis and keratoderma) (Sprecher ~~et al~~*et al*., 2005) syndromes. As such, skin diseases with manifestations in other tissues are not uncommon, meaning that the investigation of inherited skin diseases cannot always focus exclusively on the skin to the exclusion of other tissues.

1.4 Aims and scope

The aims of this thesis are to investigate the genetic and functional basis of three distinct rare inherited diseases, which variously affect the skin and gut of humans.

Chapter 2

Materials & Methods

2. Materials and Methods

2.1. Introduction

This chapter will describe the materials and methods that were used to generate the data presented in the forthcoming results chapters 3-5. Several of the methods described here were used to generate results that will be shown in all three results chapters, and as such the methods described will not be split into chapter-specific sections, but will rather all be presented together.

2.2. Materials and Methods

2.2.1. SNP Mapping and Targeted Sequence Capture

Genetic investigations into the pair of siblings affected by the early-onset inflammatory skin and bowel disease described in chapter 3, which was later discovered to be associated to homozygous loss-of-function mutations in *ADAM17,* was undertaken by Dr. Diana Blaydon (Centre for Cutaneous research, Blizard Institute, London), Dr. Franz Rüschendorf (Max-Delbrück-centrer for Molecular Medicine, Berlin), Dr. Vincent Plagnol (University College

London Institute of Child Health, London), Prof. David van Heel (Centre for Digestive Diseases, Blizard Institute) and Prof. David Kelsell (Centre for Cutaneous Research, Blizard Institute).

A combination of SNP homozygosity mapping, targeted sequence capture and sequencing were performed to identify disease-associated mutations. SNP homozygosity mapping of the two affected individuals, their parents and an unaffected sibling, was performed using Affymetrix 10K SNP arrays (Affymetrix, Santa Clara, USA); all exons in regions identified as having putative linkage were then included on a Nimblegen sequence capture array (Roche Nimblegen, Madison, USA), and were subsequently sequenced by next generation sequencing on an Illumina GAII sequencer (Illumina Inc. San Diego, USA).

Full details can be found in Blaydon ~~et al~~*et al* (~~Blaydon et al.,~~ 2011a).

Formatted: Font: Not Italic

2.2.2. SNP Homozygosity Mapping and Linkage Analysis in a severe gut disease

Entirely separately from the investigations in chapter 3, the severe inherited gut disease described in chapter 5 was investigated by a combination of SNP homozygosity mapping, linkage analysis and exome sequencing. SNP homozygosity mapping and linkage analysis was performed by Dr. Franz Rüschendorf (Max-Delbrück-centrer for Molecular Medicine, Berlin). Both of the affected siblings were genotyped using an Illumina Omni2.5-Quad v1.0 SNP array (Illumina Inc. San Diego, USA), an array that provides the position of 2.44 million SNPs genome-wide.

Linkage ~~anaylsis~~analysis was performed using the program Merlin (Abecasis ~~et al~~*et al*., 2002), and a reduced marker set of 64,983 SNPs, with the assumption of a degree of consanguinity between the parents of the two affected individuals (a second cousin marriage), a recessive genetic model with complete penetrance, and allele frequencies from a European population.

To narrow down the border of homozygous regions identified between the two siblings, information on all 2.44 million SNPs mapped by the array was used. A self-written Perl script was used to extract regions where both affected individuals were homozygous on the same allele (identical by state).

2.2.3. Whole Exome Sequencing in a severe gut disease

Whole exome sequencing of one of the individuals affected by the severe inherited gut disease was performed in tandem to the homozygosity mapping and linkage analysis described in the preceding section. Whole exome sequencing was carried out using a Sureselect Human all-exon 50Mb kit (Agilent technologies, Santa Clara, USA) and sequenced on an Illumina HiSeq (Illumina Inc. San Diego, USA).

Whole exome data ~~was~~ were analysed by Dr. Vincent Plagnol (University College London Institute of Child Health, London). Sequencing reads were aligned to the hg19 build of the human reference genome using the software novoalign (http://www.novocraft.com). SNP and insertion/deletion calling were performed using samtools V.0.18 and were annotated using the software ANNOVAR (Wang ~~et al~~*et al*., 2010). Candidate variants were filtered on the basis of function (as predicted by ANNOVAR), and 1000 Genomes (http://www.1000genomes.org) and NLHBI exome sequencing project (http://evs.gs.washington.edu/EVS/) frequencies.

2.2.4. DNA and RNA Extraction

DNA or RNA was extracted from keratinocyte cell cultures or blood specimens (collected in heparinised or citrate-lined collection tubes) using Qiagen DNeasy (DNA) or RNeasy (RNA) kits (Qiagen, Crawley, UK), according to manufacturer's instructions.

DNA and RNA concentrations in extracted specimens were measured using a Nanodrop ND-1000 spectrophotometer. Concentrations of both DNA and RNA are measured by absorbance at 260nm, with the purity of nucleic acid present in the sample analysed by measuring the ratio of absorbance at 260 and 280nm, with a 260:280nm ratio above 1.8 considered to represent pure DNA, and a ratio above 2 representing pure RNA.

2.2.5. Reverse Transcription

Conversion of extracted total RNA to cDNA was performed by reverse transcription using Superscript II reverse transcriptase (Invitrogen, California, USA) as the active enzyme. Reverse transcription was performed according to manufacturer's instructions. Briefly, for each sample undergoing reverse transcription a 12µl reaction volume was made up, containing 200ng of total RNA, 0.5µl of random hexamers (200 µM), and 1µl of dNTPs (10 mM) in addition to distilled water (dH_2O). Each reaction volume was incubated at 65°C for 5

minutes then chilled on ice, following which 4µl of 5x first strand buffer, 2 µl of 0.1 M DTT and 1 µl of RNase OUT (a recombinant ribonuclease inhibitor; all Invitrogen, California, USA) were added to each. Finally, 1µl of superscript II reverse transcriptase (200U/µl) was added, following which the samples were incubated at 42°C for 50 minutes, then 70°C for 15 minutes, in a PTC-225 Peltier thermal cycler (MJ Research, Quebec, Canada).

2.2.6. Primer Design

Primers for all standard and quantitative PCR were designed using Primer-BLAST (www.ncbi.nlm.nih.gov/tools/primer-blast), using gene sequences derived from Ensembl (www.emsembl.org; for sequencing whole exons) or Entrez gene (www.ncbi.nlm.nih.gov/gene; for mutation confirmation, and cDNA primers).

For sequencing whole genes, primers were designed to lie in the introns surrounding the exon(s) of interest, such that the entire exon(s) and the splice site immediately flanking it were present in their entirety in the PCR product. For quantitative PCR of cDNA, primers were designed such that at least one of the primers spanned an exon-exon junction within the cDNA target, meaning that the only sequence amplified by the primer pair would be cDNA, rather than any genomic DNA contamination.

For quantitative PCR, Taqman chemistry was used. In brief, this method detects the production of the targeted PCR product via the use of a fluorescently labelled probe, whose sequence is complimentary to a section of the PCR product amplified by the specific primers used. This allows for very specific detection of the specific product targeted, as unintended products of the primers used cannot be bound to by the probe. Furthermore, this allows for the simultaneous detection of two or more PCR products in a single reaction mixture (using a separate, differently-labelled probe for each), such as in this case the simultaneous measurement of a gene of interest and a control. Probes were designed using Primer-BLAST (as above), probes against genes of interest were labelled with the green fluorophore 6-FAM, whilst probes against control genes were labelled with the yellow fluorophore HEX.

Primers and probes were purchased from, and synthesised by Sigma Aldrich (Dorset, UK). The sequence of each primer and probe used is shown in appendix 1.

2.2.7. Polymerase Chain Reaction (PCR)

Standard PCR was carried out using BioTaq DNA Polymerase (Bioline, London, UK) as the primary active enzyme according to well established principles. Briefly, each 20µl reaction

mixture was made up of 2 µl 10X PCR buffer, 1.5mM $MgCl_2$, 200µM of each deoxyribonucelotide (dNTPs), 1µM of each primer, 1U Taq polymerase, 1-5ng of sample DNA, and dH_2O. PCR reactions consisted of 10 minutes at 95°C, followed by 35 cycles of 30 seconds at 95°C, 30 seconds at 60°C and 1 minute at 72°C, and a final 10 minutes at 72°C. PCR was performed using a PTC-225 Peltier thermal cycler ~~(MJ Research, Quebec, Canada)~~.

Formatted: Subscript

Primer products were visualised following PCR by first separating by electrophoresis in 1.6% agarose gels, then UV transillumination.

2.2.8. Sanger Sequencing

Di-deoxy Sanger sequencing of PCR products was performed privately by Source Bioscience (Nottingham, UK), using PCR products and primers designed as described in the preceding sections.

2.2.9. Sequence Analysis

Sequence traces were viewed and analysed using Chromas Lite 2.1 software (Technelysium, South Brisbane, Australia; www. technelysium.com.au). Control sequences and sequences of interest were aligned using the Multalin multiple alignment tool (multalin.toulouse.inra.fr/multalin).

For protein sequences and analysis of conservation, details of protein sequences for non-human species were also obtained from the NCBI Protein database (http://www.ncbi.nlm.nih.gov/protein); these were aligned and compared using the ClustalW2 multiple sequence alignment tool (www.ebi.ac.uk/tools/msa/clustalw2) and visualised using the Jalview multiple alignment editor (www.jalview.org).

2.2.10. Quantitative PCR (qPCR)

Quantitative real-time PCR was performed using a Rotorgene Q thermocycler (Qiagen, Crawley, UK), according to established principles. Briefly, each 20µl reaction mixture consisted of 2x Rotorgene multiplex PCR buffer (Qiagen, Crawley, UK), 1µM of forward and reverse primer for both the gene of interest and a control, 500nM of labelled probe for both the gene of interest and a control, 1ng cDNA, and dH_2O.

qPCR reactions consisted of 10 minutes at 95°C, followed by 46 cycles of 95°C for 15 seconds, and 60°C for 50 seconds. During each 60°C step, fluorescence acquisition was performed in the green and yellow channels to detect fluorescence resulting from the binding of 6-FAM- and HEX-labelled probes respectively. Data ~~was~~ were collected and analysed by Rotorgene software.

Expression of the gene of interest was calculated by the ΔCt method, in which expression of a gene of interest relative to a control is equal to $2^{\Delta Ct}$, where ΔCt is the difference between the cycle number at which the fluorescence of each probe rises above the level of background fluorescence (Livak and Schmittgen, 2001). Statistical analysis was performed using Student's unpaired t-test.

2.2.11. Keratinocyte Cell Culture and Stimulation Assays

Culture of K17, Neb1, TYLK1 and TYLK2 keratinocyte cell lines (to be described in more detail in chapter 4) was performed using Dulbecco's Modified Eagle's Medium (DMEM; Sigma Aldri~~t~~ch, Dorset, UK) supplemented with 2mM L-glutamine, 10% Foetal Bovine Serum (FBS; percentage by volume) 5,000U/ml Penicillin, 5,000µg/ml Streptomycin, and a keratinocyte-specific supplement containing Transferrin (at a final concentration of 5µg/ml in medium), hydrocortisone (0.4µg/ml), cholera toxin (10^{-10}M), insulin (5µg/ml), and lyothyronine ($2x10^{-11}$M). In addition, EGF was optionally added to the medium at a final concentration of 10ng/ml; EGF-containing medium was referred to as 'RM+', whilst EGF-free medium was referred to as 'RM-'. Cells were cultured at 37°C and 5% CO_2, and were passaged via the use of trypsin upon reaching 80-90% confluence.

For keratinocyte stimulation assays, normal keratinocyte growth medium was supplemented variously with 100ng/ml phorbol myristate acetate (PMA; Sigma-Aldri~~t~~ch, Dorset, UK), 1-1000ng/ml bacterial lipopolysaccharide (LPS; InvivoGen, San Diego, USA), 1µM GW280264X (an ADAM17 inhibitor; manufacturer), 2000pg/ml recombinant amphiregulin (R&D Systems, Minneapolis, USA), or dimethyl sulphoxide (DMSO; Sigma-Aldri~~t~~ch, Dorset, UK).

For cell culture secretion assays, two slightly different protocols were used, depending on whether or not siRNA knockdown of particular gene expression was performed. When siRNA was employed, cells were seeded at an initial concentration of $1.5x10^5$ cells per well of a 12-well cell culture plate in standard RM+ medium; after 24 hours, siRNA was used to knockdown gene expression as described in section 2.13. siRNA-containing transfection medium was removed from the cells 24 hours after that, and (after thorough washing)

replaced with the medium in which protein concentrations were to be measured. In the case of stimulation assays, it was this medium to which the relevant stimulant was added. This medium was left on the cells for a further 24 hours, at which point (i.e. 72 hours after the cells were initially seeded) it was removed for testing by ELISA.

When no siRNA was used, the experiment proceeded similarly, except that the initial concentration of cells seeded was $3x10^5$ per well of a 12-well plate. The medium to be tested was then added to these cells 24 hours after seeding, and removed for testing a further 24 hours after that (i.e. 48 hours after initial seeding). When the small molecule GW280264X was used to inhibit ADAM17-dependent shedding, GW280264X-containing medium was added to the cells 2 hours before the start of the 24-hour measurement period. After 2 hours this medium was replaced with fresh GW280264X-containing medium, which was then tested by ELISA after 24 hours incubation.

In all cases, each cell line was cultured in triplicate under every condition tested. In chapter 4, data ~~is~~ are often presented as pooled results from 'control' (K17 and Neb1) and 'tylosis' (TYLK1 and TYLK2) keratinocytes. Each of these therefore represents 6 biological replicates.

2.2.12. Three dimensional organotypic keratinocyte cell culture

Three-dimensional organotypic keratinocyte cell culture models were made by Prof. Spiro Getsios, and Dr. Nihal Kaplan (Northwestern University Feinberg School of Medicine, Chicago, USA), using control and TOC keratinocytes according to methods previously described (Getsios ~~et al~~*et al*., 2009, Simpson ~~et al~~*et al*., 2010).

Briefly, J2-3T3 fibroblasts maintained in DMEM containing 10% FBS were trypsinized and resuspended ($2.5x10^5$/ml) in an ice-cold, pH neutralized DMEM-rat tail collagen (4 mg/ml; BD Biosciences, San Jose, CA) solution. The collagen-fibroblast slurry was polymerized in a 12 well plate (2 ml/well) at 37~~-~~^oC for 30 minutes and maintained in J2-3T3 culture medium for 24 hours in a humidified tissue culture incubator at 37~~–~~^oC and 5% CO_2. Control or TOC keratinocyte lines were trypsinised and resuspended in RM+ DMEM. $5x10^5$/ml keratinocytes were seeded onto a collagen-fibroblast plug established in duplicate for each experiment. Keratinocyte-collagen plugs were maintained as submerged cultures for 48 hours to ensure an intact, confluent epidermal sheet of keratinocytes covered the entire surface of the dermal equivalent prior to air exposure. A sterilized metal spatula was used to transfer the keratinocyte-collagen plug to the top of a stainless steel meshed wire grid raised above the surface of a 60 mm petri dish. RM- FAD medium was added to the bottom chamber of the

wire mesh in contact with the base of the collagen plug, thereby exposing the keratinocytes to an air-liquid interface. The culture medium was replaced every two days, and the organotypic cultures were maintained in a humidified tissue culture incubator at 37°C and 5% CO_2 for 12 days. Duplicate cultures were established from each control and TOC keratinocyte cell line, and the raft culture experiment was repeated on three separate occasions.

Following the establishment of three-dimensional cultures, cell culture supernatants were removed for analysis by ELISA, and the cultures themselves were either sectioned (for histological examination, immunohistochemistry, or transglutaminase activity assays) or homogenised and lysed (for western blotting examination). Subsequent assays were then performed as described in the relevant sections of this chapter.

2.2.13. siRNA Knockdown

siRNA knockdown of ADAM17 or iRHOM2 was performed on keratinocytes in culture using OnTarget SMARTPool siRNA specific to ADAM17, iRHOM2, or non-targeting pool (NTP) siRNA (Thermo Fisher Dharmacon, Lafayette, Colorado, USA). In brief, growing cells ~~are~~ were incubated for 24 hours at 37°C and 5% CO_2 with penicillin- and streptomycin-free medium, containing 100nM ADAM17, iRHOM2 or NTP siRNA, alongside the transfection reagent DharmaFECT 1 (Thermo Fisher Dharmacon, as above). Following this, expression of ADAM17 and iRHOM2 was analysed by western blot and qPCR, as described in the relevant sections of this chapter.

2.2.14. Enzyme-linked Immunosorbent Assays (ELISA)

ELISA techniques were used to measure the secretion of TNFα, IL-6, IL-8, amphiregulin, TGFα, HB-EGF, IL-17A, IL-17F, IL-22 and IL-23 in the culture medium in which keratinocytes and PBMCs had been cultured. DuoSet ELISA kits for each of the above were purchased from R&D systems (Minneapolis, USA) and used according to manufacturer's instructions.

In brief, ELISA-specific MaxiSorp 96-well plates (Thermo Fisher Nunc) were first incubated overnight with an assay-specific primary 'capture' antibody diluted to an assay-specific concentration in 1% bovine serum albumin in PBS solution (1% BSA/PBS). Unless otherwise noted, 100µl of all solutions were added to each well of the 96-well plate. The following day, this antibody was washed off by filling each well of the 96-well plate three times with a wash

buffer made up of 0.05% Tween 20 in PBS, and drying (this standard wash was repeated between every step of the ELISA process). Next, non-specific binding was blocked by a 1-hour incubation with 1% BSA/PBS. After washing, the supernatants of interest were added to the plate and incubated for 2 hours. Depending on the assay and the concentration of the substrate expected to be present, supernatants may have been diluted in 1% BSA/PBS before being added to the ELISA plate; for example, supernantants were typically diluted 1 in 10 for amphiregulin ELISAs and 1 in 20 for IL-8 ELISAs, but were undiluted for TGFα and HB-EGF ELISAs. After washing, an assay-specific biotinylated 'detection' antibody diluted in 1% BSA/PBS ~~is~~ was next added to the plate, and incubated for a further 2 hours. The plate was then washed again, after which a solution of horseradish peroxidase (HRP)-streptavidin, diluted 1/200 in 1% BSA/PBS, was added, and incubated in darkness for 20 minutes. The plate was then washed for the final time, and a solution of HRP substrate (R&D Systems, Minneapolis, USA) was added, which produces a colour change proportionate to the HRP activity of each well, and therefore proportionate to the concentration of the ELISA target in the supernatant sample tested in each well. After 20 minutes incubation in darkness, the colour change reaction was stopped by the addition of 50µl 2N H_2SO_4 to each well, following which the absorbance readings of every well were read at 450nm.

Aside from the use of different capture and detection antibodies (and the concentrations thereof), ELISAs for all of the tested substrates described above followed the same protocol, with the sole exception of IL-8 ELISAs, in which 1% BSA/PBS was replaced throughout with 0.1% BSA/PBS containing 0.05% Tween 20, and in which the blocking step was performed using 1% BSA/PBS supplemented with 0.05% sodium azide (NaN_3), per manufacturer's instructions.

To calculate the concentration of the ELISA target protein in each well, each ELISA plate included a 1-in-2 dilution series of the relevant protein being tested, at an assay dependent series of concentrations. Each of these dilution series contained 8 dilutions of the relevant protein (including a zero). The absorbance readings of these standards were used to make a standard curve for that ELISA plate, from which the concentrations of the protein in each of the other sample wells can be calculated. Each supernatant sample being tested was assayed in duplicate on each ELISA plate, with the mean of these duplicate results then used to calculate the protein concentration of each sample.

Statistical analysis of ELISA results was performed using 2-way ANOVA and Bonferroni's post-hoc test, to analyse whether or not levels of secreted protein were significantly different

between control and tylosis keratinocytes, and between treated (with, for example, PMA, ADAM17 siRNA or GW280264X) and untreated keratinocytes.

2.2.15. Wound healing (scratch) assays

To assess the wound healing activity of keratinocytes, scratch assays were performed on monolayer keratinocytes under standard cell culture conditions (37°C and 5% CO_2). Keratinocytes were seeded in triplicate at a concentration of $4x10^5$ cells per well of a 12-well cell culture plate, in RM+ medium, and allowed to proliferate for 48 hours before the scratch assay took place. This medium was removed, and replaced (after thorough washing) with RM- medium two hours prior to scratch wounding taking place. If GW280264X was being used to block ADAM17 activity, this inhibitor was included in the RM- medium added at this point.

Each keratinocyte monolayer was then scratched using a 1000µl pipette tip, once horizontally and once vertically, to form a cross pattern. After washing, scratches were visualised using a Nikon Eclipse TE-2000S microscope (Nikon Instruments, Kingston-Upon-Thames, UK) and a picture was immediately taken of the section of the vertical scratch immediately above the centre of the cross (the 0 hour time point) using a Nikon Digital Sight DS-Fi2 Camera (Nikon Instruments, UK). The medium in which the keratinocytes were cultured was changed after 24 and 48 hours, at which points a second and third picture of the same section of each well was taken. The area of the scratch wound shown in each picture was quantified using ImageJ software (US National Institutes of Health, Bethesda, USA; www.imagej.nih.gov/ij). The differences in the size of the scratch wound after 24 and 48 hours were then used to calculate the area over which the keratinocytes had migrated in that time period. An example of this calculation can be seen in figure 2.1. Every condition tested was examined in triplicate for each cell line.

For scratch assays examining the effect of keratinocyte conditioned media, the TYLK- or Control-conditioned mediums were made by pooling equal proportions of RM- medium in which either K17 and Neb1 (Control-conditioned medium) or TYLK1 and TYLK2 (TYLK-conditioned medium) had been growing for 24 hours.

To measure growth factor secretion into the medium following scratch wounding, the medium removed from the keratinocytes after 48 hours (i.e. that representing the second 24 hour period after the scratch wound took place) was collected and analysed by ELISA. To measure amphiregulin secretion over time, each keratinocyte cell line was seeded in

triplicate into wells representing 1, 3, 6, 12, 24 and 48 hours, which were all scratched at the same time, with medium being removed from each at the appropriate time point and analysed by ELISA.

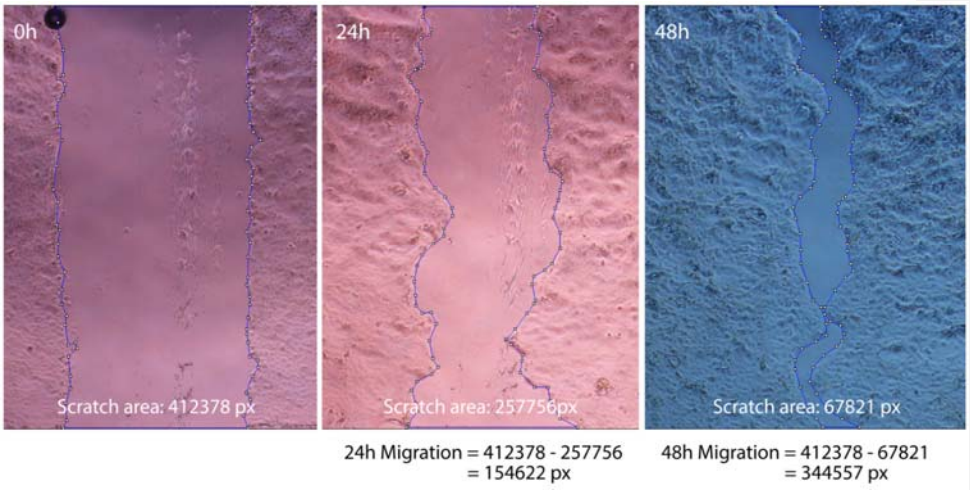

Figure 2.1: Quantification of scratch wounding assays. To quantify keratinocyte migration in scratch wounding assays, a picture was taken of the same part of the scratch wound immediately after wounding (0h) and at 24 hour intervals after wounding (24h and 48h). The area of the scratch wound in each image was then quantified as shown, using ImageJ software (US National Institutes of Health, Bethesda, USA; www.imagej.nih.gov/ij), with migration then calculated as the difference between the scratch wound areas at 0h and 24 or 48h. The pictures in this example show TYLK2 keratinocytes in control medium in the absence of exogenous EGFR ligands, and also appear in figure 4.24. Note that the pictures taken appear to be different colours due to the 0h and 24h ~~picturtes~~pictures being taken with the cells in cell culture medium, whilst the 48h picture is in PBS (the medium having been removed for ELISA analysis).

Statistical analysis of keratinocyte migration was performed using 2-way ANOVA and Bonferroni's post-hoc test, to analyse whether or not migration differed significantly different between control and tylosis keratinocytes, and between treated (with, for example, GW280264X or TYLK-conditioned medium) and untreated keratinocytes.

2.2.16. Peripheral Blood Mononuclear Cell (PBMC) Extraction and Culture

Isolation of PBMCs from whole venous blood samples of subjects for analysis was performed, following manufacturer's instructions, using Ficoll Paque Premium isolation medium (GE Healthcare Life sciences, Buckinghamshire, UK), a density gradient medium that allows for the separation of whole blood into plasma, erythrocytes, granulocytes and PBMCs. In brief, 2ml of isolated, anticoagulant-treated whole blood was mixed 1:1 with PBS; the 4ml of diluted blood was then carefully layered on top of 3ml of Ficoll Paque premium in a centrifuge tube (for larger blood samples, these volumes could also be proportionally scaled up using larger centrifuge tubes), after which the tube was centrifuged for 40 minutes at 400x g, with the centrifuge brake disabled. This process effectively splits each blood sample into the layers described above, meaning that PBMCs (the second-to-top layer) can be extracted and re-suspended in PBS once the uppermost serum layer is removed.

Rather than DMEM (as used for keratinocytes), isolated PBMCs were cultured at 37°C and 5% CO_2 in RPMI medium supplemented with 10% FBS. PBMCs were counted and $2x10^5$ PBMCs from each specimen of interest were seeded in triplicate into 96-well cell culture plates. The PBMCs were then cultured for 24 hours in either non-supplemented medium, or medium supplemented with 100ng/ml PMA (Sigma-Aldritch, Dorset, UK) or 1-1000ng/ml LPS (InvivoGen, San Diego, USA). Alternatively, the PBMCs could be seeded into 96-well cell culture plates which were coated with an anti-CD3 antibody (BD Biosciences, Oxford, UK), and treated with an anti-CD28 antibody (eBioscience, San Diego, USA) at a concentration of 1µg/ml. After 24 hours, the cell culture supernatants were removed and analysed by ELISA.

2.2.17. Immunocytochemistry

Immunofluorescence staining of keratinocyte monolayers was performed on cells which had been seeded and cultured directly on 16mm-diameter circular glass cover slips. Cells were fixed in a solution of 4% paraformaldehyde (PFA) for 30 minutes, following which cell membranes were made permeable by incubation with a solution of 0.5% Triton-X100 in PBS for 10 minutes at room temperature. After thorough washing (at least five times for five minutes) in PBS, the cells were next incubated for 30 minutes in a solution of 10% goat serum in PBS in order to block non-specific antibody binding.

For antibody incubation steps, keratinocytes were incubated with antibody solution via the inversion of the keratinocyte-coated coverslip onto a 50µl droplet of antibody solution. Cells were incubated with a solution of one or two (for co-localisation staining) primary antibodies, diluted to an assay dependent dilution in either 3% BSA or 5% goat serum in PBS, for one hour at room temperature. A list of antibodies used in immunocytochemistry, immunohistochemistry and western blotting, and the concentrations at which each was used, is shown in table 2.1. After primary antibody incubation, cells were thoroughly washed in PBS, then incubated simultaneously with one or more fluorophore-conjugated secondary antibodies, diluted in PBS only, under the same conditions as for primary antibodies. Cells were then once more thoroughly washed, before being mounted in Immuno-Mount mounting medium (Thermo Scientific, Pittsburgh, USA) containing 10µg/ml 4'6-diaminido-2-phenylindole (DAPI), a nuclear stain. Cells were viewed and imaged using a Leica DM5000 automated epifluorescence microscope (Leica, Milton Keynes, UK).

Primary Antibodies				
Antibody (species and type)	**Manufacturer & Product Code**	**Immunocyto-chemistry dilution**	**Immunohisto-chemistry dilution**	**Western blot dilution**
ADAM10 (Rabbit polyclonal)	Millipore AB19026	-	-	1/1000
ADAM17 Total (Rabbit polyclonal)	Abcam Ab2051	1/100	1/150	1/2000
ADAM17 Pro-domain (Rabbit polyclonal)	Abcam Ab39161	-	-	1/2000
Calnexin (Mouse monoclonal)	BD Biosciences 610523	1/100	-	-
Cytosolic Phospholipase A2-α (Rabbit polyclonal)	Abcam Ab58375	-	1/100	1/2000
Desmoglein 2 (Rabbit polyclonal)	Gift from Dr. My Mahoney (Jefferson Inst. Philadelphia, USA) Ab10	1/200	-	1/1000
Filaggrin (Rabbit polyclonal)	Covance PRB-417P	-	1/400	-
GAPDH (Rabbit polyclonal)	Abcam Ab9485	-	-	1/2000
GM130 (Mouse monoclonal)	BD Biosciences 610882	1/100	-	-
IL-17A (Rabbit polyclonal)	Abcam Ab79056	-	1/100	-
Involucrin (Mouse polyclonal)	Abcam SY5	-	1/100	-
iRHOM2 (Rabbit polyclonal)	Sigma-Aldritch HPA018080	-	1/100	1/500-1500
Keratin 2E (Mouse polyclonal)	Abcam Ab19122	-	1/100	
Loricrin	Covance	-	1/400	-

(Rabbit polyclonal)	PRB-145P			
Transglutaminase 1 (Mouse polyclonal)	Biogenesis Ab5500-6006	-	1/100	-
Immunofluorescence Secondary Antibodies				
AlexaFluor-488 Goat anti-rabbit	Invitrogen A11008	1/1000-2000	1/1000	-
AlexaFluor-488 Goat anti-mouse	Invitrogen A11029	1/1000-2000	1/1000	-
Alexa-Fluor-594 Donkey anti-mouse	Invitrogen A21203	1/1000-2000	-	-
Western Blot Secondary Antibodies				
HRP-conjugated Swine anti-rabbit	Dako P0399	-	-	1/2000-5000
HRP-conjugated Rabbit anti-mouse	Dako P0260	-	-	1/500-3000

Table 2.1: Antibodies used in immunofluorescence staining and western blot studies

2.2.18. Immunohistochemistry

Both frozen and paraffin embedded tissues sections were used for immunohistochemistry, which necessitated slightly different staining protocols for each. In every case, the control tissue used for each staining experiment was from the same tissue as the diseased or patient specimens, and had been either frozen or embedded in the same way.

For paraffin embedded tissue samples, sections were de-paraffinised by serial immersion in xylene (twice, for 5 minutes each), 100% ethanol (twice, 3 minutes each), 90% ethanol (3 minutes), 70% ethanol (3 minutes) and finally running water (5 minutes). Antigen retrieval was then performed on each section, which consisted of heating each section three times for 5 minutes in boiling citrate buffer (18ml 0.1M citric acid, 82ml 0.1M trisodium citrate, per 1L, in water). Frozen tissue sections were allowed to defrost and air-dry at room temperature. Following this, a protocol analogous to that used for immunocytochemistry was performed (using antibodies as shown in table 2.1), with the single exception being that antibody solutions were placed directly atop each tissues section, rather than the section being inverted onto them.

2.2.19. Western Blotting

For western blotting, whole cell lysates of keratinocytes were made by direct lysis of cells in the tissue culture plates in which they were cultured. Keratinocytes were lysed directly in a reducing and denaturing sample buffer containing 0.1M tris-HCl, 4% SDS, 20% Glycerol, 1.44M β-mercaptoethanol and 0.001% bromophenol blue. For PBMC lysates, cells were collected as described in section 2.16, suspended in PBS, and spun into a cell pellet, which

was lysed directly by the addition of the lysis buffer described above. The resulting whole cell lysates from keratinocytes or PBMCs were subsequently heated at 95°C for at least 5 minutes; if the lysates were excessively viscous, they were sonicated for 10-30 seconds.

Western blotting of the collected lysates was performed according to standard principles. Briefly, the lysates were separated by SDS-polyacrylamide gel electrophoresis (SDS-PAGE) on 8-12% polyacrylamide gels, alongside a 225-10kDa protein size marker (Rainbow Ladder, GE Healthcare, Buckinghamshire, UK). Proteins were then transferred onto Hybond C nitrocellulose membrane (GE Healthcare, Buckinghamshire, UK) by electrophoretic transfer at either 300mA for 2 hours, or 100mA overnight. SDS-PAGE and electrophoretic transfer were performed using hardware from Bio-Rad (Hercules, California, USA).

Non-specific binding was blocked by incubation of the membrane in either 10% milk or 10% BSA diluted in tris-buffered saline (TBS), supplemented with 1% Tween-20 (TBS-T), for one hour. Membranes were then cut to size, and incubated with primary antibody (at dilutions specified in table 2.1) diluted in 5% milk or 3% BSA in TBS-T, at 4°C overnight. After thorough washing in TBS-T (at least 4 washes for 5 minutes), membranes were then incubated with secondary antibody (as described in table 2.1) diluted in TBS-T for 2 hours at room temperature. After further thorough washing in TBS-T, membranes were treated with Immobilon Western chemiluminescent HRP substrate (Millipore, Bilerica, USA) to visualise proteins, which were shown using Amersham Hyperfilm ECL (GE healthcare, Buckinghamshire, UK) chemiluminescence film, developed with an automated developing machine.

2.2.20. Transglutaminase Activity (Biotinylated-monodansylcadaverine) Assay

For ~~*in situ*~~*in situ* detection of epidermal transglutaminase activity, the biotinylated monodansylcadaverine (biot-MDC) assay was used, as previously described (Raghunath ~~et al~~*et al*., 1998). This assay works on the principle of the covalent incorporation of a biotinylated amine donor (monodansylcadaverine) into the active site of a transglutaminase, which can then be detected by the addition of a fluorphore conjugated to streptavidin. Because Biot-MDC can only be incorporated into transglutaminase 1 when it is in an active conformation, this assay will effectively measure the activity of TGM1, rather than simply measuring its presence. This assay has in the past therefore proven useful for the assessment of patients affected by lamellar ichthyosis (caused by mutations in the *TGM1* gene), who may show normal levels of TGM expression in the skin, even though the associated mutations

Formatted: Font: Not Italic

have significantly reduced or entirely abrogated its enzymatic function (Raghunath ~~et al~~*et al.*, 1998). Furthermore, by controlling the pH at which the assay is performed, it is possible to specifically differentiate TGM1 activity (TGM1 is active at pHs from 7 to 9) from that of the other major epidermal transglutaminase TGM3 (which is active only in a narrow pH window of around 8-8.4).

In brief, frozen epidermal sections from normal controls and disease-affected individuals were preincubated with 1% BSA in 0.1 M Tris-HCl, at pH 7.4 (at which pH TGM1 is selectively active) for 30 min. The sections were then incubated for 2 hours with 100μM biot-MDC (or 10mM EDTA as a negative control) and 5mM $CaCl_2$ in 0.1 M Tris-HCl at pH 7.4. The reaction was halted by the addition of 10mM EDTA solution and washing with PBS, following which the sections were stained using a solution of Streptavidin conjugated to the fluorophore AlexaFluor-488 (Invitrogen, Massachusetts, USA), and mounted in medium containing DAPI. To quantify TGM1 activity in the granular layer, the average fluorescence intensity of the epidermis of negative control skin was calculated using ImageJ image analysis software (as previous), then subtracted from Biot-MDC positive specimen images. The fluorescence intensity in the granular layer of these normalised images was then isolated and measured specifically, using ImageJ.

Statistical analysis was performed using Student's unpaired t-test, to separately measure the significance of differences in the fluorescence intensity of TGM1 activity in the granular layer of control, ADAM17-null and TOC epidermis.

The biotinylated-MDC used in the transglutaminase activity assays described here was a gift from Dr. Claus-Werner Franzke (University of Freiburg, Germany).

2.2.21. Electron microscopy

For electron microscopy studies of desmosomes, TOC and control epidermis specimens were fixed in phosphate buffered 4% glutaraldehyde, post-fixed in 1% osmium tetroxide and dehydrated through a graded ethanol series. They were then cleared in propylene oxide and infiltrated with Araldite. The cells were embedded by inverting 'BEEM' capsules filled with partly cured Araldite over the monolayer and incubating them at 60°C for 48 hours. After cutting away the silicone membrane, semi-thin sections (0.5 mm) for light microscopy were cut and stained with Toluidine Blue. Ultrathin sections (60–80 nm) were cut, mounted on copper grids and stained with uranyl acetate and lead citrate. They were examined in a

J.E.O.L. JEM 1230 electron microscope and images collected with an Olympus 'Morada' 2K × 2K digital camera.

Embedding of skin specimens was performed by Graham McPhail (Department of Cellular Pathology, Barts and The London NHS Trust, London, UK), whilst electron microscopy was performed by Professor Akemi Ishida-Yamamoto (Department of Dermatology, Asahikawa Medical University, Japan).

2.2.22. Cytosolic Phospholipase A2-α activity Assays

The majority of the cPLA$_2$α activity studies described were carried out in collaboration with the research group of Prof. Tim Warner (William Harvey Research Institute, Barts and the London School of Medicine and Dentistry).

Briefly, whole venous blood specimens were collected by venepuncture into tri-sodium citrate-lined vacutainers (BD Diagnostics, UK). Platelet-rich plasma (PRP) was obtained from whole blood by centrifugation at 175x g for 15 minutes at 25°C, followed by decanting of the topmost plasma layer. Platelet-poor plasma (PPP) was obtained by centrifugation of PRP at 15000x g for 2 min. All experiments were completed within 2 hours of blood collection.

For light transmission aggregometry, responses to arachidonic acid (1mM; Sigma, UK), 'Horm' collagen (a suspension of native collagen fibrils; 0.3-3µg/ml; Nycomed, Austria) or ADP (5µM; Chronolog, UK) were measured in a Bio/Data PAP-8E turbidometric aggregometer (37°C, 1200rpm stir speed, 4min) with platelet aggregation determined as % change in absorbance PRP vs. PPP. At the end of the PRP aggregation monitoring, cyclo-oxygenase activity was halted by the addition of 1mmol/L diclofenac (Sigma, UK), the samples centrifuged at 1300g for 10min at 4°C, and the supernatants removed and frozen. Plasma thromboxane B_2 (TXB_2) levels, as a surrogate for thromboxane A_2 production, were subsequently determined using a selective, competitive enzyme immunoassay (Cayman Chemical, USA) according to manufacturer's instructions.

Platelet aggregation was also determined by a standardised optical multichannel absorbance-based method ('Optimul'), as previously described (Chan ~~et al~~*et al*., 2011, Chan and Warner, 2011). In brief, PRP was added to clear half-area 96-well microplates containing lyophilized platelet agonists: arachidonic acid (at a final concentration of 0.03-1mM), ADP (0.005-40µM), Horm collagen (0.01-40µg/ml), epinephrine (0.0004-10µM; Chronolog, UK), U46619 (a thromboxane A_2 receptor agonist; 0.005-40µM; Cayman Chemical, USA) or ristocetin (0.14-4mg/ml; Helena Bioscience, UK) or vehicle. PPP was added to some wells as reference to 100% aggregation. Plates were then vigorously mixed (1200rpm, 37°C; BioShake IQ, Q Instruments, Germany) for 5min and absorbance at 595nm measured using a standard absorbance microplate reader (Sunrise, Tecan, Switzerland). Platelet aggregation was calculated as % change in absorbance PRP vs. PPP.

In all platelet studies, responses of sibling platelets were compared to those prepared from healthy volunteers, with and without *in vitro* treatment with aspirin (30 µM; Sigma, UK). ATP and TXB_2 release data were normalised to the platelet count in PRP.

2.2.23. Figures and Graphs

All graphs presented in this thesis were produced using GraphPad Prism (GraphPad Software, San Diego, USA), and all figures were drawn using Adobe Illustrator CS6. ~~All statistical analyses were likewise performed using GraphPad Prism.~~ The $cPLA_2\alpha$ structure shown in chapter 5 was retrieved from the NCBI Conserved Domains database (accession number: cd07200) and visualised using Cn3D software (Wang ~~et al~~*et al*., 2000).

2.2.24. Statistical Analysis

All statistical analyses were ~~likewise~~ performed using GraphPad Prism (San Diego, USA). For simple pairwise comparisons, student's unpaired t-test was used, whilst for analyses comparing the effect of more than one independent variable (such as the effect of an inhibitor drug on keratinocytes derived from control or TOC-affected individuals) two-way ANOVA followed by Bonferroni's post-hoc test was used. The statistical analysis used to analyse significance is detailed in the legend of each figure, where appropriate.

Formatted: Font: Bold

Formatted: List Paragraph, Indent: Left: 0 cm, Hanging: 1.75 cm, Outline numbered + Level: 3 + Numbering Style: 1, 2, 3, … + Start at: 1 + Alignment: Left + Aligned at: 1.27 cm + Indent at: 2.16 cm

Formatted: Font: 11.5 pt

Chapter 3

ADAM17 Loss-of-function mutations in humans

3. ADAM17 Loss-of-function mutations in humans

3.1. Introduction

This chapter describes investigations into the genetic cause and pathophysiology of a rare, neo-natal onset, recessively-inherited syndrome of skin and bowel inflammation. Through a combination of SNP homozygosity mapping and targeted next-generation sequencing, this syndrome was associated in a single, consanguineous affected family with a homozygous deletion mutation in *ADAM17,* a gene encoding the multi-substrate ectodomain sheddase enzyme ADAM17 (also known as tumour necrosis factor-alpha [TNFα] converting enzyme; TACE), which is described in detail in chapter 1.

Investigations into the pathophysiology of this syndrome were carried out using blood and skin samples derived directly from one affected individual, his unaffected mother, and a number of otherwise healthy normal controls.

3.2. Results – ADAM17 mutations in a UK-based family

3.2.1. A neonatal-onset inflammatory skin and bowel syndrome – phenotype

A neonatal-onset syndrome of inflammatory skin and bowel disease was identified in two of three children (one male, one female) born to consanguineous (first cousin) parents of Lebanese origin. The clinical features involved were the same for both children, and developed very soon after birth, with skin lesions being observed on the second day of life, and diarrhoea within a week. Both siblings developed perioral and perianal erythema with fissuring, and a generalised pustular rash that developed into psoriasiform erythroderma, with flares of erythema and scaling. The skin phenotype can be observed in figure 3.1 (A-B). The skin of both affected siblings was prone to *Staphylococcus aureus* infection, which resulted in repeated instances of blepharitis (inflammation of the eyelids), and otitis externa (external ear infection) as well as skin infection. Similarly, the nails were thickened, and susceptible to frequent instances of paronychia caused by bacterial and fungal (*Candida*) infections (figure 3.1, C).

The hair of the affected individuals was short and broken, whilst the eyebrows and eyelashes were wiry and disorganised (figure 3.1, A). Microscopic examination of the hair revealed the presence of an unusual hair shaft abnormalilty, severe weathering, and a markedly damaged cuticle. In addition to the inflammatory skin phenotype, both siblings were affected by recurrent diarrhoea, which worsened in parallel with increases in the severity of the skin disease, and was predominantly bloody with malabsorbtive characteristics.

The affected girl died aged 12 from fulminant myocarditis associated to parvovirus B19 infection. On subsequent investigation, the affected boy's heart was found to have moderate left ventricular dilatation and borderline-dysfunctional systolic function (an ejection fraction of 55%, where 45% is regarded as dysfunctional) (Blaydon ~~et al~~*et al*., 2011a).

Figure 3.1: The phenotype of a neonatal-onset inflammatory skin and bowel disease. Representative images of the skin, hair and nail phenotype of the affected siblings. Adapted from Blaydon ~~et al~~*et al* (~~Blaydon et al.,~~ 2011a).

Formatted: Font: Not Italic

3.2.2. Genetic investigations

To attempt to identify a genetic cause of this inherited condition, a combination of SNP homozygosity mapping (employed due to the known consanguinity between the parents of the affected individuals), targeted sequence capture and next generation sequencing was employed. These genetic investigations were undertaken by Dr. Diana Blaydon (Centre for Cutaneous research, Blizard Institute, London), Dr. Franz Rüschendorf (Max-Delbrück-centrer for Molecular Medicine, Berlin), Dr. Vincent Plagnol (University College London Institute of Child Health, London), Prof. David van Heel (Centre for Digestive Diseases, Blizard Institute) and Prof. David Kelsell (Centre for Cutaneous Research, Blizard Institute).

SNP homozygosity mapping was performed on five members of the affected family: the two affected individuals; their unaffected brother and both parents, using Affymetrix 10K SNP arrays. Analysis of SNP array data revealed linkage to three large stretches of SNP homozygosity in the two affected siblings (on chromosomes 2, 5, and 21). After ruling out plausible candidate genes by Sanger sequencing, probes for all exons found in these three

regions of the genome were included on a custom capture array, a total of 1468 exons corresponding to 439kb of DNA. All of these exons were captured and sequenced in the affected boy, with the sequence data then analysed for single nucleotide variants and insertion/deletion variation. This analysis revealed the presence of a novel 4-base pair deletion in exon 5 of the *ADAM17* gene (c.603-606delCAGA) on chromosome 2 (Blaydon ~~et al~~*et al*., 2011a).

3.2.3. Confirmation of a mutation in *ADAM17*

To confirm the presence of the c.603-606del mutation in the two affected siblings, and its segregation with disease, Sanger sequencing was performed using primers designed specifically to amplify exon 5 of *ADAM17* (primer sequences are shown in appendix 1). Sequencing was carried out by Dr. Diana Blaydon, on genomic DNA specimens taken from the two affected individuals, their unaffected parents, and their unaffected brother.

Sequence analysis confirmed the presence of the c.603-606delCAGA mutation in the two affected individuals, where it was found in homozygosity (figure 3.2, A). Confirming the segregation of the c.603-606delCAGA mutation with disease, both parents of the affected individuals were found to be heterozygous for the mutation, which was entirely absent in their unaffected brother. This thus resulted in the family pedigree shown in figure 3.2, B.

No rare variants that were predicted to result in loss of function could be found for *ADAM17* in any of the dbSNP, 1000 genomes, or exome variant server databases. This meant that this discovery represented the first association of any mutation in *ADAM17* with disease in humans, though mouse models of *Adam17* mutation have been generated (as described in section 1.2.7).

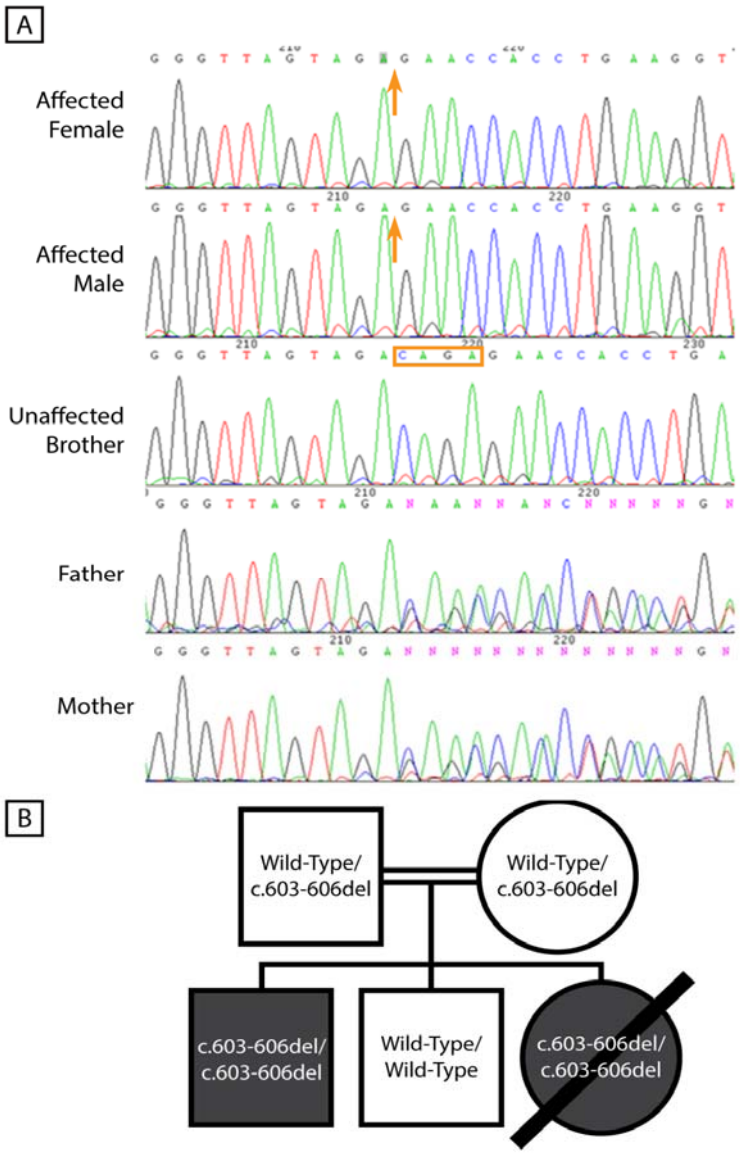

Figure 3.2 Confirmation of *ADAM17* mutations and their segregation with disease. **A:** Sanger sequence traces of a portion of the *ADAM17* exon 5 containing a deletion mutation, in five members of the family affected by the disease described. The orange box illustrates the deleted bases, and orange arrows show the position from which the residues are missing in the affected individuals. **B:** A family pedigree demonstrating the segregation of the c.603-606delCAGA mutation with disease. White shapes illustrate unaffected individuals, grey shapes illustrate affected individuals. Adapted from Blaydon ~~et al~~*et al* (~~Blaydon et al., 2011~~a).

Formatted: Font: Not Italic

3.2.4. Characterisation of the identified *ADAM17* mutation

The c.603-606delCAGA *ADAM17* mutation found homozygously in the two affected siblings results in the deletion of 4 base pairs from exon 5 of the gene. Bioinformatic analysis predicts that this 4 base pair deletion will cause a frameshift in the transcript of *ADAM17,* which would result in a transcript encoding 10 further codons after the deletion, followed by a premature stop codon. The mutation can therefore be annotated as p.D201fsX10. As the deletion mutation results in the introduction of a premature stop codon at a relatively early point in the *ADAM17* transcript (in exon 5 of 19), it would be expected to produce a severely truncated protein. This truncated transcript is predicted to encode a protein containing only the ADAM17 pro-domain (the most N-terminal domain in the complete protein), and therefore lacking the active ADAM17 metalloprotease domain, as well as the disintegrin, cysteine-rich, transmembrane and cytoplasmic domains. As such, this truncated protein would be expected to have no active protease function. The predicted structure of the truncated protein, alongside a full-length, functional ADAM17 protein, is illustrated in figure 3.3.

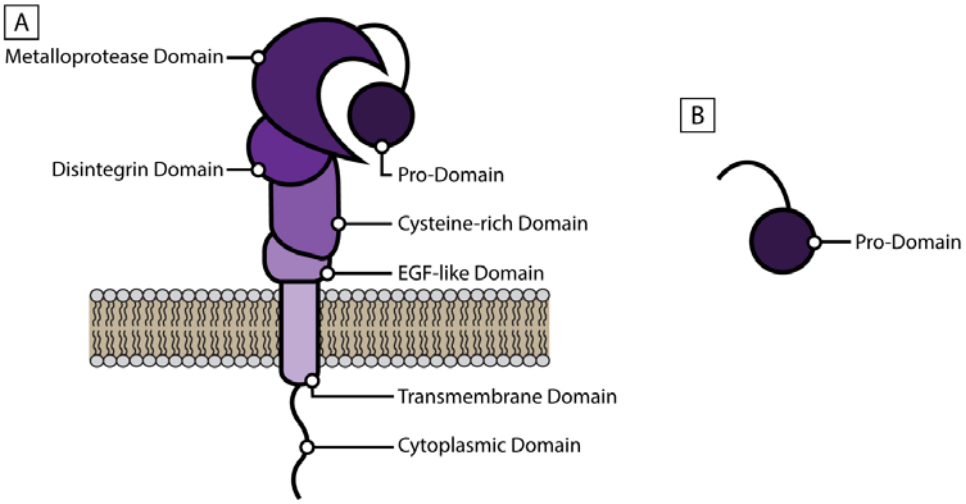

Figure 3.3 Predicted structure of the ADAM17 protein encoded by a normal ADAM17 transcript (**A**), and the transcript affected by the c.603-606delCAGA mutation- (**B**).

3.2.5. Expression of ADAM17 in the skin and blood cells of affected individuals

To assess the effect of the c.603-606delCAGA mutation on expression of ADAM17, western blotting was performed on lysates taken from the cells of the disease-affected male (the female having died aged 12), his unaffected mother (a heterozygous carrier of the c.603-606delCAGA mutation), and a number of normal controls.

ADAM17 expression was first examined in protein lysates derived from peripheral blood mononuclear cells (PMBCs) from the affected individual, his mother, and three otherwise healthy normal control individuals. Western blotting of ADAM17 was performed using an antibody that binds to an epitope in the enzyme's metalloprotease (active site) domain, and which therefore detects ADAM17 in both its pro-protein form, and the mature, active form that results from the removal of its inhibitory pro-domain during maturation. As a result, western blotting with this antibody produces a characteristic double band, representing these two forms of the protein. However, as the c.603-606delCAGA mutation would be predicted to produce a protein lacking its metalloprotease domain, this antibody would not be expected to detect this severely truncated form of the protein, if it were produced. Western blotting of these PBMCs revealed a complete lack of expression of either pro- or mature ADAM17 in the affected male's cells, whilst expression was robust in the PBMCs of each of the other four individuals tested (figure 3.4).

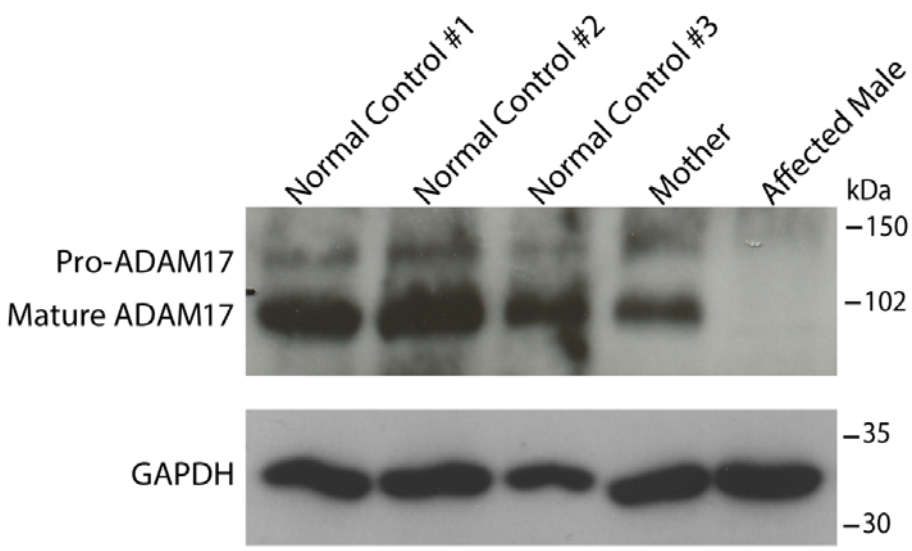

Figure 3.4 Western blotting of ADAM17 in PBMC lysates from the c.603-606delCAGA-affected individual, his unaffected mother and three normal controls. GAPDH was used as a loading control.

Next, expression of ADAM17 was examined by western blotting in primary keratinocytes derived from the affected male, and from a normal control. Once more, no ADAM17 expression could be observed in the affected male, whilst it was clearly visible in normal keratinocytes (figure 3.5, A).

Meanwhile, to examine whether loss of ADAM17 resulted in compensation from other metalloproteases, expression of the closely related ectodomain sheddase ADAM10, which cleaves similar (and in some cases the same – as shown in table 1.1) substrates as ADAM17, was also examined in keratinocytes. In this case, no difference in the expression of ADAM10 was observed between the keratinocytes of the affected male and a healthy control (figure 3.5, B), suggesting that reduced ADAM17 expression does not lead to compensatory upregulation of ADAM10.

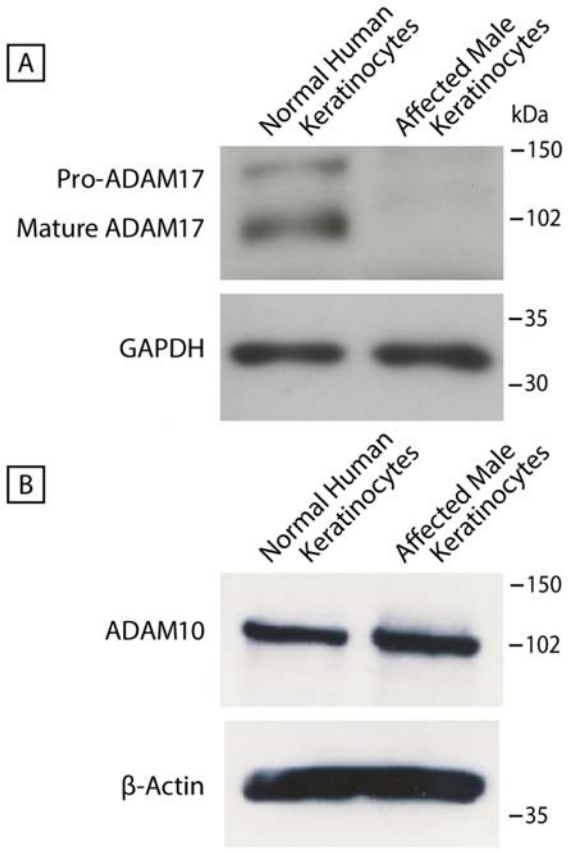

Figure 3.5 Western blotting of ADAMs in primary keratinocytes. **A:** Western blotting of ADAM17 in lysates of primary keratinocytes from the affected male and a normal control. **B:** Western blotting of ADAM10 in lysates of primary keratinocytes from the affected male and a normal control. GAPDH (for ADAM17 western blots) and β-Actin (ADAM10) were used as loading controls.

3.2.6. Expression of ADAM17 in the epidermis of affected individuals and controls

Immunohistochemical staining of ADAM17 was next performed in skin biopsies taken from the affected male and a healthy control. This immunohistochemical staining was performed by Dr. Wei-Li Di (Department of Paediatric Dermatology, University College London Institute of Child Health, London), and revealed ADAM17 staining throughout the epidermis of normal skin, whilst staining was substantially reduced in the skin of the affected male (figure 3.6, top panel).

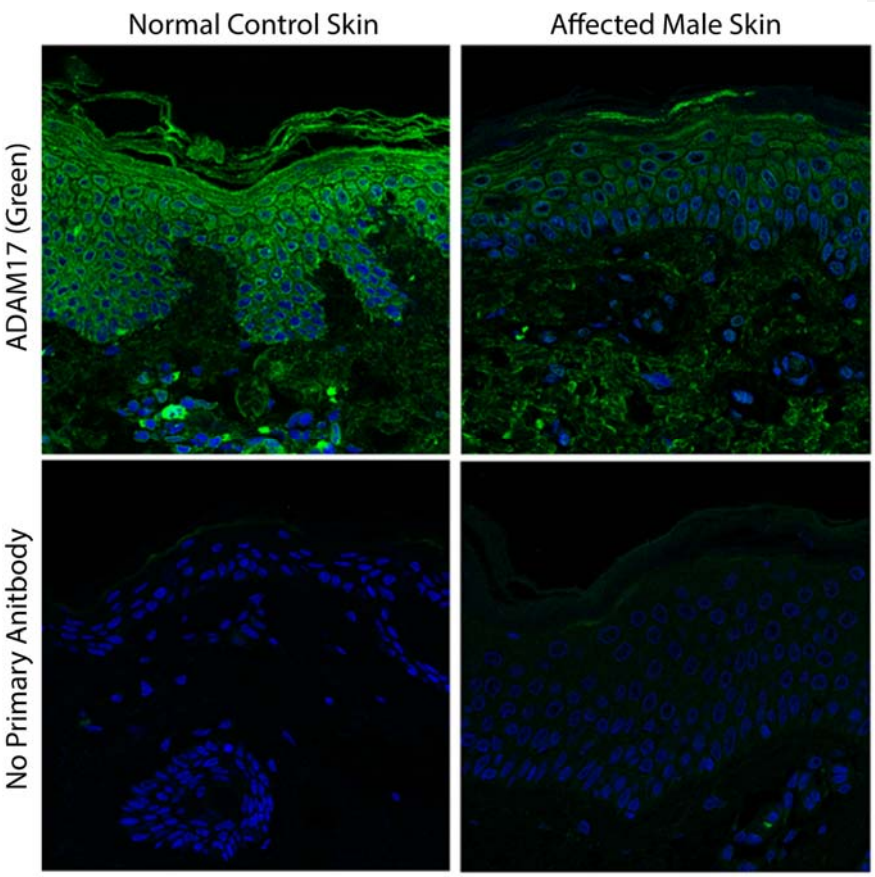

Figure 3.6 Immunohistochemical staining of ADAM17 in paraffin-embedded skin sections of the affected male and a normal control. Staining is shown when performed using an anti-ADAM17 antibody (top row), and without any primary antibody (bottom row). Staining was performed by Dr. Wei-Li Di (University College London Institute of Child Health, London). Figure ~~A~~adapted from Blaydon ~~*et al*~~*et al* (~~Blaydon et al., ~~2011a).

In addition to staining in the epidermis, immunohistochemical staining was also performed in paraffin-embedded sections of the small intestine (the other main tissue affected by this disease) taken from both affected children. Concurring with the pattern seen in the epidermis, substantially reduced ADAM17 staining was also observed in the small intestine.

Taken together, the data from western blotting and immunohistochemical studies suggested that the c.603-606delCAGA mutation in *ADAM17* resulted in the expression of no functional ADAM17 in the affected individuals.

3.2.7. ADAM17 mRNA expression

To confirm that differences in ADAM17 expression were a result of the mutation, rather than a reduction in the transcription of *ADAM17* in the affected individual, mRNA expression of the *ADAM17* transcript was measured by quantitiative PCR (qPCR). This was carried out using primers targeting a region across exons 1 and 2 of the mRNA, whose amplification of the mRNA would therefore be unaffected by the c.603-606delCAGA mutation in exon 5. qPCR was carried out on cDNA ultimately derived from the keratinocytes of the affected individual and a healthy control. This revealed that, although *ADAM17* mRNA expression was somewhat reduced, there was no significant difference between the level of expression in the affected male and a healthy control (figure 3.7).

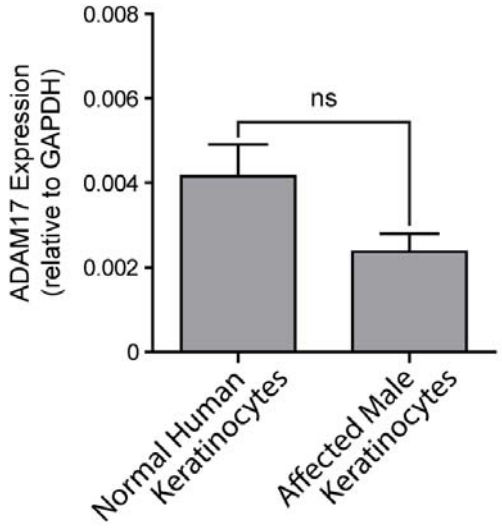

Figure 3.7 mRNA expression of ADAM17 in primary keratinocytes derived from the affected male and a healthy control. Expression was measured by qPCR and is shown relative to the expression of GAPDH. Significance was calculated using Student's unpaired t-test; ~~N~~ns: not significant.

3.2.8. ADAM17 sheddase activity in controls and affected individuals

To examine the functional effects of the reduction in ADAM17 expression in the affected individual, shedding of the ADAM17 substrate tumour necrosis factor-alpha (TNFα) from PBMCs was measured under various conditions. Shedding from PBMCs derived from the affected male, his unaffected mother and three healthy controls was measured following stimulation with either increasing concentrations of bacterial lipopolysaccharide (figure 3.8, A), activating antibodies against the T-lymphocyte co-receptors CD3 and CD28 (figure 3.8, B), or phorbol myristate acetate (PMA) and the calcium ionophore ionomycin (figure 3.8, C). Following stimulation, shedding of TNFα and other pro-inflammatory cytokines over 24 hours was measured by ELISA.

In each of these three cases, shedding of TNFα by the PBMCs of the affected male was very substantially reduced compared to his mother, and all three healthy controls. Meanwhile, the secretion of non-ADAM17-dependent cytokines (interleukin-1β and interferon-γ) by the affected male's PBMCs was unaffected, and was observed at a level comparable to that seen in his mother and healthy controls (figure 3.8).

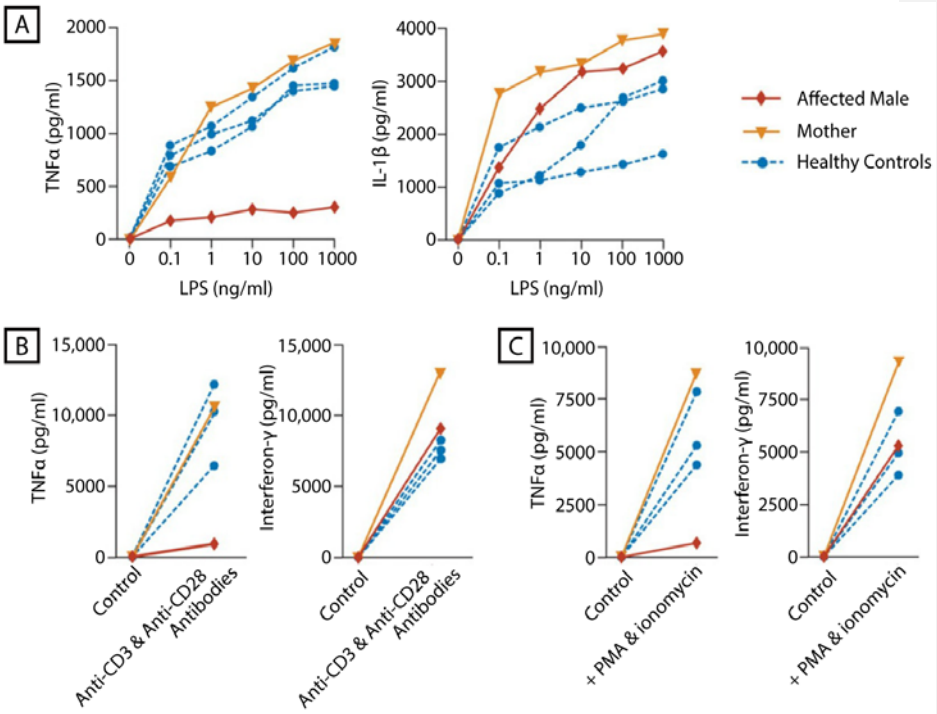

Figure 3.8 Secretion of cytokines (measured by ELISA) from stimulated PBMCs isolated from the affected male, his mother and three healthy control individuals. **A:** Measurement of TNFα and Interleukin-1β secretion from PBMCs following stimulation with increasing levels of bacterial lipopolysaccharide (LPS). **B:** Measurement of TNFα and Interferon-γ secretion from PBMCs following stimulation with anti-CD3 and anti-CD28 antibodies. **C:** Measurement of TNFα and Interferon-γ secretion from PBMCs following stimulation with phorbol myristate acetate (PMA; 100ng/ml) and ionomycin (500ng/ml). ELISA experiments were performed alongside Dr. Diana Blaydin and Dr. Paolo Biancheri (Blizard Institute, London). Figure ~~A~~adapted from Blaydon ~~et al~~*et al* (~~Blaydon et al., ~~2011a).

Formatted: Font: Not Italic

Therefore, not only was ADAM17 protein expression observed to be markedly reduced or absent in the affected male compared to controls, shedding of ADAM17 substrates was also substantially reduced, supporting the hypothesis that the c.603-606delCAGA mutation abolishes or severely abrogates ADAM17 function in the affected individual.

3.2.9. Characterisation of epidermal barrier protein expression

Because the clearest manifestation of the disease associated with the c.603-606delCAGA mutation was seen in the skin, investigations next focussed on the expression of proteins involved in the generation of the skin barrier, several of which can themselves be mutated in epidermal disease (as shown in table 1.2).

To examine this, immunohistochemical staining of filaggrin, involucrin, loricrin and keratin 2E was carried out in the skin of the affected male and a healthy control. As shown in figure 3.9, staining of each of these four barrier proteins was very similar between the affected male and a normal control, demonstrating no obvious up- or downregulation, or any aberrant staining pattern. The epidermis of the affected male was noticeably hyperproliferative and thicker than the normal control, and therefore displayed a larger amount of each of the proteins examined, but the distribution and staining intensity of the tested proteins throughout the epidermal layers was unaltered.

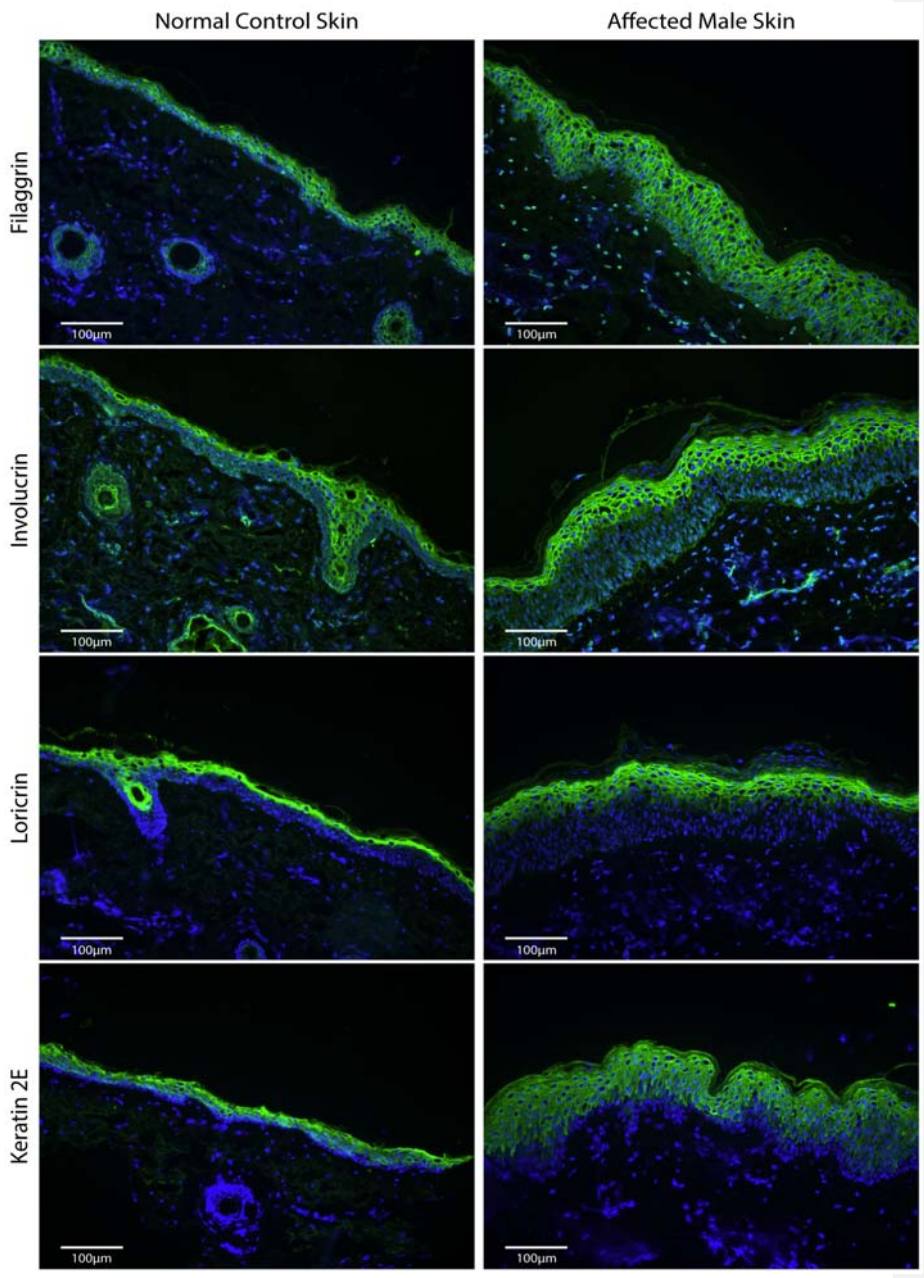

Figure 3.9 Immunohistochemical staining of proteins involved in the epidermal barrier, in frozen skin sections derived from the affected male and a healthy control. Scale bars represent 100µm in all cases.

However, in contrast to the four epidermal barrier-associated proteins shown in figure 3.9, a noticeable difference between healthy control skin and the skin of the affected male was observed when staining for transglutaminase 1 (TGM1). As shown in figure 3.10, the intensity of TGM1 staining in the granular layer of the epidermis was markedly reduced in the skin of the affected male, compared to a normal control.

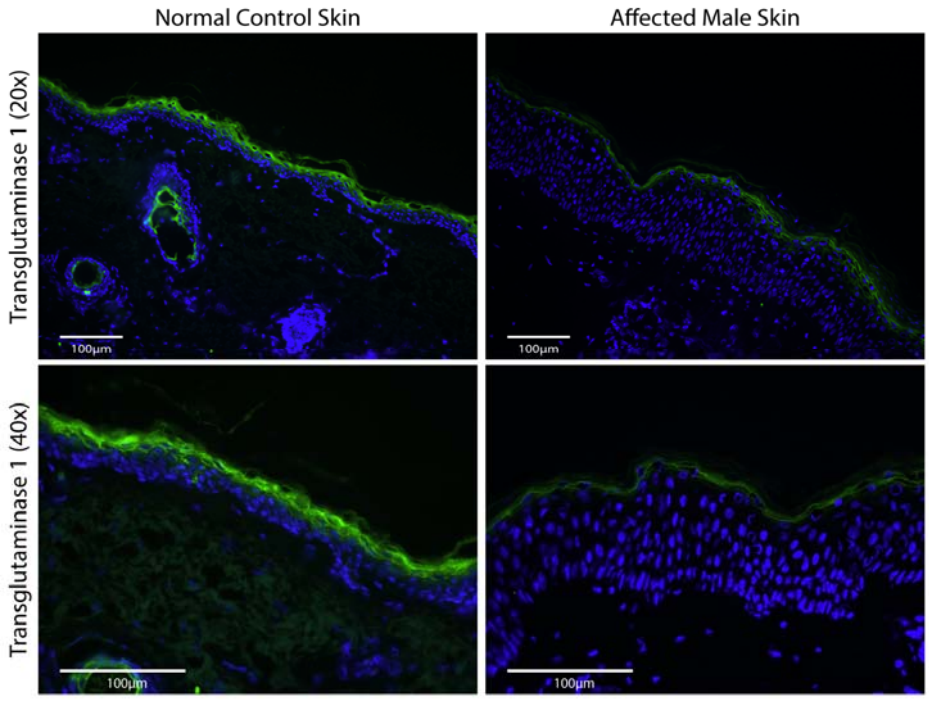

Figure 3.10 Immunohistochemical staining of transglutaminase 1 in frozen skin sections derived from the affected male and a healthy control. Scale bars represent 100µm in all cases.

3.2.10. Transglutaminase 1 activity in control and affected ~~individuals'~~ individual's skin

To investigate the observation of reduced TGM1 staining in the affected individual's upper epidermis, an assay directly measuring ~~*in situ*~~*in situ* TGM1 activity (rather than expression) was performed. This assay uses an amine donor – monodansylcadaverine (MDC) – which is covalently incorporated into the active site of transglutaminase 1 when it is in an active conformation. When MDC is biotinylated (Biot-MDC) this allows for fluorescent detection of MDC bound to active TGM1 via the use of a streptavidin-conjugated fluorophore, and

therefore the quantitative measurement of TGM1 activity ~~*in situ*~~*in situ*. As such, this assay has proven useful in the past in the diagnosis of lamellar ichthyosis (caused by mutations in the *TGM1* gene), sufferers of which may show normal levels of TGM1 expression in the skin, even though the associated mutations have significantly abrogated or entirely abolished its enzymatic function (Raghunath ~~et al~~*et al*., 1998).

In normal control skin, robust TGM1 activity can be observed in the granular layer of the epidermis (figure 3.11), corresponding to the region where TGM1 protein is most highly expressed (as shown in figure 3.10). However, in the skin of the affected male, no visible TGM1 activity could be detected by Biot-MDC incorporation in this upper epidermal layer (figure 3.11).

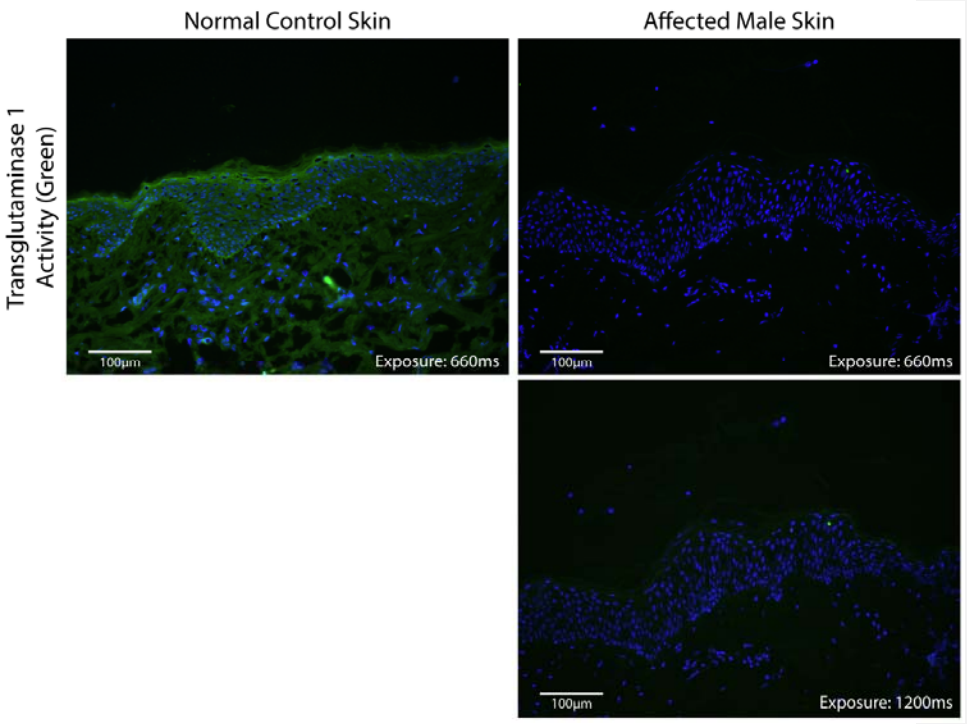

Figure 3.11 Transglutaminase 1 activity in frozen skin sections derived from the affected male and a healthy control, measured using the Biotinylated-MDC assay. Scale bars represent 100µm in all cases. Camera exposure times are given to illustrate that some signal could be seen in the affected male's skin when exposed for a lengthy period.

Taken together, the finding of substantially reduced TGM1 expression and the lack of any detectable ~~in situ~~*in situ* TGM1 activity, suggested that the function of TGM1 was severely impaired in the individual affected by the c.603-606delCAGA *ADAM17* mutation.

Formatted: Font: Not Italic

Subsequent to the finding of reduced TGM1 expression being published, it was shown that a keratinocyte-restricted knockout of *Adam17* in mouse skin led to a significantly reduced level of TGM1 activity in that skin, as a consequence of reduced ADAM17-dependent EGFR ligand shedding (which could be rescued by the topical application of the ADAM17 substrate TGFα). This reduction in TGM1 activity in mouse skin, and the reduction in epidermal barrier activity that results from it, was shown to be primarily responsible for the inflammatory skin phenotype that develops in these mice (Franzke ~~et al~~*et al*., 2012), which bears a close resemblance to the human disease seen in the affected male described here. Furthermore, mutations affecting TGM1 function underlie some types of autosomal recessive congenital ichthyosis, illustrating the importance of TGM1 activity in proper epidermal function in humans. Therefore, the reduced expression and activity of TGM1 observed in the affected male's skin offers a plausible mechanism for at least part of the inflammatory skin phenotype observed.

3.2.11. Expression of desmosome proteins in control and affected individuals

As well as its primary function in ectodomain shedding, ADAM17 is also intimately involved in the regulation of desmosomes, intercellular junction complexes which play a key role in the mechanical stability of particular tissues by providing strong adhesions between individual cells. Desmosomes are found particularly in tissues undergoing high degrees of mechanical stress, such as the skin and the heart, meaning that mutations in various desmosome components are often associated with inherited syndrome diseases affecting the skin and heart (as described in section 1.3.2). A detailed description of desmosome structure and function, and their regulation by ADAM17 and EGFR signalling, can be found in section 1.2.9-10.

The primary desmosome component regulated by ADAM17 is the cadherin desmoglein 2 (DSG2) (Bech-Serra ~~et al~~*et al*., 2006, Brennan ~~et al~~*et al*., 2012). Western blotting was used to assess the expression of desmogleins in the keratinocytes of the affected male and a normal control, by Dr. Rita Cabral (Blizard Institute). The antibody used for this western blotting was co-specific for DSG1 and DSG2; however, the keratinocytes were cultured in medium

containing FBS, which is known to greatly decrease the expression of DSG1 in cultured keratinocytes (Denning ~~et al~~*et al*., 1998), meaning that the vast majority of the expression seen represents DSG2. Western blotting revealed the presence of an increased level of DSG expression in keratinocytes from the affected male, compared to a normal control (figure 3.12).

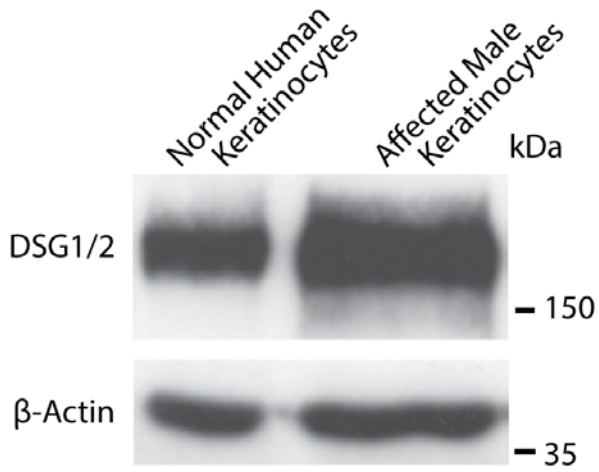

Figure 3.12 Western blotting of desmogleins 1 and 2 in primary keratinocyte lysates derived from the affected male and a healthy control. β~~B~~-actin was used as a loading control. Western blot was carried out by Dr. Rita Cabral (Blizard Institute, London). Figure ~~A~~adapted from Blaydon ~~et al~~*et al* (~~Blaydon et al., 2011a~~).

In addition, staining of DSG2 was shown to be upregulated in the affected male's skin, compared to a healthy control (Blaydon ~~et al~~*et al*., 2011a). Together, these data are indicative of reduced cleavage of DSG2 by ADAM17 in keratinocytes, leading to accumulation of the cadherin at the plasma membrane. Not only does this support the contention that ADAM17 activity is severely downregulated or absent in the individual affected by the c.603-606delCAGA mutation, but it also provides interesting clues to the phenotype observed.

Dysregulation of DSG2 processing in the affected male individual is particularly interesting in the light of the heart phenotype observed in the two affected individuals: a moderate ventricular dilatation in the affected male, as well as the fact that the affected female died from a heart-related condition (infectious myocarditis). Mutations in DSG2 can be

responsible for the inherited heart disease arrhythmogenic right ventricular cardiomyopathy (ARVC), a cause of sudden cardiac death (Brooke ~~et al~~*et al*., 2012). Meanwhile, ADAM17 can also regulate the heart during development, via its shedding of members of the EGFR ligand family, which offers a second potential route to heart dysfunction in cases of ADAM17 loss-of-function. The implications of a loss of ADAM17 activity on heart development and function will be discussed in more detail in chapter 6.

3.2.12. Investigation of the T_h17 pathway in affected individuals

The skin phenotype associated with homozygous c.603-606delCAGA *ADAM17* mutation in these two affected individuals resembled in some ways that of psoriasis, with the skin condition having being described previously as 'psoriasiform ethyroderma' (Blaydon ~~et al~~*et al*., 2011a). As such, the resemblance to psoriasis was investigated at the level of the affected male's PBMCs and skin. Accumulating evidence has suggested that signalling by the T_h17 T-lymphocyte lineage is key to the induction, development and propagation of psoriasis (Coimbra ~~et al~~*et al*., 2012, Elloso ~~et al~~*et al*., 2012).

T_h17 cells are CD4-positive (CD4+) lymphocytes that are distinct from the classically described T_h1 and T_h2 lymphocyte subsets, and are characterised by their ability to produce the cytokines IL-17A, IL-17F and IL-22 (Coimbra ~~et al~~*et al*., 2012). They differentiate from naïve CD4+ lymphocytes under stimulation from IL-1, IL-6 and TGF-β, whilst another cytokine – IL-23 – drives their proliferation (Vanden Eijnden ~~et al~~*et al*., 2005). These cells are recognised as playing a central role in the pathogenesis of a number of autoimmune and inflammatory conditions, including psoriasis. In particular, IL-17A is a critical component in the establishment and perpetuation of inflammation, due to its induction of pro-~~inflammtory~~inflammatory cytokine production (Coimbra ~~et al~~*et al*., 2012). IL-17A mRNA is detectable in psoriatic lesions (Teunissen ~~et al~~*et al*., 1998), while increased blood concentrations of it correlate with psoriasis severity (Arican ~~et al~~*et al*., 2005, Caproni ~~et al~~*et al*., 2009).

To investigate the activity of the T_h17 pathway in the affected male, PBMCs from him, his mother and two otherwise healthy normal controls were isolated, and stimulated with either PMA and ionomycin, or activating anti-CD3 and anti-CD28 antibodies for 24 hours (in the same fashion as was described in section 3.2.8), following which levels of the cytokines IL-17A, IL-17F, IL-22 and IL-23 were measured by ELISA. In order to establish whether any

potential differences observed were dependent on ADAM17 activity, PBMCs were also treated with either the small-molecule ADAM17 inhibitor GW280264X (Dreymueller et al*et al*., 2012, Ludwig et al*et al*., 2005, Rabinowitz et al*et al*., 2001), an anti-ADAM17 blocking antibody, or relevant vehicle controls for the two (DMSO and IgG, respectively), in addition to stimulation by PMA and Ionomycin, or activating anti-CD3 and anti-CD28 antibodies.

When measured by ELISA, secretion of IL-17A and IL-23 by the PBMCs of the affected individual was not substantially different to the levels of secretion seen from either his mother or a pair of healthy controls (figure 3.13). Some variation in IL-17A secretion was observed following stimulation with PMA and ionomycin, but levels did not vary notably between the affected individual and controls. IL-17A secretion following stimulation with activating anti-CD3 and anti-CD28 antibodies, and IL-23 secretion under all the tested conditions, was virtually identical (figure 3.13). Levels of secreted IL-17F and IL-22 were below the limit of detection for the ELISA kits used and are not shown.

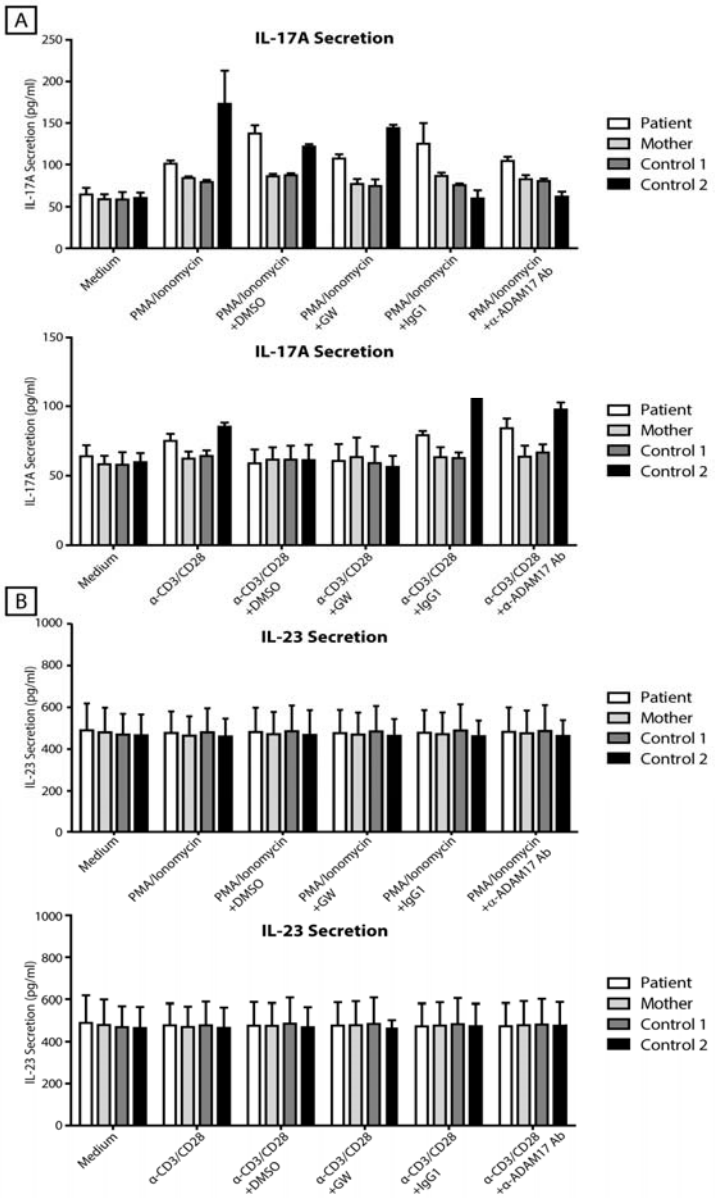

Figure 3.13 Secretion of T_h17 family cytokines, measured by ELISA by stimulated PBMCs. **A:** IL-17A secretion by PBMCs derived from the affected individual, his unaffected mother and two healthy controls, following stimulation with either PMA (100ng/ml) and ionomycin (500ng/ml) or activating anti-CD3 and anti-CD28 antibodies (α-CD3/28). In addition, PBMCs were treated with either DMSO, the ADAM17 inhibitor GW280264X (GW), IgG or an ADAM17-blocking antibody. **B:** IL-23 secretion measured under the same conditions as described for A.

From these results, it can be surmised that there was no particular enrichment of T_h17 lymphocytes in the PBMC fraction of the affected individuals blood, compared to controls, as any significantly greater level of T_h17 cells would produce notably higher levels of IL-17A upon stimulation (particularly with direct stimulation of the T cell co-receptors CD3 and CD28). This corresponds with the IL-23 secretion data, for which significantly increased IL-23 would be expected to be seen if the T_h17 compartment was especially enriched, due to the requirement for IL-23 for T_h17 cell proliferation.

As well as studies in PBMCs, expression of IL-17A was also examined in paraffin-embedded sections of the epidermis of the affected male, as well as a normal control and a specimen of psoriasis skin, by immunohistochemistry. Staining of IL-17A was relatively weak and diffuse throughout the epidermis of all three types of section tested, and no obvious differences could be observed between the affected male's epidermis and either of the other two tested (figure 3.14).

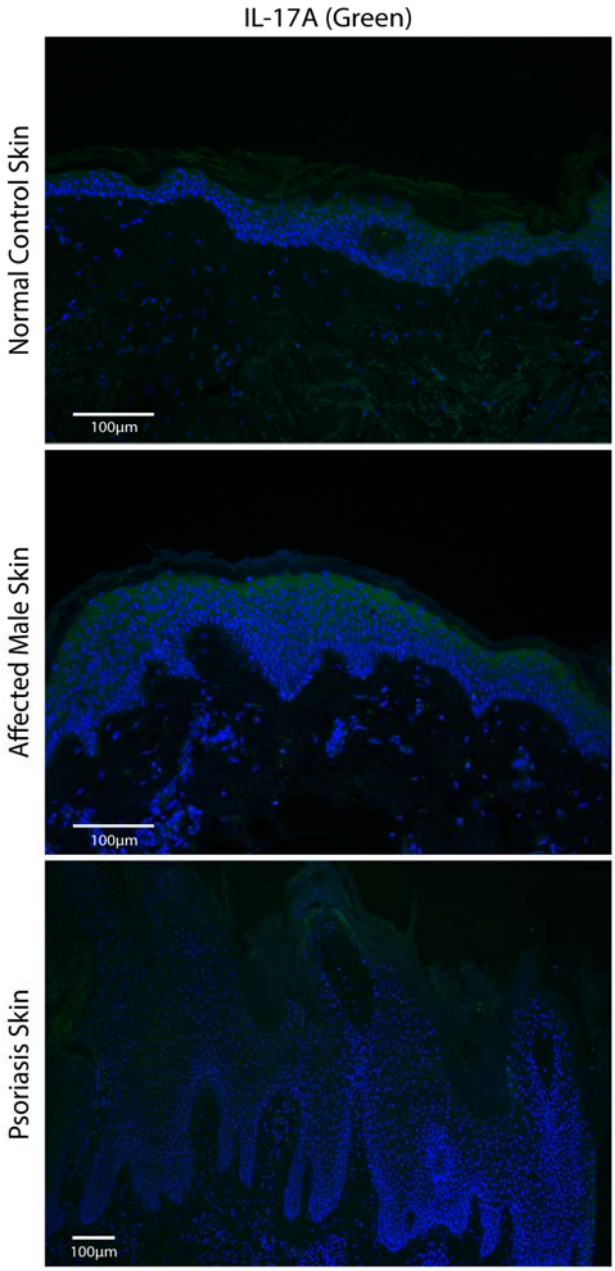

Figure 3.14 Immunohistochemical staining of IL-17A in paraffin-embedded skin sections derived from the affected male, a healthy control, and a psoriasis patient. Scale bars represent 100µm in all cases. Note the reduced magnification of the psoriasis skin picture.

In addition, simple, superficial comparison of skin sections from the affected individual with those taken from psoriatic skin reveal obvious differences in the epidermal structure. Although the epidermis of the affected male is hyperproliferative and somewhat thicker than that of a normal control individual, it lacks the extreme hyperplasia, folding, and elongated, bulbous rete ridges (extensions of the epidermis into the underlying dermis) that characterise and are clearly visible in psoriatic skin.

3.3. Results – genetic investigations in other disease candidates

In addition to the UK-based family of Lebanese origin in which the c.603-606delCAGA *ADAM17* mutation was identified, individuals who displayed skin phenotypes superficially similar to those described in section 3.2.1, belonging to three other, unrelated families, were also investigated for mutations in *ADAM17.* For this *ADAM17* genotyping, PCR primers were designed to separately amplify each of the 19 exons of the gene. Every exon of *ADAM17,* as well as the splice sites immediately before and after each, was then amplified by PCR and sequenced, in the affected individual in each family, as well as in at least one parent of that individual.

In two of these families, no novel or potentially disease-causing mutations were identified in any of the exons of *ADAM17* after thorough sequencing of the whole gene, making it unlikely that their conditions share a similar pathophysiology to the one described throughout this chapter. However, investigations into a family from the Netherlands have suggested that there may be at least one other family in which this disease is present.

3.3.1. Neonatal-onset inflammatory skin and bowel disease in a Netherlands family – phenotype

ADAM17 genotyping was performed in a single female child from the Netherlands, who suffered from an inflammatory skin and bowel disease similar to that seen in the UK-based family described in section 3.2. The affected girl had a low birth weight, and suffered from intractable diarrhea from shortly after birth, requiring full parenteral nutrition. She displayed a skin phenotype that consisted of erythema and very dry skin, which was described as almost resembling ichthyosis, and recurrent infections. She was thought to suffer from alopecia, displayed very little hair growth, developed a cardiomyopathy, and died at an early age.

The obvious similarities of this phenotype with that described in section 3.2.1 made a mutation in *ADAM17* an attractive candidate for a cause of this condition. However, unlike the individuals described in section 3.2, no consanguinity was known to exist between the parents of the affected child.

3.3.2. ADAM17 sequencing in a Netherlands individual

To establish whether or not ADAM17 mutations may contribute to the phenotype of this child, each exon of ADAM17 was sequenced in a genomic DNA sample derived from the affected girl. A single heterozygous nonsense point mutation was identified in exon 16 of *ADAM17,* annotated as c.2113C>T (figure 3.15). Bioinformatic analysis predicts that this mutation would result in the substitution of an arginine codon for a premature stop codon (p.644R>X), and thus to result in the production of a transcript encoding a truncated ADAM17 protein.

This identified mutation was completely novel, and has neither been previously been described, nor is present in any databases of genomic variation examined (including the 1000 genomes, dbSNP and exome variant server databases). Furthermore, this represents the first identification of any nonsense point mutation in *ADAM17*, strongly implying that this mutation may be disease associated. As no consanguinity is known or suspected to exist between the parents of the affected girl, a mechanism of compound heterozygous mutations in *ADAM17* would appear to be the most likely cause of a disease resulting from ADAM17 loss-of-function under these circumstances.

At present, a second ADAM17 mutation (that would be required to confirm a compound heterozygous loss-of-function of ADAM17) has yet to be identified in the affected individual. To confirm the segregation of any mutations with disease, it would be desirable to sequence both the parents of the affected individual as well. To date, only DNA from the mother has been available; sequencing of exon 16 in the mother revealed the presence of the heterozygous mutation in exon 16 (figure 3.15), indicating that any second *ADAM17* mutation would be inherited from the father.

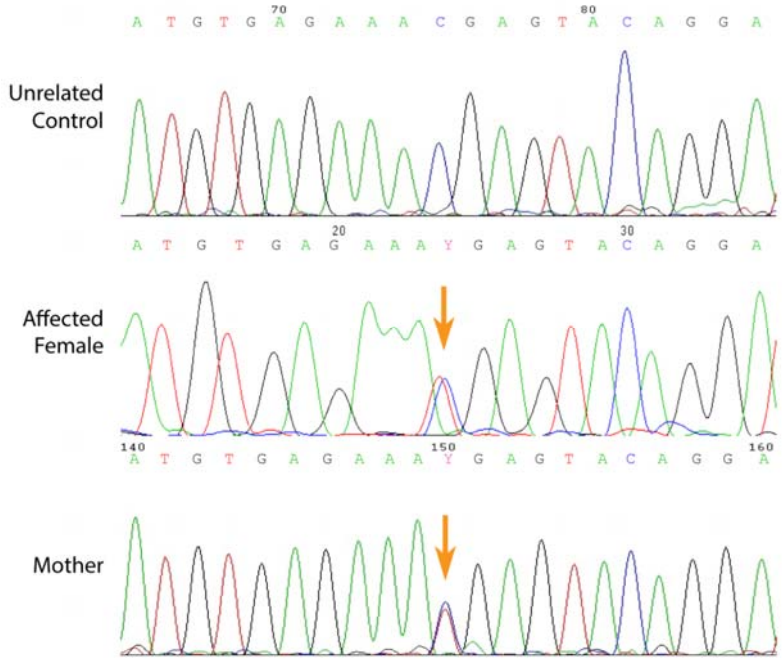

Figure 3.15 Sanger sequencing of a portion of exon 16 of *ADAM17* in a disease-affected Dutch child, her unaffected mother, and a healthy control. Orange arrows illustrate the position of the detected heterozygous mutation.

As only a single *ADAM17* mutation has been identified in this affected individual, genetic investigations into the cause of the disease in the patient described here are ongoing at the time of publication.

3.4. ~~Discussion~~ Summary of chapter

The data presented in this chapter describe investigations into the genetic causes and pathophysiology of an autosomal recessive, neonatal-onset inflammatory skin and bowel disease, which was associated in two affected individuals in the same family with a homozygous deletion mutation in *ADAM17,* a gene encoding the multi-substrate ectodomain sheddase enzyme of the same name.

The presence of this deletion was associated with an absence of ADAM17 expression in keratinocytes and peripheral blood mononuclear cells (PBMCs) of an affected individual, despite a non-significantly changed level of mRNA expression, and resulted in an inability for affected PBMCs to shed the ADAM17 substrate TNFα, and an accumulation of the substrate desmoglein 2 at the plasma membrane of keratinocytes. In investigating the inflammatory skin phenotype, it was observed that expression of the skin barrier proteins filaggrin, involucrin, loricrin and keratin 2E was normal, whilst both the expression level and ~~*in situ*~~*in situ* activity of transglutaminase 1 was severely reduced. Furthermore, despite the superficial resemblance of the skin phenotype to psoriasis, no evidence could be found of activation of the T_h17 signalling pathway in either the blood or the epidermis.

The wide range of substrates shed by cells as a result of ADAM17 activity mean that a deletion of its enzymatic activity could be expected to result in severe consequences in humans. A number of the pathogenic defects observed in individuals affected by this *ADAM17* deletion can readily be associated to the loss of shedding of one or more of its substrates, offering some rationale for the particular set of symptoms observed. The implications of this loss-of-function mutation on the disease seen will be discussed in greater detail in chapter 6.

Lastly, ongoing investigations into other individuals affected by diseases with phenotypes similar to that seen in the individuals described here, suggest the possibility that disease resulting from *ADAM17* mutation may be present in more than the single family described in section 3.2, and may reflect the existence of a novel disease entity.

Chapter 4

The iRHOM2-ADAM17 axis in Tylosis with oesophageal cancer

4. The iRHOM2-ADAM17 Axis in Tylosis with Oesophageal Cancer

4.1. Introduction

This chapter describes investigations into the pathophysiology of the rare inherited skin disease Tylosis with Oesophageal Cancer (TOC). These investigations were undertaken using material derived directly from TOC-affected individuals, including skin sections and peripheral blood cells, as well as a pair of immortalised keratinocyte cell lines derived from TOC patients in the UK.

4.1.1. Tylosis with Oesophageal Cancer

Tylosis with oesophageal cancer (TOC; OMIM: 148500) is a rare, dominantly-inherited genetic disorder comprising an early onset focal, non-epidermolytic palmoplantar keratoderma (PPK; hyperkeratosis of the skin on the palms and soles, particularly prevalent in areas which undergo significant mechanical stress), accompanied by oral leukokeratosis, follicular hyperkeratosis, and a vastly increased risk of developing oesophageal squamous cell carcinoma (OSCC) (Blaydon ~~et al~~*et al.*, 2012, Field ~~et al~~*et al.*, 1997). This phenotype is illustrated in figure 4.1. An affected individual belonging to a large, TOC-affected family in the UK has been calculated as having a 92% probability of dying from oesophageal cancer by the age of 70 (Ellis ~~et al~~*et al.*, 1994). PPK in these individuals is inherited with complete penetrance, with onset at around 7-8 years of age (Kelsell ~~et al~~*et al.*, 1996). Whilst a comparatively rare condition, TOC has been reported to date in at least five extensive family pedigrees worldwide, three reported in the mid-nineties, located in the UK (Ellis ~~et al~~*et al.*, 1994), USA (Stevens ~~et al~~*et al.*, 1996) and Germany (Hennies ~~et al~~*et al.*, 1995), and twice more very recently in Spain (Varela ~~et al~~*et al.*, 2011) and Finland (Saarinen ~~et al~~*et al.*, 2012).

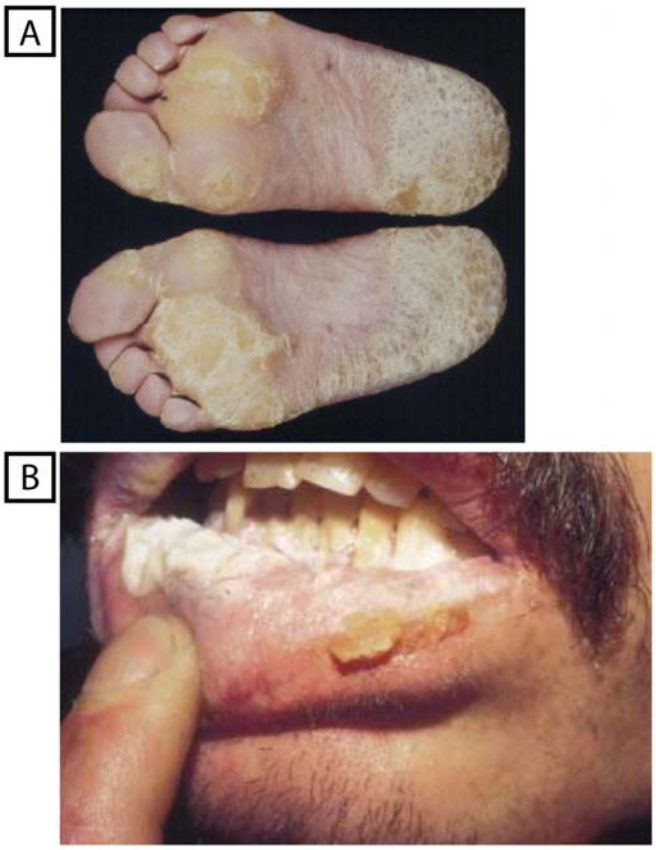

Figure 4.1: Clinical pictures illustrating the phenotype of TOC. A: palmoplantar keratoderma. B: Oral leukokeratosis. Adapted from Blaydon ~~*et al*~~*et al* (~~Blaydon et al.,~~ 2012).

4.1.2. TOC-associated mutations

The TOC locus was mapped to a region of chromosome 17q25 as long ago as 1996 (Risk ~~et al~~*et al*., 1994, Kelsell ~~et al~~*et al*., 1996, Risk ~~et al~~*et al*., 2002), though efforts to identify a causative gene by sequencing were unsuccessful (Langan ~~et al~~*et al*., 2004). However, upon re-assessing the TOC minimal region and revising the status of affected family members, the author's research group was recently able identify TOC as being associated with heterozygous mis-sense mutations (consistent with a dominant pattern of inheritance) in exon six of the *RHBDF2* gene, responsible for encoding the catalytically inactive Rhomboid protease iRHOM2, in the UK, USA and German families (Blaydon ~~et al~~*et al*., 2012). The UK

and US families share the same mutation – c.557T>C, leading to the novel isoleucine to threonine substitution p.Ile186Thr – whilst the mutation affecting the German family is distinct, but located very close by, just three residues away in the full length protein – c.566C>T, which causes the proline to leucine substitution p.Pro189Leu. Subsequent to this study, a Finnish family affected by TOC was examined, and found to harbour a third, distinct TOC-associated mutation in *RHBDF2* (Saarinen ~~et al~~*et al*., 2012). Intriguingly, this mutation was found in the exact same region as those affecting the UK and USA families, lying between the two previously described mutations at residue 188 (p.~~Asp188Ans~~Asp188Asn). Each of the three affected residues is highly conserved both between species and between iRHOM2 and its close family member iRHOM1. The obvious clustering of mutations, as well as this high level of conservation, (Figure 4.2) strongly suggests the mutations alter a site-specific function of ~~iRhom2~~ iRHOM2 to give rise to TOC. Aside from offering strong clues as to the pathogenesis of TOC, this discovery also represented the first linkage of any gene to inherited oesophageal cancer.

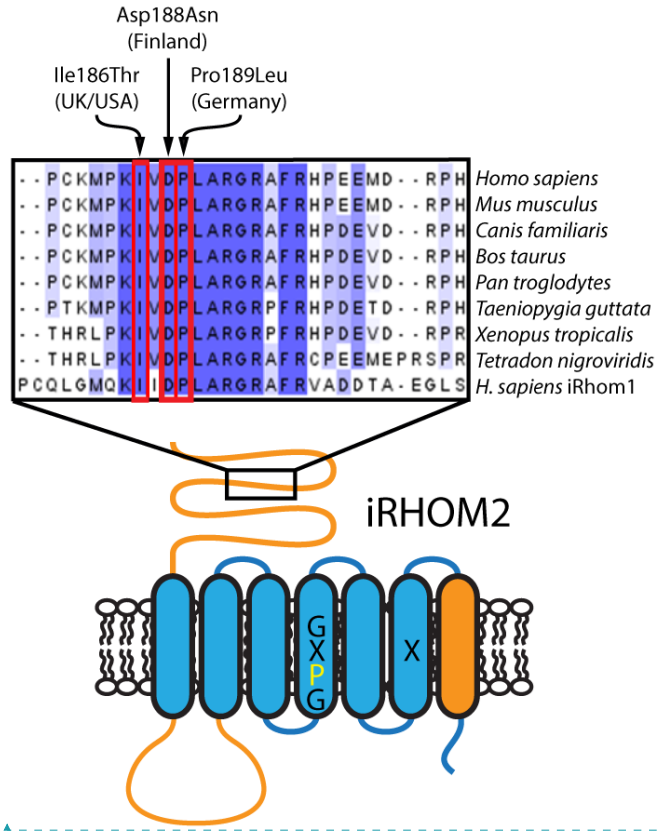

Formatted: Font: 11.5 pt

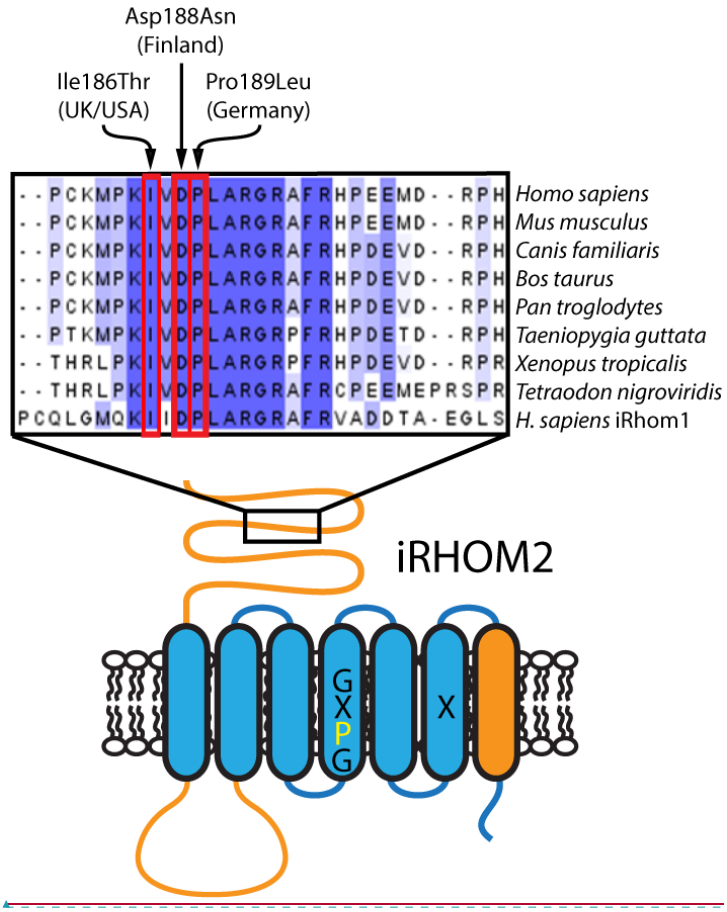

Figure 4.2: TOC-associated iRHOM2 mutations. The residues mutated in TOC, and their high degree of conservation, are illustrated in iRHOM2 protein sequences from a wide variety of animals, and in the closely related human iRHOM1. The location of the TOC-associated mutations in a long N-terminal domain of iRHOM2 is also illustrated. Adapted from Blaydon ~~et al~~*et al* (~~Blaydon et al.,~~ 2012).

Formatted: Font: 11.5 pt

Formatted: Font: Not Italic

4.1.3. The rhomboid protease family – structures

iRHOM2 is a member of the relatively recently discovered family of rhomboid proteases, named after the effect of mutations in *Drosophila*, which affect the first family member to be discovered (now known as Rhomboid-1) and produced an abnormal, rhomboid-shaped head skeleton ~~(Ha et al., 2013)~~ (Mayer and Nusslein-Volhard, 1988). Rhomboids are a family of highly conserved transmembrane serine proteases, found in all eukaryotes and many prokaryotes, which are distinct from most other protease types in that their site of proteolytic activity resides within the membrane; as such, they are referred to as 'intramembrane' proteases. Mammalian rhomboids have been divided into four subgroups, secretase A, secretase B, PARL, and the iRHOMs (Lemberg and Freeman, 2007, Etheridge ~~et al~~*et al*., 2013). The simplest of these in structure are those belonging to the secretase B subgroup (known as 'basic' rhomboids, and represented in humans by the active protease RHBDL4), which contain 6 transmembrane domains. In common with the secretase A and PARL Rhomboids, these contain the highly conserved serine (in transmembrane domain 4) and histidine (in transmembrane domain 6) residues that are required for Rhomboid catalytic activity. These two residues were first identified in *Escherichia coli* and *Haemophilus influenzae* rhomboids (named GlpG in both) as Ser201 and His254, which interact via a strong hydrogen bond (Wang ~~et al~~*et al*., 2006, Lemieux ~~et al~~*et al*., 2007, Ben-Shem ~~et al~~*et al*., 2007). In addition to the six found in secretase B rhomboids, both secretase A and PARL-type rhomboids contain an additional transmembrane domain, with the additional domain in secretase A rhomboids found at the C-terminal end of the protein, and the additional domain in PARL being found at the N-terminal end, relative to the structure of secretase B (figure 4.3). All three of these rhomboid subgroups are catalytically active, with their substrate specificity dependent on the recognition of a 'partially disordered conformation' in their substrates' transmembrane domains, a result of the presence of helix-destabilising residues such as glycine and alanine (Urban and Freeman, 2003).

In contrast to the three other subgroups of rhomboids, the iRHOMs lack the catalytic serine residue in their fourth transmembrane domain, (instead, a proline residue is invariantly found in the position immediately proximal to where the serine would be positioned) (Lemberg and Freeman, 2007) and consequently lack any active protease function. The iRHOMs do however display a clear topological homology with the other rhomboids, containing seven transmembrane domains arranged as in the secretase A subgroup. In

addition, iRHOMs contain a unique long N-terminal cytoplasmic domain and an 'iRHOM homology' loop domain found between the first two transmembrane regions, both of which are very highly conserved and unique to the family. It is in the unique long N-terminal domain that the iRHOM2 mutations associated with TOC are found.

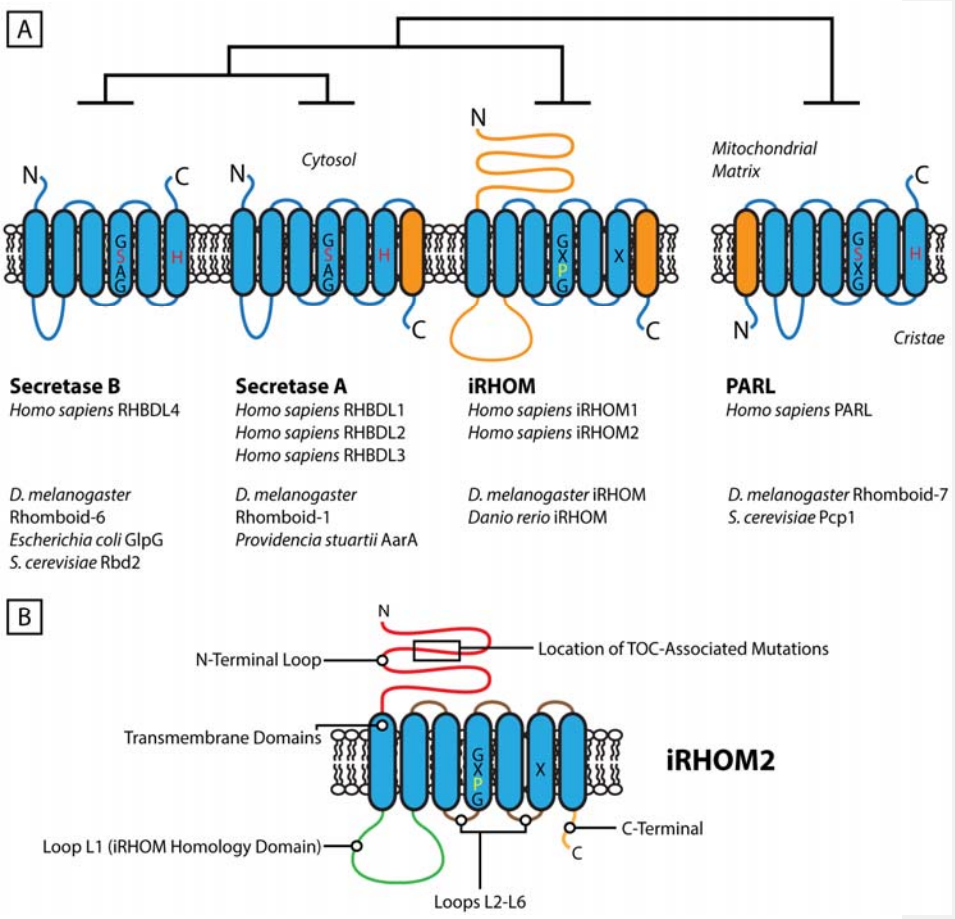

Figure 4.3: Structure of the Rhomboid family proteases. **A:** Topology models illustrating the protein structures and phylogenetic relationships between the major groups of the Rhomboid family. The catalytic dyad of serine and histidine in proteolytically active Rhomboids is illustrated in red, with the invariant proline residue of iRHOMs shown in yellow. Major differences from the most basic Rhomboid structure (as found in the secretase B family) are illustrated in orange. Examples of Rhomboids belonging to each group found in *Homo sapiens* and selected other organisms are listed below, demonstrating the highly conserved nature of the Rhomboid family. Rhomboid structures are ~~A~~adapted from Lemberg & Freeman (~~Lemberg and Freeman,~~ 2007).~~-~~ **B:** Detailed structure model of iRHOM2, illustrating each individual domain, and the location of TOC-associated mutations.

4.1.4. The rhomboid protease family – functions

As mentioned, the catalytically active rhomboids function as intramembrane serine proteases, and function to regulate diverse processes in the wide variety of organisms in which they are expressed. The first rhomboid to be discovered, now known as the *Drosophila* Rhomboid-1 was first studied due to its involvement in developmental control mediated through the EGFR (Urban ~~et al~~*et al*., 2001), which it was found to accomplish via cleavage of the EGFR ligand Spitz (a homologue of TGFα) (Lee ~~et al~~*et al*., 2001). As well as influencing the morphology of the head skeleton in development, Rhomboid-1-dependent regulation of EGFR signalling also regulates sleep patterns in *Drosophila* (Foltenyi ~~et al~~*et al*., 2007), a function which has established rhomboid activity as the key regulator of EGFR signalling in these insects. Similarly, rhomboid activity has been implicated in EGFR signalling in *Caenorhabditis elegans,* in which the EGF-like ligand Lin-3 is proteolytically released by the rhomboid ROM-1 (Dutt ~~et al~~*et al*., 2004).

Intercellular signalling is also the function of a rhomboid in an entirely different organism, the opportunistic bacterial pathogen *Providencia stuartii.* In these bacteria, the rhomboid AarA functions to cleave and thereby activate TatA, a cell wall protein translocase that functions in the transmission of bacterial cell-cell communication proteins, as part of the bacterial communication process known as quorum sensing. Despite the vast evolutionary distance between the two organisms, the rhomboids from *Drosophila* and *P. stuartii* have been shown to share substrate specificity, and are even capable of functionally replacing each other *in vivo* (Gallio ~~et al~~*et al*., 2002, Urban ~~et al~~*et al*., 2002), impressively illustrating the highly conserved nature of rhomboids.

In humans, the active rhomboid RHBDL2 has perhaps been the most closely studied in terms of its functional activity. Illustrating a conservation of function with *Drosophila* and *C. elegans* rhomboids, RHBDL2 has been found to cleave EGF (along with very low levels of betacellulin and neuregulin-1, but no other EGFR ligands) in a manner independent of ADAM10 (Adrain ~~et al~~*et al*., 2011), and therefore appears to play a role in signalling through the EGFR. The expression profile of RHBDL2 is limited to certain tissues, suggesting that RHBDL2 may play tissue-specific roles in EGFR signalling, as opposed to the widely expressed ADAM10 (Adrain

et al*et al*., 2011). As well as EGF, RHBDL2 has a number of other substrates in humans. These include thrombomodulin (Lohi et al*et al*., 2004), a glycoprotein expressed on the surface of keratinocytes and endothelial cells, the soluble form of which is involved keratinocyte proliferation and migration during in wound healing in the skin. Also substrates of RHBDL2 are members of the Ephrin B family, particularly Ephrin B3 (Pascall and Brown, 2004). Ephrins are ligands of the Eph tyrosine kinase receptors, signalling through which is bi-directional (affecting both the sending and receiving cell). Eph-Ephrin signalling is involved in a range of processes, including intercellular communication, adhesion and migration (Pasquale, 2005,; Pasquale, 2008).

In contrast to the other members of the rhomboid family, the single human PARL rhomboid is restricted in its distribution to the mitochondria. Indeed, all eukaryotes express a mitochondrial rhomboid (Freeman, 2008), which form a distinct rhomboid subgroup, as shown in figure 4.3. Rather than a secretory function, PARL is involved in the regulation of the shape of mitochondrial christae, through its cleavage of the dynamin-like mitochondrial protein OPA1. Mouse knockouts of *PARL* resulted in cells that demonstrate excessive release of cytochrome *c* from mitochrondria and a heightened sensitivity to apoptotic stimuli (Cipolat et al*et al*., 2006). The balance of cleaved and membrane bound OPA1 regulates the sealing of junctions between the christae of mitochondria, and therefore cytochrome *c* release and apoptosis, making PARL and important regulator of both mitochondrial function and the apoptotic response.

4.1.5. The functions of iRHOM2

The absence of the highly conserved catalytic serine and histidine residues found in other rhomboids suggest that the iRHOM proteins are not proteolytically active, which for many years made the extremely high level of conservation of these proteins in mammals somewhat puzzling. However, several roles for iRHOM2 have recently become apparent, which may offer interesting insights into the pathology of TOC. Although incapable of proteolysis, iRHOM2 has emerged as a novel regulator of EGFR signalling, which it can accomplish through two distinct processes. In the first of these, iRHOM2 is capable of directly binding to EGFR ligands, and regulating the level their shedding by driving pro-ligands into the ER-associated degradation (ERAD) machinery, a system which functions to degrade proteins using the proteasome. By initiating the degradation of EGFR ligands at the level of

the ER, there are therefore prevented from reaching later stages in the secretory pathway, where they can be proteolytically shed by either ADAMs or RHBDL2 (Zettl et al*et al*., 2011).

4.2. Results – the iRHOM2-ADAM17 axis in tylosis with oesophageal cancer

4.2.1. Immortalised TOC keratinocyte cell lines

To investigate the effect of TOC-associated iRHOM2 mutations in skin, studies were carried out in immortalised keratinocyte cell lines derived from two TOC patients (TYLK1 and TYLK2; a male and a female) carrying the iRHOM2 mutation associated to TOC in the UK family (p.Ile186Thr, the same as is found in the American TOC family) (Blaydon et al*et al*., 2012). These keratinocytes were immortalised by transfection with human papilloma virus (HPV)-16 open reading frames E6 and E7, which when co-expressed are necessary and sufficient to immortalise human keratinocytes (Munger et al*et al*., 1989, Hawley-Nelson et al*et al*., 1989). Though a number of cellular targets have been described for both E6 and E7, the interactions of the two with the tumour suppressors p53 (which is degraded by E6) and pRb (which is bound and degraded by E7) are the key functional activities in keratinocyte immortalisation by these proteins (Buitrago-Perez et al*et al*., 2009).

In each study, TYLK keratinocytes were compared with a pair of normal control keratinocyte cell lines which had been immortalised in the same manner, both of which have previously been described (K17 {[Morley et al*et al*., 1995}] and Neb1 {[Morley et al*et al*., 2003}]).

4.2.2. Dysregulation of EGFR signalling in TOC keratinocytes

Prior to the studies described here, dysregulation of EGFR signalling in TOC keratinocyte cell lines was described by the author's group. Proliferation of TOC keratinocytes was found to be significantly higher than controls, but was insensitive to supplementation with exogenous EGF, whilst control keratinocytes' proliferation increased significantly upon EGF supplementation. Similarly, TOC keratinocytes migrated at a significantly higher rate when cultured in the absence of exogenous EGFR ligands in a simulated wounding ('scratch') assay (Blaydon et al*et al*., 2012). As such, TOC keratinocytes were considered to act in an EGFR ligand-independent fashion.

4.2.3. iRHOM2 in ADAM17 loss-of-function skin

The observed dysregulation of EGFR signalling in TOC keratinocytes meant that the possibility of an interaction between iRHOM2 and ADAM17 – in its role as the principal sheddase of EGFR ligands – warranted investigation. To first examine this potential relationship, the expression of iRHOM2 was investigated by immunohistochemistry in the skin of the ADAM17 loss-of-function individual described in chapter 3, by Sarah Etheridge (Centre for Cutaneous Research, Blizard Institute).

As shown in figure 4.4, iRHOM2 in the epidermis is found largely at the plasma membrane. In ADAM17 loss-of-function skin, iRHOM2 displays a notably reduced level of staining and punctate localisation. These data were indicative of the possibility of an interaction between iRHOM2 and ADAM17 in the epidermis. Strikingly, siRNA knockdown of ADAM17 in keratinocytes also results in a reduction in the expression of iRHOM2 (to be discussed in section 4.2.4).

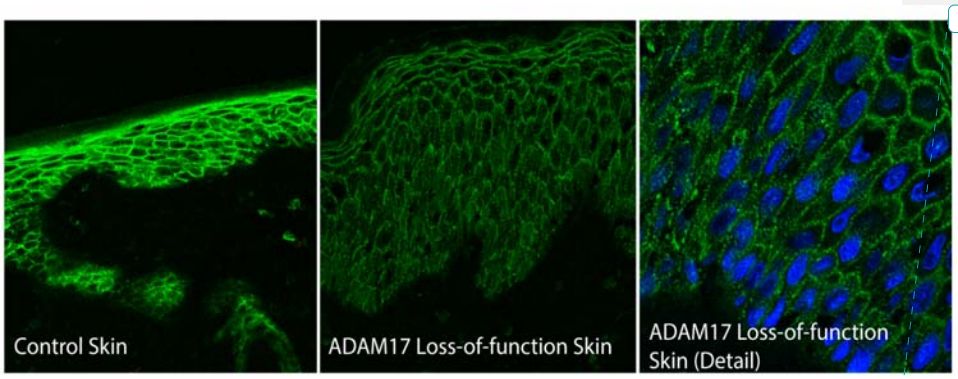

Formatted: Font: 11.5 pt, Bold

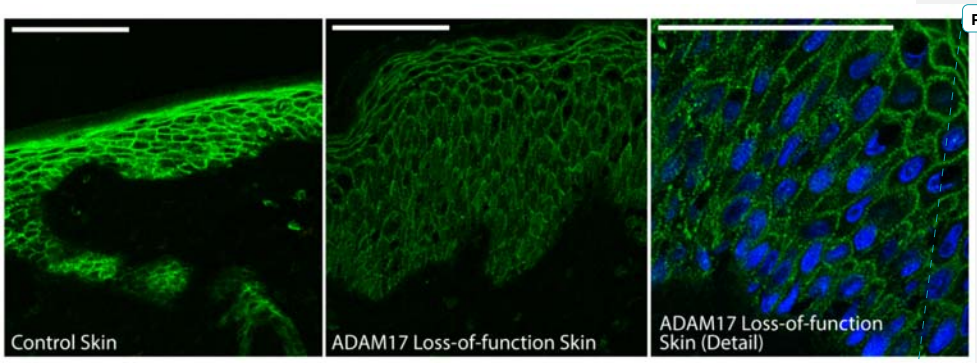

Figure 4.4: iRHOM2 staining (green) in control and ADAM17 loss-of-function epidermis. Scale bars (top left) in all cases represent 100µm. Staining was carried out by Sarah Etheridge (Blizard Institute, London).

4.2.4. ADAM17 expression in TOC and control keratinocytes

To investigate the expression of ADAM17 and its possible relationship with iRHOM2 in keratinocytes, western blotting of both ADAM17 and iRHOM2 was performed in each of the four keratinocyte cell lines investigated, with and without siRNA knockdown of ADAM17 or iRHOM2. Western blotting of ADAM17 was performed using an antibody whose epitope lies in the enzyme's active site domain – which is therefore unaffected by ADAM17 maturation – which as a result detects ADAM17 in both its pro-protein form, and the mature, active form that results from cleavage by pro-protein convertases in the Golgi apparatus. Western blotting of ADAM17 using this antibody therefore results in the presence of characteristic double band (as shown in figure 4.5), representing pro- and mature ADAM17.

Western blotting of ADAM17 in all four keratinocyte cell lines revealed an intriguing expression profile. Most notably, relative expression levels of the mature, active form of ADAM17 were significantly increased in non-targeting pool (NTP)-treated TOC keratinocytes, compared to controls ($p<0.01$; figure 4.5, *symbols).

As would be expected, siRNA knockdown of ADAM17 led to a significant reduction in both pro- and mature ADAM17 in all four cell lines ($p<0.05$ in all cases; figure 4.5, # symbol), but also interestingly caused a corresponding reduction in expression of iRHOM2 in all four cell lines. This observation not only further illustrates the close relationship between the two proteins in keratinocytes, but also tallies with previous observations, such as the reduced level of iRHOM2 staining in the epidermis of the ADAM17 loss-of-function patient (shown in figure 4.4) and a subsequently published study showing a reduction in the overall level of ADAM17 expression in murine iRHOM1 and 2 knockouts (Christova ~~et al~~*et al*., 2013).

Interestingly, siRNA knockdown of iRHOM2 was found to abolish the increased level of mature ADAM17 in TOC keratinocytes, with mature ADAM17 expression significantly reduced in anti-iRHOM2 siRNA-treated TYLK1 and TYLK2 cell lines ($p<0.01$; figure 4.5, § symbols) but not the two control cell lines, suggesting that the increased level of mature ADAM17 in the TYLK cell lines is iRHOM2-dependent.

The western blot shown in figure 4.5 was performed by Sarah Etheridge (Centre for Cutaneous Research, Blizard Institute), whilst the results in the graph below the western blot represent data from three individual experiments, performed by the author and Sarah Etheridge.

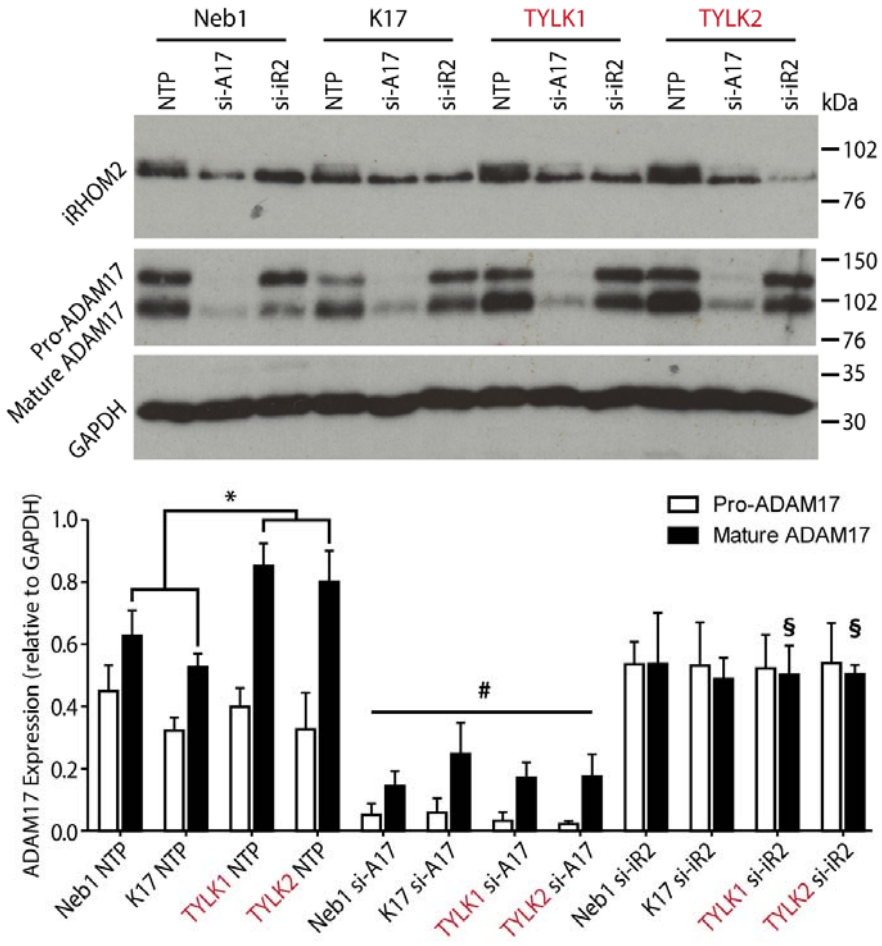

Figure 4.5: ADAM17 and iRHOM2 expression in control and TOC keratinocyte cell lines. Expression of iRHOM2 and ADAM17 is shown in two control (Neb1 and K17) and two TOC (TYLK1 and 2) keratinocyte cell lines in whole cell lysates collected 24 hours after transfection with non-targeting pool (NTP) siRNA, or siRNA against either ADAM17 (si-A17) or iRHOM2 (si-iR2). The western blot shown was performed by Sarah Etheridge (BLIzard Institute, London), whilst ~~T~~the graph shown represents results from three separate experiments carried out by both Sarah Etheridge and the author. Statistical analysis was performed using two-way ANOVA with Bonferroni's post-hoc test; * signifies that expression of mature ADAM17 is individually significantly higher in both TOC cell lines than both control cell lines ($p<0.01$ in all cases); # signifies that expression of both pro- and mature ADAM17 is significantly reduced in all keratinocytes treated with si-A17, compared to those treated with NTP ($p<0.01$ in all cases); § symbols signify that expression of mature ADAM17 is significantly reduced in both TOC cell lines treated with si-iR2 compared to NTP, but not in either of the control cell lines ($p<0.05$ in each case).

Next, an antibody was used that binds to the ADAM17 pro-domain, and therefore detects the presence of the free pro-domain released upon ADAM17 maturation. Blotting with this antibody demonstrated an increase in this free pro-domain in TOC keratinocytes relative to controls, as shown in figure 4.6.

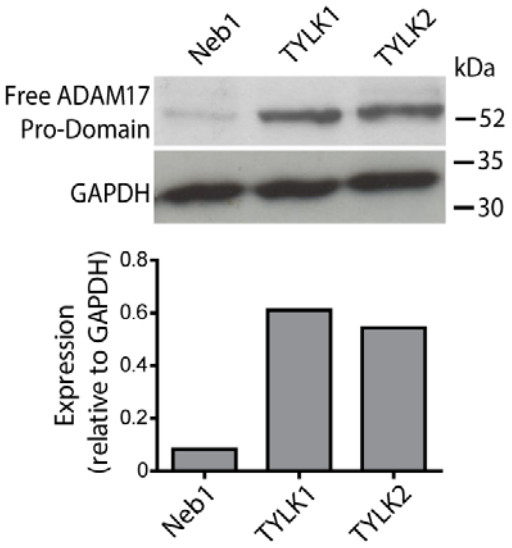

Figure 4.6: Expression of the free ADAM17 pro-domain in control and TOC keratinocyte cell lines, in whole cell lysates.

4.2.5 iRHOM2 and ADAM17 interaction

These data are particularly interesting in light of the findings of a pair of subsequent studies, which illustrated that, in addition to its role in regulating the intracellular degradation of EGFR ligands, iRHOM2 can act as a novel regulator of ADAM17. As previously discussed, in order for Pro-ADAM17 to become activated, removal of its inhibitory pro-domain must occur, a process catalysed by the pro-protein convertase furin. iRHOM2 is capable of regulating this maturation process, as it is required for the transit of Pro-ADAM17 from the ER into the Golgi apparatus (Adrain ~~et al~~*et al*., 2012, McIlwain ~~et al~~*et al*., 2012). Activity of iRHOM2 is therefore absolutely required for ADAM17 activity in some cell types. iRHOM2 can therefore be considered to play a dual role in the ER, both in regulating the availability of

EGFR ligands for shedding (as discussed in section 1.2.5), and in the regulation of ADAM17. This dual role is illustrated in figure 4.7.

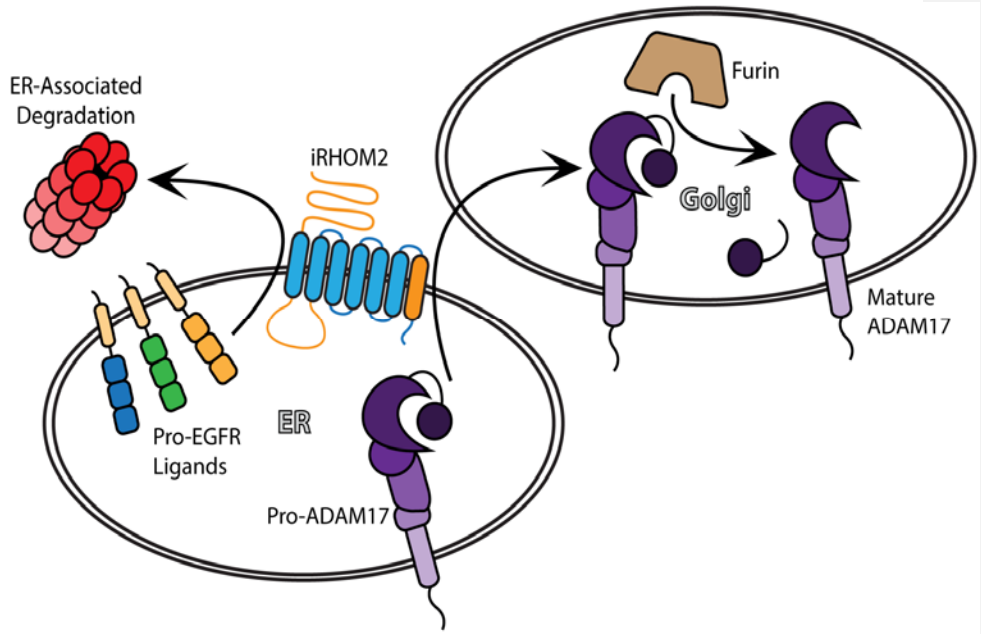

Figure 4.7: The Dual role of iRHOM2**.** An illustration of iRHOM2's two distinct roles in the ER: targeting membrane bound pro-EGFR ligands (multi-coloured) for ER-associated degradation in the proteasome (red); and facilitating the transit of pro-ADAM17 (purple) from the ER into the Golgi, where its pro-domain is removed by the actions of the pro-protein convertase furin (brown).

Interestingly, the function of iRHOM2 in supporting ADAM17 maturation has recently been shown to be shared with its close relative iRHOM1, with a high degree of redundancy having been observed between the two iRHOMs in tissues where both are highly expressed (including the skin) (Christova ~~et al~~*et al*., 2013). The fact that only the iRHOMs, and not any other rhomboid, are capable of supporting ADAM17 maturation in this way, implies that this function may be related to one of the unique domains specific to the iRHOMs. Indeed, it has recently been shown that the abrogation of KitL2 (a model ADAM17 substrate) shedding in *iRhom2*$^{-/-}$ mouse embryonic fibroblasts could be rescued by overexpression of wild-type

iRhom2, but not by an iRHOM2 mutant lacking its iRHOM-specific N-terminal cytoplasmic domain, in which TOC-associated mutations are located (Maretzky ~~et al~~*et al.*, 2013).

The key function of iRHOM2 in supporting the maturation of ADAM17 was discovered as a result of *iRhom2* knockout mice, which are viable and show no obvious defects, but fail to control the replication of the pathogenic bacteria *Listeria monocytogenes,* as a result of impaired shedding of the ADAM17 substrate TNFα (McIlwain ~~et al~~*et al.*, 2012). Similarly, *iRhom2*$^{-/-}$ mice were recently shown to be protected from inflammatory arthritis to the same extent as mice lacking either ADAM17 or TNFα (Issuree ~~et al~~*et al.*, 2013). Although they do display an obvious phenotype, *iRhom2* knockout mice did not display a phenotype of anything like the same severity as that seen in *Adam17* knockout mice, which die perinatally of severe morphological defects resulting from the inability to shed EGFR ligands (Peschon ~~et al~~*et al.*, 1998). The apparent paradox of iRHOM2 being required for ADAM17 maturation, the lethality of *Adam17* knockouts in mice and the seeming lack of effect of *iRhom2* knockouts may be explained by recent reports showing that the closely related iRHOM1 is also capable of supporting ADAM17 maturation in the same way as iRHOM2, in a number of different cell types (Issuree ~~et al~~*et al.*, 2013, Christova ~~et al~~*et al.*, 2013).

Murine knockouts of *iRhom1* result in lethality between 9 days and 6 weeks (dependent on mouse genetic background), and a much more severe phenotype than knockout of *iRhom2* (Christova ~~et al~~*et al.*, 2013). This phenotype included pronounced intracerebral haemorrhages, a lack of any detectable white fat deposits, morphological defects of the bone marrow, spleen and pancreas, and evidence of neurological defects. Interestingly, mouse *iRhom1* knockouts do not exactly phenocopy *Adam17* knockouts, which characteristically display open eyes at birth and hair follicle defects, neither of which were present in *iRhom1* knockout mice. Double knockouts of both iRHOMs resulted in embryonic lethality in mice, at a much earlier stage than even *Adam17* knockouts. From these data it can therefore be inferred that iRHOMs may have a larger role than the regulation of ADAM17 alone, due to the increased severity of double *iRhom* knockouts compared to *Adam17,* and the presence of not-obviously-ADAM17-related phenotypes in *iRhom* knockout mice, such as brain haemorrhages and organ dysfunction. These functions do not however include supporting the maturation of other ADAMs: while double *iRhom* knockout mice display no detectable mature ADAM17, maturation of all other widely expressed ADAMs is not affected, nor is the trafficking of other transmembrane proteins – including various EGFR ligands and ErbB2 – adversely affected (Christova ~~et al~~*et al.*, 2013). Furthermore, the fact that a double *iRhom*

knockout results in a more severe phenotype than would be expected from a simple combination of two single knockouts implies that there is a large degree of functional redundancy between the two.

As could therefore be expected, the two iRHOMs are often co-expressed in a number of tissues; interestingly, the tissue with the highest level of expression of both iRHOM1 and iRHOM2 is the skin, offering some rationale for why a syndrome related to iRHOM2 mutations would manifest itself in the first instance as a cutaneous disease.

In the light of these studies, these data illustrate that although both iRHOMs are expressed in keratinocytes, iRHOM2 ~~in~~ is particularly important in the process of ADAM17 maturation in this cell type. Furthermore, the increased expression of mature ADAM17 in TOC keratinocytes suggests that TOC-associated iRHOM2 mutations may directly affect its role in the ADAM17 maturation, and lead to an upregulation of this process. iRHOM2 knockdown would not be expected to completely block ADAM17 maturation, due to the co-expression of iRHOM1 in keratinocytes.

4.2.6 Three-dimensional organotypic culture of TOC and control keratinocytes

In order to investigate the phenotype of TOC in circumstances more similar to those found *in vivo,* experiments involving TOC keratinocytes were performed in organotypic, three-dimensional cultures, as well as in keratinocyte monolayers under standard cell culture conditions (as shown in the preceding section). Three-dimensional cultures of both TOC cell lines and one control (K17) were performed by Prof. Spiro Getsios and Dr. Nihal Kaplan at Northwestern University, Chicago, USA. All staining of three-dimensional culture sections was performed at Northwestern University, whilst western blotting of lysates derived from the cultures were performed primarily at Northwestern, and in part by the author. All ELISAs of supernatants derived from the cultures were performed by the author.

These three-dimensional cultures yielded fully differentiated skin equivalent models for each cell line (figure 4.8, A), which expressed a range of differentiation markers, including loricrin, involucrin and transglutaminase 1 (TGM1; figure 4.8, B), and displayed robust TGM1 activity in their upper layers (to be discussed in section 4.2.18). The two TOC cell lines yielded stratified epithelial tissues with distinct morphologies; however, all lines generate epidermal equivalents that express differentiation products similar to controls. Also importantly, the

effects on ADAM17 and the EGFR observed (to be discussed in detail below) were consistent between TYLK1 and TYLK2.

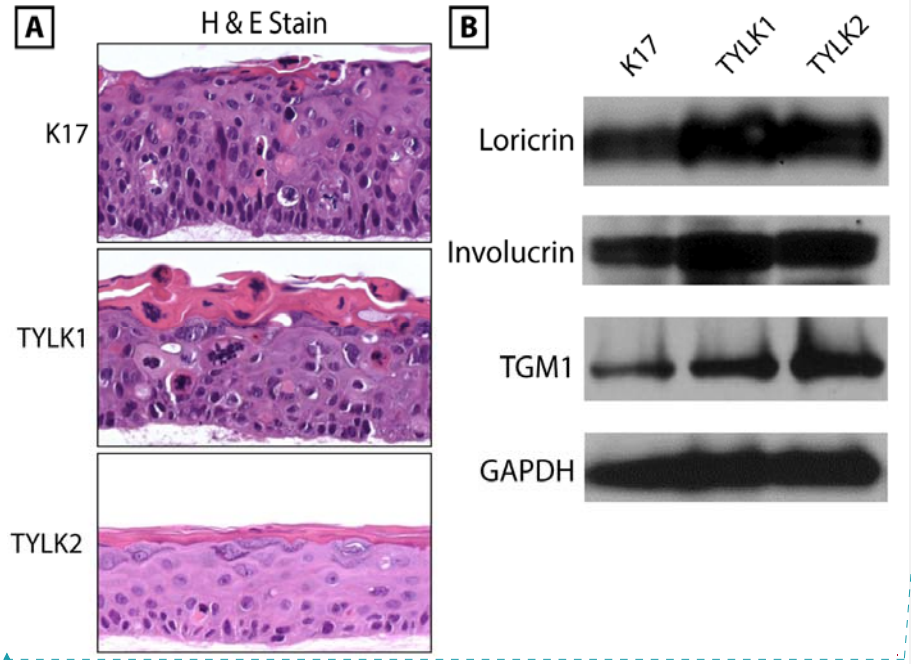

Formatted: Font: 11.5 pt, Bold

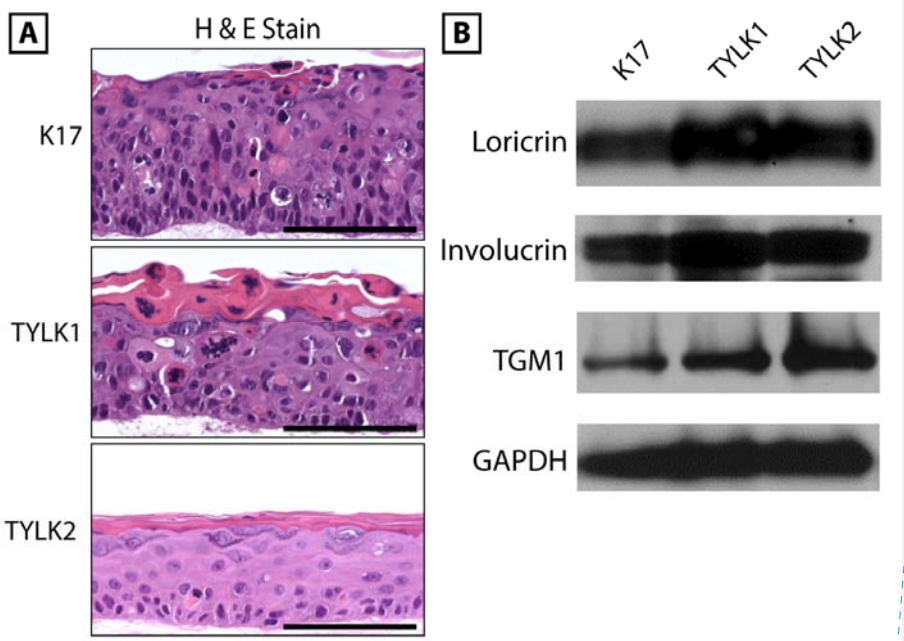

Formatted: Font: 11.5 pt, Bold

Figure 4.8: Three-dimensional organotypic cultures of TOC and control keratinocytes. **A:** Haematoxylin and Eosin (H&E) stain of three-dimensional culture models of one control (K17 and two TOC (TYLK1 and TYLK2) cell lines, illustrating their stratified, three-dimensional structure. 3D cultures were performed by Prof. Sipro Getsios and Dr. Nihal Kaplan (Northwestern University, Chicago, USA). Scale bars (black) in each case represent 100µm. **B:** Western blotting of the differentiation markers loricrin, involucrin and transglutaminase 1 (TGM1) in each three-dimensional culture, illustrating that full terminal differentiation is taking place in each culture model. Robust TGM1 activity is also seen in each model (see section ~~5~~4.2.18).

4.2.7 Expression of ADAM17 in three-dimensional organotypic keratinocyte culture

To investigate ADAM17 expression, the same western blotting strategy as was used in monolayer keratinocytes was adopted in protein lysates taken from the three-dimensional keratinocyte cultures described in section 4.2.6. Expression of ADAM17 in these cultures displayed a very similar pattern to that seen in keratinocyte monolayers, in that TOC keratinocytes were characterised by relatively increased levels of mature ADAM17 compared to pro-ADAM17, and increased levels of the free ADAM17 pro-domain (figure 4.9).

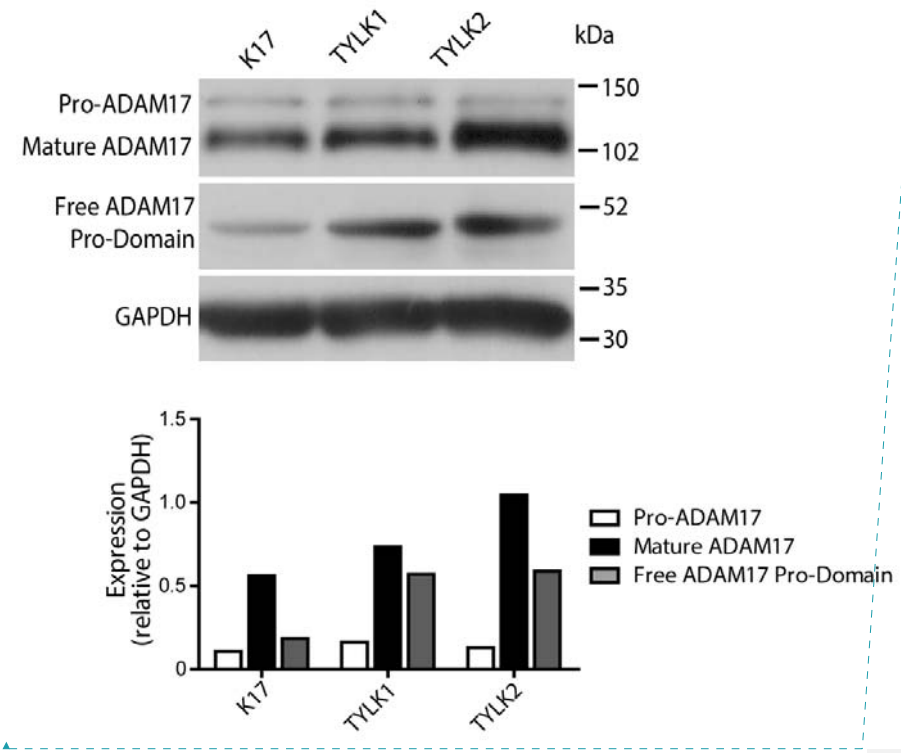

Formatted: Font: 11.5 pt

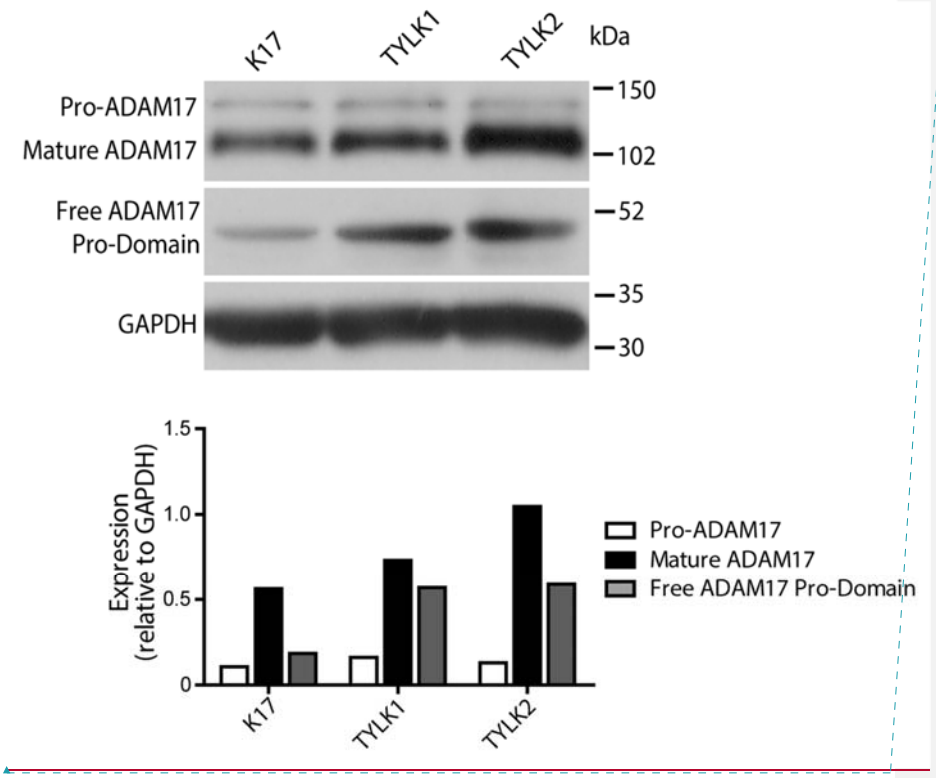

Figure 4.9: ADAM17 expression in three-dimensional organotypic cultures. Expression of pro- and mature ADAM17 and the free ADAM17 pro-domain is shown in whole cell lysates taken from three-dimensional organotypic cultures of a control (K17) and two TOC (TYLK1 and TYLK2) cell lines.

Taken together, these results imply that ADAM17 maturation is increased in TOC keratinocytes relative to controls, and that this increase is dependent on TOPC-associated mutations in iRHOM2 – a protein intimately involved in the generation of mature ADAM17, and whose knockdown significantly reduces ADAM17 maturation, with a particularly potent effect in TOC keratinocytes.

Formatted: Font: 11.5 pt

4.2.8 Localisation of ADAM17 in TOC and control keratinocytes in monolayer and in ~~3D~~ three-dimensional culture

To further investigate the observation of increased ADAM17 maturation in TOC keratinocytes, immunocytochemical co-staining of ADAM17 – alongside markers of the endoplasmic reticulum (ER), Golgi apparatus and plasma membrane – was performed in the four cell lines previously described. ADAM17 displayed clear staining at the plasma membrane (its primary site of ectodomain sheddase activity) and also within the Golgi apparatus (figure 4.10, A). The clear staining of ADAM17 in the Golgi in both TOC and control cell lines demonstrated that TOC-associated iRHOM2 mutations were not negatively affecting the ability of iRHOM2 to traffic pro-ADAM17 into the Golgi. When comparing all four cell lines it was noticeable that the two TOC cell lines displayed greater levels of ADAM17 at the plasma membrane (as shown in detail in figure 4.10, B).

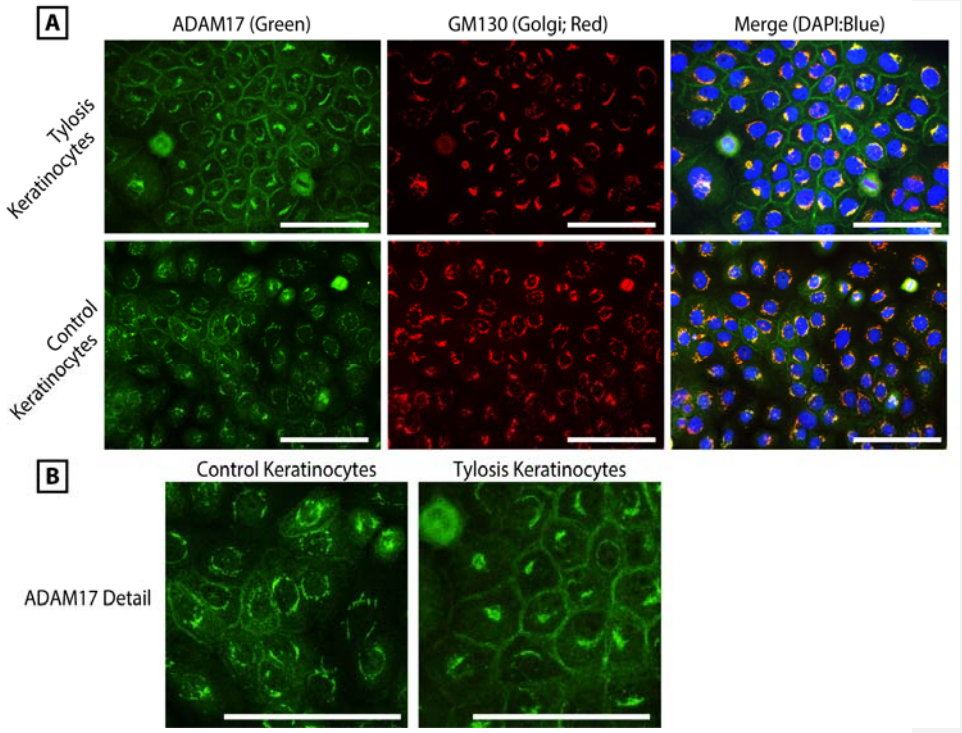

Figure 4.10: Immunocytochemical staining of control and TOC keratinocyte cell lines. **A:** Staining of ADAM17 (green) and the Golgi apparatus marker GM130 (red) is shown in control and TOC keratinocytes in monolayer culture. **B:** Detail of ADAM17 staining. Scale bars in all cases represent 100µm.

Immunohistochemical staining of ADAM17 was next performed in three-dimensional organotypic keratinocyte cultures, where findings once again corresponded with those seen in keratinocyte monolayers. ADAM17 staining at the plasma membrane of TOC keratinocyte three-dimensional cultures was significantly higher than controls, as shown in figure 4.11.

These findings of increased ADAM17 localisation to its primary site of activity, in addition to the increased expression of mature ADAM17 in TOC keratinocytes shown by western blot, further suggested an upregulation of ADAM17 maturation in TOC, which was present in both keratinocyte monolayers and three-dimensional cultures.

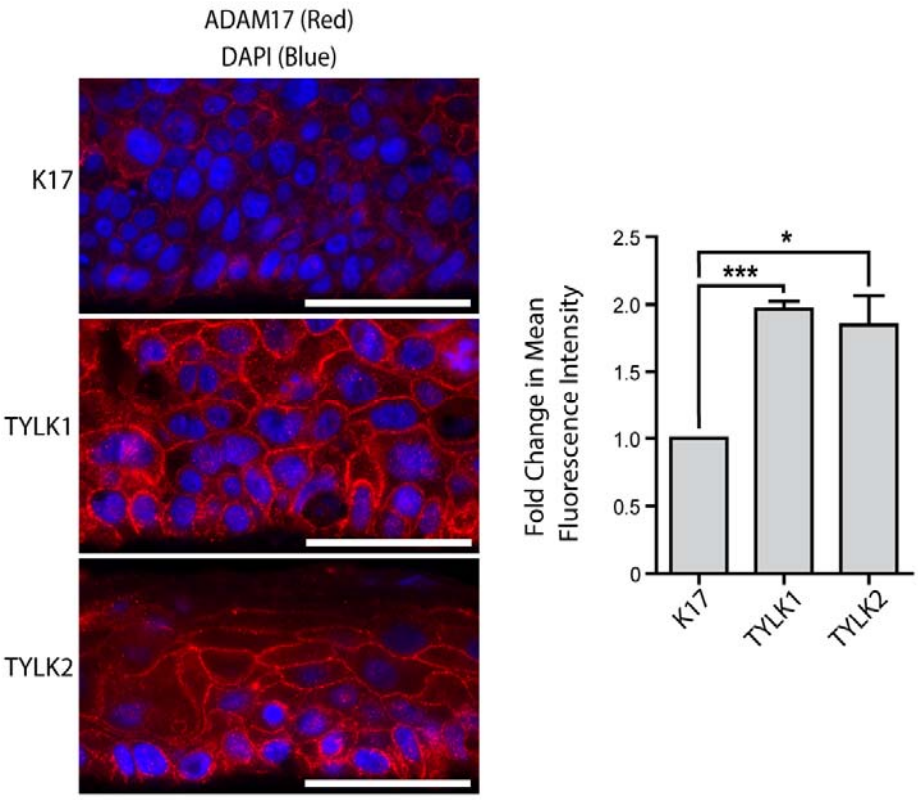

Figure 4.11: Immunohistochemical staining of ADAM17 (red) in three-dimensional organotypic culture models of control (K17) and TOC (TYLK1 and TYLK2) keratinocytes. Data quantified in the graph represent results from three separate experiments. 3D cultures were performed by Prof. Sipro Getsios and Dr. Nihal Kaplan (Northwestern University, Chicago, USA). Scale bars in all cases represent 100µm; Statistical analysis was performed using student's unpaired t-test to individually compare the TYLK1 and TYLK2 cell line results against K17; *p<0.05; **p<0.01; ***p<0.001.

Formatted: Font: 4 pt

4.2.9 Shedding of pro-inflammatory cytokines and EGFR ligands by TOC and control keratinocytes

To examine the effect of the apparent upregulation of mature ADAM17 in TOC keratinocytes, shedding of ADAM17 substrates was examined in the four cell lines studied, and in peripheral blood mononuclear cells (PBMCs) derived from TOC patients and controls.

Tumour necrosis factor-α (TNFα) – arguably ADAM17's best known substrate – was shed at a significantly higher level by TOC keratinocytes than controls (in which levels of TNFα shed

were below the limit of detection; figure 4.12, A) when these cells were stimulated with phorbol myristate acetate (PMA; 100ng/ml). Importantly, this excess TNFα shedding was found to be dependent on ADAM17, as siRNA mediated knockdown of ADAM17 (illustrated in figure 4.5) was sufficient to significantly reduce the excess shedding observed. Similarly, secretion of TNFα from PBMCs isolated from three TOC patients was also significantly higher than matched controls following PMA stimulation (figure 4.12, B). No significant difference in TNFα secretion was observed constitutively, or when these cells were stimulated with varying concentrations of lipopolysaccharide (LPS; not shown). These findings show that TOC keratinocytes harbouring mutant iRHOM2 protein are not only capable of shedding TNFα (in contrast to macrophages of iRHOM2-knockout mice, which cannot ~~{~~[Adrain ~~et al~~*et al.*, 2012~~}~~]) but do so in a more efficient manner than wild-type cells.

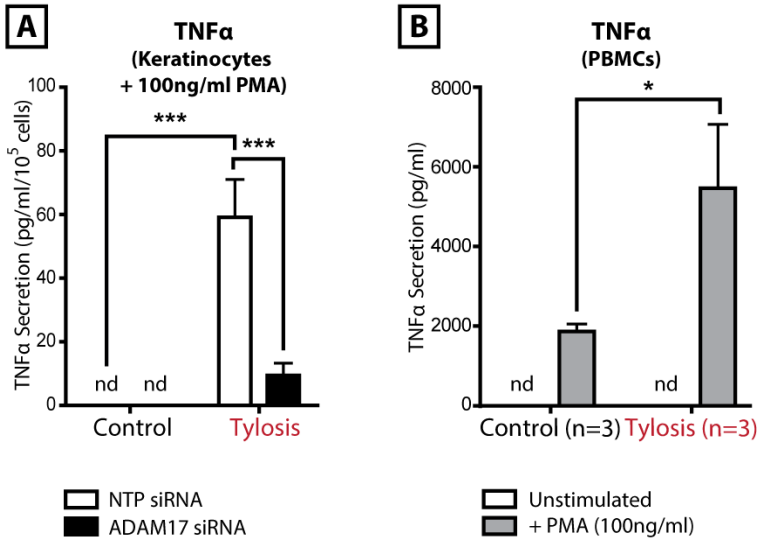

Figure 4.12: TNFα shedding. **A:** Shedding of TNFα from control and TOC keratinocytes following stimulation with 100ng/ml phorbol myristate acetate (PMA). Results represent shedding over a 24 hour period, beginning 24 hours after transfection of keratinocytes with non-targeting pool (NTP) or anti-ADAM17 siRNA. **B:** Shedding of TNFα from peripheral blood mononuclear cells (PBMCs) derived from TOC patients or controls (n=3 each) with or without 100ng/ml PMA stimulation. Data in all cases represent results from three separate experiments. "Control" results represent pooled data from K17 and Neb1 cell lines, "Tylosis" results represent pooled

data from TYLK1 and TYLK2 cell lines. Statistical analysis was performed using 2-way ANOVA with Bonferroni's post-hoc test (A) or student's unpaired t-test (B); nd: not detected; *p<0.05; **p<0.01; ***p<0.001.

As described in section 4.2.2, TOC keratinocytes have previously been shown to proliferate and migrate at a significantly higher rate than controls in a scratch assay, and do so independently of exogenous EGFR ligands (Blaydon ~~et al~~*et al.*, 2012). Consequently, the shedding of ADAM17's substrates in the EGF growth factor family, specifically amphiregulin, TGFα and HB-EGF, was examined when cells were cultured in the absence of exogenous EGFR ligands. Constitutive shedding of all three growth factors (i.e. in the absence of any stimulation, by PMA or otherwise) was shown to be significantly higher in TOC keratinocytes than controls, with amphiregulin shedding around two orders of magnitude higher than that of TGFα and HB-EGF (figure 4.13). In each of these cases, the elevated shedding observed could be significantly reduced by siRNA mediated knockdown of ADAM17 in TOC keratinocytes, illustrating the ADAM17-dependent nature of the observed increase.

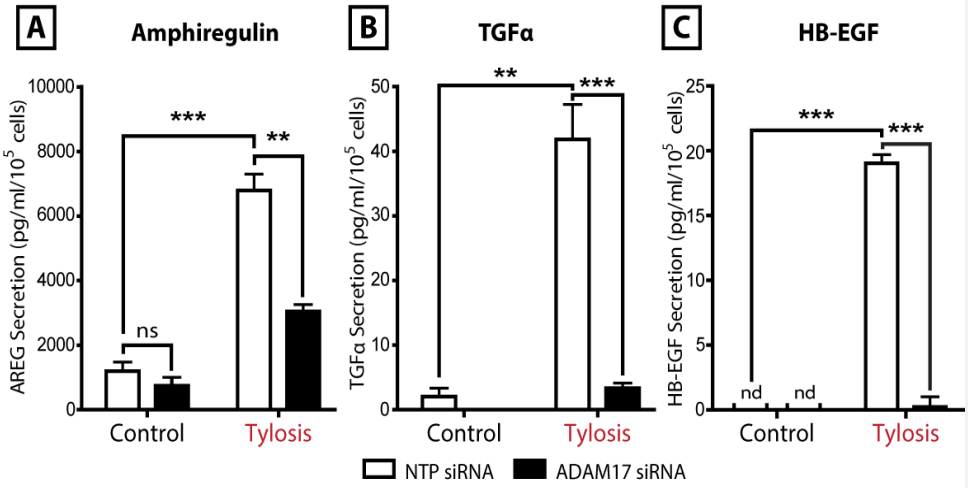

Figure 4.13: Shedding of ADAM17 substrate EGFR ligands from control and TOC keratinocytes. Shedding of amphiregulin (A), TGFα (B), and HB-EGF (C) from control and TOC keratinocytes measured by ELISA, representing shedding over a 24 hour period, beginning 24 hours after transfection of keratinocytes with non-targeting pool (NTP) or anti-ADAM17 siRNA. Data in all cases represent results from three separate experiments. "Control" results represent pooled data from K17 and Neb1 cell lines, "Tylosis" results represent pooled data from TYLK1 and TYLK2 cell

lines. Statistical analysis was performed using 2-way ANOVA with Bonferroni's post-hoc test; nd: not detected; ns: not-significant; *p<0.05; **p<0.01; ***p<0.001.

Secretion of EGFR ligands from organotypic culture models of TOC was also examined. Amphiregulin secretion was again observed to be significantly higher in TOC cells than controls (figure 4.14), whilst TGFα and HB-EGF shedding levels were below the limit of detection (not shown).

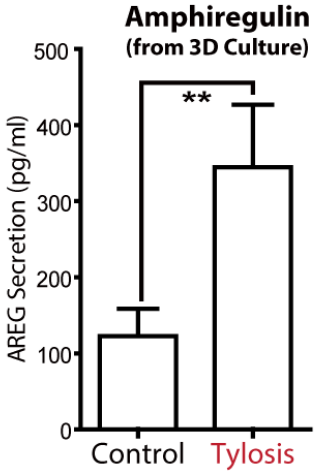

Figure 4.14: Amphiregulin shedding, measured by ELISA, from three dimensional (3D) organotypic cultures of control and TOC keratinocytes. Data represent results from three separate experiments. Statistical analysis was performed using student's unpaired t-test; *p<0.05; **p<0.01; ***p<0.001.

The secretion of a number of pro-inflammatory cytokines – specifically IL-6 and IL-8 – was also examined in TOC and control keratinocytes. Although not directly shed by ADAM17, secretion of both of these cytokines can be regulated downstream of ADAM17 substrate activity, and both are important mediators of inflammation, epidermal wound healing and keratinocyte migration. For example, IL-8 synthesis and release in the skin depend on the activation of the EGFR (Frankart ~~et al~~*et al*., 2012), and the release of both IL-6 and IL-8 require EGFR transactivation by ADAM17 in skin injury models (Buchau, 2010) (the same is

also true of other cytokines and anti-microbial peptides). Furthermore, IL-6 signalling is regulated in large part by shedding of the soluble IL-6 receptor (as discussed in section 1.1.4), a direct ADAM17 substrate.

Constitutive secretion of both IL-6 and IL-8 was found to be significantly upregulated in TOC keratinocytes compared to controls, with IL-8 secretion in particular hugely upregulated. Secretion of both was sensitive to siRNA knockdown of ADAM17 in TOC cells, but not controls, illustrating that the excessive secretory phenotype of TOC keratinocytes is dependent at least in part on ADAM17 (figure 4.15).

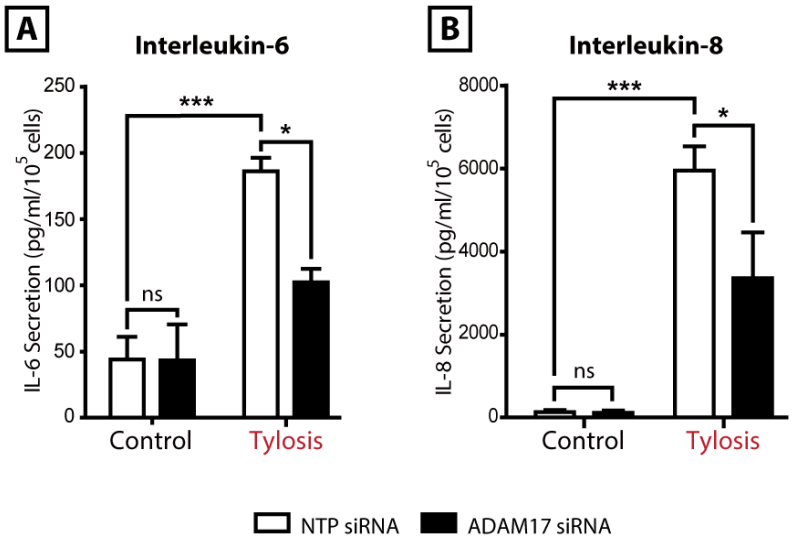

Figure 4.15: Interleukin (IL)-6 and IL-8 secretion, measured by ELISA, from control and TOC keratinocytes. These data represent secretion over a 24 hour period, beginning 24 hours after transfection of keratinocytes with non-targeting pool (NTP) or anti-ADAM17 siRNA. Data in all cases represent results from three separate experiments. "Control" results represent pooled data from K17 and Neb1 cell lines, "Tylosis" results represent pooled data from TYLK1 and TYLK2 cell lines. Statistical analysis was performed using 2-way ANOVA with Bonferroni's post-hoc test; -ns: not-significant; *p<0.05; **p<0.01; ***p<0.001.

4.2.10 mRNA expression of ADAM17 substrates in keratinocytes

To illustrate the ADAM17-dependent nature of the increased shedding observed, and that shedding reductions in cells treated with anti-ADAM17 siRNA were ADAM17-dependent, mRNA expression of each of the shed factors described above, and of ADAM17 itself, was also performed.

Other than ADAM17, no significant change at the mRNA transcript level of any protein was observed when ADAM17 siRNA was applied (figure 4.16), illustrating that differences in shedding observed were dependent on the activity of ADAM17. In general, mRNA transcript levels of EGFR ligands were marginally higher in TOC keratinocytes, which would be expected, as signalling through the EGFR promotes the production of more EGFR ligands. Additionally, these differences would not appear to explain the large degree to which shedding levels were elevated in TOC cells.

siRNA knockdown of ADAM17 robustly reduces ADAM17 mRNA levels, as would be expected. Additionally, expression of ADAM17 mRNA in TOC and control keratinocytes is comparable, meaning that increased levels of mature ADAM17 and the increased presence of ADAM17 at the plasma membrane cannot be explained simply by upregulation of ADAM17 expression at the transcription level, further implicating iRHOM2-dependent ADAM17 maturation as a key event in ADAM17 activity in TOC keratinocytes.

It is also interesting to observe that shedding levels of various substrates of ADAM17 often do not correlate with expression at the mRNA level. For example, expression of amphiregulin, TGFα and HB-EGF mRNA is broadly comparable, yet amphiregulin shedding is around two orders of magnitude higher than either of the other two growth factors, illustrating the importance of regulation at levels beyond mRNA expression.

In common with the very high levels of secretion observed, IL-8 mRNA expression was notably higher in TOC keratinocytes than controls, and was by far the highest expressed of the mRNA transcripts examined.

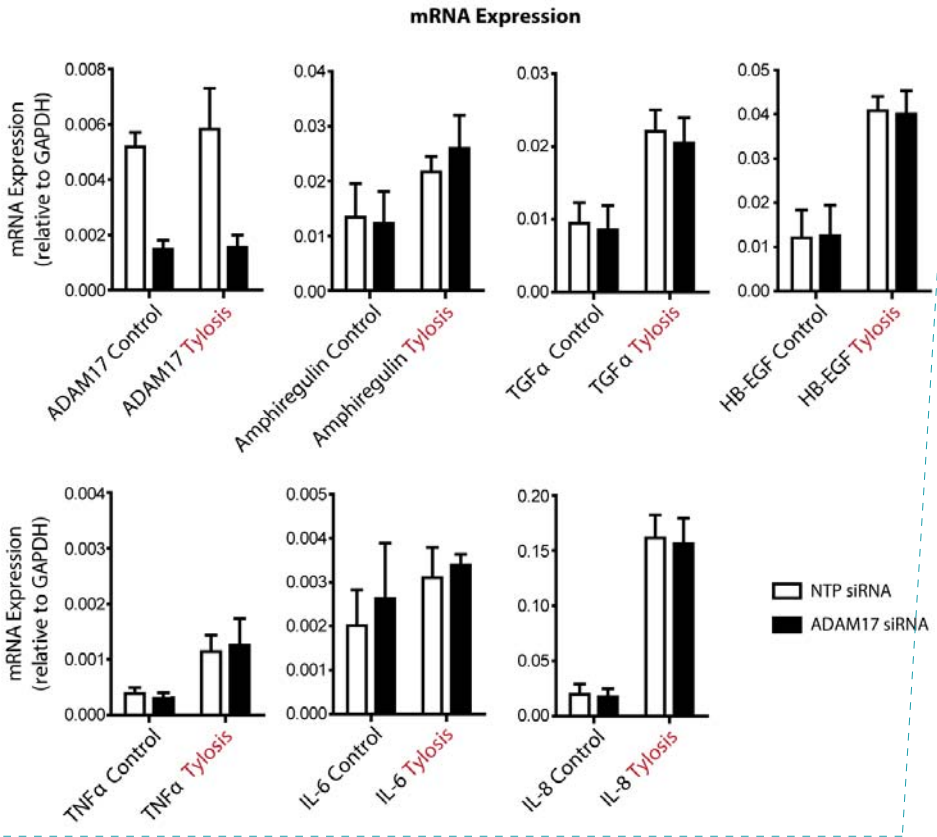

Formatted: Font: 11.5 pt, Bold

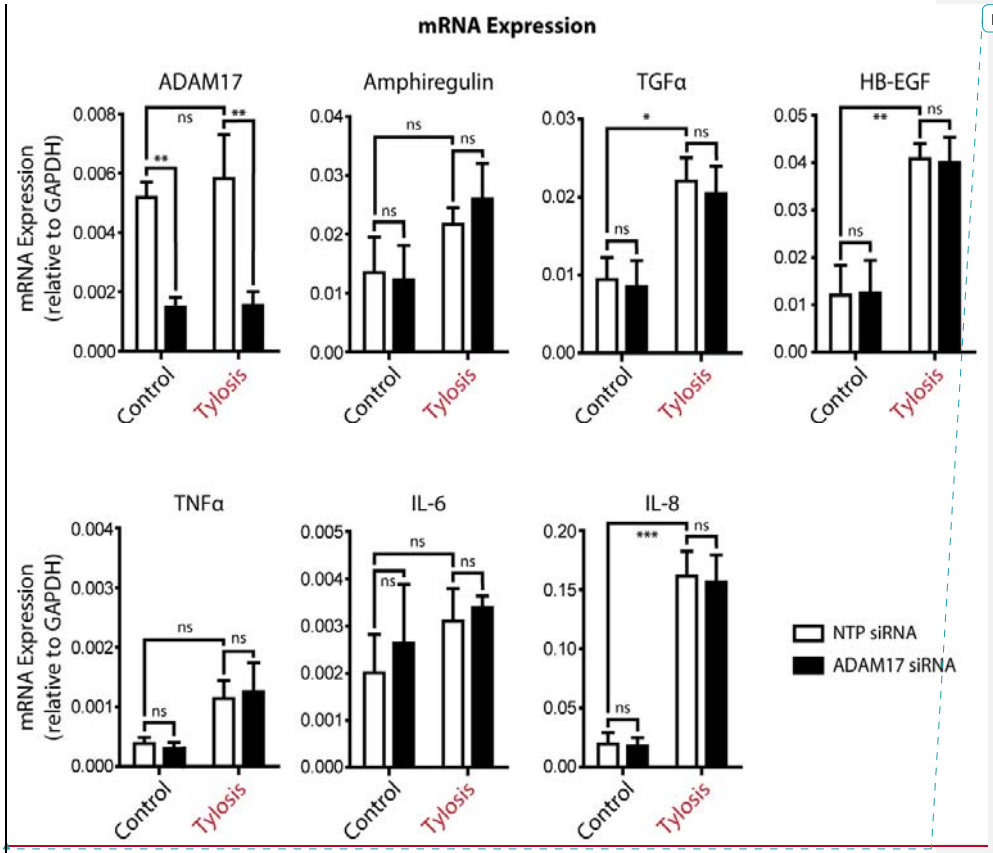

Figure 4.16: mRNA levels of various proteins in control and TOC keratinocytes. mRNA levels were measured in RNA extracted from whole cell lysates 48 hours after transfection with non-targeting pool (NTP) or anti-ADAM17 siRNA (the same cells responsible for the ligand shedding displayed in figures 4.8, 4.9 and 4.11). Data in all cases represent results from three separate experiments. "Control" results represent pooled data from K17 and Neb1 cell lines, "Tylosis" results represent pooled data from TYLK1 and TYLK2 cell lines. Statistical analysis was performed using 2-way ANOVA with Bonferroni's post-hoc test; ns: not significant; *p<0.05; **p<0.01; ***p<0.001

4.2.11 EGFR phosphorylation in TOC and control keratinocytes in three dimensional organotypic culture

Next, the consequences of increase EGFR ligand shedding by TOC keratinocytes were investigated. Western blotting of the EGFR in three-dimensional culture models revealed variable expression of total EGFR, but notably increased EGFR phosphorylation at three separate tyrosine residues (Y845, Y1045 and Y1068) in TOC cultures (figure 4.17), suggesting that increased EGFR ligand shedding is accompanied by increased EGFR signalling in these models.

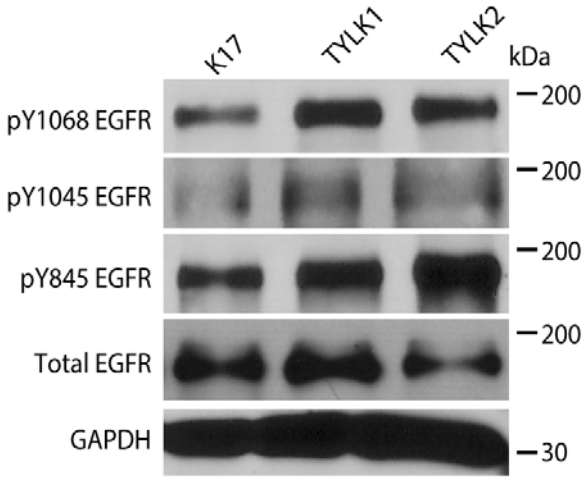

Figure 4.17: Phosphorylation of the EGFR at three separate tyrosine residues in three-dimensional organotypic culture models of a control (K17) and two TOC (TYLK1 and TYLK2) keratinocyte cell lines. Western blotting was performed by Prof. Sipro Getsios and Dr. Nihal Kaplan (Northwestern University, Chicago, USA).

4.2.12 Scratch assays as a measure of keratinocyte migration and wound healing

As previously mentioned, TOC keratinocytes have been shown to proliferate and migrate at significantly higher rates than controls keratinocytes in scratch wounding assays. These assays measure the migration of keratinocytes across a scratch made in a keratinocyte monolayer, and as such simulate the wound healing response in keratinocytes.

The increased migration of TOC keratinocytes has been described as being EGFR ligand independent. That is, when keratinocytes are cultured in medium lacking any exogenous EGFR ligands, TOC keratinocyte migration is significantly higher than that seen in controls. To confirm this finding, scratch assays were performed in the absence of exogenous EGFR ligands on all four keratinocyte cell lines described previously, with keratinocyte migration measured 24 and 48 hours after scratching. As shown in figure 4.18, migration of both TYLK1 and TYLK2 cell lines was significantly higher than both K17 and Neb1 cell lines after 24 and 48 hours ($p < 0.001$ in all cases).

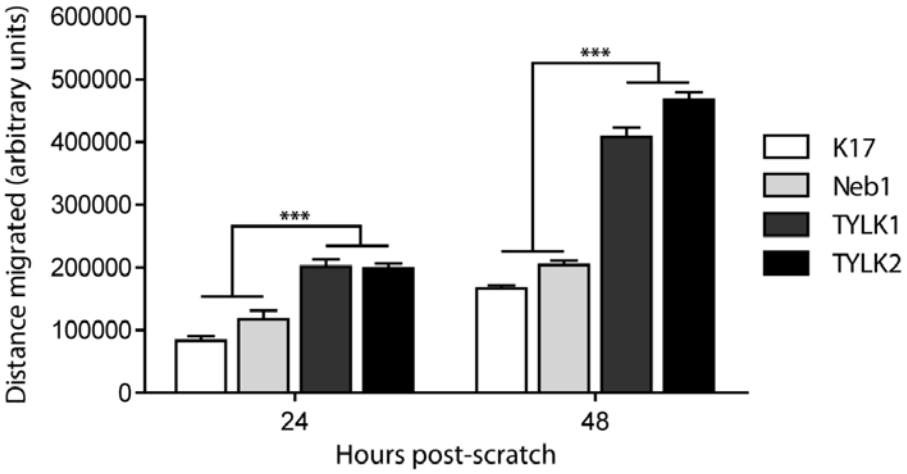

Figure 4.18: Migration of control and TOC keratinocytes 24 and 48 hours following simulated wounding, in medium lacking any exogenous EGFR ligands. Data represent three separate experiments for each cell line. Statistical analysis was performed using Student's unpaired t-test; *p<0.05; **p<0.01; ***p<0.001. Significance lines represent that both (non-pooled) TYLK1 and TYLK2 migration was significantly higher than both K17 and Neb1, at both 24 and 48 hours (p<0.001 in all cases).

4.2.13 The effect of secreted factors on keratinocyte migration

As the increased TOC keratinocyte migration observed is independent of exogenous EGFR ligands, it was reasonable to hypothesise that the significantly increased level of EGFR ligand shedding observed in TOC keratinocytes would contribute to the excessive migratory phenotype.

To investigate this, shedding of amphiregulin (the growth factor present at by far the highest levels in cell culture supernatants derived from TOC keratinocytes) was first examined over time, in supernatants derived from all four cell lines following scratch wounding. Amphiregulin production was upregulated very quickly after scratch wounding in TOC cells relative to controls, was significantly higher after only one hour (figure 4.19), and remained at a significantly higher level than controls over 48 hours after scratch wounding.

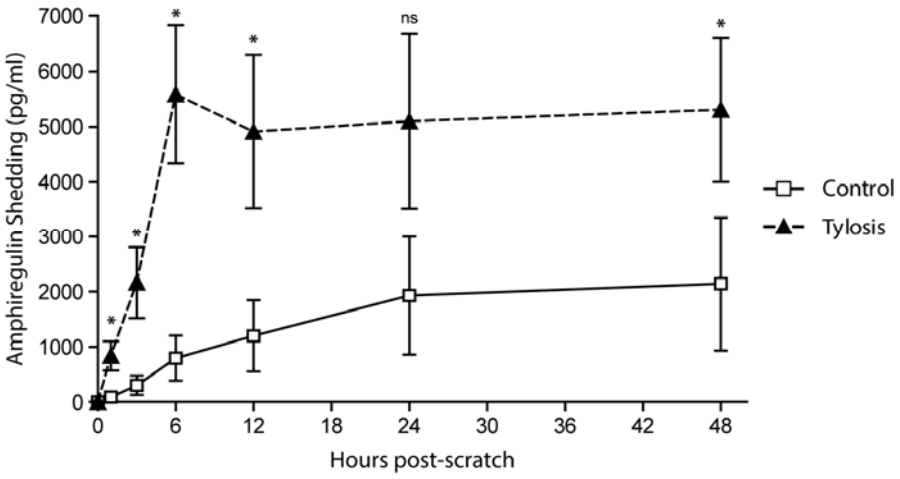

Figure 4.19: Amphiregulin shedding following scratch wounding. Amphiregulin shedding, measured by ELISA, is shown at 1, 3, 6, 12, 24 and 48 hours following scratch wounding, in control and TOC keratinocytes. Data in all cases represent results from three separate experiments on each cell line. "Control" results represent pooled data from K17 and Neb1 cell lines, "Tylosis" results represent pooled data from TYLK1 and TYLK2 cell lines. Statistical analysis

was performed using student's unpaired t-test for pairwise comparisons at each time point; ns: not-significant; *p<0.05.

To investigate the effect of shed growth factors on keratinocyte migration, cell culture medium in which TOC keratinocytes had previously been grown (TYLK-conditioned medium, composed of a 1:1 blend of medium – otherwise containing no exogenous EGFR ligands – derived from TYLK1 and TYLK2 cells) and which therefore contained the high levels of shed growth factors that characterise TOC keratinocytes, was used in place of otherwise normal medium containing no exogenous EGFR ligands, in a scratch assay of all four cell lines.

As shown in figure 4.16, the use of TYLK-conditioned medium significantly increased the migration of control keratinocytes after both 24 and 48 hours (figure 4.20, B), though the level of migration seen was still lower than that of TOC keratinocytes in otherwise normal medium. TYLK-conditioned medium also increased the migration of TOC keratinocytes, though this increase was not significant.

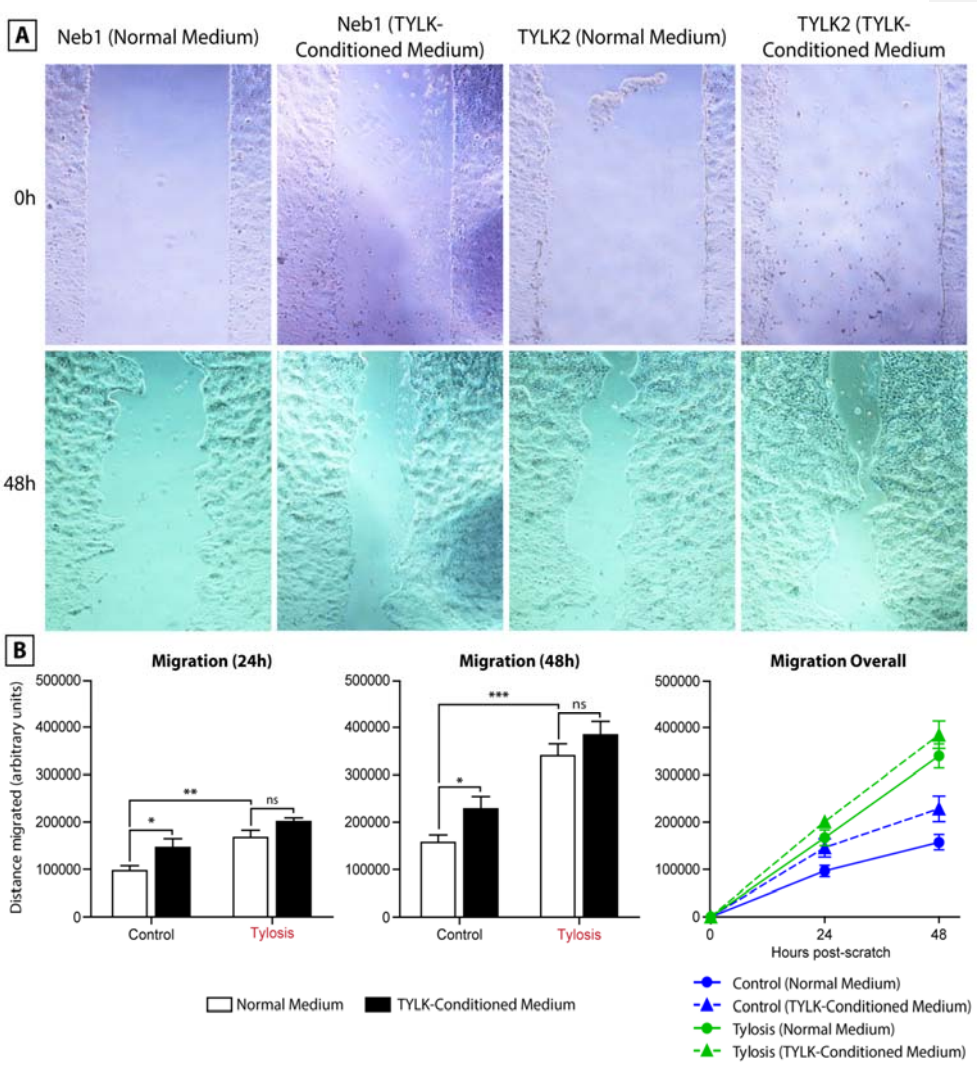

Figure 4.20: The effect of TYLK-conditioned medium on migration of control and TOC keratinocytes. **A:** representative pictures of scratch wounding of Neb1 (control) and TYLK2 (TOC) keratinocytes, at 0 and 48 hours after scratch wounding, when cultured in otherwise normal or TYLK-conditioned medium (both lacking exogenous EGFR ligands). **B:** Quantification of keratinocyte migration 24 and 48 hours after scratch wounding. Data in all cases represent results from three separate experiments on each cell line. "Control" results represent pooled data from K17 and Neb1 cell lines, "Tylosis" results represent pooled data from TYLK1 and TYLK2 cell lines. Statistical analysis was performed using 2-way ANOVA with Bonferroni's post-hoc test; ns: not-significant; *p<0.05; **p<0.01; ***p<0.001.

Next, the effect of medium conditioned by control keratinocytes in the same fashion (control-conditioned medium) was examined, to investigate whether or not the increase in migration observed could be explained by those factors shed excessively by TOC keratinocytes in particular.

As shown in figure 4.21, control-conditioned medium had no significant effect on migration of either control or TOC keratinocytes; though a small but insignificant reduction in the migration of control keratinocytes was observed.

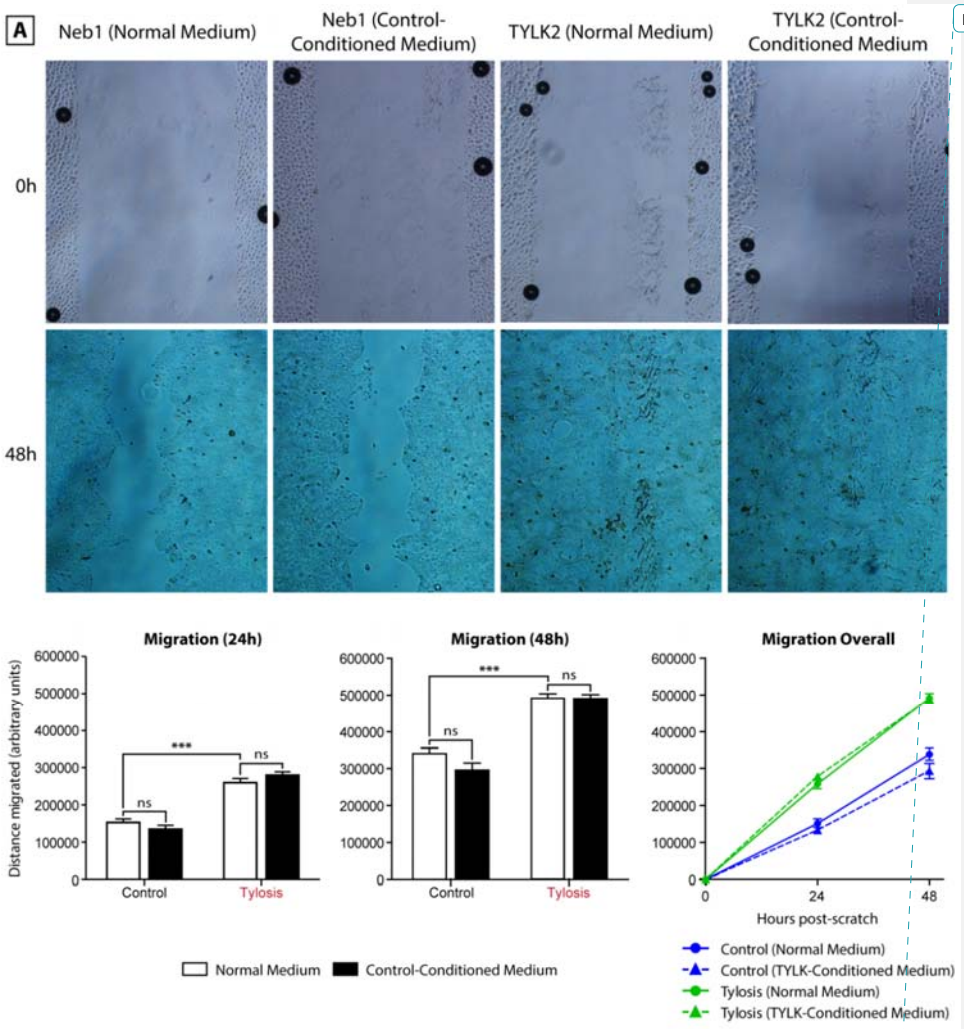

Formatted: Font: 11.5 pt, Bold

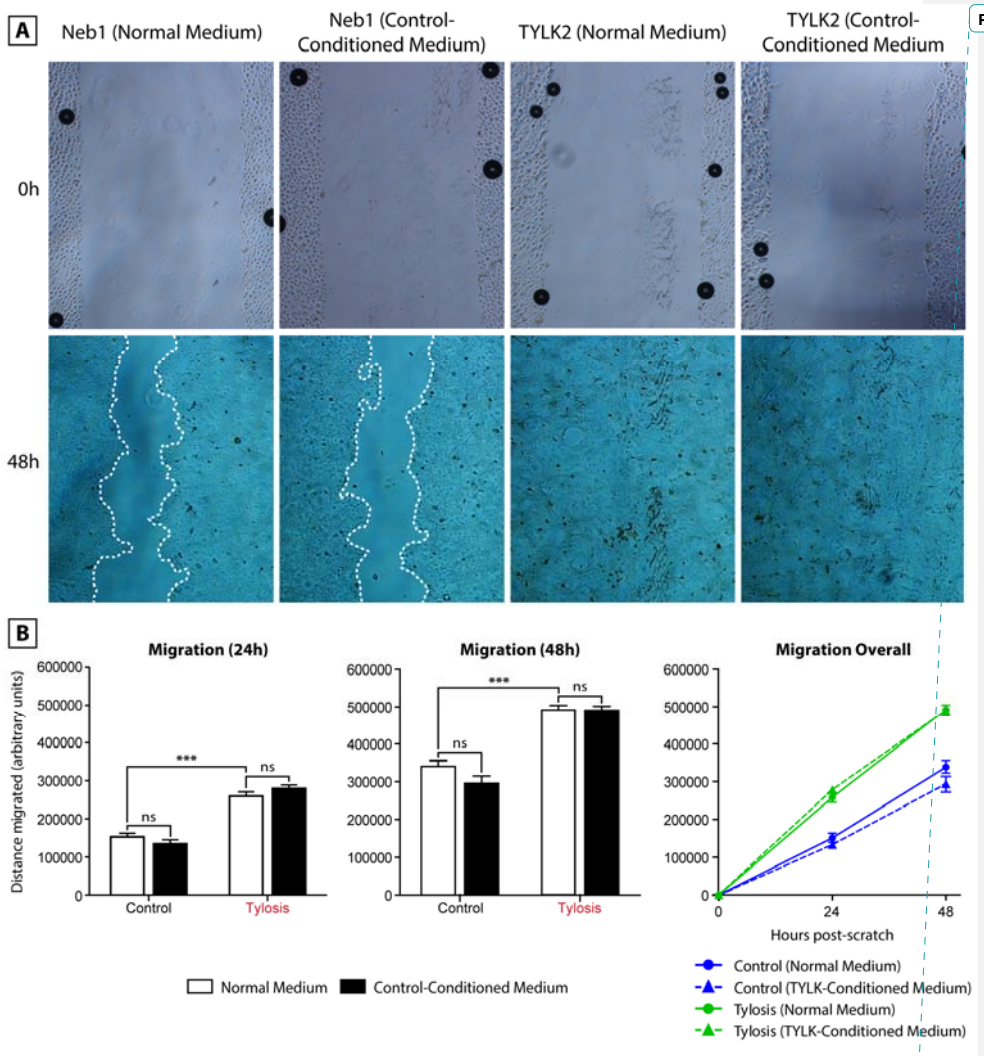

Figure 4.21: The effect of Control-conditioned medium on migration of control and TOC keratinocytes. **A:** representative pictures of scratch wounding of Neb1 (control) and TYLK2 (TOC) keratinocytes, at 0 and 48 hours after scratch wounding, when cultured in otherwise normal or Control-conditioned medium (both lacking exogenous EGFR ligands). **B:** Quantification of keratinocyte migration 24 and 48 hours after scratch wounding. Data in all cases represent results from three separate experiments on each cell line. "Control" results represent pooled data from K17 and Neb1 cell lines, "Tylosis" results represent pooled data from TYLK1 and TYLK2 cell lines. ns: not-significant; Statistical analysis was performed using 2-way ANOVA with Bonferroni's post-hoc test; *p<0.05; **p<0.01; ***p<0.001.

Therefore, medium conditioned by TOC keratinocytes is sufficient to significantly increase the migration of control keratinocytes, whilst medium conditioned by control cells has no effect on migration by any cell type, implying that factors shed by TOC cells only are important in the excessive cell migration phenotype observed in these keratinocytes.

Next, the effect of TYLK-conditioned medium on EGFR ligand production was observed. Culturing control keratinocytes in TYLK-conditioned medium resulted in the presence of significantly increased levels of amphiregulin in supernatants from these cells after 24 hours (figure 4.22), an increase which correlates with the observed increase in migration. However, whether this represents increased amphiregulin shedding in response to increased EGFR signalling, or residual amphiregulin ultimately derived from the TOC keratinocytes used to produce the TYLK-conditioned medium, remains unclear, though some combination of the two would be expected.

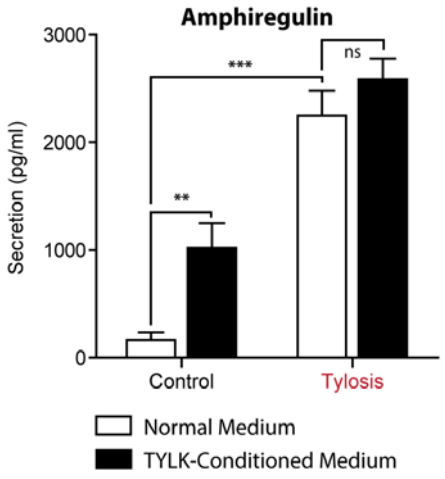

Figure 4.22: The effect of TYLK-conditioned medium on amphiregulin shedding in control and TOC keratinocytes. Amphiregulin concentrations were measured 24 hours after scratch wounding, in otherwise normal or TYLK-conditioned medium in which control or TOC keratinocytes had been cultured. Data in all cases represent results from three separate experiments on each cell line. "Control" results represent pooled data from K17 and Neb1 cell lines, "Tylosis" results represent pooled data from TYLK1 and TYLK2 cell lines. Statistical analysis was performed using 2-way ANOVA with Bonferroni's post-hoc test; -ns: not-significant; *p<0.05; **p<0.01; ***p<0.001.

4.2.14 Inhibition of ADAM17 with the small molecule GW280264X

Next, the degree to which ADAM17 contributes to the phenotype of excessive migration was investigated via chemical inhibition of ADAM17. This was performed with the use of GW280264X, a small molecule ADAM17 inhibitor used to potently inhibit ADAM17 activity (Dreymueller ~~et al~~*et al.*, 2012, Ludwig ~~et al~~*et al.*, 2005, Rabinowitz ~~et al~~*et al.*, 2001). Treatment with GW280264X at 1µM potently and significantly reduces the shedding of the ADAM17 substrates amphiregulin and TGFα (figure 4.23) from both control and TOC keratinocytes, with a particularly pronounced effect on TOC cells.

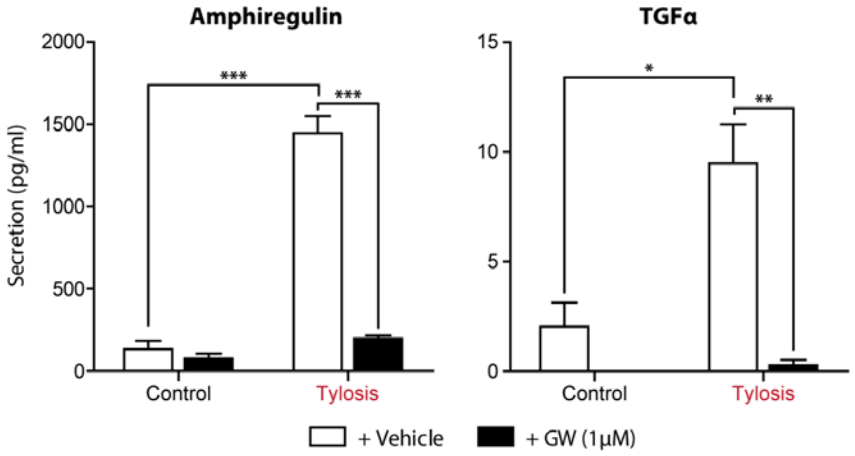

Figure 4.23: The effect of GW280264X on ADAM17 substrate shedding. Shedding of amphiregulin and TGFα from control and TOC keratinocytes measured by ELISA, representing shedding over a 24 hour period, when keratinocytes were cultured in the presence of 1µM GW280264X (GW) or a vehicle control (DMSO). Data in all cases represent results from three separate experiments. "Control" results represent pooled data from K17 and Neb1 cell lines, "Tylosis" results represent pooled data from TYLK1 and TYLK2 cell lines. Statistical analysis was performed using 2-way ANOVA with Bonferroni's post-hoc test; -*p<0.05; **p<0.01; ***p<0.001.

4.2.15 The effect of ADAM17 inhibition on EGFR ligand shedding and keratinocyte migration

In addition to potently blocking EGFR ligand shedding by keratinocytes, treatment with GW280264X was also effective in significantly reducing the migration of both control and TOC keratinocytes following scratch wounding. As with its effects on ADAM17 shedding,

GW280264X had a particularly potent effect on TOC keratinocyte migration, where it significantly reduced migration at both 24 and 48 hours (control keratinocyte migration was significantly reduced only after 48 hours) and reduced migration down to a level below that seen in control keratinocytes either with or without GW280264X treatment (figure 4.24).

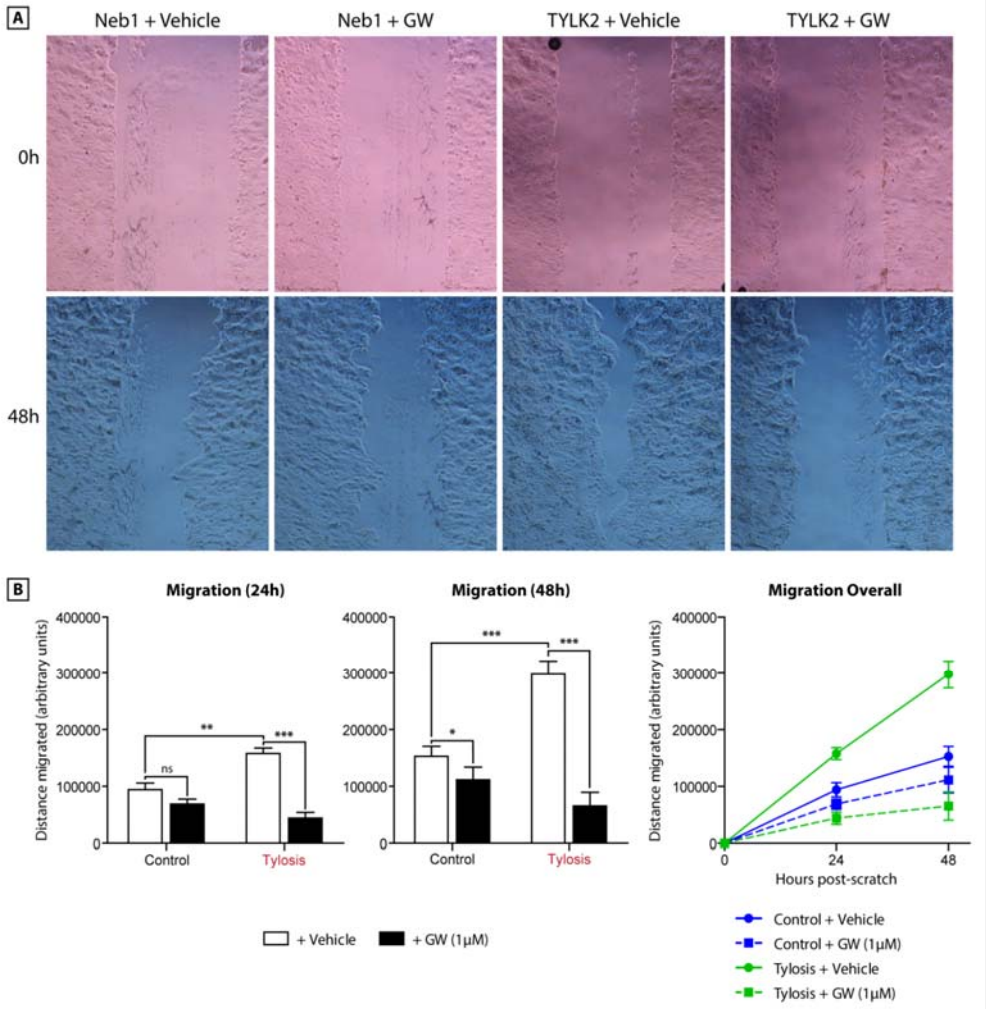

Figure 4.24: The effect of the ADAM17 inhibitor GW280264X on migration of control and TOC keratinocytes. **A:** representative pictures of scratch wounding of Neb1 (control) and TYLK2 (TOC) keratinocytes, at 0 and 48 hours after scratch wounding, when cultured in medium (lacking exogenous EGFR ligands) supplemented with either a vehicle control (DMSO) or 1µM GW280264X (GW). **B:** Quantification of keratinocyte migration 24 and 48 hours after scratch wounding. Data in all cases represent results from three separate experiments on each cell line.

"Control" results represent pooled data from K17 and Neb1 cell lines, "Tylosis" results represent pooled data from TYLK1 and TYLK2 cell lines. Statistical analysis was performed using 2-way ANOVA with Bonferroni's post-hoc test; ns: not-significant; *p<0.05; **p<0.01; ***p<0.001.

These data indicate that the excessive migration observed in TOC keratinocytes cultured in the absence of EGFR ligands is dependent on the sheddase actions of ADAM17, which corresponds with the earlier observation that factors shed by TOC keratinocytes are able to stimulate the migration of control keratinocytes.

4.2.16 The effect of EGFR ligand supplementation on keratinocyte migration

Having established that inhibition of ADAM17 is sufficient to block the excessive migration of TOC keratinocytes in EGFR ligand-free medium, the possibility of overcoming the effects of ADAM17 inhibition by exogenous supplementation with EGFR ligands was next investigated. As amphiregulin is the growth factor present at by far the highest level, and as increased amphiregulin levels correlate with increased migration (figure 4.22), it appeared to be the best candidate for supplementation studies.

As shown in figure 4.25, the addition of amphiregulin at 2000pg/ml (a concentration resembling that found in supernatants conditioned by TOC keratinocytes) does significantly increase migration by control keratinocytes, but not TOC keratinocytes (figure 4.25, A), in a fashion similar to that seen when supplementing with TYLK-conditioned medium (figure 4.20). However, amphiregulin supplementation had no effect on the migration inhibition mediated by GW280264X in either control or TOC keratinocytes.

Similarly, amphiregulin supplementation did not induce any significant upregulation of its own shedding in either control or TOC cells (though a small but insignificant increase was observed in controls cells).

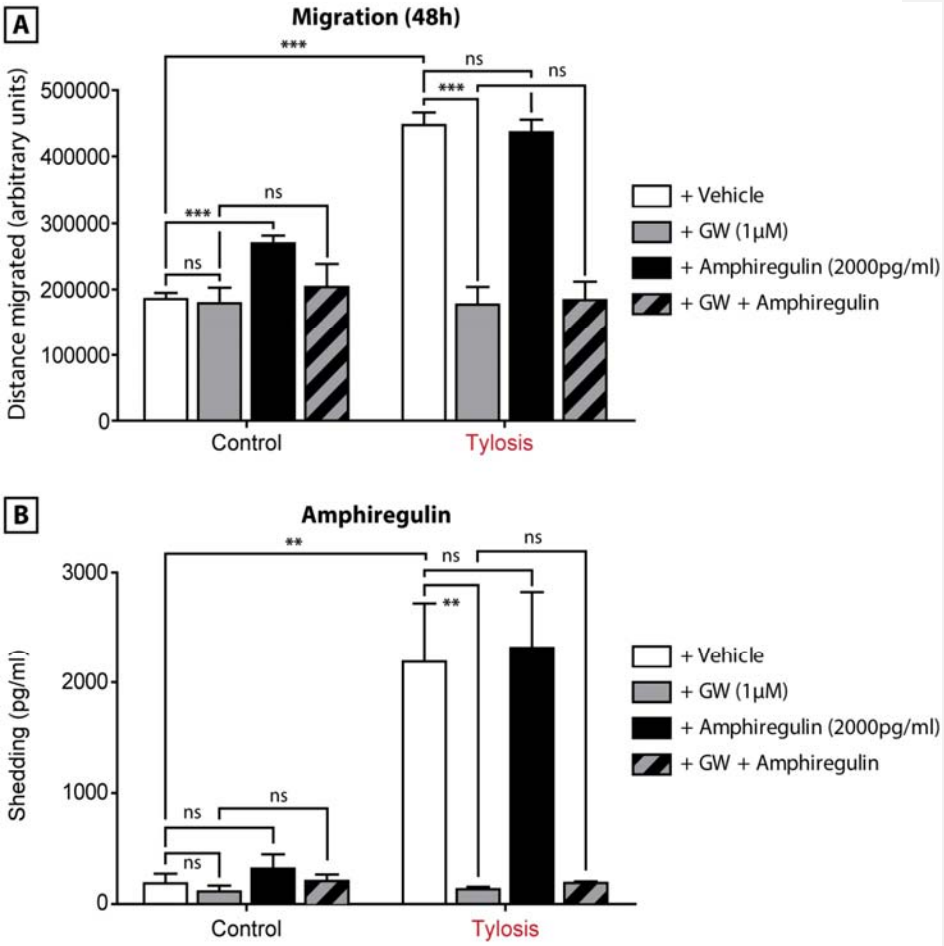

Figure 4.25: The effect of amphiregulin supplementation on migration of control and TOC keratinocytes, GW280264X-induced migration inhibition, and amphiregulin shedding. **A:** Quantification of keratinocyte migration 48 hours after scratch wounding, when cultured in medium (lacking exogenous EGFR ligands) supplemented with either a vehicle control (DMSO), 2000 pg/ml amphiregulin, 1μM GW280264X (GW), or both amphiregulin and GW280264X (both at the same concentrations) **B:** Shedding of amphiregulin from control and TOC keratinocytes measured by ELISA, representing shedding over a 24 hour period, when keratinocytes were cultured in the same conditions as described for A. Data in all cases represent results from three separate experiments on each cell line. "Control" results represent pooled data from K17 and Neb1 cell lines, "Tylosis" results represent pooled data from TYLK1 and TYLK2 cell lines. Statistical analysis was performed using 2-way ANOVA with Bonferroni's post-hoc test; ns: not significant; *p<0.05; **p<0.01; ***p<0.001.

Therefore, although it is capable of stimulating increased migration in the presence of functional ADAM17, amphiregulin alone is not capable of compensating for the loss of ADAM17 function mediated by GW280264X. These data therefore imply that either other factors than amphiregulin, or a combination of amphiregulin and other factors shed by ADAM17, are responsible for the migratory activity seen in TOC keratinocytes. Considering the wide range of substrates shed by ADAM17, and the influence these substrates can have on other signalling pathways (such as on IL-6 and IL-8 secretion), it would be expected that the interplay of several shed factors would influence the migratory phenotype observed.

4.2.17 **Electron microscopy of desmosomes in TOC and control epidermis**

As well as its sheddase activities, ADAM17 plays a key role in the regulation of desmosomes, intercellular junction complexes which function to provide strong adhesions between cells in tissues subject to high levels of mechanical stress, particularly the skin and heart. The structure and function of desmosomes, and their regulation be ADAM17 and EGFR signalling, are described in sections 1.1.14-15.

To investigate the status of desmosomes in TOC, keratinocytes from the spinous layer of TOC-affected individuals' skin were examined by electron microscopy, and their desmosomes studied. When analysed, it was observed that the desmosomes in TOC skin lacked the electron-dense midline found in mature desmosomes of control skin (figure 4.26, white arrows). This absence of a midline is indicative of the desmosomes being in a calcium-dependent, immature state associated with wound healing, keratinocyte motility and mitosis (Brooke ~~et al~~*et al*., 2012), that contrasts with the hyperadhesive, calcium-independent state of midline-containing desmosomes that are found in normal epidermis under standard conditions.

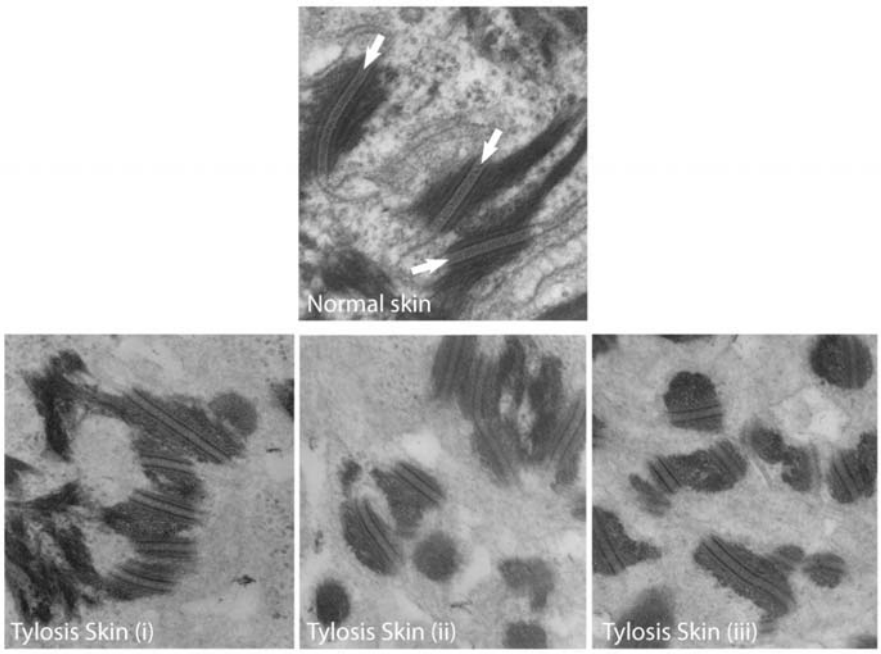

Figure 4.26: Control and TOC desmosome electron microscopy. Analysis of desmosomes in TOC skin from three TOC-affected individuals, compared to controls showed the presence in TOC skin of desmosomes lacking the electron-dense midline (white arrows) found in mature, calcium-independent desmosomes of control skin.

4.2.18 Desmoglein expression in TOC and control keratinocytes

Next, the expression of the desmosomal cadherin desmoglein 2 (DSG2), whose cleavage is dependent on ADAM17 and EGFR signalling, was examined by western blotting. The importance of ADAM17 in DSG2 cleavage is illustrated by the ADAM17-null individual described in chapter 3. This individual displayed increased expression of DSG2 by western blotting in his keratinocytes, and an increased presence of DSG2 at the plasma membrane of keratinocytes in epidermal sections (see section 3.2.11).

When keratinocytes expressing ADAM17 are grown in the presence of EGF, DSG2 shedding can be expected to occur constitutively, due to the presence of active EGFR signalling, and result in the presence of a relatively low level of DSG2 (figure 4.27, A, left panel). However, removal of EGF can be expected to lead to a reduction in EGFR signalling, and therefore DSG2 cleavage, in control cell lines and thereby increase levels of DSG2 in cell lysates. Meanwhile,

TOC keratinocytes will retain a similar level of DSG2 shedding, and hence show no increase in the presence of DSG2 by western blot, as a result of the increased level of constitutive EGFR ligand shedding displayed by them. As expected, this pattern of DSG2 expression was observed (figure 4.27, A, right panel). When grown in the presence of EGF, levels of DSG2 expression did not differ significantly between any of the four cell lines tested; whereas in the absence of EGF, DSG2 expression in both TYLK1 and 2 cells was significantly lower than either control cell line ($p<0.05$ in all cases).

To further investigate ADAM17-mediated DSG2 cleavage, expression of its specific intracellular cleavage product (Nava ~~et al~~*et al*., 2007) was measured in all cell lines, in the presence and absence of EGF. Corresponding with expression of full-length DSG2, expression of this cleavage product did not differ between all cell lines in the presence of EGF, but was noticeably reduced in control cells in the absence of EGF, whilst remaining present in TYLK1 and 2 cells (figure 4.27, B).

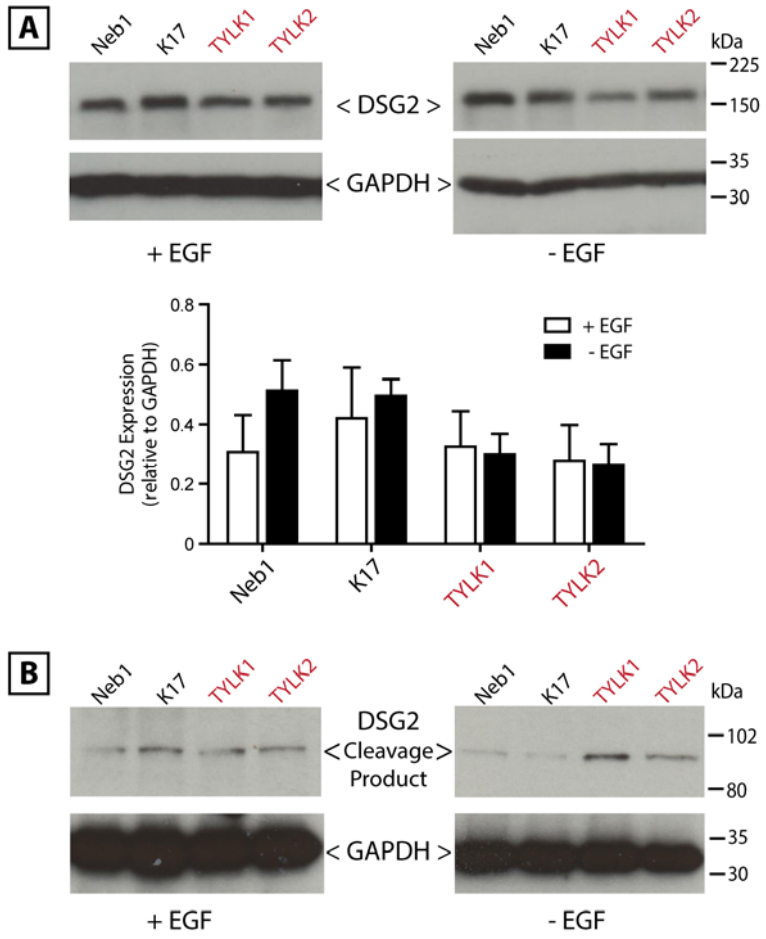

Figure 4.27: Desmoglein 2 expression in control and TOC keratinocytes. **A:** Western blotting of full-length desmoglein 2 (DSG2) in control and TOC keratinocytes, in whole cell lysates of keratinocytes cultured for 24 hours in the presence (left) or absence (right) of exogenous EGF. Data shown in the graph ~~is~~ are representative of three separate experiments. **B:** Western blotting of a specific intracellular DSG2 cleavage product in the same whole cell lysates described for A.

4.2.19 Transglutaminase activity in TOC and control epidermis, and in 3D culture of TOC and control keratinocytes

ADAM17-dependent signalling through the EGFR has recently been shown to regulate the function of Transglutaminase 1 (TGM1) in the epidermal barrier ~~(Franzke et al., 2012)(Franzke et al., 2012)(Franzke et al., 2012)(Franzke et al., 2012)(Franzke et al., 2012)~~. In keratinocyte-restricted ADAM17-knockout mice, loss of ADAM17 sheddase activity significantly reduced TGM1 activity in the upper layers of the epidermis (Franzke ~~et al~~*et al.*, 2012), a phenotype which could be reversed by the application of topical TGFα. Similarly, in a human ADAM17 loss-of-function individual (whose inflammatory skin disease superficially resembles that seen in mice lacking epidermal ADAM17 or EGFR expression) TGM1 activity was significantly reduced in the epidermis (as shown in section 3.2.10).

TGM1 activity in the epidermis of TOC patients and controls was quantified using an assay based on the incorporation of the biotinylated amine donor mono-dansylcadaverine (Biot-MDC), as described in section 3.2.10 Significantly increased TGM1 activity staining was observed in the granular layer of TOC skin compared to controls (figure 4.28, A), indicative of increased activity. Furthermore, a significant increase in TGM1 activity was also observed in three-dimensional, organotypic culture models of TOC keratinocytes, where the enzyme activity was more broadly distributed throughout the suprabasal epidermal layers (figure 4.28, B). These data suggest an increased level of EGFR-dependent TGM1 function in TOC skin, and imply that TOC epidermis may demonstrate improved barrier function.

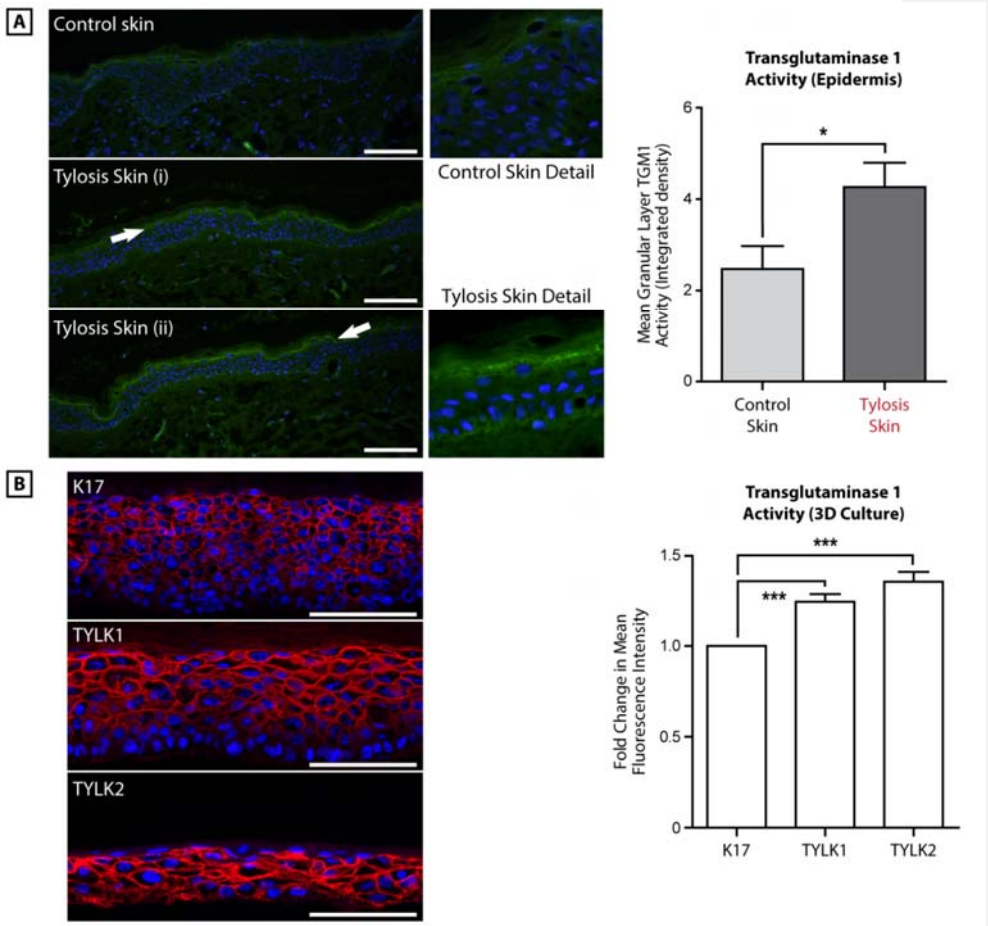

Figure 4.28: Transglutaminase 1 (TGM1) activity in control and tylosis epidermis and epidermal equivalents. **A:** TGM1 activity in the granular layer (white arrows) of control and TOC-affected epidermis, assayed by the Biot-MDC amine donor assay.. **B:** TGM1 activity (measured by the Biot-MDC assay) in three-dimensional organotypic culture models of a control (K17) and two TOC (TYLK1 and TYLK2) keratinocyte cell lines. Data in the graphs shown represent results from three separate experiments each. Statistical analysis was performed using student's unpaired t-test to compare between control and tylosis skin (A) or to individually compare the results of both TYLK cell lines with K17; *p<0.05; **p<0.01; ***p<0.001.

4.3 ~~Discussion~~ Summary of chapter

In this chapter, the relationship between iRHOM2 and ADAM17, and its downstream effects, is examined in the inherited skin disease Tylosis with Oesophageal Cancer (TOC). Western blotting and immunofluorescence staining of ADAM17 in keratinocytes derived from TOC-affected individuals revealed the presence of an increased level of mature, active ADAM17, and increased localisation of ADAM17 to the plasma membrane (its primary site of sheddase activity) in TOC keratinocytes compared to controls. This increased expression of mature ADAM17 was dependent on iRHOM2, and implies that TOC-associated iRHOM2 mutations – which affect an iRHOM2 domain required for interaction with ADAM17 during its maturation process – contribute to an upregulation of ADAM17 maturation and activity in TOC keratinocytes. This increase in maturation is accompanied by increased, ADAM17-dependent shedding of ADAM17 substrates, notably including numerous members of the EGFR ligand family, and other cytokines from these keratinocytes. Importantly, the effects of TOC on ADAM17 are consistently observed in two different TOC cell lines, and are apparent when these cells are cultured under standard monolayer conditions, and in three-dimensional, organotypic, epidermal-equivalent cultures. Upregulation of ADAM17 substrate shedding is also observed in peripheral blood mononuclear cells from TOC patients, illustrating the physiological relevance of these findings.

Prior to the investigations described here, TOC keratinocytes had notably been described as displaying increased proliferation and migration, and to act in an EGFR ligand-independent manner in both these aspects. In the studies described here, growth factors shed by TOC keratinocytes, but not control keratinocytes, were shown to be able to significantly increase keratinocyte migration. Inhibition of ADAM17 sheddase activity with the small molecule inhibitor GW280264X led to an almost total abrogation of ADAM17-dependent EGFR ligand shedding, and a concurrent, highly significant reduction in keratinocyte migration, an effect which was particularly potent in TOC keratinocytes compared to controls. Application of the ADAM17 substrate amphiregulin (the EGFR ligand shed at the highest level by TOC keratinocytes) also led to increased control keratinocyte migration, in a fashion resembling that seen with the application of medium conditioned by TOC keratinocytes, but could not however compensate for the migration reduction resulting from ADAM17 inhibition.

As well as substrate shedding, other processes regulated by ADAM17 in keratinocytes also showed signs of perturbation in TOC. Desmosomes in TOC epidermis were noticeably lacking in the electron dense midlines found in the mature desmosomes of otherwise normal control

skin – an arrangement indicative of desmosomes being present in a calcium-dependent, immature state associated with keratinocyte migration and wound-healing activity. Corresponding with this finding, turnover of the ADAM17 substrate (and desmosome component) desmoglein 2 appeared to be upregulated in TOC keratinocytes compared to controls. Finally, activity of the differentiation-dependent enzyme transglutaminase 1, which is regulated by ADAM17-dependent EGFR signalling, was found to be significantly upregulated in TOC, in both skin sections from TOC patients, and organotypic keratinocyte cell line cultures. This is indicative of increased EGFR signalling in the TOC epidermis (a suggestion borne out by increased EGFR phosphorylation in organotypic TOC keratinocyte cultures), and implies that increased barrier function may be present in TOC skin.

The findings of increased ADAM17 activity, and particularly of upregulated EGFR ligand shedding, offer several potential clues to the pathogenesis of TOC in the skin, and to the striking susceptibility to oesophageal squamous cell carcinoma that is observed in TOC patients. The implications of these finding will be discussed in greater detail in chapter 6.

Chapter 5

Cytosolic phospholipase A2-α mutation in cryptogenic multifocal ulcerative stenosing enteritis

5 Cytosolic Phospholipase A2-α mutation in Cryptogenic Multifocal Ulcerative Stenosing Enteritis

5.1. Introduction

This chapter describes investigations into the cause and pathogenesis of a severe, autosomal recessive gastrointestinal disease, in a single family of Serbian origin. This condition has been lifelong, and features multiple severe extra-intestinal complications. Genetic analyses (to be described below) associated this condition to a homozygous deletion mutation in the *PLA2G4A* gene, which segregates with disease in the siblings' family.

This chapter will describe in detail the role of *PLA2G4A*'s gene product cytosolic phospholipase A2-α (henceforth cPLA$_2$α; also known as phospholipase A2 group IVA) in the small intestine, the disease observed, the genetic investigations that led to the identification of *PLA2G4A* mutations as being associated with it, and the predicted functional consequences of the mutation. Expression of cPLA$_2$α will be examined in the intestine and peripheral blood cells of the affected ~~individuals,~~individuals and the function of cPLA$_2$α will be analysed, using the platelet-aggregating activity of the cPLA$_2$α product thromboxane A$_2$ as a measure of enzyme function.

5.1.1 The small intestine

The small intestine (small bowel) is the section of the gastrointestinal tract that immediately follows the stomach. Made up of three distinct sections (the duodenum, jejunum and ileum), it is the primary site where the digestion and absorption of food takes place. Unlike other parts of the gastrointestinal tract, cancer of the small intestine remains relatively rare (Matsumoto ~~et al~~*et al*., 2004), though inflammatory small bowel conditions represent a significant health burden. The intestinal lumen is lined with a specialised columnar epithelium which is described in detail in section 1.1.2.

5.1.2 Cryptogenic Multifocal Ulcerative Stenosing Enteritis

The syndrome known as cryptogenic multifocal ulcerative stenosing enteritis (CMUSE) is an extremely rare condition characterised by recurrent upper small intestinal ulceration and stenosis (the abnormal narrowing of the small bowel resulting from the development of numerous fibrous strictures) of unknown aetiology. The condition was probably first described in the late fifties and early sixties (Kohoutova ~~et al~~*et al*., 2013), and remains very rarely diagnosed, with only around sixty cases published so far. However, there is a high likelihood that the condition may frequently be misdiagnosed and mistaken for more common causes of small bowel ulceration, such as Crohn's disease and non-steroidal anti-inflammatory drug (NSAID)-induced enteropathy (to be discussed in 5.1.3).

The pathophysiology of CMUSE has not presently been clarified. The suggestion that the pathology of CMUSE may be immunological in nature is supported by a favourable response to treatment with systemic glucocorticosteroids in numerous CMUSE-affected individuals (Kohoutova ~~et al~~*et al*., 2010). Intestinal ulceration can also be caused by a number of medications, including thiazides and potassium tablets (Campbell and Knapp, 1966). Most strikingly however, the numerous small bowel lesions that are observed in these patients resemble those associated with the use of ~~non-steroidal anti-inflammatory drugs (~~NSAIDs~~)~~, an extremely common class of analgesic and anti-inflammatory drugs that includes medications such as aspirin and ibuprofen.

5.1.3 Non-steroidal anti-inflammatory drugs (NSAIDs) in bowel inflammation

NSAID use is extremely well described as a cause of gastro-duodenal (Soll ~~et al~~*et al*., 1991, Griffin ~~et al~~*et al*., 1991) and small intestinal (Higuchi ~~et al~~*et al*., 2009, Allison ~~et al~~*et al*., 1992) ulceration, as well as strictures of the small intestine (so-called 'diaphragm disease') that result in multiple concentric stenoses of the intestinal lumen (Bjarnason ~~et al~~*et al*., 1988, Matsuhashi ~~et al~~*et al*., 1992, De Petris and Lopez, 2008, Fellows ~~et al~~*et al*., 1992), which are observed following long-term use of NSAIDs at high doses. NSAIDs mechanism of action is as inhibitors of the cyclooxygenase (COX-1 and -2) enzymes, which function as the rate limiting synthases in the production of prostaglandins, prostacyclins and thromboxanes (a sub-group of eicosanoids together known as prostanoids). Reduction in the synthesis of prostanoids is considered to be primarily responsible for NSAID-induced small bowel disease (Yamada ~~et al~~*et al*., 1993, Higuchi ~~et al~~*et al*., 2009).

5.1.4 Prostanoids

Prostanoids are a group of lipid intercellular mediators derived from fatty acids. They are part of a larger grouping known as eicosanoids – all of which are synthesised ultimately from the polyunsaturated omega-6 fatty acid arachidonic acid (Vane ~~et al~~*et al*., 1998) – within which they are defined by the requirement for COX enzymes in their synthesis. An illustration of the prostanoid synthesis pathway is shown in figure 5.1, which also shows the structures of the common prostanoids prostaglandin E_2 (PGE_2), D_2 (PGD_2), and I_2 (PGI_2, also known as prostacyclin), and thromboxane A_2 (TxA_2). Prostanoids signal through specific G-protein coupled receptors; a single receptor each exists for TxA_2, PGI_2 and PGF_2 (a derivative of PGD_2), whilst two exist for PGD_2, and four for PGE_2 (Smyth ~~et al~~*et al*., 2009).

As described, prostanoid synthesis is dependent on the actions of COX enzymes, which convert arachidonic acid into prostaglandin H_2, which can then be converted into the various prostanoids through the actions of specific synthase enzymes. Two closely related COX enzymes (COX-1 and -2) exist; COX-1 is expressed constitutively in most mammalian cells, and is the dominant source of prostanoids involved in normal housekeeping functions, including gastrointestinal cytoprotection. Meanwhile COX-2 is inducible by stimuli such as pro-inflammatory cytokines and mechanical stress (FitzGerald and Loll, 2001).

Prostanoids have wide ranging effects on numerous tissues in mammals. For example, prostanoid synthesis is significantly increased in inflammation (largely as a result of COX-2 induction), during which PGE_2 and PGI_2 promote blood flow to inflamed areas, enhancing oedema and leukocyte infiltration (Hata and Breyer, 2004). The same two prostaglandins reduce the activation threshold of peripheral nociceptor (pain-sensing) neurons to stimulation, potentiating the effects of locally acting autocoids such as bradykinin in producing pain (Smyth ~~et al~~*et al*., 2009). The importance of prostanoids in pain generation is underlined both by the use of COX-1 and -2 inhibitors as analgesics, and by prostaglandin receptor-knockout mice, who display increased tolerance to pain (Minami ~~et al~~*et al*., 2001). Among other tissues, prostanoids also play important roles in the kidney, modulating renal blood flow and glomerular filtration (Breyer and Breyer, 2000), and the lungs, where they are involved in airway inflammation.

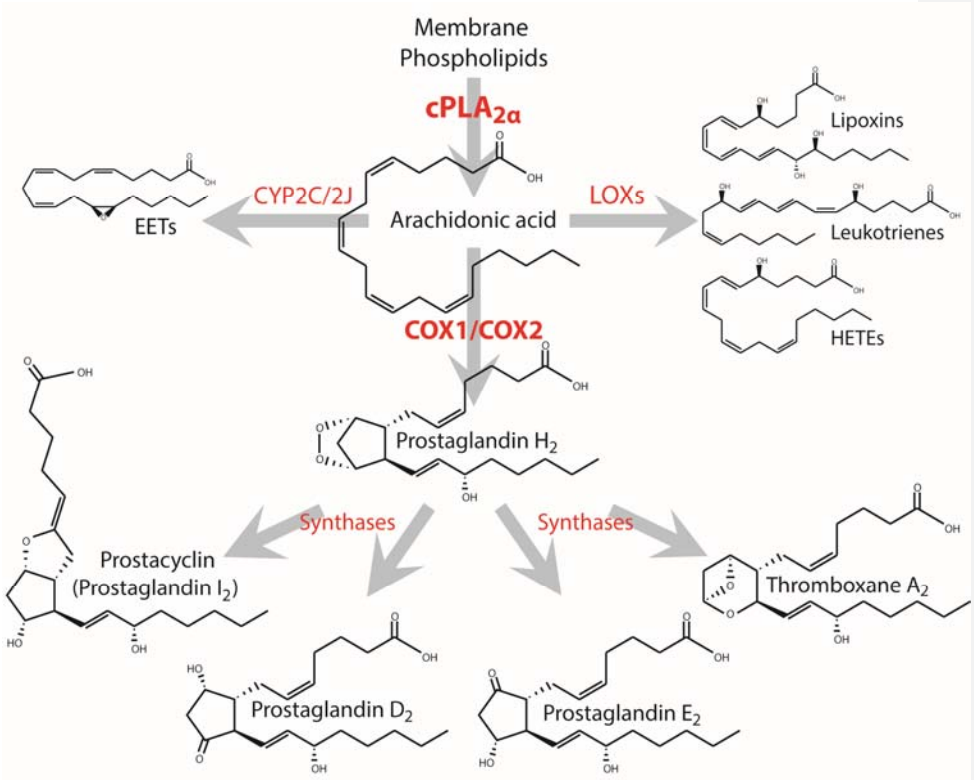

Figure 5.1: The eicosanoid synthesis pathway. An illustration of the eicosanoid synthesis pathway downstream of cytosolic phospholipase A2-α (cPLA$_2$α). Particular focus is given to those members of the prostaglandin family which lie downstream of the cyclooxygenase enzymes COX-1 and COX-2, as these are the eicosanoids whose absence is considered the principal cause of NSAID-induced enteropathy.

5.1.5 Prostanoids in gastrointestinal defence

The most easily disrupted role of prostanoids in mammals is their function in gastrointestinal defence. To protect against the numerous potentially damaging factors present in the gastrointestinal environment (such as very strong acid, tissue digesting enzymes and microorganisms), a variety of strategies are employed to protect the gastrointestinal mucosa. These include a high level of epithelial cell production (as discussed in section 1.1.10), and the production of a mucus barrier lining the epithelium, which both physically protects epithelial cells, and also traps secreted bicarbonate ions to protect against acid (principally important in the stomach, where large amounts of hydrochloric acid are generated) (Laine ~~et~~

~~al~~*et al*., 2008). Gastrointestinal mucus is made up of 95% water, and around 5% mucin glycoproteins, which form into large multimeric structures (Laine ~~et al~~*et al*., 2008). Mucus has different properties in different sections of the GI tract, being more penetrable to nutrients in the small intestine, whilst adopting a complex dual-layer structure in the stomach and colon to provide better protection against acid and bacteria respectively (Ermund ~~et al~~*et al*., 2013).

Continuous generation of prostanoids is of key importance to the maintenance of GI mucosal integrity, a fact which has been clear since prostanoid inhibition was identified as the major method by which NSAIDs produce GI damage in 1971 (Vane, 1971). PGE_2 and PGI_2 play particularly important roles, stimulating the secretion of mucus (and bicarbonate in the stomach), increasing blood flow to the epithelium and accelerating restitution of the epithelium in case of damage. In the latter case, PGE_2 in particular has been shown to stimulate cell proliferation, via transactivation of the EGFR in a process dependent on Src, metalloproteases and TGFα (Pai ~~et al~~*et al*., 2002), and which therefore can be presumed to involve ADAM17. The importance of prostanoids in GI epithelial healing is illustrated by the fact that depletion of prostaglandins during the healing of gastric ulcers both reduces the rate of healing, and predisposes the future ulcer relapse (Kobayashi and Arakawa, 1995). Furthermore, treatment with neutralising antibodies against PGE_2 and PGI_2 results in the formation of gastric and duodenal ulcers in rabbits and dogs (Redfern and Feldman, 1989, Redfern ~~et al~~*et al*., 1988).

5.1.6 The phospholipase family

Production of prostanoids is dependent on the activity of the COX enzymes, using free arachidonic acid as a substrate. In mammals, the release of arachidonic acid is one of a number of processes that come under the control of the phospholipase family, a large group of diversely expressed and often structurally unrelated enzymes responsible for the hydrolysis of phospholipids. In mammals, the phospholipases are grouped into four broad categories, phospholipases A (further subdivided into A_1 and A_2), C and D, according to the type of reaction they catalyse (De Maria ~~et al~~*et al*., 2007). All phospholipases hydrolyse reactions in the region of the glycerol 'backbone' of a phospholipid, but in differing positions and with different products. The structure of a typical phospholipid, and the different cleavage sites of the phospholipase enzymes, is illustrated in figure 5.2.

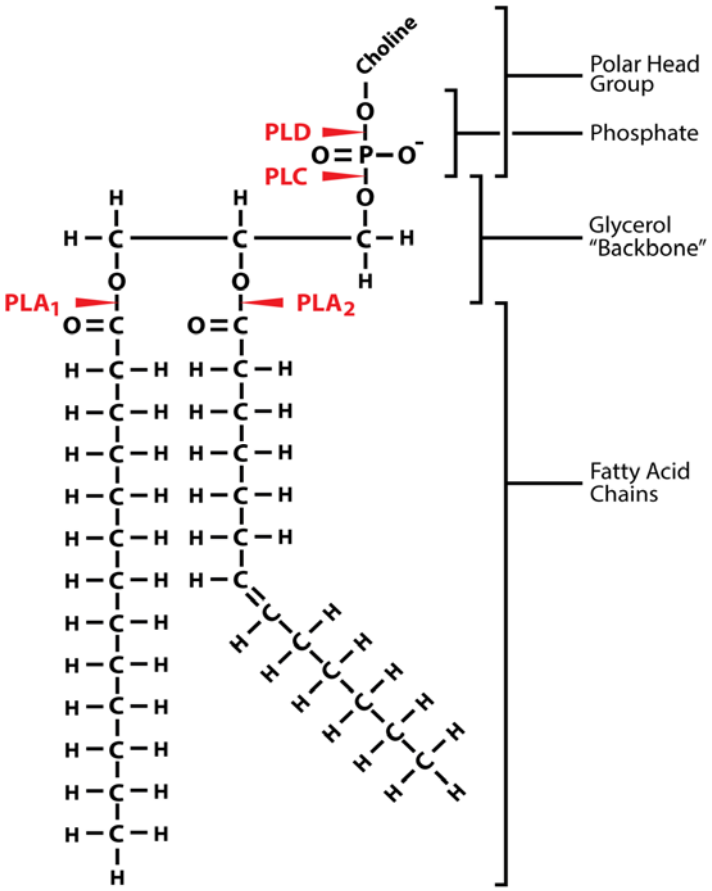

Figure 5.2: An illustration of the structure of a typical phospholipid (a phosphatidylcholine), showing the different positions that are hydrolysed by the four major families of phospholipase (PLA_1, A_2, C and D). Note that the fatty acid chains shown are for representative purposes and may not represent a conformation found in nature, and that the choline group can be replaced with a number of other groups, such as serine or ethanolamine.

In brief, enzymes of the phospholipase A class are known as deacylating phospholipases, as they are responsible for the release of acyl chains associated with phospholipids. PLA_1 phospholipases cleave the *sn-1* position of phospholipids, which is enriched in saturated fatty acids, to release the fatty acid chain associated to that position (Ghosh ~~et al~~*et al.*, 2006); whilst the PLA_2 class cleave at the *sn-2* position – enriched for unsaturated fatty acids – to release the fatty acid chain found associated there (Leslie, 1997, Ghosh ~~et al~~*et al.*, 2006). The numerous members of the PLC class hydrolyse phospholipids between the glycerol head and

phosphate group, and are responsible for the hydrolysis of the inner membrane phospholipid phosphatidylinositol-4,5-bisphosphate (PIP_2), generating the release of the second messengers inositol-1,4,5-triphosphate (IP_3) and diacylglycerol (DAG) (Lyon and Tesmer, 2013). This is an important cellular signalling process, involved in the regulation of multiple physiological processes, including muscle contraction, chemotaxis, cell proliferation and survival (Lyon and Tesmer, 2013), making PLCs among the best studied of the phospholipases. Meanwhile, the phospholipase D enzymes catalyse hydrolysis of phospholipids after the phosphate group, and are classically involved in the hydrolysis of phosphatidylcholine, to yield phosphatidic acid and a free choline (Jenkins and Frohman, 2005).

Of particular interest are those enzymes belonging to the PLA_2 family, as it is to this subgroup that the enzyme responsible for intracellular arachidonic acid generation – cytosolic phospholipase A2-α – belongs. There are approximately 20 human genes that encode members of the PLA_2 family (Six and Dennis, 2000). Ten of these are members of the subgroup of secreted PLA_2s ($sPLA_2$s), while the remainder are intracellular, belonging to either the group VI, calcium-independednt PLA2s ($iPLA_2$s), or the group IV, cytosolic PLA_2s ($cPLA_2$s) (Ghosh ~~et al~~*et al.*, 2006). The $sPLA_2$s have diverse functions, including hydrolysis of cell surface phospholipids (Bezzine ~~et al~~*et al.*, 2000), potent anti-microbial activity via the degradation of bacterial phospholipids (Koduri ~~et al~~*et al.*, 2002), and regulation of serum lipoproteins (Webb, 2005). The intracellular PLA_2s have no structural homology to the $sPLA_2$s (Ghosh ~~et al~~*et al.*, 2006), and play a wide variety of roles within the cell, which depend largely on their specificity for particular phospholipids or acyl chains.

5.1.7 Cytosolic Phospholipase A2-α and eicosanoid synthesis

Cytosolic phospholipase A2-α ($cPLA_2\alpha$) is a very highly conserved member of the PLA_2 family: human and mouse $cPLA_2\alpha$ homologues share over 95% amino acid identity, and over 80% identity is shared between the human enzyme and its homologues in the chicken, zebrafish, and *Xenopus* (Clark ~~et al~~*et al.*, 1991). $cPLA_2\alpha$ is joined in the cytosolic PLA_2 family by five other members, commonly referred to as $cPLA_2\beta$, γ, δ, ε, and ζ, which share 30-37% amino acid identity with $cPLA_2\alpha$ (Ghosh ~~et al~~*et al.*, 2006). All members of the subgroup contain an aspartic acid residue in the active site (Asp549 in $cPLA_2\alpha$) which forms an active dyad with a serine residue (Ser228), with the presence of an arginine (Arg200) residue also required for

catalytic activity. All but one of the cytosolic PLA_2 family contain a C2 domain, a calcium-binding domain found in many mammalian proteins which promotes interaction with phospholipid membranes (Nalefski and Falke, 1996). Calcium binding to specific loops in the C2 domain is critical for its penetration into the membrane (Murray and Honig, 2002), making the $cPLA_2$ enzymes highly calcium-dependent. Differences in the C2 domains of each enzyme are thought to contribute to the specificity of the enzyme, by regulating the membrane-binding properties of each, and therefore the types of phospholipid each enzyme will interact with. $cPLA_2\alpha$ differs from the other members of the $cPLA_2$ family in being almost ubiquitously expressed, where most other members of the family, excluding the also widely expressed $cPLA_2\beta$, are limited to specific tissues or disease states. These include $cPLA_2\gamma$, found only in the heart, skeletal muscle and brain; and $cPLA_2\delta$, found only in the cervix, foetal skin, and psoriatic lesions (Ghosh ~~et al~~*et al*., 2006). Crystal structure models of $cPLA_2\alpha$ are shown in figure 5.3, illustrating the major domains.

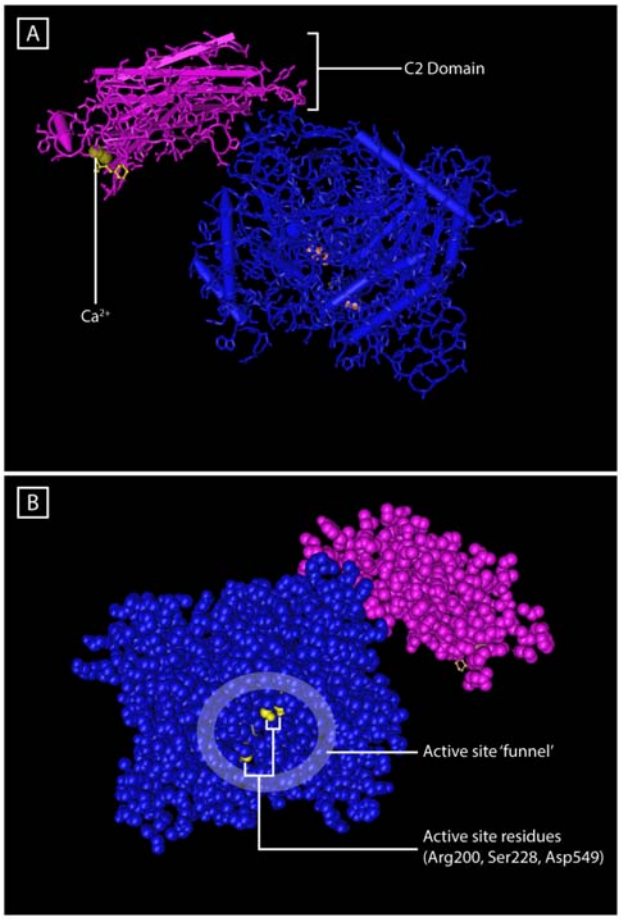

Figure 5.3: Crystal structure models of cPLA$_2$α. **A:** A tubular model of cPLA$_2$α, showing secondary and tertiary structures of the enzyme, and the two major domains: the C2 domain (pink), and catalytic domain (blue). The binding sites of Ca^{2+} atoms in the C2 domain are shown in yellow. **B:** Space filling model of cPLA$_2$α (from the reverse angle) illustrating the location of the active site residues (yellow), which are found at the end of a 'funnel-shaped' cavity. The cPLA$_2$α structure was retrieved from the NCBI Conserved Domains database (accession number: cd07200) and visualised using Cn3D software.

Of the PLA$_2$ enzymes, cPLA$_2$α has attracted most interest due to its ability to selectively cleave arachidonic acid – from phospholipids such as phosphatidylcholines, phosphatidylethanolamine, and phosphatidylinositides – a function not shared by any other member of the cPLA$_2$ family. The specificity of cPLA$_2$α for arachidonic acid is dependent on

the architecture of its 'funnel-shaped' active site (Dessen et al et al., 1999). The composition of the active site cleft of the closely related cPLA$_2$γ differs from that of cPLA$_2$α by only 2 amino acid residues; however, this is sufficient to render cPLA$_2$γ unable to cleave arachidonic acid (Dessen et al et al., 1999). cPLA$_2$α activity, and therefore intracellular arachidonic acid production, is tightly regulated by intracellular calcium concentration and phosphorylation of the enzyme at two separate sites (Ser505 and Ser727) by mitogen-activated protein (MAP) kinases and MNK1-related kinases (Hefner et al et al., 2000, Tian et al et al., 2008). cPLA$_2$α activity is also upregulated by numerous stimuli, including TNFα (Lee et al et al., 2013), ceramide-1-phosphate (Pettus et al et al., 2004) and binding to PIP$_2$ (Mosior et al et al., 1998).

As previously described, arachidonic acid serves as the substrate for a broad spectrum of enzymes involved in the synthesis of eicosanoids, including COX-1 and -2, lipooxygenases, and cytochrome P450 eoxygenase. cPLA$_2$α-mediated arachidonic acid release is thus a rate limiting step in eicosanoid production, and cPLA$_2$α activity therefore plays an important role in the wide variety of physiological and pathological processes affected by eicosanoids. An illustration of the eicosanoid synthesis pathway dependent on cPLA$_2$α activity is shown in figure 5.1.

Mice deficient in cPLA$_2$α show normal development and life-span, but demonstrate defects in reproduction (Bonventre et al et al., 1997), parturition (Uozumi et al et al., 1997), renal function (Uozumi and Shimizu, 2002) and the allergic response (Uozumi et al et al., 1997), alongside exaggerated heart and striated muscle growth (Haq et al et al., 2003), and the presence of numerous ulcerative lesions of the small intestine (Takaku et al et al., 2000). These effects can be associated with particular eicosanoid pathways. For instance, mice deficient in COX-2 demonstrate impaired inflammatory responses, impaired resolution of inflammation, impaired renal development, and impaired female reproduction (Yu and Funk, 2007),(Rouzer and Marnett, 2009). However, these mice also demonstrate a degree of resistance to inflammatory diseases; for example, they are highly resistant to experimental autoimmune encephalomyelitis, a mouse model of multiple sclerosis (Marusic et al et al., 2005).

5.1.8 The importance of cPLA$_2$α in humans

Considering its central role in the synthesis of prostanoids and other members of the eicosanoid family, it would be expected that any disruption in cPLA$_2$α function would have significant effects on health, in particular on the gastrointestinal tract.

A single case of ileo-jejunal ulceration, accompanied by gastrointestinal blood loss, anaemia, and impaired eicosanoid biosynthesis (symptoms of which developed in the 4th decade of life), has previously been reported to be associated with compound heterozygous single base-pair missense mutations in *PLA2G4A.* These rare (not previously described) missense mutations were expected to alter the conformation of cPLA$_2$α in the individual studied, who was found to have reduced (but not absent) cPLA$_2$α protein expression, and reduced eicosanoid secretion (TxA$_2$, PGI$_2$ and PGE$_2$ were found at 16, 30 and 43% of normal expression levels respectively) (Adler ~~et al~~*et al.*, 2008).

5.2 Results – cytosolic phospholipase A2-α mutation in cryptogenic multifocal ulcerative stenosing enteritis

5.2.1 Case reports

This report describes a disease present in a pair of siblings (one male, born 1963; and one female, born 1966), of Serbian origin. The parents of the affected siblings were not known to be consanguineous, though both did hail from the same small, isolated community in Serbia. The case reports below are adapted from those written by Dr. Hilary Longhurst (Consultant Immunologist, Barts Health NHS Trust, London).

Both siblings have suffered from severe gastrointestinal (GI) disease from an early age, first presenting at age 4 in the male, and age 2 in the female. Both have suffered from repeated episodes of severe gastric (stomach) and duodenal ulceration, and multiple instances of stenosis (abnormal narrowing of the GI tract resulting from the development of fibrous strictures), particularly affecting the duodenum, ileum and pylorus (the most distal part of the stomach, immediately preceding the duodenum). The severe ulceration has resulted in the formation of perforated ulcers of the stomach and ileum, in the male and female respectively. Multiple adhesions of the small intestine (scar tissue forming across the intestinal lumen in response to damage; particularly in the male sibling), and volvulus (twisting of the intestine) have also been seen, often resulting in bowel obstruction, and gangrene in one case. Both siblings have been affected by gastrointestinal fistulae. In most cases, this disease has been limited to the upper GI tract, with a normal terminal ileum and large intestine having been observed in the male sibling.

Treatments for this in both patients have included vagotomy (resection of the vagus nerve), gastrojejunostomy (the creation of a connection between the stomach and jejunum), and pyloroplasy (widening of the pylorus), as well as emergency surgeries to treat perforated ulcers (in both individuals) and a gangrenous ileum. Secondary to the severe gastrointestinal disease, complications have included dysphagia (difficulty swallowing), oesophagitis, vitamin B_{12} deficiency, and bile duct ulceration and fibrosis. Both individuals have developed severe malnutrition and hypoalbuminaemia, requiring total parenteral nutrition.

As well as gastrointestinal disease, both individuals have been affected by a differing spectrum of other disease, including anaemia, renal failure and osteoporosis in both; liver

abcesses, type 2 diabetes and peripheral neuropathy in the male; and gall stones, left ventricular cardiac hypertrophy, bladder fibrosis, ~~endometrosis~~endometriosis and infertility in the female. Furthermore, the female sibling in particular has suffered from repeated infectious disease, with multiple episodes of severe *Campylobacter* enteritis, *Salmonella enteriditis* and *Candida albicans* infections, and infectious xanthogranulomatous pyelonephritis. Full details of the clinical history of the two sibling can be found in Brooke ~~et al~~*et al* (~~Brooke et al., 2014b~~).

Based on the clinical history and histology, the siblings are considered to have severe cryptogenic multifocal ulcerating stenosing enteritis (CMUSE), accompanied by wide ranging complications which may or may not be secondary to the severe gut disease. Symptoms in both siblings have progressed despite maximal medical therapy – most recently with high dose proton pump inhibitors – including eradication of *Helicobacter pylori.* Short courses of moderate-dose corticosteroids were unhelpful in the male sibling, and have not been evaluated in the female. The siblings' mother, father and brother are healthy and have no family history of similar symptoms, with the single exception of a peptic ulcer in the father's middle age, which resolved with a typical clinical course.

5.2.2 SNP homozygosity mapping and exome sequencing

To attempt to identify a genetic cause for the condition observed in the two siblings, a combination of whole genome single nucleotide polymorphism (SNP) array analysis – to search for regions of homozygosity shared between the two siblings – and exome sequencing was performed.

Whole-genome SNP array analysis of the two affected siblings was performed by Dr. Franz Rüschendorf (Max Delbrück Center for molecular medicine, Berlin, Germany), to identify shared regions of homozygosity. Linkage analysis was performed using two different marker sets, containing 64,983 and 2.44 million SNPs across the entire genome, based on a hypothetical pedigree which assumed a degree of consanguinity between the parents of the affected siblings (a 2nd degree cousin marriage), allele frequencies from a European population, and a model of disease assuming recessive inheritance and complete penetrance. Using this pedigree, the maximum LOD score possible was around 2.38. This linkage analysis revealed two long stretches of the genome with the maximal LOD score of 2.38, on chromosomes 1 and 10. On chromosome 1, the stretch was 9.5Mb in length, and

Formatted: Font: Not Italic

was bordered by the markers rs6425457 and rs4607826, whilst the stretch on chromosome 10 was 5.42 Mb long, between rs11201179 and rs12265445 (figure 5.4). These two stretches were considered to be identical by descent in the two affected individuals.

In tandem, whole exome sequencing was performed on the affected female. Insertion/deletion variation analysis of this exome sequencing data was performed by Dr. Vincent Plagnol (University College London, London) and revealed the presence of a homozygous 4 base-pair deletion (g.155574_77delGTAA) in the *PLA2G4A* gene, located in the splice donor site directly following exon 17 (the penultimate exon) of the gene. *PLA2G4A* (Accession Number: NG_012203.1) maps within the common region of homozygosity found on chromosome 1, at 1q25.

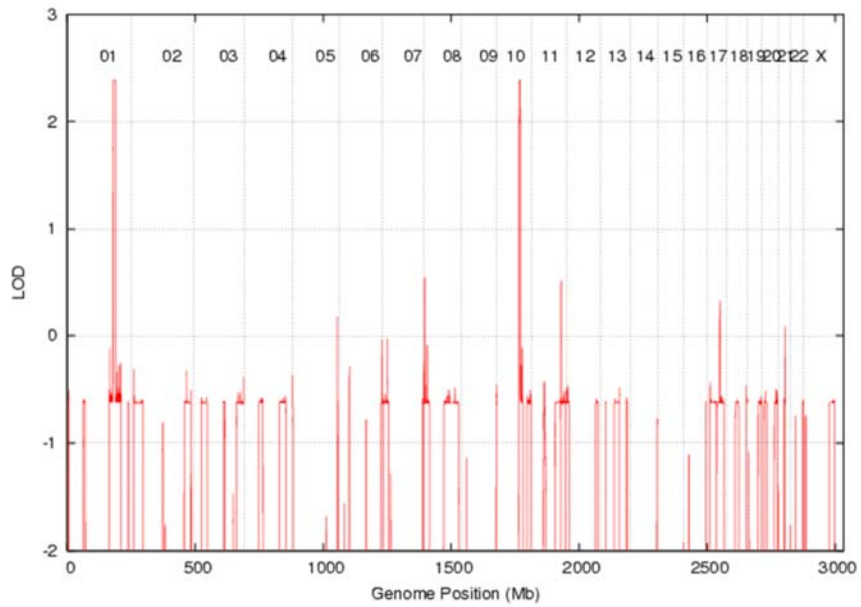

Figure 5.4: Homozygosity mapping revealed the presence of two regions of the genome (on chromosomes 1 and 10) with the maximum possible LOD score of 2.383, which were shared by the affected individuals identically by descent. These same two regions were identified by homozygosity mapping as being homozygous between the two affected individuals. SNP array analysis was performed by Dr. Franz Rüschendorf (Max-Delbrück Center for molecular medicine, Berlin, Germany).

5.2.3 Confirmation of mutations in *PLA2G4A*

To confirm the presence of the g.155574_77delGTAA mutation in both affected siblings, and its segregation with disease, PCR and Sanger sequencing was performed, using primers designed to amplify the mutated region of *PLA2G4A* (primer sequences are shown in appendix 1). Sequencing was performed on the DNA of the two affected individuals, their mother, father and brother (all of whom are unaffected by the disease), and an unrelated, otherwise normal control.

Sequencing confirmed the homozygous presence of the four base-pair deletion in both of the affected individuals, with the mother, father and brother of the siblings all found to be heterozygous carriers of the mutation (figure 5.5), which was absent in an unrelated control. This deletion has never been described before, and is not present in either the dbSNP or 1000 Genomes databases of genetic variation. Although one individual has been identified who carries two compound heterozygous mutations in *PLA2G4A* which result in disease (Adler ~~et al~~*et al*., 2008), this represents the first identification of a deletion mutation being associated with disease in *PLA2G4A,* and only the second identification of any disease-associated mutation in that gene.

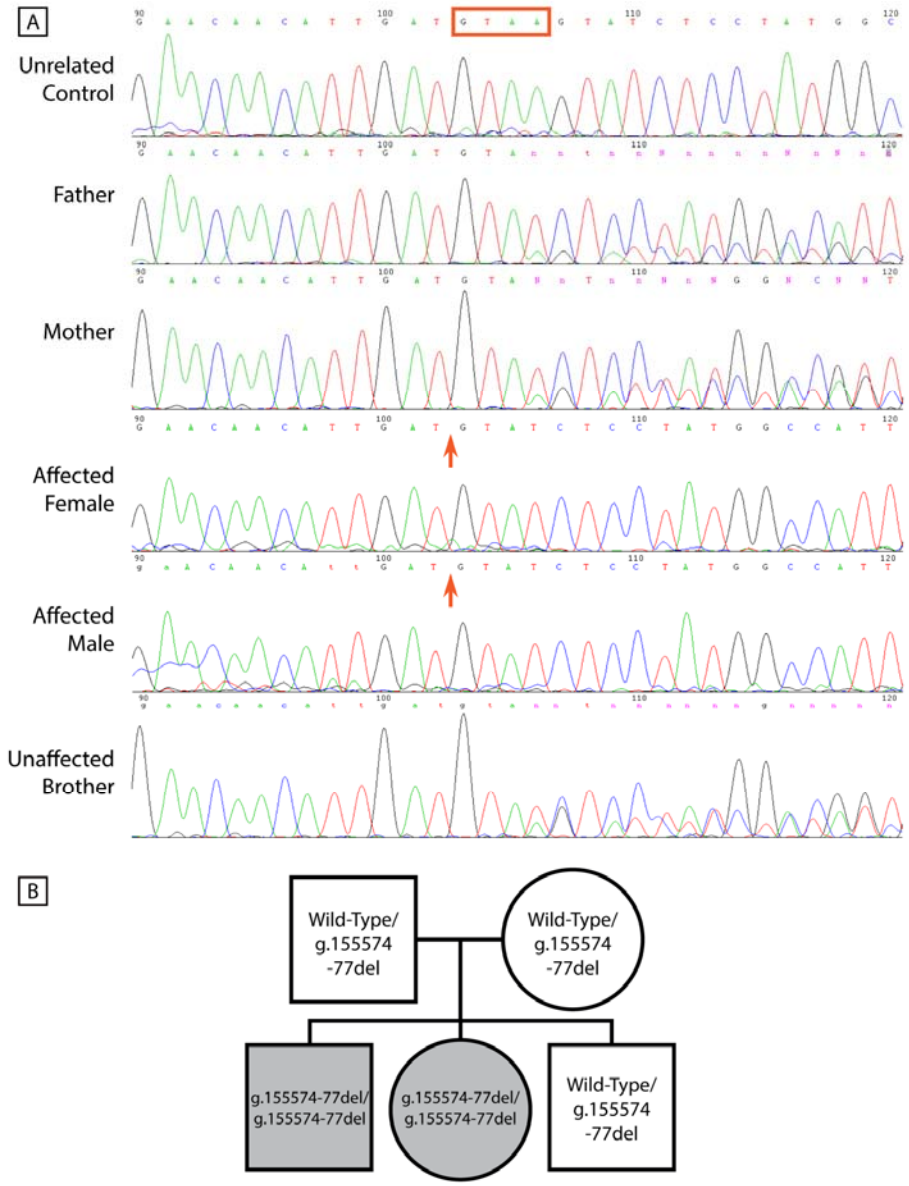

Figure 5.5: Confirmation of *PLA2G4A* mutations segregating with disease in the affected family. **A:** Sanger sequence traces of the g.155574_77delGTAA mutation site in the affected individuals, their immediate family members, and an unrelated control. **B:** A family pedigree based on the presence of the g.155574_77delGTAA mutation illustrates that this mutation segregates with disease in this family (white: unaffected individuals; grey: affected individuals)

5.2.4 Characterisation of *PLA2G4A* mutations

To predict the consequences of the g.155574_77delGTAA mutation in humans, bioinformatic analysis was performed. The mutation is located in the splice donor site that directly follows exon 17 (the penultimate exon) of *PLA2G4A*, the gene encoding cPLA$_2$α, and is predicted to result in the loss of the affected splice donor site, and introduce a frameshift predicted to encode 10 amino acids before a premature stop codon (p.V707fsX10). This would result in the loss of 43 codons from the C-terminus of cPLA$_2$α mRNA, and the loss of 24 amino acids (residues 707-732) from the mature cPLA$_2$α protein product (figure 5.6, A). The deleted area makes up part of the large region known as the cPLA$_2$α catalytic domain, though it does not lie directly adjacent to any of the active site residues, or the 'funnel-shaped' cavity which defines the substrate selectivity of the enzyme. The loss of the deleted region would however be expected to affect the shape of the enzyme. Furthermore, the deleted region is highly conserved between species (figure 5.6, B). In addition to this, the deleted region contains a key regulatory site (serine-727) at which phosphorylation is required for cPLA$_2$α activity (Tian ~~et al~~*et al.*, 2008). Taken together, this analysis suggests that this region would be expected to play an important role in the correct functioning of the enzyme, and its deletion would negatively impact enzymatic activity.

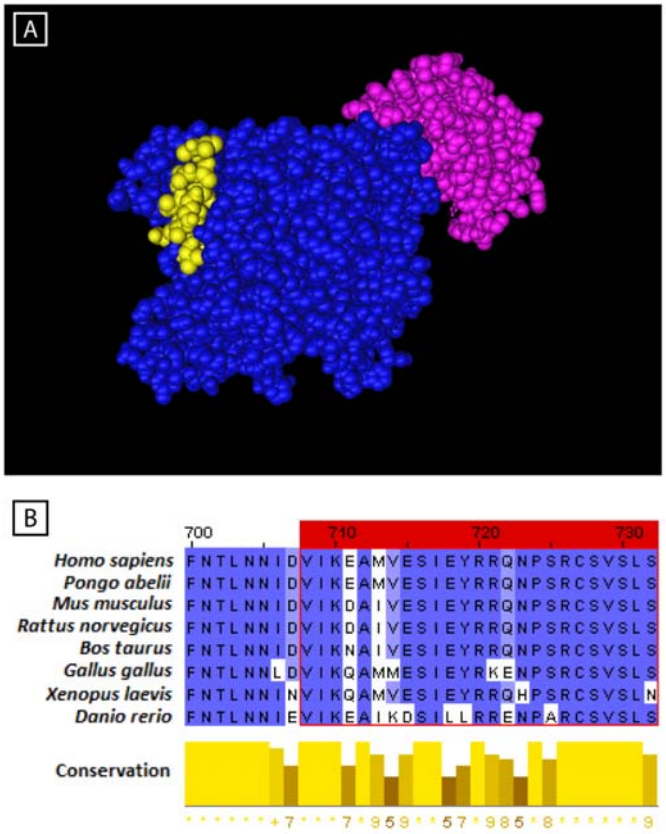

Figure 5.6: Analysis of the consequences of cPLA$_2$α mutation. **A:** Space-filling model of cPLA$_2$α, with the C2 domain in pink, and catalytic domain in blue. The yellow highlighted region represents the region deleted as a result of the g.155574_77delGTAA mutation. Note that some deleted residues are inside the protein structure and thus are not visible. The cPLA$_2$α structure was retrieved from the NCBI Conserved Domains database (accession number: cd07200) and visualised using Cn3D software. **B:** Conservation of amino acids residues in part of the cPLA$_2$α catalytic domain across species. The region predicted to be deleted is highlighted in red. The lower yellow graph illustrates the degree of conservation of each residue, a full-height yellow bar indicating complete conservation between species.

5.2.5 Expression of cPLA$_2$α in affected individuals and controls

To examine how the detected g.155574_77delGTAA mutation affected the expression of cPLA$_2$α, immunohistochemical staining of paraffin-embedded small intestine sections was performed, using an antibody against cPLA$_2$α which targets the protein at a site around serine-505 (i.e. in a location upstream the region predicted to be deleted, and distant from it in the tertiary structure of the enzyme). This staining revealed the presence of high levels of cPLA$_2$α staining in the intestinal epithelium of an unrelated control individual, particularly along the apical membrane of enterocytes. However, no cPLA$_2$α expression could be detected in the small intestine of the affected female or male, with the pattern of staining indistinguishable from the background autofluorescence observed when staining the tissue in the absence of an anti-cPLA$_2$α primary antibody (figure 5.7, A).

Next, expression of cPLA$_2$α was examined by western blotting, in protein lysates derived from the peripheral blood mononuclear cells (PBMCs) of the two affected individuals, and their unaffected father (a heterozygous carrier of the g.155574_77delGTAA mutation). This revealed a complete absence of cPLA$_2$α protein in both affected individuals, whilst the father displayed robust expression (figure 5.7, B).

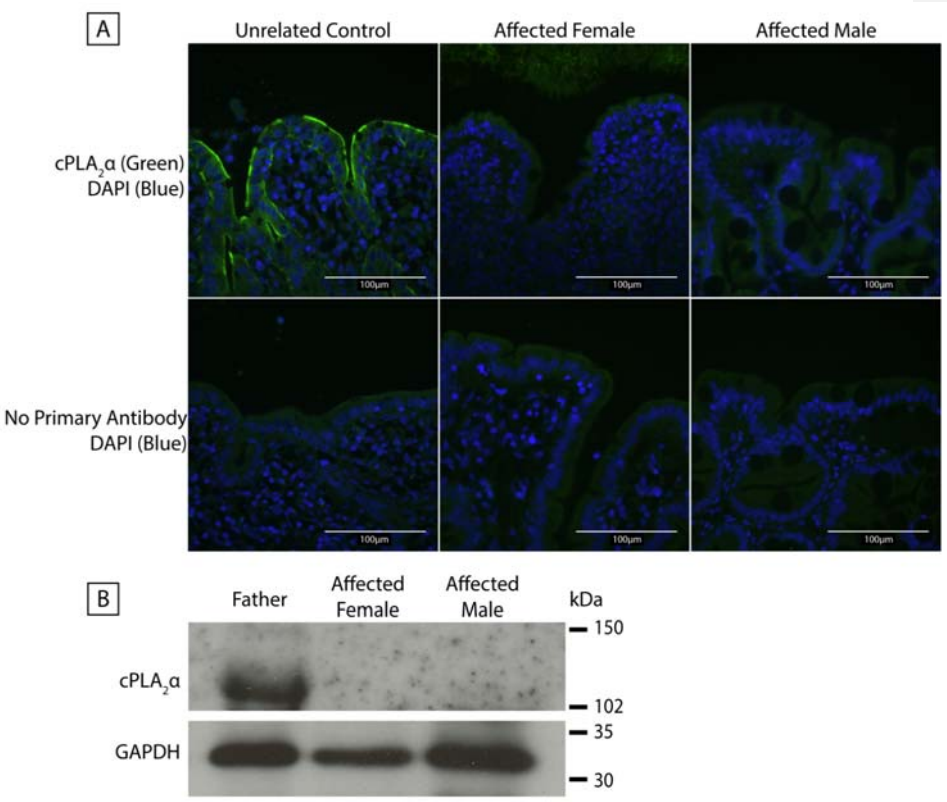

Figure 5.7: cPLA$_2$α expression. **A:** Immunofluorescence of cPLA$_2$α in paraffin-embedded small intestinal sections from an unrelated control and the affected individuals. **B:** Western blotting of cPLA$_2$α in the PBMCs of both affected individuals and their unaffected father.

5.2.6 Thromboxane A$_2$ as a measure of cPLA$_2$α function

Thromboxane A$_2$ (TxA$_2$) is an eicosanoid produced primarily in platelets, which is synthesised from arachidonic acid by the sequential actions of COX-1 or -2 and thromboxane-A synthase 1 (as shown in figure 5.3). As such, its synthesis is dependent on the actions of cPLA$_2$α. TxA$_2$ generated by platelets acts in an autocrine manner on the TxA$_2$ receptor (TP) (Smyth ~~et al~~*et al*., 2009), a G-protein coupled receptor expressed on platelets, as well as a variety of other cell types, such as macrophages, vascular endothelial cells and smooth muscle cells (Nisar ~~et al~~*et al*., 2014). Activated platelets secrete TxA$_2$, which in turn activates other platelets via binding to the TP, which when activated predominantly couples to the G-proteins G$_q$ and G$_{12/13}$. Respectively, these G-proteins facilitate platelet aggregation (via protein kinase C-

dependent pathways), and platelet shape changes (via Rho/Rho kinase-dependent signalling). TxA_2 is therefore a potent stimulant of platelet aggregation. Aggregation of platelets can be induced in plasma *in vitro* by the addition of stimuli such as collagen and adrenaline. Collagen is a strong stimulant of platelet activation *in vivo*, typically in cases where vascular damage exposes collagen in the sub-vasculature to platelets, inducing platelet activation mediated (particularly at lower collagen concentrations) through the production of TxA_2 (Roberts ~~et al~~*et al*., 2004). This makes measuring the aggregation of platelets in the plasma a good measure of TxA_2 production, and therefore of $cPLA_2\alpha$ function.

A second advantage to this method is that inhibition of TxA_2 production can be artificially induced in serum via the use of NSAIDs, in particular aspirin. As with all NSAIDs, aspirin inhibits COX activity; however, aspirin is unique in that it covalently acetylates serine residues in the COX enzymes (ser-529 in COX-1, ser-516 in COX-2) to inhibit enzyme activity irreversibly (Smyth ~~et al~~*et al*., 2009). Irreversible COX inhibition, combined with platelets' limited capacity for *de novo* protein synthesis, means that aspirin inhibits TxA_2 production in a sustained manner. This sustained COX inhibition – and therefore inhibition of platelet aggregation – contributes to aspirin's cardioprotective activity. The addition of aspirin to plasma can therefore act as a control, to study how platelets incapable of TxA_2 production would be expected to act in response to aggregating stimuli.

5.2.7. Platelet aggregation and thromboxane A_2 production in affected individuals and controls

Platelet aggregation was measured in the plasma of the two affected individuals and unrelated controls by light transmission aggregometry, a method by which the amount of light passing through a sample of platelet-rich plasma over time gives an indication of the degree of platelet aggregation in response to a given stimulus. These experiments were performed in collaboration with the laboratory of Prof. Tim Warner (William Harvey Research Institute, Barts and The London School of Medicine and Dentistry, London). Examples of light transmission over a time course are shown in figure 5.8, in which platelet aggregation in response to collagen in the plasma of a healthy volunteer is represented by a large fall in light transmission. However, the response in the plasma of the affected male is significantly abrogated, and follows almost exactly the pattern of a healthy volunteer treated with 30μM aspirin (figure 5.8, A). Note that, in addition to its function as a stimulant of TxA_2

production, collagen acts as a direct physical substrate for platelet aggregation (platelets can directly adhere to it, independent of the influence of TxA_2 [~~(~~Roberts ~~et al~~*et al*., 2004, Morton ~~et al~~*et al*., 1989~~)~~]) meaning that some degree of platelet aggregation would be expected when stimulating with collagen, even in cells completely incapable of producing TxA_2.

Next, the effect of arachidonic acid on platelet aggregation was examined. In this case, the addition of 1mM arachidonic acid potently induced the aggregation of platelets in both healthy controls and the affected male, whilst no aggregation was observed in healthy controls treated with aspirin (figure 5.8, B). This result is consistent with a fully functional TxA_2 synthesis pathway being present downstream of arachidonic acid in the affected male's platelets, suggesting that a lack of arachidonic acid production is the limiting factor in the reduced aggregation observed. Conversely, aspirin inhibits the COX enzymes that are immediately downstream of arachidonic acid in the TxA_2 synthesis pathway (see figure 5.3), meaning that arachidonic acid supplementation would not be expected to increase TxA_2 production (and therefore aggregation) in plasma treated with aspirin. Note that collagen was not used as an aggregation stimulant in this case, so no degree of platelet aggregation dependent on platelets adhering directly to collagen would be expected.

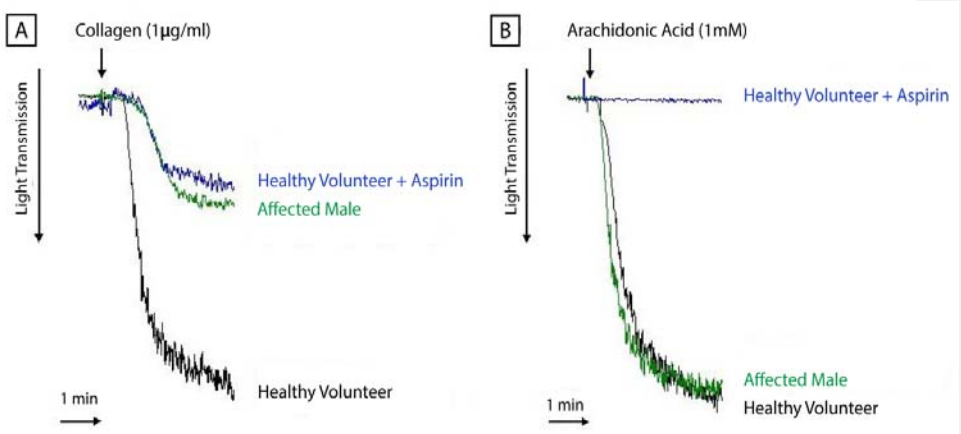

Figure 5.8: Light transmission aggregometry of platelet-rich plasma **A:** Platelet aggregation measured by light transmission through platelet-rich plasma against time. Light transmission changes in response to 1µg collagen are shown in a healthy volunteer, a healthy volunteer treated with 30µM aspirin, and the affected male. **B:** Platelet aggregation in response to 1mM arachidonic acid in the same individuals. Experiments were performed in collaboration with the

group of Prof. Tim Warner (William Harvey Research Institute, Barts and The London School of Medicine & Dentistry, London).

In addition to measuring aggregation in platelet-rich plasma, secretion of TxA_2 was also measured indirectly, by measurement of levels of its stable and inactive hydration metabolite thromboxane B_2 (TxB_2; to which TxA_2 is converted with a half-life of approximately 30 seconds {[Hamberg et al*et al.*, 1975}]). As shown in figure 5.9, stimulation with increasing concentrations of collagen resulted in increasing levels of TxB_2 production in healthy control platelets, whilst TxB_2 could not be detected in the plasma of either the affected female or male. The addition of 1mM arachidonic acid led to greatly increased TxB_2 production in the healthy controls, whilst high levels were also produced by the platelets of both affected individuals (higher than many healthy controls). As with the light transmission aggregometry results, this suggests that the thromboxane synthesis pathway remains intact and functional in the affected individuals, with TxA_2 production abolished as a result of a lack of arachidonic acid.

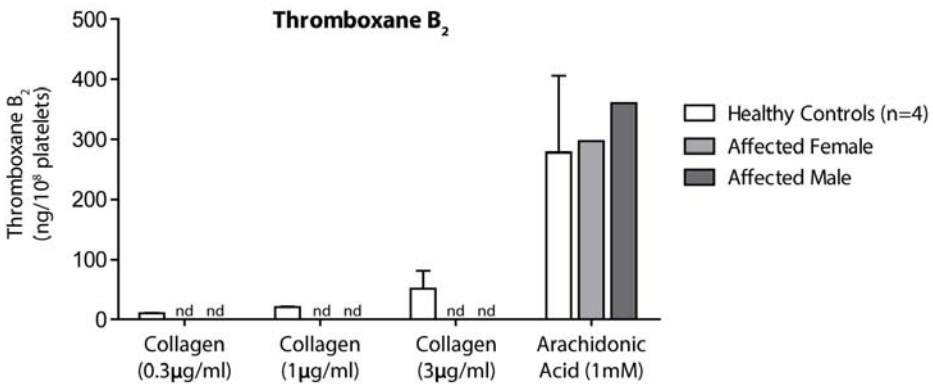

Figure 5.9: TxB_2 levels in platelet-rich plasma of healthy controls (n=4) and the two affected individuals, measured by ELISA, in response to stimulation with increasing levels of collagen and 1mM arachidonic acid. Nd = not detected. Experiments were performed in collaboration with the group of Prof. Tim Warner (William Harvey Research Institute, Barts and The London School of Medicine & Dentistry, London).

Platelet aggregation was next measured using a standardised optical multichannel absorbance-based method ('Optimul'), in which platelet-rich plasma was added to 96-well

microplates containing lyophilised agonists, following which absorbance was read at 595nm to measure aggregation. Once more, aggregation was measured in healthy controls (n=4) with and without aspirin treatment, and both affected individuals. As shown in figure 5.10, platelet aggregation in the two affected individuals' plasma was markedly reduced in response to stimulation by both collagen (3µg/ml) and adrenaline (10µM); with levels of aggregation again comparable to that seen in healthy individuals treated with aspirin, compared to healthy controls. Once more, treatment with 1mM arachidonic acid restored levels of platelet aggregation in both affected individuals to levels comparable to those seen in healthy volunteers, whilst aggregation in healthy volunteers treated with aspirin remained very low.

The addition of a synthetic analogue of TxA_2 (U46619, at 40 µM) resulted in comparable levels of platelet aggregation in all four groups, illustrating that no dysfunction exists in either the thromboxane receptor (TP), or its downstream, G-protein-dependent signalling pathway. Finally, stimulation with ristocetin – an antibiotic compound that stimulates the agglutination (as opposed to aggregation) of platelets in a manner dependent on adhesion between the platelet glycoprotein (GP)Ib/IX complex and the blood glycoprotein Von Willebrand Factor (Coller, 1978, Takata ~~et al~~*et al*., 2012), and which is thus thromboxane-independent – also produced agglutination which was very similar between healthy volunteers with or without aspirin and the two affected individuals.

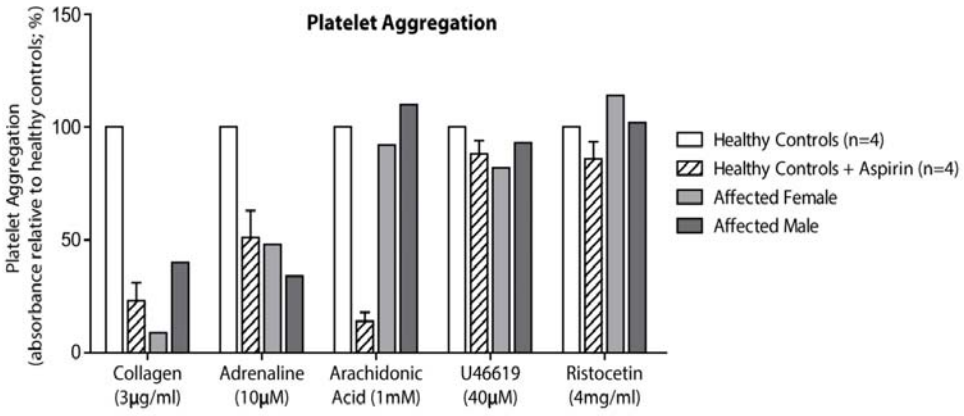

Figure 5.10: Platelet aggregation in healthy volunteers with and without aspirin treatment (both n=4), and the two affected individuals, measured by standardised optical multichannel

('Optimul') platelet aggregometry. Aggregation was measured as absorbance at 595nm, and is displayed as absorbance relative to that seen in healthy controls with no aspirin treatment, as a percentage. Experiments were performed in collaboration with the group of Prof. Tim Warner (William Harvey Research Institute, Barts and The London School of Medicine & Dentistry, London).

These results were consistent with the hypothesis that $cPLA_2\alpha$ activity is absent or significantly reduced in the affected individuals, and that defects in platelet aggregation result from a lack of arachidonic acid production owing to this abrogated activity.

5.2.8. Genetic investigations in other individuals with CMUSE-like disease

Subsequent to the association of the disease described above in the two siblings of Serbian origin, genetic investigations have taken place in two other candidate families (one from Bosnia-Herzegovina, the other from Turkey), whose gastrointestinal symptoms appeared similar to those described previously.

To investigate these cases, PCR primers were designed to separately amplify each of the 18 exons of *PLA2G4A,* all of which were then sequenced in the individuals suspected to harbour the disease, and the mother and father of both. Primer sequences are shown in appendix one. This strategy allowed for the successful sequencing of every exon, and the splice sites immediately preceding and following each, in each individual tested. No novel or potentially disease-causing mutations were observed in the *PLA2G4A* genes of any of these individuals, making it unlikely that the conditions they suffer from share the same aetiology as the one described above.

5.3 ~~Discussion~~Summary of chapter

Formatted: Font: 11.5 pt

These data describe a pair of siblings with a catastrophic 40 year clinical history of intestinal and extra-intestinal disease. A combination of genome SNP homozygosity mapping and whole exome sequencing revealed the siblings to be homozygous for a 4 base pair deletion in the *PLA2G4A* gene, which encodes the enzyme cytosolic Phospholipase A2-α (Phospholipase A2 Group IV-A, cPLA$_2$α) (Adler ~~et al~~*et al*., 2008), which is predicted to entirely eliminate enzymatic activity. No expression of cPLA$_2$α could be observed in the affected individuals' small intestine or PBMCs. Functional studies revealed absent production of the eicosanoid thromboxane A$_2$, and severely impaired platelet aggregation in response to collagen, which was restored by the addition of exogenous arachidonic acid - cPLA$_2$α's enzymatic product.

As such, it would be expected that these two affected individuals would have a global defect in the production of arachidonic acid, and therefore of eicosanoid synthesis. It is straightforward to hypothesise how a complete lack of prostanoid production that would follow from ablated cPLA$_2$α activity would be expected to cause gastrointestinal disease, as this would be expected to be analogous to NSAID mediated enteropathy. The pathophysiology of this enteropathy and of many of the extra-intestinal conditions observed can reasonably be expected to be a consequence of a lack of cPLA$_2$α function, and will be discussed in more detail in chapter 6.

Chapter 6

Discussion

6. Discussion

6.1. An ADAM17 loss-of-function syndrome

The third chapter of this thesis describes investigations into a neonatal-onset inflammatory skin and bowel disease, which was associated to a homozygous deletion mutation in *ADAM17.* This deletion was associated with severely reduced or absent ADAM17 protein expression and activity, and would therefore be expected to result in the abolition of the shedding of its many substrates *in vivo.*

The clearest manifestations of *ADAM17* loss-of-function mutations in the two affected individuals described in chapter 3 are inflammatory disease of the skin and bowel, accompanied by clear abnormalities in the nails, hair and heart. Considering the wide variety of ADAM17 substrates that can be assumed to be affected by loss-of-function mutations in ADAM17, a number of pathophysiological processes could plausibly lead to the different aspects of the phenotype that was observed. One of the most notable aspects of the disease described here is its relative lack of severity compared with an equivalent *Adam17*-knockout mouse model. Mice lacking ADAM17 expression die perinatally, with a phenotype involving severe developmental defects that can be shown to result from the absence of signalling by one or more of the five EGFR ligands that ADAM17 sheds (TGFα, amphiregulin, HB-EGF, betacellulin and epiregulin). Phenotypes of these mice are described in detail in section 1.1.15. Notably, the syndromes observed in these mice included severe defects in epithelial development (including that of the skin) that resembled TGFα-knockout mice (Peschon ~~et al~~*et al*., 1998), lungs, and heart (resembling amphiregulin ~~{~~[Luetteke ~~et al~~*et al*., 1999~~}~~] and HB-EGF ~~{~~[Jackson ~~et al~~*et al*., 2003, Shi ~~et al~~*et al*., 2003~~}~~] null mice respectively). Knockouts of the mouse ~~*Egfr*~~ *Egfr* produce an even more severe phenotype, with severely impaired skin development and differentiation (Miettinen ~~et al~~*et al*., 1995), as well as heavily defective

development of numerous other tissues. Interestingly however, when a novel gene-targeting strategy was used to generate a mouse model expressing severely reduced (but not absent) levels of *Adam17* (hypomorphic *Adam17* mice), skin development was observed to be relatively normal, but an obvious skin inflammatory phenotype was observed (Chalaris ~~et al~~*et al*., 2010), among other defects.

In attempting to better understand pathophysiology of the skin disease observed in the *ADAM17* mutation-affected individuals, keratinocyte-restricted *Adam17* knockout (*Adam17*$^{\Delta KC}$) mice have provided interesting insights into a potential disease mechanism. These *Adam17*$^{\Delta KC}$ mice display relatively normal skin architecture, but suffer from a pronounced chronic inflammatory dermatitis, a phenotype which superficially resembles the inflammatory skin phenotype seen in the *ADAM17* mutation-affected individuals described here (Franzke ~~et al~~*et al*., 2012). This dermatitis is accompanied by an epidermal barrier defect, shown to result from significantly reduced transglutaminase 1 (TGM1) activity in the upper layers of the epidermis, accompanied by a reduction in the expression of TGM1 mRNA. This reduction in TGM1 activity was itself a result of reduced EGFR signalling activity due to absent (ADAM17 substrate) EGFR ligand shedding, closely resembles the phenotype seen in keratinocyte-restricted *Egfr* knockout mice, and could be rescued by the application of topical TGFα (Franzke ~~et al~~*et al*., 2012). Mirroring this mouse phenotype, the affected individual described in chapter 3 was found to have substantially reduced TGM1 expression in the granular layer of his skin, and virtually undetectable ~~*in situ*~~*in situ* TGM1 activity. In addition, the skin of the *ADAM17* mutation-affected individual displayed a notable infiltration of T lymphocytes (of both CD4+ and CD8+ lineages) (Blaydon ~~et al~~*et al*., 2011a), which was also seen in *Adam17*$^{\Delta KC}$ mice. Given that shedding of ADAM17 substrates from the keratinocytes of the affected individual was shown to be virtually absent, it can be hypothesised that a lack of EGFR ligand shedding, and a downregulation of TGM1 expression and activity that results from it, may therefore make a substantial contribution to the inflammatory skin phenotype seen in the affected individuals, and as such that this phenotype is analogous to that seen in *Adam17*$^{\Delta KC}$ mice. Furthermore, the fact that topical treatment with recombinant TGFα was sufficient to rescue the inflammatory dermatitis phenotype observed in *Adam17*$^{\Delta KC}$ mice offers the intriguing suggestion that a treatment for the inflammatory skin disease observed in this individual may already exist, in the form of topical EGFR ligand supplementation.

As well as offering a plausible mechanism for the inflammatory skin disease observed, it is also interesting to note that, in common with the affected humans described here, the development and differentiation of *Adam17*$^{\Delta KC}$ mouse skin appears otherwise normal. This may serve to illustrate the differing requirements for EGFR signalling in development, compared to the requirement for it in normal epidermal homeostasis. In ~~each of~~ the affected ~~male~~ individual described here, *Adam17*$^{\Delta KC}$ mice, hypomorphic *Adam17* mice, and mice with a spontaneous *Adam17* mutation (*waved with open eyelids* mice ~~(Hassemer et al~~*et al*~~.,~~ ~~2010)~~~~{~~[Hassemer ~~et al~~*et al*., 2010~~}~~]), skin development and differentiation appears to proceed normally, whilst EGFR activity in each of these models was insufficient to maintain epidermal homeostasis, in terms of TGM1 activity and epidermal barrier maintenance.

Related to the skin phenotype seen in these individuals was a clear abnormality in the hair: the eyebrows, eyelashes and scalp hair being found to be wiry, disorganised and easily broken, with hair follicles appearing severely weathered and abnormal under microscopic examination. These features bear a similarity to those seen in mice with knockouts of the *tgfa* (TGFα) gene, whose hair is disorganised (follicles are unaligned, and point in random directions), kinked and curly, giving an overall 'wavy' appearance. Interestingly, this hair phenotype is present in mice with a knockout of *tgfa* (Luetteke ~~et al~~*et al*., 1993), with spontaneous null mutations in *tgfa* (the *waved-1* mouse ~~{~~[Mann ~~et al~~*et al*., 1993~~}~~]), and in a mouse that is spontaneously hypomorphic for *Adam17* (the *waved with open eyelids* mouse ~~{~~[Hassemer ~~et al~~*et al*., 2010~~}~~]). A deficiency of TGFα signalling would in this case therefore appear to be the most logical explanation for the hair phenotype seen.

Recently, the first example of an inherited human disease associated with loss-of-function missense mutations in the *EGFR* gene has been identified, which was characterised by inflammatory skin disease that resembled that seen in patients treated with EGFR-inhibiting drugs, as well as bowel and lung inflammation (Campbell ~~et al~~*et al*., 2014). The skin and bowel disease observed in the single individual affected by this condition bore a resemblance to that seen in the *ADAM17*-null individual described in this thesis, lending credence to the suggestion that reduction in EGFR ligand shedding, and therefore of EGFR signalling, may be a highly important pathological process in the disease resulting from *ADAM17* mutations. In contrast to *ADAM17*-null individuals, the child affected by *EGFR* mutation died at around 2.5 years old (Campbell ~~et al~~*et al*., 2014). This lethality may reflect the fact that *EGFR* loss-of-function mutations would result in a reduction in signalling mediated by the binding of all EGFR ligands, whilst *ADAM17* loss-of-function mutations would adversely affect signalling

mediated only by ADAM17-specific substrates (TGFα, HB-EGF, amphiregulin, epigen and epiregulin), whilst EGF and betacellulin signalling would be unaffected, as these are shed under the control of ADAM10.

As well as inflammatory disease, the skin and nails of the individuals affected by *ADAM17* mutations were also noticeably susceptible to infection, by organisms such as *Staphylococcus aureus, Psuedomonas* and *Candida* species. The defective epidermal barrier function that would be expected to result from the reduced expression and activity of TGM1 in the upper epidermal layers, can plausibly be expected to result in reduced resistance to bacterial infection in the epidermis, which may contribute to the increased infection susceptibility. Further, an inability to shed TNFα, a cytokine with numerous important roles in the innate inflammatory response, would also be expected to result in reduced resistance to bacterial infection. This latter point is clearly illustrated by the example of *iRhom2* knockout mice, whose macrophages cannot produce mature ADAM17, and thus cannot shed TNFα. Although viable, these mice fail to adequately control the replication of inoculated bacteria (*Listeria monocytogenes*), and as such succumb to infection as a direct consequence of impaired TNFα shedding (McIlwain ~~et al~~*et al.*, 2012).

In addition to its functions in the maintenance of an effective skin (and gut, to be discussed below) barrier, the functions of ADAM17 at the level of individual cells may also be important in the response to infection. Work by Dr. Charlotte Simpson (Blizard Institute, London) has shown that knockdown of ADAM17 in keratinocytes results in increased susceptibility to infection by *S. aureus* bacteria*,* which are able to both adhere to and invade keratinocytes at a higher rate in the absence of ADAM17. Conversely, keratinocytes derived from TOC patients (which appear to have upregulated ADAM17 activity) demonstrate significantly increased resistance to bacterial invasion and adherence, which can be abolished by knockdown of ADAM17 in the same way as normal control keratinocytes (Brooke ~~et al~~*et al.*, 2014a).

In a fashion similar to the skin disease observed, complete abrogation of ADAM17 could plausibly be expected to result in an inflammatory gut disease through a number of different pathophysiological processes. Signalling through the EGFR is important in the development of the intestinal epithelium, with *efgr* null mice found to have fewer, shorter intestinal villi and reduced epithelial proliferation, though all of the four intestinal epithelial cell types do develop (Miettinen ~~et al~~*et al.*, 1995). The intestines of *egfr* null mice are fragile and strongly susceptible to damage, with numerous intestinal haemorrhages and disintegration of the villi

visible a few days after birth. As well as in development, EGFR signalling is required in the response to damage to the intestinal epithelium (McElroy ~~et al~~*et al*., 2012, Dvorak ~~et al~~*et al*., 2002), suggesting that abrogated EGFR ligand shedding in ADAM17 null individuals would be expected to adversely affect both the development of, and the response to injury in, the intestinal epithelium.

This is borne out by the severe gut sensitivity seen in mice expressing severely reduced levels of ADAM17 (hypomorphic for *Adam17*). In contrast to ~~*Egfr*~~ *egfr* knockout mice, the gastrointestinal tract in these mice appears superficially normal. They were however strongly susceptible to inflammatory colitis following challenge with dextran sulphate, with this sensitivity found to result from defective regeneration of intestinal epithelium due to an inability to shed EGFR ligands (Chalaris ~~et al~~*et al*., 2010). High levels of EGFR ligands, in particular TGFα, were generated in the enterocytes of these mice following challenge, but remained at the plasma membrane due to the inability to effectively shed them, whilst treatment with soluble TGFα was sufficient to restore normal intestinal epithelial function. It is however worth noting that the gut inflammation observed in hypomorphic *Adam17* mice was observed only after challenge with dextran sulphate (Chalaris ~~et al~~*et al*., 2010), whereas diarrhoea was seen in affected humans within hours of birth, without any obvious challenge to the gut epithelium. Therefore, whilst the gut disease observed in hypomorphic *Adam17* mice may offer a good model of the intestinal inflammation seen in the ADAM17 null individual, further investigation is required to understand the precise pathology of this condition.

Interestingly, much of the stimulus for regeneration after damage to the intestinal epithelium is mediated through the signalling actions of prostaglandins, particularly prostaglandin E_2 (PGE_2). PGE_2 stimulates intestinal epithelial cell proliferation via transactivation of the EGFR (as described in section 1.2.6), a process which is dependent on the cleavage of TGFα, and therefore on the activity of ADAM17 (Pai ~~et al~~*et al*., 2002). This therefore offers the intriguing possibility that the otherwise entirely unrelated gut diseases that are described in the individual in chapter 3 (affected by loss-of-function mutation in *ADAM17*) and the two individuals described in chapter 5 (affected by loss-of-function mutations in *PLA2G4A,* and who therefore cannot synthesise prostaglandins) may share some degree of common pathophysiology, in that proliferation of the intestinal epithelium cannot be stimulated by the actions of PGE_2 in either disease, which would be assumed to result in defective regeneration of the gut epithelium and breakdown of the intestinal

barrier. It is also worth noting that the intestinal epithelium also expresses a transglutaminase enzyme, TGM2, which is notable for the fact that it is the main target for autoantibodies in the autoimmune inflammatory bowel condition coeliac disease (Dieterich ~~et al~~*et al*., 1997). EGFR signalling has been shown to upregulate TGM2 activity in some cell types (Li ~~et al~~*et al*., 2010, Li ~~et al~~*et al*., 2011b), meaning that reduced EGFR signalling in the intestinal epithelium may also plausibly lead to barrier defects, in a fashion analogous to depleted TGM1 activity in the skin.

Another important aspect of the disease observed in the *ADAM17* null individuals is a notable heart phenotype. In the male individual, this consists of moderate left ventricular dilatation and borderline-dysfunctional systolic function (an ejection fraction of 55%, where 45% is regarded as dysfunctional). The female sibling died suddenly at 12 years of age from fulminant myocarditis associated with Parvovirus B19 infection (Blaydon ~~et al~~*et al*., 2011a). Given the lack of material available from the female child, it is impossible to investigate whether or not her heart displayed any abnormality prior to this infectious disease; however, the presence of heart dysfunction in these individuals is particularly interesting in the light of the phenotype of *Adam17* knockout mice, who die perinatally as a result of severe heart abnormalities (Peschon ~~et al~~*et al*., 1998). Intriguingly, mice hypomorphic for ADAM17 are also affected by an obvious heart dysfunction, which primarily takes the form of massive left ventricular hyperplasia (i.e. affecting the same part of the heart as in the human affected individual). Despite this, these mice remain viable. Whilst the wide variety of potential ADAM17 substrates makes it difficult to pinpoint precisely whether or not a shedding defect may underlie this observed cardiomyopathy, a number of potential mechanisms could plausibly underlie the development of cardiac disease in these individuals.

The first of these is that the cardiomyopathy represents a developmental defect in the heart, analogous to the lethal failure of proper heart development in knockout mice. In these mice, the cardiac developmental defect closely resembles that seen in mice which cannot express the growth factor HB-EGF, which is required in heart development for the proper development and morphogenesis of the ventricles and the semilunar and atrioventricular valves (Iwamoto ~~et al~~*et al*., 2003, Jackson ~~et al~~*et al*., 2003), with mice lacking HB-EGF developing grossly enlarged and dilated ventricular chambers and cardiac valves, resulting in severe heart failure (Iwamoto ~~et al~~*et al*., 2003). Similarly, mice that express an un-sheddable mutant form of HB-EGF develop severe heart defects analogous to those seen in HB-EGF-null mice, rather than the milder cardiomyopathy seen in mice expressing severely reduced

Adam17 (Yamazaki ~~et al~~*et al.*, 2003); this illustrates that a degree of active HB-EGF shedding is required for proper heart development. Therefore, it is interesting to note that a degree of functional redundancy has been shown between ADAM17 and the related sheddase ADAM19, in which ADAM19 can contribute to HB-EGF shedding in the heart in the absence of functional ADAM17 (Horiuchi ~~et al~~*et al.*, 2005). Although it was not directly studied, there is no reason to expect that ADAM19 levels would be different in the individuals described here compared to normal controls, suggesting that the relatively minor heart defects (compared to knockout mice) observed in the affected male may reflect only a partial abrogation of HB-EGF signalling in heart development.

The second possibility chiefly concerns ADAM17's substrate Desmoglein 2 (DSG2), a cadherin component of desmosomes, intercellular junction complexes which serve to robustly link adjacent cells (Brooke ~~et al~~*et al.*, 2012). ADAM17's functions in the regulation of DSG2 are described in detail in section 1.2.9-10. Desmosomes are especially important in maintaining the integrity of tissues subject to high levels of mechanical stress, such as the skin, the bladder and the heart. The various desmosomal cadherins (desmogleins and desmocollins) are expressed in tissue- and differentiation-dependent patterns across numerous tissues; with DSG2 the primary cadherin present in the myocardium. The importance of DSG2 in the heart is illustrated by the association of mutations in DSG2 with arrhythmogenic right ventricular cardiomyopathy (ARVC) (Simpson ~~et al~~*et al.*, 2009), an inherited disorder causing cardiac arrhythmias and sudden cardiac death, (which can be associated with mutations in a variety of desmosomal components ~~(~~[Brooke ~~et al~~*et al.*, 2012~~)~~]). Keratinocytes derived from the affected male were shown to have dysregulation in the processing of DSG2, and to accumulate DSG2 at their plasma membrane, suggesting that DSG2 dynamics were abnormal in this individual. However, the contribution of ADAM17-dependent DSG2 turnover to normal desmosomal homeostasis in the heart has not been extensively studied, and it is notable that the phenotype observed in the affected male does not exactly phenocopy ARVC (left- rather than right-ventricular dilatation, for example). Despite this, a cause of this heart disease dependent on desmosomal dynamics cannot be ruled out and bears further investigation.

Thirdly, it remains possible that the infectious myocarditis observed in the affected female did not reflect a developmental or structural abnormality, but rather reflected an impairment in immune function resulting from ADAM17 loss-of-function. Notably, this is supported by evidence from TNFα-knockout mice, in which TNFα was shown to play a key

protective role in acute viral myocarditis (Wada ~~et al~~*et al*., 2001), the very condition from which the affected female died. This hypothesis would not however explain the moderate cardiac defect observed in the affected male, making it most likely that some combination of the factors described here contribute to the cardiac disease seen.

As previously described, *Adam17* null mice die perinatally, and suffer from severe developmental defects which appear to be related to a lack of shedding of various EGFR ligands, and are analogous to complete knockouts of one or more EGFR ligands. However, in contrast to complete mouse knockouts of EGFR ligands, and despite the inflammatory disease and moderate hyperplasia, the overall structure of the skin in the human ADAM17 loss-of-function individuals is relatively normal (though their hair did show obvious abnormality).

Although loss-of-function mutations in ADAM17 would be expected to result in substantially reduced ADAM17-dependent EGFR ligand shedding in humans, the situation in these affected individuals cannot be considered to be analogous to a complete knockout of any of the EGFR ligands, or of the EGFR itself, for two reasons. Firstly, although these ligands cannot be shed, interaction between cell surface-bound EGFR ligands and the EGFR on neighbouring cells (juxtacrine signalling) can be used to activate EGFR signalling; such as in signalling by membrane-bound TGFα through the EGFR in bone marrow stroma (Anklesaria ~~et al~~*et al*., 1990). Secondly, a degree of functional redundancy appears to exist in humans in the shedding of EGFR ligands by ADAMs. For example, in addition to ADAM17, HB-EGF can also be shed by ADAMs 9 (Izumi ~~et al~~*et al*., 1998), 12 (Asakura ~~et al~~*et al*., 2002), 15 (Hart ~~et al~~*et al*., 2005) and 19 (with evidence having demonstrated a degree of mutual compensatory activity between ADAMs 17 and 19 in terms of HB-EGF secretion in heart development ~~{~~[Horiuchi ~~et al~~*et al*., 2005~~}~~]), amphiregulin by ADAM15 (Schafer ~~et al~~*et al*., 2004) and neuregulin by ADAM19 (Yokozeki ~~et al~~*et al*., 2007). Whilst ADAM17 may act as the primary sheddase for these ligands under normal circumstances, shedding by these other ADAMs in the absence of ADAM17 may be sufficient for normal development in humans. This is in addition to the fact that two members of the EGFR ligand family (EGF and epigen) are shed by ~~ADAM10,~~ADAM10; meaning that a degree of EGFR signalling would be expected to be activated even if no ADAM17 ligands could be shed at all. As such, although EGFR signalling can be expected to be reduced in the absence of ADAM17-mediated ligand shedding, it does not appear that this reduction in shedding is sufficient – in the context of normal skin

development and differentiation – to produce the severe phenotypes associated with a complete lack of one or more EGFR ligands, or of the EGFR itself.

The differences seen between *Adam17*-null mice and a human ADAM17-null individual could therefore plausibly be explained in a number of ways. The first of these is that some degree of residual ADAM17 activity can be found in the cells of the affected individuals. In support of this, it is notable that a small amount of TNFα could be shed by the PBMCs of the affected male, rather than none at all. Furthermore, the phenotype seen in the affected humans most closely resembles that seen in hypomorphic *Adam17* mice, in that both have fully developed but inflammatory skin, significant intestinal inflammation, hair abnormalities, and left ventricular hyperplasia, without the lethal developmental defects that result from complete ablation of ADAM17. Second, the differences between human and mouse models of ADAM17 loss-of-function may plausibly represent subtle but significant differences in ADAM and EGFR ligand physiology between humans and mice. A less severe human disease may therefore reflect more effective compensation for ADAM17 loss by other ADAMs, which may or may not include other ADAMs having a broader spectrum of substrates in humans. Similarly, the various members of the EGFR ligand family may have slightly different roles in development and homeostasis in humans, such as the ability for EGF or epigen signalling to compensate for the loss of shedding of ADAM17 substrates, for example.

These results illustrate the existence of a novel inherited genetic disease associated with *ADAM17* mutations. In recent years, ADAM17 has emerged as an attractive pharmacological target for the potential treatment of inflammatory diseases, in particular those driven by TNFα (Saftig and Reiss, 2011, Arribas and Esselens, 2009). However, the dramatically deleterious phenotype seen in *Adam17* null mice dampened enthusiasm for this therapeutic approach. The results seen in the individuals affected by *ADAM17* loss-of-function mutations however illustrate that loss of ADAM17 activity is not incompatible with human survival, and therefore suggest that pharmacological treatment of this pathway should be considered plausible in humans.

6.2. Tylosis with oesophageal cancer, and the iRHOM2-ADAM17 axis

The fourth chapter of this thesis described investigations into the pathophysiology of tylosis with oesophageal cancer (TOC), a dominantly inherited disease characterised by palmoplantar keratoderma, oral and oesophageal leukoplakia, and a striking susceptibility to oesophageal squamous cell carcinoma. TOC was associated in three large family groups (from the UK, USA and Finland) to dominantly inherited, notably clustered mutations in the gene *RHBDF2* (Blaydon ~~et al~~*et al*., 2012), the gene encoding iRHOM2; an association which was subsequently confirmed by analysis of another TOC-affected family in Finland (Saarinen ~~et al~~*et al*., 2012). The linkage of iRHOM2 mutations to TOC represents the first and only linkage of inherited oesophageal cancer susceptibility to any gene.

Subsequent to the association of *RHBDF2* mutations to TOC, the role of iRHOM2 in regulating the maturation and activity of ADAM17 was revealed. In chapter 4, studies on immortalised keratinocytes, skin sections and PBMCs derived from TOC sufferers showed that TOC-associated iRHOM2 mutations result in an increase in the processing of ADAM17, increased localisation of mature ADAM17 to its major site of activity (the plasma membrane), and increased constitutive and stimulated shedding of ADAM17 substrates (and other pro-inflammatory cytokines), notably including the EGFR ligands amphiregulin, TGFα and HB-EGF. These changes were accompanied by the presence of desmosomes lacking electron dense midlines (in an immature, calcium dependent state), increased desmosome processing and increased epidermal transglutaminase 1 activity. TOC keratinocytes displayed a marked increase in their migration compared to controls, which was independent of exogenous EGFR ligand supplementation. This increase on migration was found to be associated with factors released by TOC keratinocytes (which could increase the migration of control keratinocytes),

and could be blocked via the inhibition of ADAM17-dependent EGFR ligand shedding by the small molecule ADAM17 inhibitor GW280264X.

The finding that TOC-associated iRHOM2 mutations are associated with an increased rate of ADAM17 maturation implies that these mutations can be classified as gain-of-function in nature, and result in increased processing and activity of ADAM17. This hypothesis is supported by a number of factors. Firstly, gain-of-function mutations are consistent with the dominant pattern of inheritance observed for TOC, in that only one copy of the mutated gene would be required to increase iRHOM2's function in ADAM17 maturation beyond the background level provided by wild-type iRHOM2. Secondly, the iRHOM2 mutations associated with TOC display a remarkable degree of clustering, with all three mutations described (in four entirely unrelated families) resulting in amino acid substitutions within the space of only four residues (see figure 4.2), strongly implying that these mutations affect a particular function in which the mutated motif is intimately involved. Importantly, these three TOC-associated iRHOM2 mutations are found within a long N-terminal loop domain that is unique to the two iRHOM proteins, and is very highly conserved between species and across large evolutionary distances (the mutated residues in iRHOM2 are conserved identically in humans, finches, toads and pufferfish, for example), implying that its function is subject to strong selection pressure. The fact that this domain is found only in the two iRHOM proteins in also revealing, as iRHOM1 has also been shown to share the ability of iRHOM2 to support ADAM17 maturation, with a large degree of functional redundancy having been observed between the two iRHOMs in tissues where they are co-expressed (Christova ~~et al~~*et al*., 2013). The residues affected by TOC-associated mutations are expressed identically in iRHOM1. In fact, this N-terminal domain has been shown to be absolutely required for iRHOM2 to function correctly in regulating ADAM17 maturation: shedding of ADAM17 substrates in *iRhom2*-null mouse embryonic fibroblasts can be rescued by the addition of wild-type mouse iRHOM2, but not by a mutant iRHOM2 lacking the N-terminal domain where TOC-associated mutations are found (Maretzky ~~et al~~*et al*., 2013). Therefore, since the TOC-associated mutations affect extremely highly conserved residues in a domain that is absolutely required for ADAM17 maturation, and that is found only in those proteins capable of supporting ADAM17 maturation, it is reasonable to hypothesise that these mutations would influence the process of ADAM17 maturation. Furthermore, siRNA knockdown of iRHOM2 specifically abolished the increased level of mature ADAM17 in TOC keratinocytes, illustrating that – although both iRHOMs are expressed in skin, and both can

effectively support the maturation of ADAM17 – the increased level of mature ADAM17 observed is iRHOM2-dependent.

As well as providing evidence that ADAM17 maturation in keratinocytes is strongly influenced by iRHOM2, siRNA knockdown experiments also suggested that reciprocal regulation of iRHOM2 by ADAM17 may exist. Knocking down expression of ADAM17 by siRNA led to noticeable downregulation of iRHOM2 expression, in TOC keratinocytes as well as controls. Although not expected, this corresponded with the observation of reduced iRHOM2 staining in the epidermis of the ADAM17-null individual described in chapter 3, and suggests that expression of iRHOM2 may depend on the activity of ADAM17 in some form.

The upregulation of mature ADAM17, and its increased localisation to the plasma membrane, was accompanied by increased constitutive and stimulated shedding of many ADAM17 substrates. As well as upregulation of stimulated TNFα shedding from both keratinocytes and PBMCs, there was a highly significant increase in shedding of the EGFR ligands dependent on ADAM17 for release.

In culture, keratinocytes express high levels of ~~amphiregulin,~~amphiregulin and much lower levels of TGFα and HB-EGF (Pastore ~~et al~~*et al*., 2008). It was therefore especially interesting to note that shedding of all three of these growth factors was upregulated in TOC keratinocytes, even in unstimulated conditions. Amphiregulin – the growth factor known to provide by far the strongest degree of autocrine stimulation of keratinocyte growth (Piepkorn ~~et al~~*et al*., 1994) - was shed at a particularly high level. It was noticeable that, although the level of mRNA expression of TGFα and HB-EGF was comparable to that of amphiregulin, the levels of these two proteins in the medium were much lower than amphiregulin. This may however represent the differing importance of EGFR ligands in transactivation of the EGFR by triple membrane pass signalling. As described in section 1.2.6, the ligand involved in EGFR transactivation is commonly HB-EGF (Prenzel ~~et al~~*et al*., 1999), whilst a role for TGFα in EGFR transactivation has been described in some tissues (such as the intestine ~~(~~[Pai ~~et al~~*et al*., 2002~~)~~]). Conversely, a role for amphiregulin is not well described in EGFR transactivation. The relatively increased level of amphiregulin in the medium of TOC cells may therefore be representative of this growth factor being freely shed into keratinocytes' surroundings, whilst shed HB-EGF and TGFα is bound by the EGFR in an autocrine fashion shortly after release, during EGFR transactivation.

Upregulation of EGFR ligands *in vivo* is characteristic of numerous benign and malignant hyperproliferative conditions of the skin. For example, hyperproliferative psoriatic lesions overexpress TGFα (Elder ~~et al~~*et al*., 1989), HB-EGF (Zheng ~~et al~~*et al*., 2003) and amphiregulin (Piepkorn, 1996) as well as the EGFR (Nanney ~~et al~~*et al*., 1986). Amphiregulin is also known to be strongly upregulated in actinic keratoses, verrucas and squamous cell carcinomas (Piepkorn, 1996). Meanwhile, transgenic overexpression of TGFα in murine epidermis leads to cutaneous hyperplasia and hyperkeratosis, accompanied by the spontaneous formation of squamous papillomas at sites of wounding (Dominey ~~et al~~*et al*., 1993). EGFR ligand signalling also underlies the hyperproliferative effects of retinoids (a class of chemical compounds related to vitamin A) on keratinocytes, with retinoid-induced hyperplasia mediated by the marked induction of HB-EGF and amphiregulin shedding (Rittie ~~et al~~*et al*., 2006, Stoll and Elder, 1998). The highly significant increases in shedding of these factors by keratinocytes from TOC affected areas could therefore plausibly be expected to play a role in the epidermal hyperproliferation that characterises TOC, and may offer a rationale for the development of the palmoplantar keratoderma seen.

As well as the direct detection of increased EGFR ligand shedding, and the finding of increased EGFR phosphorylation in three-dimensional culture models of TOC keratinocytes, evidence of upregulated EGFR signalling in TOC epidermis can also be inferred from the activity of transglutaminase 1 (TGM1) in TOC skin. As described previously for an ADAM17-null individual (and *Adam17*$^{\Delta KC}$ mice), TGM1 activity is regulated by EGFR signalling, and is dependent on shedding of ADAM17-substrate EGFR ligands (Franzke ~~et al~~*et al*., 2012). Both TOC epidermis and three-dimensional culture models of TOC keratinocytes display increased TGM1 activity in their upper layers. As well as offering a stark contrast to ADAM17-null skin (where TGM1 activity is undetectable), this increased TGM1 activity implies antecedent upregulation of EGFR activity, and suggests that individuals affected by TOC may display increased epidermal barrier function.

As well as functioning to increase epidermal barrier function, upregulation of ADAM17 activity may also have a direct effect on cells' susceptibility to infection. As described previously, work by Dr. Charlotte Simpson has shown a direct role for ADAM17 in regulating individual keratinocytes' susceptibility to attachment and invasion by *Staphylococcus aureus* bacteria. TOC keratinocytes have displayed a natural resistance to *S. aureus* attachment and invasion, which was found to be dependent on the activity of ADAM17 (Brooke ~~et al~~*et al*., 2014a). Combined with the finding of increased epidermal barrier function, this raises the

intriguing possibility that the skin of TOC-affected individuals may display a naturally heightened resistance to infection. Rates of infection in TOC patients have never been examined in detail, though it would undoubtedly be interesting to investigate this aspect of the phenotype resulting from TOC-associated iRHOM2 mutations.

Signalling through the EGFR is also known to play an important role in cutaneous wound healing – particularly in the early phase response to wounding – by increasing keratinocyte proliferation and migration (Barrientos et al*et al*., 2008). The importance of this response is illustrated in mice with *egfr*-null epidermis, whose skin lesions heal at a slower rate compared to controls (Repertinger et al*et al*., 2004). ADAM-mediated shedding of EGFR ligands is required for keratinocyte migration during wound healing and is immediately induced upon wounding (Tokumaru et al*et al*., 2000), with factors upregulated in wounded skin including amphiregulin, TGFα and HB-EGF (but not EGF or betacellulin) (Barrientos et al*et al*., 2008). In particular, TGFα is responsible for approximately 80% of keratinocyte migration activity during wound healing (Li et al*et al*., 2006) and also promotes proliferation (Cha et al*et al*., 1996); whilst HB-EGF promotes re-epithelialisation (Hashimoto et al*et al*., 1994) and accelerates cutaneous wound healing when applied topically (Tolino et al*et al*., 2011, Shirakata et al*et al*., 2005).

As such, it may be plausible to consider that the significant, constitutive upregulation of EGFR ligand shedding by TOC keratinocytes can be thought of as representing a constitutive 'wound healing-like' state in the epidermis and keratinocytes of TOC sufferers. This hypothesis is supported by other lines of evidence, such as the presence in TOC skin of desmosomes lacking the electron-dense midline that characterises mature, 'hyperadhesive', calcium-independent desmosomes. This immature desmosomal state is associated with keratinocyte motility (Brooke et al*et al*., 2012), and is especially prominent in skin undergoing wound healing (Garrod et al*et al*., 2005). Secondly, in addition to high levels of EGFR ligands, TOC keratinocytes also secrete particularly high levels of IL-6 and IL-8, both of which are correlated with, and important for, wound healing processes (Werner and Grose, 2003). For example, IL-6 is strongly upregulated at sites of wounding (Grellner et al*et al*., 2000), persists in chronic wounds (Barrientos et al*et al*., 2008, Finnerty et al*et al*., 2006), and is strongly reduced in glucocorticoid treated mice, which display significant impairment in wound healing (Grose et al*et al*., 2002). IL-6-knockout mice heal wounds significantly more slowly than controls, a phenotype which can be rescued by topical IL-6 application (Gallucci et al*et al*., 2004, McFarland-Mancini et al*et al*., 2010). Meanwhile, IL-8 is also upregulated in

wounded tissue (Werner and Grose, 2003) and may enhance keratinocyte proliferation and wound healing (Rennekampff ~~et al~~*et al*., 2000, Jiang ~~et al~~*et al*., 2012), though high IL-8 levels have conversely been associated to impaired wound healing (Iocono ~~et al~~*et al*., 2000).

As with rates of infection in TOC patients, wound healing in TOC patients has also never been directly studied. No mouse model of TOC-associated iRHOM2 mutation is available at the time of writing, but any differences in wound healing in the epidermis that arise as a consequence of these mutations would be an extremely interesting aspect of the TOC phenotype that would benefit from closer examination.

As well as the skin phenotype, by far the most prominent aspect of TOC – and the primary cause of mortality amongst TOC-affected individuals – is the striking susceptibility to oesophageal squamous cell carcinoma (OSCC) that has been described. Oesophageal cancer (of which OSCC is the predominant type) is the eighth most common cancer worldwide and the sixth leading cause of cancer related mortality, with overall 5-year survival rates ranging from 15 to 25% (Pennathur ~~et al~~*et al*., 2013). Environmental risk factors for OSCC prominently include tobacco smoking, alcohol and caustic injury, whilst TOC is the only known syndrome of highly penetrant inherited OSCC susceptibility (Blaydon ~~et al~~*et al*., 2012, Enzinger and Mayer, 2003). An affected individual belonging to a large, TOC-affected family in the UK has been calculated as having a 92% probability of dying from oesophageal cancer by the age of 70 (Ellis ~~et al~~*et al*., 1994).

The observed excessive secretion of EGFR ligands may offer clues to this OSCC susceptibility observed in TOC patients. In sporadic ~~OSSC~~OSCC, EGFR overexpression has been observed in 45.6-72.1% of primary tumours (Gibault ~~et al~~*et al*., 2005, Abedi-Ardekani ~~et al~~*et al*., 2012), 88% of OSCC lymph node metastases, and 90% of oesophageal squamous dysplasias (Itakura ~~et al~~*et al*., 1994) – suggesting that signalling through the EGFR may make a substantial contribution to tumour initiation. Direct *EGFR* gene amplification is seen in 12-28% of OSCC (Kitagawa ~~et al~~*et al*., 1996, Itakura ~~et al~~*et al*., 1994, Hanawa ~~et al~~*et al*., 2006) and is associated with significantly reduced cumulative survival (Kitagawa ~~et al~~*et al*., 1996), whilst EGFR overexpression has been shown to correlate with poor prognosis (Okines ~~et al~~*et al*., 2011). Increased levels of EGFR ligand secretion have been associated with the development and progression of squamous cell carcinomas in the oesophagus, where upregulation of TGFα is associated with poor OSCC prognosis (Yamabuki ~~et al~~*et al*., 2006), and numerous other tissues, including the epidermis (Rittie ~~et al~~*et al*., 2007, Cataisson ~~et al~~*et al*., 2012), lung (Fujimoto ~~et al~~*et al*., 2005), mouth (Tsai ~~et al~~*et al*., 2006), and head and neck tissues (Rubin

Formatted: Font: Italic

Grandis et al*et al*., 1998). Independently of the EGFR, expression of ADAM17 itself has also been recently shown to correlate with progression of OSCC (Liu et al*et al*., 2013). Upregulation of ADAM17 activity in TOC, and the increased EGFR ligand shedding that accompanies it, may therefore plausibly play a role in the initiation of OSCC in TOC patients.

Together, the data presented here illustrate that TOC-associated iRHOM2 mutations affect the process of iRHOM2-regulated ADAM17 maturation, leading to upregulation of ADAM17 activity. The consequences of this demonstrate that the iRHOM2-ADAM17 axis plays a key role in epidermal proliferation, skin barrier maintenance, inflammation and migration, and represents a novel oncogenic pathway in the oesophagus. This pathway may therefore have important roles in normal epidermal homeostasis, the response to injury in the skin, and oesophageal oncogenesis, and represents an attractive target for further research.

6.3. *PLA2G4A* mutations in cryptogenic multifocal ulcerative stenosing enteritis

In the fifth chapter of this thesis, genetic mutations underlying an inherited syndrome of severe intestinal disease, whose symptoms corresponded to cryptogenic multifocal ulcerative stenosing enteritis (CMUSE) accompanied by multiple extra-intestinal complications, were investigated. This condition was associated, in two affected siblings from a consanguineous family, with homozygous deletion mutations (g.155574_77delGTAA) in *PLA2G4A,* the gene encoding cytosolic phospholipase A2-α (cPLA$_2$α), an enzyme responsible for the production of arachidonic acid from membrane phospholipids, and which therefore catalyses a rate-limiting reaction in the production of eicosanoids. No expression of cPLA$_2$α could be observed in the affected individuals' small intestine or PBMCs. Functional studies of platelet aggregation demonstrated that both individuals were unable to synthesise the eicosanoid thromboxane A$_2$, a situation which could be rescued by the addition of exogenous arachidonic acid.

The intestinal disease observed in the two affected individuals bore a striking resemblance to the enteropathy that results from long-term use of high dose non-steroidal anti-inflammatory drugs (NSAIDs), which function to block synthesis of prostaglandins (a class of eicosanoid) by their actions as cyclooxygenase (COX) inhibitors (see section 5.1.3). In particular, gastro-duodenal and small intestinal ulceration and concentric strictures of the small bowel are known consequences of high-dose, long-term NSAID use (Bjarnason et al*et al*., 1988, Matsuhashi et al*et al*., 1992, De Petris and Lopez, 2008, Fellows et al*et al*., 1992),

and (but for the greater severity of the disease) closely resemble the phenotype of the affected individuals described here. As such, it seems likely that the enteropathy affecting these two siblings is a direct consequence of their inability to produce prostaglandins and other eicosanoids.

As described in section 5.1.5, prostaglandins, particularly PGE_2 and PGI_2, play especially important roles in gastrointestinal defence, by stimulating the secretion of mucus (and bicarbonate in the stomach), increasing blood flow to the intestinal epithelium and accelerating cellular proliferation in the intestinal epithelium following damage, via EGFR transactivation. As mentioned previously, cell proliferation stimulated by prostaglandins (especially PGE_2) requires transactivation of the EGFR, in a process dependent on ADAM17 shedding of TGFα (Pai ~~et al~~*et al*., 2002), meaning that the intestinal disease described in the two $cPLA_2\alpha$-deficient individuals can be expected to share, in part, a common pathophysiology with that seen in the ADAM17-deficient individual described in chapter 3. In addition to the roles of PGE_2 and PGI_2, other prostaglandins have been shown to have important gastro-protective effects, including PGD_2, and its derivative 15-deoxy-$\Delta^{12,14}$-PGJ_2, which has a potent anti-inflammatory role that results from its ability to specifically inhibit the NF-κB signalling pathway (a key activator of inflammatory response genes) (Straus ~~et al~~*et al*., 2000). PGD_2 has meanwhile been shown to be specifically upregulated in the long-term remission of ulcerative colitis (Vong ~~et al~~*et al*., 2010), illustrating a gastro-protective effect which would presumably also be lacking in $cPLA_2\alpha$-deficiency. As well as the absence of these prostaglandins, the increased severity of the enteropathy seen in the two individuals described here (relative to that seen in NSAID-associated enteropathy) may reflect the wider spectrum of eicosanoids that cannot be produced by the $cPLA_2\alpha$-deficient individuals. For example, lipoxins are a class of eicosanoid produced by the sequential actions of two or more lipoxygenase enzymes from arachidonic acid; lipoxins can therefore be produced in NSAID-treated individuals, whilst the $cPLA_2\alpha$-deficient individuals described here will be unable to synthesise them. Lipoxins A_4 and B_4 have potent anti-inflammatory and pro-resolution functions, and have been shown to have gastro-protective actions (Serhan, 2005, Pajdo ~~et al~~*et al*., 2011), as well as anti-inflammatory roles in other tissues.

A single case of ileo-jejunal ulceration, accompanied by gastrointestinal blood loss, anaemia, and impaired eicosanoid biosynthesis, has previously been reported to be associated with compound heterozygous single base-pair mutations in *PLA2G4A.* Interestingly, this patient only developed disease requiring surgery in the 4th decade of life, although milder symptoms

of gastrointestinal ulceration were described as having been lifelong. In addition, unlike the cPLA$_2$α-deficient siblings described here, who have severe duodenal, gastric and oesophageal disease, this compound heterozygous individual had a normal upper bowel. Although the mutations observed in the compound heterozygote were expected to affect the conformation of cPLA$_2$α, a reasonable (though reduced) degree of protein expression could be observed in this individual. Furthermore, although also significantly reduced, expression of multiple eicosanoids was observed in the compound heterozygote (TxA$_2$, PGI$_2$ and PGE$_2$ were found at 16, 30 and 43% of normal expression levels respectively, for example) (Adler ~~et al~~*et al*., 2008). This is in contrast to the pair of individuals carrying the g.155574_77delGTAA mutation, who demonstrated no cPLA$_2$α expression in the small intestine or PBMCs, and no detectable production of TxA$_2$ in the absence of arachidonic acid, although metabolites of other eicosanoids were not examined. Moreover, aggregation of platelets in the plasma of the two affected individuals was identical to that of healthy volunteers treated with aspirin, a drug which irreversibly blocks TxA$_2$ production. It is therefore reasonable to assume that cPLA$_2$α activity is completely absent in these two individuals (carrying the g.155574_77delGTAA mutation), in contrast to the previously described compound heterozygote, whose cPLA$_2$α deficiency is clearly less marked, and whose associated disease is consequently of a much less severe nature.

As well as the pronounced and severe enteropathy, both cPLA$_2$α-deficient individuals were affected by multiple extra-intestinal complications. Considering the lifelong nature of their disease, it is in some cases difficult to determine whether these systemic complications were secondary to their severe enteropathy, or represent separate phenomena. Both siblings have shown clear pathologies of the biliary tree, such as fibrosis and ulceration of the common bile duct, accompanied variously by liver abscesses, evidence of fibrosis in the liver and gall stones. Due to the intimate connection between the GI tract and biliary tree, these pathologies may most likely represent mechanical damage, arising from the increased susceptibility of the bile duct and related tissues to stress and injury in the absence of eicosanoid-mediated protection. However, cPLA$_2$α also plays an important role in the direct protection of hepatocytes from Fas-induced apoptosis (mediated through upregulation of EGFR activity), illustrating another potential mechanism of liver injury in the absence of cPLA$_2$α (Li ~~et al~~*et al*., 2011a). The female sibling has meanwhile developed pernicious anaemia, which could be hypothesised to result from a deficiency of vitamin B$_{12}$ absorption as a consequence of the extensive gastrointestinal damage. This possibility is supported by the fact that vitamin B$_{12}$ deficiency has also been previously noted in the male sibling.

However, the pathogenesis of other extra-intestinal disease developed by the siblings, including bladder fibrosis, endometrosis, infertility and cardiac ventricular hypertrophy in the female, and diabetes in the male, cannot be obviously ~~be~~ explained as secondary complications of severe enteropathy. Many of the symptoms seen in the cPLA$_2$α-deficient individuals do however bear similarities to those seen in *Pla2g4a*-null mice, which do demonstrate defects in reproduction (Bonventre ~~et al~~*et al*., 1997) and parturition (Uozumi ~~et al~~*et al*., 1997) and exaggerated cardiac muscle growth (Haq ~~et al~~*et al*., 2003), as well as ulcerative small intestinal lesions (Takaku ~~et al~~*et al*., 2000). In addition, a naturally occurring genotypic variant of *PLA2G4A* has been strongly associated with the development of type-2 diabetes in the Pima Native American population, a population with an extremely high prevalence of that disease (Wolford ~~et al~~*et al*., 2003).

The female sibling in particular has also suffered repeatedly from infectious diseases, including infections by *Candida albicans, Campylobacter* and *Salmonella* species, as well as repeated, severe *Staphylococcus* infections. This susceptibility to infection may be related to the role cPLA$_2$α is known to play in innate immunity. For example, cPLA$_2$α has been shown to be required for the efficient killing of bacteria by neutrophils (Rubin ~~et al~~*et al*., 2005), which some reports have suggested may be related to a requirement for cPLA$_2$α in the activation of NADPH oxidase, an enzyme necessary for the generation of reactive oxygen species, in a process known as respiratory burst (Shmelzer ~~et al~~*et al*., 2003, Murakami ~~et al~~*et al*., 2011). Abscesses of the skin and other tissues are frequently seen in diseases such as chronic granulomatous disease, which are related to an inability to generate such reactive oxygen species in immune cells, frequently as a result of mutations in the NADPH oxidase-2 gene *CYBB* (Holland, 2010). The presence of multiple abscesses in the cPLA$_2$α-deficient individuals described here could thus plausibly be related to deficiencies in this pathway. Furthermore, immunity to intracellular pathogens such as *Chlamydia trachomatis* requires cPLA$_2$α, since in its absence production of type I interferon is deficient (Vignola ~~et al~~*et al*., 2010); whilst *Candida albicans* has been shown to rapidly upregulate cPLA$_2$α in macrophages, suggesting that its absence may compromise innate immunity to that yeast (Parti ~~et al~~*et al*., 2010). Lastly, cPLA$_2$α is involved in the induction, by pro-inflammatory cytokines, of expression of the intercellular adhesion molecule ICAM-1 on the surface of endothelial cells, suggesting that cPLA$_2$α-deficient individuals may be affected by impaired mobilisation and transmigration of leukocytes from the bloodstream into tissues to deal with infectious agents (Hadad ~~et al~~*et al*., 2011).

In conclusion, mutations in *PLA2G4A* were found to segregate with the severe CMUSE-like syndrome observed in two affected individuals over a 40-year period. CMUSE remains a very rarely diagnosed condition, despite its severe consequences, and has until now never been associated with any inherited mutations. As such, investigations of *PLA2G4A* offer a novel diagnostic strategy in cases of otherwise unexplained gastrointestinal ulceration and stricturing.

6.4. Future work

The findings presented in this thesis offer specific insights into the pathophysiology of the inherited diseases studied, but also into the wider biology of the particular proteins affected by mutations in each instance. As such, these findings could be used as the basis for further investigations in numerous fields.

In the first instance, the most immediate potential impact of understanding these genetic disorders is in informing the treatment of patients affected by them. To at least some extent, the inflammatory skin phenotype described in chapter 3 could plausibly result from downregulation of transglutaminase 1 (TGM1) activity in the upper epidermal layers of the affected individual studied. As described in section 6.1, the TGM1-dependent inflammatory skin phenotype seen in mice with a keratinocyte restricted *Adam17* knockout could be reversed by the application of topical TGFα; this suggests that EGFR ligand supplementation, for example by topical creams, may offer a route to treatment of this skin condition. However, the epidermis of this individual is already notably hyperproliferative, meaning that further growth factor supplementation would have to be carefully monitored, to avoid exacerbating this phenotype.

Next, the finding that the pathology of tylosis with oesophageal cancer (TOC) is associated with upregulation of ADAM17 activity suggests that direct pharmacological targeting of this pathway may prove useful in the treatment of at least the skin manifestations of this condition. Targeting of ADAM17 has in the past been considered as a potential strategy in treatment of inflammatory diseases driven by TNFα (Saftig and Reiss, 2011, Arribas and Esselens, 2009), until the severe phenotype of *Adam17* knockout mice dampened enthusiasm for this approach. However, the relatively (in comparison to mouse models) minor phenotype seen in the individuals affected by *ADAM17* loss-of-function mutations (as described in chapter 3) illustrates ADAM17 inhibition would not necessarily result in the same severe disease in adult humans, and suggesting that pharmacological treatment of this pathway should be considered plausible in future. Furthermore, the majority of the most serious defects observed in *Adam17* null mice result from impaired shedding of EGFR ligands (and therefore of reduced EGFR signalling). It is therefore pertinent to note that therapeutic targeting of the EGFR is a widely used and proven strategy in cancer treatment; and although inflammatory skin disease is a consequence of this approach, the effects seen are by no means as severe as those in *egfr*-null mice, suggesting that ADAM17 inhibition need not be expected to result in the same effects.

Treatment of the two individuals affected by CMUSE, as a result of *PLA2G4A* mutations, could also plausibly follow from the identification of cPLA$_2$α mutations as the cause of their inherited disease. In this case, replacement of prostaglandins, the inability to synthesise which may contribute significantly to the disease observed, would appear to be the most obvious treatment strategy. Indeed, subsequent to the findings of *PLA2G4A* mutations as the causative factor in this disease, both affected individuals began to be treated with the synthetic PGE$_2$ analogue misoprostol. Neither individual initially tolerated the treatment very well, complaining of gastrointestinal upset and an unusual 'fuzzy' feeling, which may reflect the fact that they were unaccustomed to having any circulating prostaglandins at all. However, in the female sibling at least, renal function has stabilised, the need for oesophageal dilatation has reduced, and there have been no severe, acute episodes of gastrointestinal disease since treatment began (Dr. Hilary Longhurst, personal communication). Notably, the previously described American individual with compound heterozygous *PLA2G4A* mutations improved only slightly when treated with misoprostol, but improved significantly when the nitric oxide donor sildenafil was added, suggesting a potential treatment strategy in future.

Other patient-focussed investigations could include the genetic screening of other individuals who have displayed symptoms similar to those seen in the three diseases described here. In the case of the diseases associated to *ADAM17* and *PLA2G4A* mutations, investigation of other potentially-disease-affected individuals and families can and has been performed by direct sanger sequencing of those genes, as previously described. A number of potentially affected individuals have already been screened by this method, without the finding of any potentially disease-causing mutations in these genes, with the possible exception of a ~~dutch~~Dutch individual described in section 3.3. In these cases, further investigations into a genetic cause for these diseases could involve more general next generation sequencing techniques, such as whole exome sequencing.

Beyond patient focussed investigations, the findings of TOC-associated iRHOM2 mutations having a significant effect on ADAM17 maturation can also form the basis of further experiments. The particular localisation of iRHOM2 mutations associated with TOC within the protein structure suggests that ADAM17 maturation is heavily influenced by interactions involving the iRHOM2 N-terminal domain generally, and the highly-conserved motif affected by TOC-associated mutations in particular. This association could be further investigated by the knock-in of these mutations into animal models. No mouse model of TOC yet exists, but the effects of TOC-associated iRHOM2 mutations on epidermal and oesophageal homeostasis in this system would be very interesting, and could also be used to shed light on the cancer susceptibility that is a key feature of TOC. Conversely, the finding that these three very specific residues are intimately involved in ADAM17 maturation would make studies into the particular iRHOM2 residues necessary for ADAM17-iRHOM2 of particular interest. For example, targeted knock out of, or the introduction of deleterious mutations to, the specific residues involved could be used to establish which particular features of the iRHOM2 N-terminal domain are necessary for ADAM17 maturation. Similarly, the introduction of TOC-associated mutations into iRHOM1 (which shares the function of iRHOM2 in ADAM17 maturation, and in which the TOC-associated residues are identical) in cell or animal models could be used to further investigate the iRHOM-ADAM17 interaction, and its importance in cellular signalling.

Similarly, the finding in TOC epidermis of many features associated to epidermal wound healing make the function of iRHOM2 in skin regeneration an aspect of TOC that bears further scrutiny. As well as wound healing studies in any potential TOC mouse model, zebrafish have in recent years emerged as valuable models of cutaneous wound healing

(Richardson ~~et al~~*et al*., 2013), and could be used to investigate wound healing in TOC. Zebrafish do express a single iRHOM protein, meaning that a model of TOC wound healing could be generated either by mutation of the zebrafish iRHOM, or by engineering zebrafish to express human TOC-associated-mutant iRHOM2.

Further investigations of iRHOM biology could focus on their roles beyond the regulation of ADAM17 maturation. It is interesting to note that a mouse double knockout of both iRHOMs results in a phenotype that does not exactly phenocopy that seen in *Adam17*-null mice. This double iRHOM knockout phenotype is both more severe than *Adam17* knockout, in that it leads to lethality at a much earlier stage, but also results in effects that are not obviously related to ADAM17 dysfunction, such as brain haemorrhages and dysfunctions in multiple organs (Christova ~~et al~~*et al*., 2013). This therefore implies that iRHOMs regulate processes other than ADAM17 maturation, and that investigation of other iRHOM functions would provide fruitful insights into the development and homeostasis of numerous tissues.

Returning to the particular disease phenotype of TOC, the particular effects of TOC-associated iRHOM2 mutations in oesophageal carcinogenesis would be of particular interest. In particular, considering the specific upregulation of EGFR ligand shedding in TOC, investigating the ADAM17-EGFR axis in oesophageal squamous cell carcinoma (OSCC) further, by histological, genetic and functional analyses of TOC-associated OSCC cells and tissue samples, as well as samples of the oesophageal precursor lesions that develop in TOC patients, would be a priority in further research. This would provide meaningful insights into the biology of both TOC-associated and sporadic oesophageal tumours, a cancer type which remains severely under-researched, despite its high incidence and rate of mortality.

At a wider level, investigations into TOC highlight the potential utility of the skin in investigating syndromic disease. In a similar fashion to TOC, and as described in section 1.3.2, numerous inherited syndromes exist that feature skin disease as only one of a number of pathologies, accompanied by other conditions such as the oesophageal cancer susceptibility in TOC. Because of the high visibility and accessibility of the skin, investigations of skin cells affected by a disease can provide useful insights into the pathophysiology of conditions affecting otherwise inaccessible tissues. For example, examination of the effects of mutations in desmosomal components in keratinocytes could be used to understand the desmosomal defect that could cause the cardiac condition arrhythmogenic right ventricular cardiomyopathy (ARVC), which would otherwise be intensely difficult due to the unavailability of heart tissue. Taken further, the availability of skin cells that carry a particular

inherited mutation could be exploited by harvesting these cells and reprogramming them into induced pluripotent stem cells (iPS cells), which could then be differentiated into other cell types and used to investigate syndromic diseases affecting other, non-skin tissues.

6.5. Concluding remarks

This thesis has focussed on investigations into the pathophysiology of three rare, inherited diseases, and has sought to offer physiological explanations as to the mechanisms by which mutations in the associated genes – *ADAM17, RHBDF2* and *PLA2G4A* – result in the various phenotypes that characterise these conditions. It is particularly interesting to have observed that two distinct diseases, an ADAM17 loss-of-function-associated syndrome and tylosis with oesophageal cancer, have pathophysiologies that essentially reflect the down- and upregulation of the same gene (ADAM17), with entirely different consequences.

Taken together, the data presented here underscore both the power of next-generation genotyping technologies, and the utility of combining these with well-understood cell and molecular biology techniques, in the investigation and understanding of rare and complex inherited diseases.

Chapter 7

Appendices

7. Appendices

7.1. Appendix 1: Primers and probes used in genotyping and qPCR studies

Table A1.1: Primers used for *ADAM17* genotyping

Formatted: Font: Italic

ADAM17 Exon (s)	Forward Primer	Reverse Primer	Product Size (bp)
1	CTGCTCTTCCCTCAAACGAG	CTTCCGGCTGTGGGTGG	411
2	CCCAAGATTTCAGTAGATACCCTT	GTCTGGCACTCTCATTTTAACGA	302
3	CTGCACCAGAAAAGAATATGCA	TGAGACTTAAAATTTGTGTGCTT	271
4	CTGAGCAGCTTTTTGAAAATCAG	TTGAGAGTAATGCATAGTTTCTTAT	221
5	AAGAACAAGCAAAGAATGTTAGAAGA	GGAACAAACCTCTTATTTTCATGC	306
6	CATGGAATGTACCCACCCAA	ACTCCTTGTTTTGGTGAATTTTGA	246
7	AGGTTTTGAATACAAGTGACAAA	CAGGAGAGGTAAAGAGTTACAT	217
8	TCCTTCATTAAAACACATACAATCC	GAGCCTTCTGACTTATTTTGGA	250
9 & 10	ACTGAGGTTCTACTACAATAAACT	CATCTTTTAGTCTGATGTAATTGTT	477
11	TGATCATTATACACAGCCTCTTTCC	TTTAAGACAGCATAGGCCCAAC	294
12	CCTGCAAGTTCAGTCTTCTCTTA	ATTGCATGGGAATACATTTTTATGA	340
13	TCATCTGAACAAAACATAATCTTGT	CGTTTGATTTGATATGGGGCC	253
14	GCAGACAAAGGCCATGTTTTC	GCACCTGTAGAACTGGTGGA	252
15	ACTTCCTATCTGGCTGTTACA	AGAGGCAGGTCTCAGAACAA	228
16	TCATCACAGAAATTGACTCAGCT	TGCTTCTGAATACATTGTGTTTGG	189
17	CCAGAGATTACATGGTTGGAGT	TTTGTGAAGTACTTGGTCAAGA	209

18	CTAACAGGGCCTCAGACCA	CTGAATTGTATTTGTAGGGAATGAC	152
19	ACAAGCTGTGATTGATTTGTAGG	TGAGGACCTCCGATTCATCTT	476

Table A1.2: Primers used for *PLA2G4A* (cPLA$_2\alpha$) genotyping

***PLA2G4A* Exon (s)**	**Forward Primer**	**Reverse Primer**	**Product Size (bp)**
1	AAAGCGCAAGGAGACCAGCCC	GAGGGTGGGAGAGAGAAGTGGAGC	190
2	ACTGCATCCAAGAGGAAGCTTAACA	AGCAACACCCGCAATATTCACAGA	224
3	GTTTCTGGTATGCATGCTACTTGTT	AGGCAGAACCTCCGATTTGTCA	288
4	ACCTCCTTCTTGTTTGTGTTTACT	GGACAAACTCAAGCATGTCTCTCA	249
5	TCCATGGGAAATTTTATTTTTGTGC	CCAAGTGTTAAACCCAACTTCCC	239
6	AGGGTCTTCATGGAGCTGTGT	AGTGGATCACTCACAATATTTCTCA	239
7	AAACCAGACCACTGGGAGCA	TTGGGGAAATTGTCCAAGCTAAA	261
8	GTGTACAAATCTCTCTGTTGCATCG	TCCCCTTTTCTCTTCTAGTGCTTG	251
9	ACAGAGTGTGCCTTCTTTCTTTGG	ACGCATAGTTGGACAAATAAGTAGA	437
10	TGAATAGCATTCTTTCTGTGTCTGT	TGCAATTCAGAGGTTCCAGGAAGT	229
11 & 12	TAATTGTGCACACCATGCCA	AGCAAGATTTGTATCAATGTAAGCA	431
13	GATCTCACTCTGTGGTTTTGCTCA	ATCCTTTCCTCATGGATCTGGGC	220
14	TTTGGAGTCTGTATGGTGACCTTTT	TCTCCTGCATTAGCTCCCACT	321
15	GTCTCCAAAGCCTGAGGGCCTA	AAGGCAAGCAAGAGAATGTGGT	362
16	TGCTGGCACACAGTAGACACCT	GCTGGTACAGCAGTGACAGAGTGA	394
17	TGGGGACTCCCACTGCTGTCT	AGTGGCATATTTTGGGTGGTGTCAT	392
18	GCAGCGCTAATTATACAACTTCTGT	GGGATTGCAAACTGCCTCAGC	222

Table A1.3: Primers used for TaqMan qPCR

Gene	**Forward Primer**	**Reverse Primer**	**Product Size (bp)**
ADAM17	GGTTCCTTTCGTGCTGGCGC	AAGCTTCTCGAGTCTCTGGTGGG	73
GAPDH	TGGCCCCTCCGGGAAACTGT	CCTTGCCCACAGCCTTGGCA	92
AREG	AAGGACCAATGAGAGCCCCG	TAATGGCCTGAGCCGAGTATC	82
TGFA	AGCATGTGTCTGCCATTCTG	TGTGATGATAAGGACAGCCAGG	96
HBEGF	TTCTGGCTGCAGTTCTCTCG	TGGATACAGTGGGAGGGTC	105
TNF	GCCCATGTTGTAGCAAACCC	TATCTCTCAGCTCCACGCCA	97
IL6	CAGTTCCTGCAGAAAAAGGCAA	CTGCAGCCACTGGTTCTGT	108
IL8	ACCACCGGAAGGAACCATCT	GGCAAAACTGCACCTTCACAC	111

Table A1.4: Fluorescently-labelled probes used for TaqMan qPCR

Gene	**Probe**	**5' Modification**	**3' modification**
ADAM17	CGCGACCTCCGGATGACCCGGGCT	6-FAM	BHQ-1
GAPDH	GCGTGATGGCCGCGGGGCTCTCCA	HEX	BHQ-1
AREG	GCCGGCGCCGGTGGTGCTGT	6-FAM	BHQ-1
TGFA	TGGCCGTGGTGGCTGCCAGCCA	6-FAM	BHQ-1
HBEGF	GGCGAGAGCCTGGAGCGGCTTCGG	6-FAM	BHQ-1
TNF	CGCCGGGCCAATGCCCTCCTGGCC	6-FAM	BHQ-1
IL6	GCCAGCCTGCTGACGAAGCTGCAGGC	6-FAM	BHQ-1

IL8	GCTGGCCGTGGCTCTCTTGGCAGCC	6-FAM	BHQ-1

Chapter 8

Bibliography

ABECASIS, G. R., CHERNY, S. S., COOKSON, W. O. & CARDON, L. R. 2002. Merlin--rapid analysis of dense genetic maps using sparse gene flow trees. *Nat Genet,* 30**,** 97-101.

ABEDI-ARDEKANI, B., DAR, N. A., MIR, M. M., ZARGAR, S. A., LONE, M. M., MARTEL-PLANCHE, G., VILLAR, S., MOUNAWAR, M., SAIDI, F., MALEKZADEH, R. & HAINAUT, P. 2012. Epidermal growth factor receptor (EGFR) mutations and expression in squamous cell carcinoma of the esophagus in central Asia. *BMC Cancer,* 12**,** 602.

ADLER, D. H., COGAN, J. D., PHILLIPS, J. A., 3RD, SCHNETZ-BOUTAUD, N., MILNE, G. L., IVERSON, T., STEIN, J. A., BRENNER, D. A., MORROW, J. D., BOUTAUD, O. & OATES, J. A. 2008. Inherited human cPLA(2alpha) deficiency is associated with impaired eicosanoid biosynthesis, small intestinal ulceration, and platelet dysfunction. *J Clin Invest,* 118**,** 2121-31.

ADRAIN, C., STRISOVSKY, K., ZETTL, M., HU, L., LEMBERG, M. K. & FREEMAN, M. 2011. Mammalian EGF receptor activation by the rhomboid protease RHBDL2. *EMBO Rep,* 12**,** 421-7.

ADRAIN, C., ZETTL, M., CHRISTOVA, Y., TAYLOR, N. & FREEMAN, M. 2012. Tumor necrosis factor signaling requires iRhom2 to promote trafficking and activation of TACE. *Science,* 335**,** 225-8.

AGGARWAL, B. B., GUPTA, S. C. & KIM, J. H. 2012. Historical perspectives on tumor necrosis factor and its superfamily: 25 years later, a golden journey. *Blood,* 119**,** 651-65.

AGUS, D. B., AKITA, R. W., FOX, W. D., LEWIS, G. D., HIGGINS, B., PISACANE, P. I., LOFGREN, J. A., TINDELL, C., EVANS, D. P., MAIESE, K., SCHER, H. I. & SLIWKOWSKI, M. X. 2002. Targeting ligand-activated ErbB2 signaling inhibits breast and prostate tumor growth. *Cancer Cell,* 2**,** 127-37.

ALLISON, M. C., HOWATSON, A. G., TORRANCE, C. J., LEE, F. D. & RUSSELL, R. I. 1992. Gastrointestinal damage associated with the use of nonsteroidal antiinflammatory drugs. *N Engl J Med,* 327**,** 749-54.

ALTSHULER, D., DALY, M. J. & LANDER, E. S. 2008. Genetic mapping in human disease. *Science,* 322**,** 881-8.

ANKLESARIA, P., TEIXIDO, J., LAIHO, M., PIERCE, J. H., GREENBERGER, J. S. & MASSAGUE, J. 1990. Cell-cell adhesion mediated by binding of membrane-anchored transforming growth factor alpha to epidermal growth factor receptors promotes cell proliferation. *Proc Natl Acad Sci U S A,* 87**,** 3289-93.

ARICAN, O., ARAL, M., SASMAZ, S. & CIRAGIL, P. 2005. Serum levels of TNF-alpha, IFN-gamma, IL-6, IL-8, IL-12, IL-17, and IL-18 in patients with active psoriasis and correlation with disease severity. *Mediators Inflamm,* 2005**,** 273-9.

ARNOTT, C. H., SCOTT, K. A., MOORE, R. J., ROBINSON, S. C., THOMPSON, R. G. & BALKWILL, F. R. 2004. Expression of both TNF-alpha receptor subtypes is essential for optimal skin tumour development. *Oncogene,* 23**,** 1902-10.

ARRIBAS, J., BECH-SERRA, J. J. & SANTIAGO-JOSEFAT, B. 2006. ADAMs, cell migration and cancer. *Cancer Metastasis Rev,* 25**,** 57-68.

ARRIBAS, J. & ESSELENS, C. 2009. ADAM17 as a therapeutic target in multiple diseases. *Curr Pharm Des,* 15**,** 2319-35.

ASAKURA, M., KITAKAZE, M., TAKASHIMA, S., LIAO, Y., ISHIKURA, F., YOSHINAKA, T., OHMOTO, H., NODE, K., YOSHINO, K., ISHIGURO, H., ASANUMA, H., SANADA, S., MATSUMURA, Y., TAKEDA, H., BEPPU, S., TADA, M., HORI, M. & HIGASHIYAMA, S. 2002. Cardiac hypertrophy is inhibited by antagonism of ADAM12 processing of HB-EGF: metalloproteinase inhibitors as a new therapy. *Nat Med,* 8**,** 35-40.

BALKWILL, F. 2006. TNF-alpha in promotion and progression of cancer. *Cancer Metastasis Rev,* 25**,** 409-16.

BALKWILL, F. 2009. Tumour necrosis factor and cancer. *Nat Rev Cancer,* 9**,** 361-71.

BARRIENTOS, S., STOJADINOVIC, O., GOLINKO, M. S., BREM, H. & TOMIC-CANIC, M. 2008. Growth factors and cytokines in wound healing. *Wound Repair Regen,* 16**,** 585-601.

BECH-SERRA, J. J., SANTIAGO-JOSEFAT, B., ESSELENS, C., SAFTIG, P., BASELGA, J., ARRIBAS, J. & CANALS, F. 2006. Proteomic identification of desmoglein 2 and activated leukocyte cell adhesion molecule as substrates of ADAM17 and ADAM10 by difference gel electrophoresis. *Mol Cell Biol,* 26**,** 5086-95.

BECHERER, J. D. & BLOBEL, C. P. 2003. Biochemical properties and functions of membrane-anchored metalloprotease-disintegrin proteins (ADAMs). *Curr Top Dev Biol,* 54**,** 101-23.

BECKER, C., FANTINI, M. C., SCHRAMM, C., LEHR, H. A., WIRTZ, S., NIKOLAEV, A., BURG, J., STRAND, S., KIESSLICH, R., HUBER, S., ITO, H., NISHIMOTO, N., YOSHIZAKI, K., NISHIMOTO, N., GALLE, P. R., BLESSING, M., ROSE-JOHN, S. & NEURATH, M. F. 2004. TGF-beta suppresses tumor progression in colon cancer by inhibition of IL-6 trans-signaling. *Immunity,* 21**,** 491-501.

BECKER, C., FANTINI, M. C., WIRTZ, S., NIKOLAEV, A., LEHR, H. A., GALLE, P. R., ROSE-JOHN, S. & NEURATH, M. F. 2005. IL-6 signaling promotes tumor growth in colorectal cancer. *Cell Cycle,* 4**,** 217-220.

BEN-SHEM, A., FASS, D. & BIBI, E. 2007. Structural basis for intramembrane proteolysis by rhomboid serine proteases. *Proceedings of the National Academy of Sciences of the United States of America,* 104**,** 462-466.

BEZZINE, S., KODURI, R. S., VALENTIN, E., MURAKAMI, M., KUDO, I., GHOMASHCHI, F., SADILEK, M., LAMBEAU, G. & GELB, M. H. 2000. Exogenously added human group X secreted phospholipase A(2) but not the group IB, IIA, and V enzymes efficiently release arachidonic acid from adherent mammalian cells. *Journal of Biological Chemistry,* 275**,** 3179-3191.

BJARNASON, I., PRICE, A. B., ZANELLI, G., SMETHURST, P., BURKE, M., GUMPEL, J. M. & LEVI, A. J. 1988. Clinicopathological features of nonsteroidal antiinflammatory drug-induced small intestinal strictures. *Gastroenterology,* 94**,** 1070-4.

BLACK, R. A., RAUCH, C. T., KOZLOSKY, C. J., PESCHON, J. J., SLACK, J. L., WOLFSON, M. F., CASTNER, B. J., STOCKING, K. L., REDDY, P., SRINIVASAN, S., NELSON, N., BOIANI, N.,

SCHOOLEY, K. A., GERHART, M., DAVIS, R., FITZNER, J. N., JOHNSON, R. S., PAXTON, R. J., MARCH, C. J. & CERRETTI, D. P. 1997. A metalloproteinase disintegrin that releases tumour-necrosis factor-alpha from cells. *Nature,* 385**,** 729-33.

BLANCHOT-JOSSIC, F., JARRY, A., MASSON, D., BACH-NGOHOU, K., PAINEAU, J., DENIS, M. G., LABOISSE, C. L. & MOSNIER, J. F. 2005. Up-regulated expression of ADAM17 in human colon carcinoma: co-expression with EGFR in neoplastic and endothelial cells. *J Pathol,* 207**,** 156-63.

BLAYDON, D. C., BIANCHERI, P., DI, W. L., PLAGNOL, V., CABRAL, R. M., BROOKE, M. A., VAN HEEL, D. A., RUSCHENDORF, F., TOYNBEE, M., WALNE, A., O'TOOLE, E. A., MARTIN, J. E., LINDLEY, K., VULLIAMY, T., ABRAMS, D. J., MACDONALD, T. T., HARPER, J. I. & KELSELL, D. P. 2011a. Inflammatory skin and bowel disease linked to ADAM17 deletion. *N Engl J Med,* 365**,** 1502-8.

BLAYDON, D. C., ETHERIDGE, S. L., RISK, J. M., HENNIES, H. C., GAY, L. J., CARROLL, R., PLAGNOL, V., MCRONALD, F. E., STEVENS, H. P., SPURR, N. K., BISHOP, D. T., ELLIS, A., JANKOWSKI, J., FIELD, J. K., LEIGH, I. M., SOUTH, A. P. & KELSELL, D. P. 2012. RHBDF2 mutations are associated with tylosis, a familial esophageal cancer syndrome. *Am J Hum Genet,* 90**,** 340-6.

BLAYDON, D. C., NITOIU, D., ECKL, K. M., CABRAL, R., BLAND, P., HAUSSER, I., VAN HEEL, D. A., RAJPOPAT, S., FISCHER, J., OJI, V., ZVULUNOV, A., TRAUPE, H., HENNIES, H. C. & KELSELL, D. P. 2011b. Mutations in cystatin A underlie autosomal recessive exfoliative ichthyosis and reveal a role for this protease inhibitor in cell-cell adhesion. *Am J Hum Genet,* 89**,** 1-8.

BLOBEL, C. P. 2005. ADAMs: key components in EGFR signalling and development. *Nat Rev Mol Cell Biol,* 6**,** 32-43.

BODE, W., GOMIS-RUTH, F. X. & STOCKLER, W. 1993. Astacins, serralysins, snake venom and matrix metalloproteinases exhibit identical zinc-binding environments (HEXXHXXGXXH and Met-turn) and topologies and should be grouped into a common family, the 'metzincins'. *FEBS Lett,* 331**,** 134-40.

BONVENTRE, J. V., HUANG, Z., TAHERI, M. R., O'LEARY, E., LI, E., MOSKOWITZ, M. A. & SAPIRSTEIN, A. 1997. Reduced fertility and postischaemic brain injury in mice deficient in cytosolic phospholipase A2. *Nature,* 390**,** 622-5.

BORRELL-PAGES, M., ROJO, F., ALBANELL, J., BASELGA, J. & ARRIBAS, J. 2003. TACE is required for the activation of the EGFR by TGF-alpha in tumors. *EMBO J,* 22**,** 1114-24.

BRENNAN, D., PELTONEN, S., DOWLING, A., MEDHAT, W., GREEN, K. J., WAHL, J. K., DEL GALDO, F. & MAHONEY, M. G. 2012. A role for caveolin-1 in desmoglein binding and desmosome dynamics. *Oncogene,* 31**,** 1636-1648.

BREYER, M. D. & BREYER, R. M. 2000. Prostaglandin receptors: their role in regulating renal function. *Curr Opin Nephrol Hypertens,* 9**,** 23-9.

BROOKE, M. A., ETHERIDGE, S. L., KAPLAN, N., SIMPSON, C., O'TOOLE, E., ISHIDA-YAMAMOTO, A., MARCHES, O., GETSIOS, S. & KELSELL, D. P. 2014a. iRHOM2-dependent regulation of ADAM17 in cutaneous disease and epidermal barrier function. *Hum Mol Genet*.

BROOKE, M. A., LONGHURST, H. J., PLAGNOL, V., KIRKBY, N. S., MITCHELL, J. A., RUSCHENDORF, F., WARNER, T. D., KELSELL, D. P. & MACDONALD, T. T. 2014b. Cryptogenic multifocal ulcerating stenosing enteritis associated with homozygous deletion mutations in cytosolic phospholipase A2-alpha. *Gut,* 63**,** 96-104.

BROOKE, M. A., NITOIU, D. & KELSELL, D. P. 2012. Cell-cell connectivity: desmosomes and disease. *J Pathol,* 226**,** 158-71.

BROU, C., LOGEAT, F., GUPTA, N., BESSIA, C., LEBAIL, O., DOEDENS, J. R., CUMANO, A., ROUX, P., BLACK, R. A. & ISRAEL, A. 2000. A novel proteolytic cleavage involved in Notch signaling: the role of the disintegrin-metalloprotease TACE. *Mol Cell,* 5**,** 207-16.

BUCHAU, A. S. 2010. EGFR (trans)activation mediates IL-8 and distinct human antimicrobial peptide and protein production following skin injury. *J Invest Dermatol,* 130**,** 929-32.

BUCHON, N., BRODERICK, N. A., KURAISHI, T. & LEMAITRE, B. 2010. Drosophila EGFR pathway coordinates stem cell proliferation and gut remodeling following infection. *BMC Biol,* 8**,** 152.

BUITRAGO-PEREZ, A., GARAULET, G., VAZQUEZ-CARBALLO, A., PARAMIO, J. M. & GARCIA-ESCUDERO, R. 2009. Molecular Signature of HPV-Induced Carcinogenesis: pRb, p53 and Gene Expression Profiling. *Curr Genomics,* 10**,** 26-34.

CAMPBELL, J. R. & KNAPP, R. W. 1966. Small bowel ulceration associated with thiazide and potassium therapy: review of 13 cases. *Ann Surg,* 163**,** 291-6.

CAMPBELL, P., MORTON, P., TAKEICHI, T., SALAM, A., ROBERTS, N., PROUDFOOT, L. E., MELLERIO, J. E., AMINU, K., WELLINGTON, C., PATIL, S. N., AKIYAMA, M., LIU, L., MCMILLAN, J. R., ARISTODEMOU, S., ISHIDA-YAMAMOTO, A., ABDUL-WAHAB, A., PETROF, G., FONG, K., HARNCHOOWONG, S., STONE, K., HARPER, J. I., MCLEAN, W. H., SIMPSON, M. A., PARSONS, M. & MCGRATH, J. A. 2014. Epithelial Inflammation Resulting from an Inherited Loss-of-Function Mutation in EGFR. *J Invest Dermatol*.

CAPRONI, M., ANTIGA, E., MELANI, L., VOLPI, W., DEL BIANCO, E. & FABBRI, P. 2009. Serum levels of IL-17 and IL-22 are reduced by etanercept, but not by acitretin, in patients with psoriasis: a randomized-controlled trial. *J Clin Immunol,* 29**,** 210-4.

CARRAWAY, K. L., WEBER, J. L., UNGER, M. J., LEDESMA, J., YU, N., GASSMANN, M. & LAI, C. 1997. Neuregulin-2, a new ligand of ErbB3/ErbB4-receptor tyrosine kinases. *Nature,* 387**,** 512-516.

CARSWELL, E. A., OLD, L. J., KASSEL, R. L., GREEN, S., FIORE, N. & WILLIAMSON, B. 1975. An endotoxin-induced serum factor that causes necrosis of tumors. *Proc Natl Acad Sci U S A,* 72**,** 3666-70.

CATAISSON, C., SALCEDO, R., HAKIM, S., MOFFITT, B. A., WRIGHT, L., YI, M., STEPHENS, R., DAI, R. M., LYAKH, L., SCHENTEN, D., YUSPA, H. S. & TRINCHIERI, G. 2012. IL-1R-MyD88 signaling in keratinocyte transformation and carcinogenesis. *J Exp Med,* 209**,** 1689-702.

CHA, D., O'BRIEN, P., O'TOOLE, E. A., WOODLEY, D. T. & HUDSON, L. G. 1996. Enhanced modulation of keratinocyte motility by transforming growth factor-alpha (TGF-alpha) relative to epidermal growth factor (EGF). *J Invest Dermatol,* 106**,** 590-7.

CHALARIS, A., ADAM, N., SINA, C., ROSENSTIEL, P., LEHMANN-KOCH, J., SCHIRMACHER, P., HARTMANN, D., CICHY, J., GAVRILOVA, O., SCHREIBER, S., JOSTOCK, T., MATTHEWS, V., HASLER, R., BECKER, C., NEURATH, M. F., REISS, K., SAFTIG, P., SCHELLER, J. & ROSE-JOHN, S. 2010. Critical role of the disintegrin metalloprotease ADAM17 for intestinal inflammation and regeneration in mice. *J Exp Med,* 207**,** 1617-24.

CHALARIS, A., RABE, B., PALIGA, K., LANGE, H., LASKAY, T., FIELDING, C. A., JONES, S. A., ROSE-JOHN, S. & SCHELLER, J. 2007. Apoptosis is a natural stimulus of IL6R shedding and contributes to the proinflammatory trans-signaling function of neutrophils. *Blood,* 110**,** 1748-55.

CHAN, M. V., ARMSTRONG, P. C., PAPALIA, F., KIRKBY, N. S. & WARNER, T. D. 2011. Optical multichannel (optimul) platelet aggregometry in 96-well plates as an additional method of platelet reactivity testing. *Platelets,* 22**,** 485-94.

CHAN, M. V. & WARNER, T. D. 2011. Standardised optical multichannel (optimul) platelet aggregometry using high-speed shaking and fixed time point readings. *Platelets*.

CHANG, H., RIESE, D. J., GILBERT, W., STERN, D. F. & MCMAHAN, U. J. 1997. Ligands for ErbB-family receptors encoded by a neuregulin-like gene. *Nature,* 387**,** 509-512.

CHESNEAU, V., BECHERER, J. D., ZHENG, Y., ERDJUMENT-BROMAGE, H., TEMPST, P. & BLOBEL, C. P. 2003. Catalytic properties of ADAM19. *J Biol Chem,* 278**,** 22331-40.

CHO, C., BUNCH, D. O., FAURE, J. E., GOULDING, E. H., EDDY, E. M., PRIMAKOFF, P. & MYLES, D. G. 1998. Fertilization defects in sperm from mice lacking fertilin beta. *Science,* 281**,** 1857-9.

CHOI, M., SCHOLL, U. I., JI, W., LIU, T., TIKHONOVA, I. R., ZUMBO, P., NAYIR, A., BAKKALOGLU, A., OZEN, S., SANJAD, S., NELSON-WILLIAMS, C., FARHI, A., MANE, S. & LIFTON, R. P. 2009. Genetic diagnosis by whole exome capture and massively parallel DNA sequencing. *Proc Natl Acad Sci U S A,* 106**,** 19096-101.

CHRISTOVA, Y., ADRAIN, C., BAMBROUGH, P., IBRAHIM, A. & FREEMAN, M. 2013. Mammalian iRhoms have distinct physiological functions including an essential role in TACE regulation. *EMBO Rep,* 14**,** 884-90.

CIPOLAT, S., RUDKA, T., HARTMANN, D., COSTA, V., SERNEELS, L., CRAESSAERTS, K., METZGER, K., FREZZA, C., ANNAERT, W., D'ADAMIO, L., DERKS, C., DEJAEGERE, T., PELLEGRINI, L., D'HOOGE, R., SCORRANO, L. & DE STROOPER, B. 2006. Mitochondrial rhomboid PARL regulates cytochrome c release during apoptosis via OPA1-dependent cristae remodeling. *Cell,* 126**,** 163-175.

CLARK, J. D., LIN, L. L., KRIZ, R. W., RAMESHA, C. S., SULTZMAN, L. A., LIN, A. Y., MILONA, N. & KNOPF, J. L. 1991. A Novel Arachidonic Acid-Selective Cytosolic Pla2 Contains a Ca2+-Dependent Translocation Domain with Homology to Pkc and Gap. *Cell,* 65**,** 1043-1051.

COFFEY, R. J., DERYNCK, R., WILCOX, J. N., BRINGMAN, T. S., GOUSTIN, A. S., MOSES, H. L. & PITTELKOW, M. R. 1987. Production and Autoinduction of Transforming Growth Factor-Alpha in Human Keratinocytes. *Nature,* 328**,** 817-820.

COIMBRA, S., FIGUEIREDO, A., CASTRO, E., ROCHA-PEREIRA, P. & SANTOS-SILVA, A. 2012. The roles of cells and cytokines in the pathogenesis of psoriasis. *Int J Dermatol,* 51**,** 389-95; quiz 395-8.

COLLER, B. S. 1978. The effects of ristocetin and von Willebrand factor on platelet electrophoretic mobility. *J Clin Invest,* 61**,** 1168-75.

CONTIN, C., PITARD, V., ITAI, T., NAGATA, S., MOREAU, J. F. & DECHANET-MERVILLE, J. 2003. Membrane-anchored CD40 is processed by the tumor necrosis factor-alpha-converting enzyme. Implications for CD40 signaling. *J Biol Chem,* 278**,** 32801-9.

COOK, P. W., MATTOX, P. A., KEEBLE, W. W., PITTELKOW, M. R., PLOWMAN, G. D., SHOYAB, M., ADELMAN, J. P. & SHIPLEY, G. D. 1991. A Heparin Sulfate-Regulated Human Keratinocyte Autocrine Factor Is Similar or Identical to Amphiregulin. *Molecular and Cellular Biology,* 11**,** 2547-2557.

CROSNIER, C., STAMATAKI, D. & LEWIS, J. 2006. Organizing cell renewal in the intestine: stem cells, signals and combinatorial control. *Nat Rev Genet,* 7**,** 349-59.

DANG, M., ARMBRUSTER, N., MILLER, M. A., CERMENO, E., HARTMANN, M., BELL, G. W., ROOT, D. E., LAUFFENBURGER, D. A., LODISH, H. F. & HERRLICH, A. 2013. Regulated ADAM17-dependent EGF family ligand release by substrate-selecting signaling pathways. *Proc Natl Acad Sci U S A,* 110**,** 9776-81.

DE MARIA, L., VIND, J., OXENBOLL, K. M., SVENDSEN, A. & PATKAR, S. 2007. Phospholipases and their industrial applications. *Applied Microbiology and Biotechnology,* 74**,** 290-300.

DE PETRIS, G. & LOPEZ, J. I. 2008. Histopathology of diaphragm disease of the small intestine: a study of 10 cases from a single institution. *Am J Clin Pathol,* 130**,** 518-25.

DENNING, M. F., GUY, S. G., ELLERBROEK, S. M., NORVELL, S. M., KOWALCZYK, A. P. & GREEN, K. J. 1998. The expression of desmoglein isoforms in cultured human keratinocytes is regulated by calcium, serum, and protein kinase C. *Exp Cell Res,* 239**,** 50-9.

DESSEN, A., TANG, J., SCHMIDT, H., STAHL, M., CLARK, J. D., SEEHRA, J. & SOMERS, W. S. 1999. Crystal structure of human cytosolic phospholipase A(2) reveals a novel topology and catalytic mechanism. *Cell,* 97**,** 349-360.

DIAZ-RODRIGUEZ, E., MONTERO, J. C., ESPARIS-OGANDO, A., YUSTE, L. & PANDIELLA, A. 2002. Extracellular signal-regulated kinase phosphorylates tumor necrosis factor alpha-converting enzyme at threonine 735: a potential role in regulated shedding. *Mol Biol Cell,* 13**,** 2031-44.

DIETERICH, W., EHNIS, T., BAUER, M., DONNER, P., VOLTA, U., RIECKEN, E. O. & SCHUPPAN, D. 1997. Identification of tissue transglutaminase as the autoantigen of celiac disease. *Nat Med,* 3**,** 797-801.

DING, X., YANG, L. Y., HUANG, G. W., WANG, W. & LU, W. Q. 2004. ADAM17 mRNA expression and pathological features of hepatocellular carcinoma. *World J Gastroenterol,* 10**,** 2735-9.

DOEDENS, J. R., MAHIMKAR, R. M. & BLACK, R. A. 2003. TACE/ADAM-17 enzymatic activity is increased in response to cellular stimulation. *Biochem Biophys Res Commun,* 308**,** 331-8.

DOMINEY, A. M., WANG, X. J., KING, L. E., JR., NANNEY, L. B., GAGNE, T. A., SELLHEYER, K., BUNDMAN, D. S., LONGLEY, M. A., ROTHNAGEL, J. A., GREENHALGH, D. A. & ~~ET AL~~*ET AL*. 1993. Targeted overexpression of transforming growth factor alpha in the epidermis of transgenic mice elicits hyperplasia, hyperkeratosis, and spontaneous, squamous papillomas. *Cell Growth Differ,* 4**,** 1071-82.

DREYMUELLER, D., MARTIN, C., KOGEL, T., PRUESSMEYER, J., HESS, F. M., HORIUCHI, K., UHLIG, S. & LUDWIG, A. 2012. Lung endothelial ADAM17 regulates the acute inflammatory response to lipopolysaccharide. *EMBO Mol Med,* 4**,** 412-23.

DUTT, A., CANEVASCINI, S., FROEHLI-HOIER, E. & HAJNAL, A. 2004. EGF signal propagation during C-elegans vulval development mediated by ROM-1 rhomboid. *PLoS Biol,* 2**,** 1799-1814.

DVORAK, B., HALPERN, M. D., HOLUBEC, H., WILLIAMS, C. S., MCWILLIAM, D. L., DOMINGUEZ, J. A., STEPANKOVA, R., PAYNE, C. M. & MCCUSKEY, R. S. 2002. Epidermal growth factor reduces the development of necrotizing enterocolitis in a neonatal rat model. *Am J Physiol Gastrointest Liver Physiol,* 282**,** G156-64.

DYCZYNSKA, E., SUN, D., YI, H., SEHARA-FUJISAWA, A., BLOBEL, C. P. & ZOLKIEWSKA, A. 2007. Proteolytic processing of delta-like 1 by ADAM proteases. *J Biol Chem,* 282**,** 436-44.

EDWARDS, D. R., HANDSLEY, M. M. & PENNINGTON, C. J. 2008. The ADAM metalloproteinases. *Mol Aspects Med,* 29**,** 258-89.

EL-ABASERI, T. B., PUTTA, S. & HANSEN, L. A. 2006. Ultraviolet irradiation induces keratinocyte proliferation and epidermal hyperplasia through the activation of the epidermal growth factor receptor. *Carcinogenesis,* 27**,** 225-231.

ELDER, J. T., FISHER, G. J., LINDQUIST, P. B., BENNETT, G. L., PITTELKOW, M. R., COFFEY, R. J., JR., ELLINGSWORTH, L., DERYNCK, R. & VOORHEES, J. J. 1989. Overexpression of transforming growth factor alpha in psoriatic epidermis. *Science,* 243**,** 811-4.

ELLIS, A., FIELD, J. K., FIELD, E. A., FRIEDMANN, P. S., FRYER, A., HOWARD, P., LEIGH, I. M., RISK, J., SHAW, J. M. & WHITTAKER, J. 1994. Tylosis associated with carcinoma of the oesophagus and oral leukoplakia in a large Liverpool family--a review of six generations. *Eur J Cancer B Oral Oncol,* 30B**,** 102-12.

ELLOSO, M. M., GOMEZ-ANGELATS, M. & FOURIE, A. M. 2012. Targeting the Th17 pathway in psoriasis. *J Leukoc Biol,* 92**,** 1187-97.

ENZINGER, P. C. & MAYER, R. J. 2003. Esophageal cancer. *N Engl J Med,* 349**,** 2241-52.

ERMUND, A., SCHUTTE, A., JOHANSSON, M. E., GUSTAFSSON, J. K. & HANSSON, G. C. 2013. Studies of mucus in mouse stomach, small intestine, and colon. I. Gastrointestinal mucus layers have different properties depending on location as well as over the Peyer's patches. *Am J Physiol Gastrointest Liver Physiol,* 305**,** G341-7.

ETHERIDGE, S. L., BROOKE, M. A., KELSELL, D. P. & BLAYDON, D. C. 2013. Rhomboid proteins: a role in keratinocyte proliferation and cancer. *Cell Tissue Res,* 351**,** 301-7.

EVANS, J. P. 2001. Fertilin beta and other ADAMs as integrin ligands: insights into cell adhesion and fertilization. *Bioessays,* 23**,** 628-39.

FARQUHAR, M. G. & PALADE, G. E. 1963. Junctional complexes in various epithelia. *J Cell Biol,* 17**,** 375-412.

FELDMAN, A. M., COMBES, A., WAGNER, D., KADAKOMI, T., KUBOTA, T., LI, Y. Y. & MCTIERNAN, C. 2000. The role of tumor necrosis factor in the pathophysiology of heart failure. *J Am Coll Cardiol,* 35**,** 537-44.

FELLOWS, I. W., CLARKE, J. M. & ROBERTS, P. F. 1992. Non-steroidal anti-inflammatory drug-induced jejunal and colonic diaphragm disease: a report of two cases. *Gut,* 33**,** 1424-6.

FIELD, E. A., ELLIS, A., FRIEDMANN, P. S., LEIGH, I. M. & FIELD, J. K. 1997. Oral tylosis: A re-appraisal. *Oral Oncol,* 33B**,** 55-57.

FINNERTY, C. C., HERNDON, D. N., PRZKORA, R., PEREIRA, C. T., OLIVEIRA, H. M., QUEIROZ, D. M., ROCHA, A. M. & JESCHKE, M. G. 2006. Cytokine expression profile over time in severely burned pediatric patients. *Shock,* 26**,** 13-9.

FITZGERALD, G. A. & LOLL, P. 2001. COX in a crystal ball: current status and future promise of prostaglandin research. *J Clin Invest,* 107**,** 1335-7.

FOLTENYI, K., GREENSPAN, R. J. & NEWPORT, J. W. 2007. Activation of EGFR and ERK by rhomboid signaling regulates the consolidation and maintenance of sleep in Drosophila. *Nature Neuroscience,* 10**,** 1160-1167.

FORBES, S. A., BINDAL, N., BAMFORD, S., COLE, C., KOK, C. Y., BEARE, D., JIA, M., SHEPHERD, R., LEUNG, K., MENZIES, A., TEAGUE, J. W., CAMPBELL, P. J., STRATTON, M. R. & FUTREAL, P. A. 2011. COSMIC: mining complete cancer genomes in the Catalogue of Somatic Mutations in Cancer. *Nucleic Acids Res,* 39**,** D945-50.

FRANKART, A., COQUETTE, A., SCHROEDER, K. R. & POUMAY, Y. 2012. Studies of cell signaling in a reconstructed human epidermis exposed to sensitizers: IL-8 synthesis and release depend on EGFR activation. *Arch Dermatol Res,* 304**,** 289-303.

FRANZKE, C. W., COBZARU, C., TRIANTAFYLLOPOULOU, A., LOFFEK, S., HORIUCHI, K., THREADGILL, D. W., KURZ, T., VAN ROOIJEN, N., BRUCKNER-TUDERMAN, L. & BLOBEL, C. P. 2012. Epidermal ADAM17 maintains the skin barrier by regulating EGFR ligand-dependent terminal keratinocyte differentiation. *J Exp Med,* 209**,** 1105-19.

FRANZKE, C. W., TASANEN, K., BORRADORI, L., HUOTARI, V. & BRUCKNER-TUDERMAN, L. 2004. Shedding of collagen XVII/BP180: structural motifs influence cleavage from cell surface. *J Biol Chem,* 279**,** 24521-9.

FRAYNE, J. & HALL, L. 1998. The gene for the human tMDC I sperm surface protein is non-functional: implications for its proposed role in mammalian sperm-egg recognition. *Biochem J,* 334 (Pt 1)**,** 171-6.

FREEMAN, M. 2008. Rhomboid proteases and their biological functions. *Annu Rev Genet,* 42**,** 191-210.

FUJIMOTO, N., WISLEZ, M., ZHANG, J., IWANAGA, K., DACKOR, J., HANNA, A. E., KALYANKRISHNA, S., CODY, D. D., PRICE, R. E., SATO, M., SHAY, J. W., MINNA, J. D., PEYTON, M., TANG, X., MASSARELLI, E., HERBST, R., THREADGILL, D. W., WISTUBA, II & KURIE, J. M. 2005. High expression of ErbB family members and their ligands in lung adenocarcinomas that are sensitive to inhibition of epidermal growth factor receptor. *Cancer Res,* 65**,** 11478-85.

GALLIO, M., STURGILL, G., RATHER, P. & KYLSTEN, P. 2002. A conserved mechanism for extracellular signaling in eukaryotes and prokaryotes. *Proceedings of the National Academy of Sciences of the United States of America,* 99**,** 12208-12213.

GALLUCCI, R. M., SLOAN, D. K., HECK, J. M., MURRAY, A. R. & O'DELL, S. J. 2004. Interleukin 6 indirectly induces keratinocyte migration. *J Invest Dermatol,* 122**,** 764-72.

GARROD, D. R., BERIKA, M. Y., BARDSLEY, W. F., HOLMES, D. & TABERNERO, L. 2005. Hyper-adhesion in desmosomes: its regulation in wound healing and possible relationship to cadherin crystal structure. *J Cell Sci,* 118**,** 5743-54.

GARTON, K. J., GOUGH, P. J., PHILALAY, J., WILLE, P. T., BLOBEL, C. P., WHITEHEAD, R. H., DEMPSEY, P. J. & RAINES, E. W. 2003. Stimulated shedding of vascular cell adhesion molecule 1 (VCAM-1) is mediated by tumor necrosis factor-alpha-converting enzyme (ADAM 17). *J Biol Chem,* 278**,** 37459-64.

GETSIOS, S., SIMPSON, C. L., KOJIMA, S., HARMON, R., SHEU, L. J., DUSEK, R. L., CORNWELL, M. & GREEN, K. J. 2009. Desmoglein 1-dependent suppression of EGFR signaling promotes epidermal differentiation and morphogenesis. *J Cell Biol,* 185**,** 1243-58.

GHOSH, M., TUCKER, D. E., BURCHETT, S. A. & LESLIE, C. C. 2006. Properties of the Group IV phospholipase A2 family. *Prog Lipid Res,* 45**,** 487-510.

GIBAULT, L., METGES, J. P., CONAN-CHARLET, V., LOZAC'H, P., ROBASZKIEWICZ, M., BESSAGUET, C., LAGARDE, N. & VOLANT, A. 2005. Diffuse EGFR staining is associated with reduced overall survival in locally advanced oesophageal squamous cell cancer. *Br J Cancer,* 93**,** 107-15.

GOULD, R. J., POLOKOFF, M. A., FRIEDMAN, P. A., HUANG, T. F., HOLT, J. C., COOK, J. J. & NIEWIAROWSKI, S. 1990. Disintegrins: a family of integrin inhibitory proteins from viper venoms. *Proc Soc Exp Biol Med,* 195**,** 168-71.

GREEN, K. J. & GAUDRY, C. A. 2000. Are desmosomes more than tethers for intermediate filaments? *Nat Rev Mol Cell Biol,* 1**,** 208-16.

GRELLNER, W., GEORG, T. & WILSKE, J. 2000. Quantitative analysis of proinflammatory cytokines (IL-1beta, IL-6, TNF-alpha) in human skin wounds. *Forensic Sci Int,* 113**,** 251-64.
GRIFFIN, M. R., PIPER, J. M., DAUGHERTY, J. R., SNOWDEN, M. & RAY, W. A. 1991. Nonsteroidal anti-inflammatory drug use and increased risk for peptic ulcer disease in elderly persons. *Ann Intern Med,* 114**,** 257-63.
GROSE, R., WERNER, S., KESSLER, D., TUCKERMANN, J., HUGGEL, K., DURKA, S. & REICHARDT, H. M. 2002. A role for endogenous glucocorticoids in wound repair. *EMBO Rep,* 3**,** 575-82.
GSCHWIND, A., HART, S., FISCHER, O. M. & ULLRICH, A. 2003. TACE cleavage of proamphiregulin regulates GPCR-induced proliferation and motility of cancer cells. *EMBO J,* 22**,** 2411-21.
HADAD, N., TUVAL, L., ELGAZAR-CARMOM, V. & LEVY, R. 2011. Endothelial ICAM-1 protein induction is regulated by cytosolic phospholipase A2alpha via both NF-kappaB and CREB transcription factors. *J Immunol,* 186**,** 1816-27.
HALL, P. A., COATES, P. J., ANSARI, B. & HOPWOOD, D. 1994. Regulation of cell number in the mammalian gastrointestinal tract: the importance of apoptosis. *J Cell Sci,* 107 (Pt 12)**,** 3569-77.
HAMBERG, M., SVENSSON, J. & SAMUELSSON, B. 1975. Thromboxanes: a new group of biologically active compounds derived from prostaglandin endoperoxides. *Proc Natl Acad Sci U S A,* 72**,** 2994-8.
HANAWA, M., SUZUKI, S., DOBASHI, Y., YAMANE, T., KONO, K., ENOMOTO, N. & OOI, A. 2006. EGFR protein overexpression and gene amplification in squamous cell carcinomas of the esophagus. *Int J Cancer,* 118**,** 1173-80.
HANSEN, L. A., WOODSON, R. L., HOLBUS, S., STRAIN, K., LO, Y. C. & YUSPA, S. H. 2000. The epidermal growth factor receptor is required to maintain the proliferative population in the basal compartment of epidermal tumors. *Cancer Research,* 60**,** 3328-3332.
HAQ, S., KILTER, H., MICHAEL, A., TAO, J., O'LEARY, E., SUN, X. M., WALTERS, B., BHATTACHARYA, K., CHEN, X., CUI, L., ANDREUCCI, M., ROSENZWEIG, A., GUERRERO, J. L., PATTEN, R., LIAO, R., MOLKENTIN, J., PICARD, M., BONVENTRE, J. V. & FORCE, T. 2003. Deletion of cytosolic phospholipase A2 promotes striated muscle growth. *Nat Med,* 9**,** 944-51.
HARARI, D., TZAHAR, E., ROMANO, J., SHELLY, M., PIERCE, J. H., ANDREWS, G. C. & YARDEN, Y. 1999. Neuregulin-4: a novel growth factor that acts through the ErbB-4 receptor tyrosine kinase. *Oncogene,* 18**,** 2681-2689.
HART, S., FISCHER, O. M., PRENZEL, N., ZWICK-WALLASCH, E., SCHNEIDER, M., HENNIGHAUSEN, L. & ULLRICH, A. 2005. GPCR-induced migration of breast carcinoma cells depends on both EGFR signal transactivation and EGFR-independent pathways. *Biol Chem,* 386**,** 845-55.
HARTMANN, D., DE STROOPER, B., SERNEELS, L., CRAESSAERTS, K., HERREMAN, A., ANNAERT, W., UMANS, L., LUBKE, T., LENA ILLERT, A., VON FIGURA, K. & SAFTIG, P. 2002. The disintegrin/metalloprotease ADAM 10 is essential for Notch signalling but not for alpha-secretase activity in fibroblasts. *Hum Mol Genet,* 11**,** 2615-24.
HASHIMOTO, K., HIGASHIYAMA, S., ASADA, H., HASHIMURA, E., KOBAYASHI, T., SUDO, K., NAKAGAWA, T., DAMM, D., YOSHIKAWA, K. & TANIGUCHI, N. 1994. Heparin-binding epidermal growth factor-like growth factor is an autocrine growth factor for human keratinocytes. *J Biol Chem,* 269**,** 20060-6.
HASSEMER, E. L., LE GALL, S. M., LIEGEL, R., MCNALLY, M., CHANG, B., ZEISS, C. J., DUBIELZIG, R. D., HORIUCHI, K., KIMURA, T., OKADA, Y., BLOBEL, C. P. & SIDJANIN, D. J. 2010. The waved with open eyelids (woe) locus is a hypomorphic mouse mutation in Adam17. *Genetics,* 185**,** 245-55.
HATA, A. N. & BREYER, R. M. 2004. Pharmacology and signaling of prostaglandin receptors: multiple roles in inflammation and immune modulation. *Pharmacol Ther,* 103**,** 147-66.
HAWLEY-NELSON, P., VOUSDEN, K. H., HUBBERT, N. L., LOWY, D. R. & SCHILLER, J. T. 1989. HPV16 E6 and E7 proteins cooperate to immortalize human foreskin keratinocytes. *EMBO J,* 8**,** 3905-10.
HEFNER, Y., BORSCH-HAUBOLD, A. G., MURAKAMI, M., WILDE, J. I., PASQUET, S., SCHIELTZ, D., GHOMASHCHI, F., YATES, J. R., 3RD, ARMSTRONG, C. G., PATERSON, A., COHEN, P.,

FUKUNAGA, R., HUNTER, T., KUDO, I., WATSON, S. P. & GELB, M. H. 2000. Serine 727 phosphorylation and activation of cytosolic phospholipase A2 by MNK1-related protein kinases. *J Biol Chem,* 275**,** 37542-51.
HENNIES, H. C., HAGEDORN, M. & REIS, A. 1995. Palmoplantar keratoderma in association with carcinoma of the esophagus maps to chromosome 17q distal to the keratin gene cluster. *Genomics,* 29**,** 537-40.
HIGUCHI, K., UMEGAKI, E., WATANABE, T., YODA, Y., MORITA, E., MURANO, M., TOKIOKA, S. & ARAKAWA, T. 2009. Present status and strategy of NSAIDs-induced small bowel injury. *J Gastroenterol,* 44**,** 879-88.
HIKITA, A., YANA, I., WAKEYAMA, H., NAKAMURA, M., KADONO, Y., OSHIMA, Y., NAKAMURA, K., SEIKI, M. & TANAKA, S. 2006. Negative regulation of osteoclastogenesis by ectodomain shedding of receptor activator of NF-kappaB ligand. *J Biol Chem,* 281**,** 36846-55.
HITOMI, K. 2005. Transglutaminases in skin epidermis. *European Journal of Dermatology,* 15**,** 313-319.
HOLLAND, S. M. 2010. Chronic granulomatous disease. *Clin Rev Allergy Immunol,* 38**,** 3-10.
HOLTHOFER, B., WINDOFFER, R., TROYANOVSKY, S. & LEUBE, R. E. 2007. Structure and function of desmosomes. *Int Rev Cytol,* 264**,** 65-163.
HORIUCHI, K., KIMURA, T., MIYAMOTO, T., TAKAISHI, H., OKADA, Y., TOYAMA, Y. & BLOBEL, C. P. 2007a. Cutting edge: TNF-alpha-converting enzyme (TACE/ADAM17) inactivation in mouse myeloid cells prevents lethality from endotoxin shock. *J Immunol,* 179**,** 2686-9.
HORIUCHI, K., LE GALL, S., SCHULTE, M., YAMAGUCHI, T., REISS, K., MURPHY, G., TOYAMA, Y., HARTMANN, D., SAFTIG, P. & BLOBEL, C. P. 2007b. Substrate selectivity of epidermal growth factor-receptor ligand sheddases and their regulation by phorbol esters and calcium influx. *Mol Biol Cell,* 18**,** 176-88.
HORIUCHI, K., ZHOU, H. M., KELLY, K., MANOVA, K. & BLOBEL, C. P. 2005. Evaluation of the contributions of ADAMs 9, 12, 15, 17, and 19 to heart development and ectodomain shedding of neuregulins beta1 and beta2. *Dev Biol,* 283**,** 459-71.
HORN, S., FIGL, A., RACHAKONDA, P. S., FISCHER, C., SUCKER, A., GAST, A., KADEL, S., MOLL, I., NAGORE, E., HEMMINKI, K., SCHADENDORF, D. & KUMAR, R. 2013. TERT promoter mutations in familial and sporadic melanoma. *Science,* 339**,** 959-61.
HUOVILA, A. P., TURNER, A. J., PELTO-HUIKKO, M., KARKKAINEN, I. & ORTIZ, R. M. 2005. Shedding light on ADAM metalloproteinases. *Trends Biochem Sci,* 30**,** 413-22.
HYNES, N. E. & LANE, H. A. 2005. ERBB receptors and cancer: the complexity of targeted inhibitors. *Nat Rev Cancer,* 5**,** 341-54.
IKAWA, M., INOUE, N., BENHAM, A. M. & OKABE, M. 2010. Fertilization: a sperm's journey to and interaction with the oocyte. *J Clin Invest,* 120**,** 984-94.
IOCONO, J. A., COLLERAN, K. R., REMICK, D. G., GILLESPIE, B. W., EHRLICH, H. P. & GARNER, W. L. 2000. Interleukin-8 levels and activity in delayed-healing human thermal wounds. *Wound Repair Regen,* 8**,** 216-25.
IRELAND, H., KEMP, R., HOUGHTON, C., HOWARD, L., CLARKE, A. R., SANSOM, O. J. & WINTON, D. J. 2004. Inducible Cre-mediated control of gene expression in the murine gastrointestinal tract: effect of loss of beta-catenin. *Gastroenterology,* 126**,** 1236-46.
ISSUREE, P. D., MARETZKY, T., MCILWAIN, D. R., MONETTE, S., QING, X., LANG, P. A., SWENDEMAN, S. L., PARK-MIN, K. H., BINDER, N., KALLIOLIAS, G. D., YARILINA, A., HORIUCHI, K., IVASHKIV, L. B., MAK, T. W., SALMON, J. E. & BLOBEL, C. P. 2013. iRHOM2 is a critical pathogenic mediator of inflammatory arthritis. *J Clin Invest,* 123**,** 928-32.
ITAKURA, Y., SASANO, H., SHIGA, C., FURUKAWA, Y., SHIGA, K., MORI, S. & NAGURA, H. 1994. Epidermal growth factor receptor overexpression in esophageal carcinoma. An immunohistochemical study correlated with clinicopathologic findings and DNA amplification. *Cancer,* 74**,** 795-804.
IWAMOTO, R., YAMAZAKI, S., ASAKURA, M., TAKASHIMA, S., HASUWA, H., MIYADO, K., ADACHI, S., KITAKAZE, M., HASHIMOTO, K., RAAB, G., NANBA, D., HIGASHIYAMA, S., HORI, M.,

KLAGSBRUN, M. & MEKADA, E. 2003. Heparin-binding EGF-like growth factor and ErbB signaling is essential for heart function. *Proc Natl Acad Sci U S A,* 100**,** 3221-6.
IZUMI, Y., HIRATA, M., HASUWA, H., IWAMOTO, R., UMATA, T., MIYADO, K., TAMAI, Y., KURISAKI, T., SEHARA-FUJISAWA, A., OHNO, S. & MEKADA, E. 1998. A metalloprotease-disintegrin, MDC9/meltrin-gamma/ADAM9 and PKCdelta are involved in TPA-induced ectodomain shedding of membrane-anchored heparin-binding EGF-like growth factor. *EMBO J,* 17**,** 7260-72.
JACKSON, L. F., QIU, T. H., SUNNARBORG, S. W., CHANG, A., ZHANG, C., PATTERSON, C. & LEE, D. C. 2003. Defective valvulogenesis in HB-EGF and TACE-null mice is associated with aberrant BMP signaling. *EMBO J,* 22**,** 2704-16.
JANES, P. W., SAHA, N., BARTON, W. A., KOLEV, M. V., WIMMER-KLEIKAMP, S. H., NIEVERGALL, E., BLOBEL, C. P., HIMANEN, J. P., LACKMANN, M. & NIKOLOV, D. B. 2005. Adam meets Eph: an ADAM substrate recognition module acts as a molecular switch for ephrin cleavage in trans. *Cell,* 123**,** 291-304.
JENKINS, G. M. & FROHMAN, M. A. 2005. Phospholipase D: a lipid centric review. *Cellular and Molecular Life Sciences,* 62**,** 2305-2316.
JENSEN, U. B., LOWELL, S. & WATT, F. M. 1999. The spatial relationship between stem cells and their progeny in the basal layer of human epidermis: a new view based on whole-mount labelling and lineage analysis. *Development,* 126**,** 2409-18.
JIANG, W. G., SANDERS, A. J., RUGE, F. & HARDING, K. G. 2012. Influence of interleukin-8 (IL-8) and IL-8 receptors on the migration of human keratinocytes, the role of PLC-gamma and potential clinical implications. *Exp Ther Med,* 3**,** 231-236.
JURY, J. A., FRAYNE, J. & HALL, L. 1997. The human fertilin alpha gene is non-functional: implications for its proposed role in fertilization. *Biochem J,* 321 (Pt 3)**,** 577-81.
KARAN, D., LIN, F. C., BRYAN, M., RINGEL, J., MONIAUX, N., LIN, M. F. & BATRA, S. K. 2003. Expression of ADAMs (a disintegrin and metalloproteases) and TIMP-3 (tissue inhibitor of metalloproteinase-3) in human prostatic adenocarcinomas. *Int J Oncol,* 23**,** 1365-71.
KELLY, D. E. 1966. Fine structure of desmosomes. , hemidesmosomes, and an adepidermal globular layer in developing newt epidermis. *J Cell Biol,* 28**,** 51-72.
KELSELL, D. P., RISK, J. M., LEIGH, I. M., STEVENS, H. P., ELLIS, A., HENNIES, H. C., REIS, A., WEISSENBACH, J., BISHOP, D. T., SPURR, N. K. & FIELD, J. K. 1996. Close mapping of the focal non-epidermolytic palmoplantar keratoderma (PPK) locus associated with oesophageal cancer (TOC). *Hum Mol Genet,* 5**,** 857-60.
KITAGAWA, Y., UEDA, M., ANDO, N., OZAWA, S., SHIMIZU, N. & KITAJIMA, M. 1996. Further evidence for prognostic significance of epidermal growth factor receptor gene amplification in patients with esophageal squamous cell carcinoma. *Clin Cancer Res,* 2**,** 909-14.
KLESSNER, J. L., DESAI, B. V., AMARGO, E. V., GETSIOS, S. & GREEN, K. J. 2009. EGFR and ADAMs cooperate to regulate shedding and endocytic trafficking of the desmosomal cadherin desmoglein 2. *Mol Biol Cell,* 20**,** 328-37.
KOBAYASHI, K. & ARAKAWA, T. 1995. Arachidonic acid cascade and gastric mucosal injury, protection, and healing: topics of this decade. *J Clin Gastroenterol,* 21 Suppl 1**,** S12-7.
KODURI, R. S., GRONROOS, J. O., LAINE, V. J. O., LE CALVEZ, C., LAMBEAU, G., NEVALAINEN, T. J. & GELB, M. H. 2002. Bactericidal properties of human and murine groups I, II, V, X, and XII secreted phospholipases A(2). *Journal of Biological Chemistry,* 277**,** 5849-5857.
KOHOUTOVA, D., BARTOVA, J., TACHECI, I., REJCHRT, S., REPAK, R., KOPACOVA, M. & BURES, J. 2013. Cryptogenic Multifocal Ulcerous Stenosing Enteritis: A Review of the Literature. *Gastroenterology Research and Practice*.
KOHOUTOVA, D., BURES, J., TYCOVA, V., BARTOVA, J., TACHECI, I., REJCHRT, S., VACEK, Z., REPAK, R. & KOPACOVA, M. 2010. Severe cryptogenic multifocal ulcerous stenosing enteritis. A report of three cases and review of the literature. *Acta Medica (Hradec Kralove),* 53**,** 25-9.

KOIKE, H., TOMIOKA, S., SORIMACHI, H., SAIDO, T. C., MARUYAMA, K., OKUYAMA, A., FUJISAWA-SEHARA, A., OHNO, S., SUZUKI, K. & ISHIURA, S. 1999. Membrane-anchored metalloprotease MDC9 has an alpha-secretase activity responsible for processing the amyloid precursor protein. *Biochem J,* 343 Pt 2**,** 371-5.

KRAUSE, D. S. & VAN ETTEN, R. A. 2005. Tyrosine kinases as targets for cancer therapy. *N Engl J Med,* 353**,** 172-87.

LACOUTURE, M. E. 2006. Mechanisms of cutaneous toxicities to EGFR inhibitors. *Nature Reviews Cancer,* 6**,** 803-812.

LAINE, L., TAKEUCHI, K. & TARNAWSKI, A. 2008. Gastric mucosal defense and cytoprotection: bench to bedside. *Gastroenterology,* 135**,** 41-60.

LAMBERT, J. C., PASQUIER, F., COTTEL, D., FRIGARD, B., AMOUYEL, P. & CHARTIER-HARLIN, M. C. 1998. A new polymorphism in the APOE promoter associated with risk of developing Alzheimer's disease. *Hum Mol Genet,* 7**,** 533-40.

LANGAN, J. E., COLE, C. G., HUCKLE, E. J., BYRNE, S., MCRONALD, F. E., ROWBOTTOM, L., ELLIS, A., SHAW, J. M., LEIGH, I. M., KELSELL, D. P., DUNHAM, I., FIELD, J. K. & RISK, J. M. 2004. Novel microsatellite markers and single nucleotide polymorphisms refine the tylosis with oesophageal cancer (TOC) minimal region on 17q25 to 42.5 kb: sequencing does not identify the causative gene. *Hum Genet,* 114**,** 534-40.

LEE, I. T., LIN, C. C., CHENG, S. E., HSIAO, L. D., HSIAO, Y. C. & YANG, C. M. 2013. TNF-alpha Induces Cytosolic Phospholipase A(2) Expression in Human Lung Epithelial Cells via JNK1/2-and p38 MAPK-Dependent AP-1 Activation. *PLoS One,* 8.

LEE, J. R., URBAN, S., GARVEY, C. F. & FREEMAN, M. 2001. Regulated intracellular ligand transport and proteolysis control EGF signal activation in Drosophila. *Cell,* 107**,** 161-171.

LEMBERG, M. K. & FREEMAN, M. 2007. Functional and evolutionary implications of enhanced genomic analysis of rhomboid intramembrane proteases. *Genome Res,* 17**,** 1634-46.

LEMIEUX, M. J., FISCHER, S. J., CHERNEY, M. M., BATEMAN, K. S. & JAMES, M. N. G. 2007. The crystal structure of the rhomboid peptidase from Haemophilus influenzae provides insight into intramembrane proteolysis. *Proceedings of the National Academy of Sciences of the United States of America,* 104**,** 750-754.

LESLIE, C. C. 1997. Properties and regulation of cytosolic phospholipase A2. *J Biol Chem,* 272**,** 16709-12.

LI, B., ANTONYAK, M. A., DRUSO, J. E., CHENG, L., NIKITIN, A. Y. & CERIONE, R. A. 2010. EGF potentiated oncogenesis requires a tissue transglutaminase-dependent signaling pathway leading to Src activation. *Proc Natl Acad Sci U S A,* 107**,** 1408-13.

LI, G., CHEN, W., HAN, C. & WU, T. 2011a. Cytosolic phospholipase A(2)alpha protects against Fas- but not LPS-induced liver injury. *J Hepatol,* 55**,** 1281-90.

LI, Y., FAN, J., CHEN, M., LI, W. & WOODLEY, D. T. 2006. Transforming growth factor-alpha: a major human serum factor that promotes human keratinocyte migration. *J Invest Dermatol,* 126**,** 2096-105.

LI, Z., XU, X., BAI, L., CHEN, W. & LIN, Y. 2011b. Epidermal growth factor receptor-mediated tissue transglutaminase overexpression couples acquired tumor necrosis factor-related apoptosis-inducing ligand resistance and migration through c-FLIP and MMP-9 proteins in lung cancer cells. *J Biol Chem,* 286**,** 21164-72.

LINDER, B. & HEINLEIN, U. A. 1997. Decreased in vitro fertilization efficiencies in the presence of specific cyritestin peptides. *Dev Growth Differ,* 39**,** 243-7.

LIU, H. B., YANG, Q. C., SHEN, Y., ZHU, Y., ZHANG, X. J. & CHEN, H. 2013. [Clinicopathological and prognostic significance of the expression of ADAM17 mRNA and protein in esophageal squamous cell carcinoma]. *Zhonghua Zhong Liu Za Zhi,* 35**,** 361-5.

LIU, P. C., LIU, X., LI, Y., COVINGTON, M., WYNN, R., HUBER, R., HILLMAN, M., YANG, G., ELLIS, D., MARANDO, C., KATIYAR, K., BRADLEY, J., ABREMSKI, K., STOW, M., RUPAR, M., ZHUO, J., LI, Y. L., LIN, Q., BURNS, D., XU, M., ZHANG, C., QIAN, D. Q., HE, C., SHARIEF, V., WENG, L., AGRIOS, C., SHI, E., METCALF, B., NEWTON, R., FRIEDMAN, S., YAO, W., SCHERLE, P., HOLLIS, G. & BURN, T. C. 2006. Identification of ADAM10 as a major source of HER2

ectodomain sheddase activity in HER2 overexpressing breast cancer cells. *Cancer Biol Ther,* 5**,** 657-64.
LIVAK, K. J. & SCHMITTGEN, T. D. 2001. Analysis of relative gene expression data using real-time quantitative PCR and the 2(-Delta Delta C(T)) Method. *Methods,* 25**,** 402-8.
LOECHEL, F., FOX, J. W., MURPHY, G., ALBRECHTSEN, R. & WEWER, U. M. 2000. ADAM 12-S cleaves IGFBP-3 and IGFBP-5 and is inhibited by TIMP-3. *Biochem Biophys Res Commun,* 278**,** 511-5.
LOHI, O., URBAN, S. & FREEMAN, M. 2004. Diverse substrate recognition mechanisms for rhomboids; thrombomodulin is cleaved by Mammalian rhomboids. *Curr Biol,* 14**,** 236-41.
LORCH, J. H., KLESSNER, J., PARK, J. K., GETSIOS, S., WU, Y. L., STACK, M. S. & GREEN, K. J. 2004. Epidermal growth factor receptor inhibition promotes desmosome assembly and strengthens intercellular adhesion in squamous cell carcinoma cells. *J Biol Chem,* 279**,** 37191-200.
LUDWIG, A., HUNDHAUSEN, C., LAMBERT, M. H., BROADWAY, N., ANDREWS, R. C., BICKETT, D. M., LEESNITZER, M. A. & BECHERER, J. D. 2005. Metalloproteinase inhibitors for the disintegrin-like metalloproteinases ADAM10 and ADAM17 that differentially block constitutive and phorbol ester-inducible shedding of cell surface molecules. *Comb Chem High Throughput Screen,* 8**,** 161-71.
LUETTEKE, N. C., QIU, T. H., FENTON, S. E., TROYER, K. L., RIEDEL, R. F., CHANG, A. & LEE, D. C. 1999. Targeted inactivation of the EGF and amphiregulin genes reveals distinct roles for EGF receptor ligands in mouse mammary gland development. *Development,* 126**,** 2739-50.
LUETTEKE, N. C., QIU, T. H., PEIFFER, R. L., OLIVER, P., SMITHIES, O. & LEE, D. C. 1993. TGF alpha deficiency results in hair follicle and eye abnormalities in targeted and waved-1 mice. *Cell,* 73**,** 263-78.
LUNDBLAD, L. K., THOMPSON-FIGUEROA, J., LECLAIR, T., SULLIVAN, M. J., POYNTER, M. E., IRVIN, C. G. & BATES, J. H. 2005. Tumor necrosis factor-alpha overexpression in lung disease: a single cause behind a complex phenotype. *Am J Respir Crit Care Med,* 171**,** 1363-70.
LYON, A. M. & TESMER, J. J. G. 2013. Structural Insights into Phospholipase C-beta Function. *Molecular Pharmacology,* 84**,** 488-500.
MAATTA, J. A., SUNDVALL, M., JUNTTILA, T. T., PERI, L., LAINE, V. J., ISOLA, J., EGEBLAD, M. & ELENIUS, K. 2006. Proteolytic cleavage and phosphorylation of a tumor-associated ErbB4 isoform promote ligand-independent survival and cancer cell growth. *Mol Biol Cell,* 17**,** 67-79.
MADISON, K. C. 2003. Barrier function of the skin: "la raison d'etre" of the epidermis. *J Invest Dermatol,* 121**,** 231-41.
MANN, G. B., FOWLER, K. J., GABRIEL, A., NICE, E. C., WILLIAMS, R. L. & DUNN, A. R. 1993. Mice with a null mutation of the TGF alpha gene have abnormal skin architecture, wavy hair, and curly whiskers and often develop corneal inflammation. *Cell,* 73**,** 249-61.
MANTOVANI, A., ALLAVENA, P., SICA, A. & BALKWILL, F. 2008. Cancer-related inflammation. *Nature,* 454**,** 436-44.
MARETZKY, T., EVERS, A., ZHOU, W., SWENDEMAN, S. L., WONG, P. M., RAFII, S., REISS, K. & BLOBEL, C. P. 2011a. Migration of growth factor-stimulated epithelial and endothelial cells depends on EGFR transactivation by ADAM17. *Nat Commun,* 2**,** 229.
MARETZKY, T., MCILWAIN, D. R., ISSUREE, P. D., LI, X., MALAPEIRA, J., AMIN, S., LANG, P. A., MAK, T. W. & BLOBEL, C. P. 2013. iRhom2 controls the substrate selectivity of stimulated ADAM17-dependent ectodomain shedding. *Proc Natl Acad Sci U S A,* 110**,** 11433-8.
MARETZKY, T., REISS, K., LUDWIG, A., BUCHHOLZ, J., SCHOLZ, F., PROKSCH, E., DE STROOPER, B., HARTMANN, D. & SAFTIG, P. 2005. ADAM10 mediates E-cadherin shedding and regulates epithelial cell-cell adhesion, migration, and beta-catenin translocation. *Proc Natl Acad Sci U S A,* 102**,** 9182-7.

MARETZKY, T., ZHOU, W., HUANG, X. Y. & BLOBEL, C. P. 2011b. A transforming Src mutant increases the bioavailability of EGFR ligands via stimulation of the cell-surface metalloproteinase ADAM17. *Oncogene,* 30**,** 611-8.

MARUSIC, S., LEACH, M. W., PELKER, J. W., AZOITEI, M. L., UOZUMI, N., CUI, J. Q., SHEN, M. W. H., DECLERCQ, C. M., MIYASHIRO, J. S., CARITO, B. A., THAKKER, P., SIMMONS, D. L., LEONARD, J. P., SHIMIZU, T. & CLARK, J. D. 2005. Cytosolic phospholipase A2 alpha-deficient mice are resistant to experimental autoimmune encephalomyelitis. *Journal of Experimental Medicine,* 202**,** 841-851.

MATSUHASHI, N., YAMADA, A., HIRAISHI, M., KONISHI, T., MINOTA, S., SAITO, T., SUGANO, K., YAZAKI, Y., MORI, M. & SHIGA, J. 1992. Multiple strictures of the small intestine after long-term nonsteroidal anti-inflammatory drug therapy. *Am J Gastroenterol,* 87**,** 1183-6.

MATSUMOTO, T., IIDA, M., MATSUI, T., YAO, T., WATANABE, H. & OKABE, H. 2004. Non-specific multiple ulcers of the small intestine unrelated to non-steroidal anti-inflammatory drugs. *J Clin Pathol,* 57**,** 1145-50.

MAYER, U. & NUSSLEIN-VOLHARD, C. 1988. A group of genes required for pattern formation in the ventral ectoderm of the Drosophila embryo. *Genes Dev,* 2**,** 1496-511.

MAZZOCCA, A., COPPARI, R., DE FRANCO, R., CHO, J. Y., LIBERMANN, T. A., PINZANI, M. & TOKER, A. 2005. A secreted form of ADAM9 promotes carcinoma invasion through tumor-stromal interactions. *Cancer Res,* 65**,** 4728-38.

MCDERMOTT, M. F., AKSENTIJEVICH, I., GALON, J., MCDERMOTT, E. M., OGUNKOLADE, B. W., CENTOLA, M., MANSFIELD, E., GADINA, M., KARENKO, L., PETTERSSON, T., MCCARTHY, J., FRUCHT, D. M., ARINGER, M., TOROSYAN, Y., TEPPO, A. M., WILSON, M., KARAARSLAN, H. M., WAN, Y., TODD, I., WOOD, G., SCHLIMGEN, R., KUMARAJEEWA, T. R., COOPER, S. M., VELLA, J. P., AMOS, C. I., MULLEY, J., QUANE, K. A., MOLLOY, M. G., RANKI, A., POWELL, R. J., HITMAN, G. A., O'SHEA, J. J. & KASTNER, D. L. 1999. Germline mutations in the extracellular domains of the 55 kDa TNF receptor, TNFR1, define a family of dominantly inherited autoinflammatory syndromes. *Cell,* 97**,** 133-44.

MCELROY, S. J., HOBBS, S., KALLEN, M., TEJERA, N., ROSEN, M. J., GRISHIN, A., MATTA, P., SCHNEIDER, C., UPPERMAN, J., FORD, H., POLK, D. B. & WEITKAMP, J. H. 2012. Transactivation of EGFR by LPS induces COX-2 expression in enterocytes. *PLoS One,* 7**,** e38373.

MCFARLAND-MANCINI, M. M., FUNK, H. M., PALUCH, A. M., ZHOU, M., GIRIDHAR, P. V., MERCER, C. A., KOZMA, S. C. & DREW, A. F. 2010. Differences in wound healing in mice with deficiency of IL-6 versus IL-6 receptor. *J Immunol,* 184**,** 7219-28.

MCGOWAN, P. M., MCKIERNAN, E., BOLSTER, F., RYAN, B. M., HILL, A. D., MCDERMOTT, E. W., EVOY, D., O'HIGGINS, N., CROWN, J. & DUFFY, M. J. 2008. ADAM-17 predicts adverse outcome in patients with breast cancer. *Ann Oncol,* 19**,** 1075-81.

MCILWAIN, D. R., LANG, P. A., MARETZKY, T., HAMADA, K., OHISHI, K., MANEY, S. K., BERGER, T., MURTHY, A., DUNCAN, G., XU, H. C., LANG, K. S., HAUSSINGER, D., WAKEHAM, A., ITIE-YOUTEN, A., KHOKHA, R., OHASHI, P. S., BLOBEL, C. P. & MAK, T. W. 2012. iRhom2 regulation of TACE controls TNF-mediated protection against Listeria and responses to LPS. *Science,* 335**,** 229-32.

MICHALAKI, V., SYRIGOS, K., CHARLES, P. & WAXMAN, J. 2004. Serum levels of IL-6 and TNF-alpha correlate with clinicopathological features and patient survival in patients with prostate cancer. *Br J Cancer,* 90**,** 2312-6.

MIETTINEN, P. J., BERGER, J. E., MENESES, J., PHUNG, Y., PEDERSEN, R. A., WERB, Z. & DERYNCK, R. 1995. Epithelial Immaturity and Multiorgan Failure in Mice Lacking Epidermal Growth-Factor Receptor. *Nature,* 376**,** 337-341.

MINAMI, T., NAKANO, H., KOBAYASHI, T., SUGIMOTO, Y., USHIKUBI, F., ICHIKAWA, A., NARUMIYA, S. & ITO, S. 2001. Characterization of EP receptor subtypes responsible for prostaglandin E2-induced pain responses by use of EP1 and EP3 receptor knockout mice. *Br J Pharmacol,* 133**,** 438-44.

MOCHIZUKI, S. & OKADA, Y. 2007. ADAMs in cancer cell proliferation and progression. *Cancer Sci,* 98**,** 621-8.

MONTPETIT, A., COTE, S., BRUSTEIN, E., DROUIN, C. A., LAPOINTE, L., BOUDREAU, M., MELOCHE, C., DROUIN, R., HUDSON, T. J., DRAPEAU, P. & COSSETTE, P. 2008. Disruption of AP1S1, causing a novel neurocutaneous syndrome, perturbs development of the skin and spinal cord. *PLoS Genet,* 4**,** e1000296.

MOORE, R. J., OWENS, D. M., STAMP, G., ARNOTT, C., BURKE, F., EAST, N., HOLDSWORTH, H., TURNER, L., ROLLINS, B., PASPARAKIS, M., KOLLIAS, G. & BALKWILL, F. 1999. Mice deficient in tumor necrosis factor-alpha are resistant to skin carcinogenesis. *Nat Med,* 5**,** 828-31.

MORI, S., TANAKA, M., NANBA, D., NISHIWAKI, E., ISHIGURO, H., HIGASHIYAMA, S. & MATSUURA, N. 2003. PACSIN3 binds ADAM12/meltrin alpha and up-regulates ectodomain shedding of heparin-binding epidermal growth factor-like growth factor. *J Biol Chem,* 278**,** 46029-34.

MORLEY, S. M., D'ALESSANDRO, M., SEXTON, C., RUGG, E. L., NAVSARIA, H., SHEMANKO, C. S., HUBER, M., HOHL, D., HEAGERTY, A. I., LEIGH, I. M. & LANE, E. B. 2003. Generation and characterization of epidermolysis bullosa simplex cell lines: scratch assays show faster migration with disruptive keratin mutations. *Br J Dermatol,* 149**,** 46-58.

MORLEY, S. M., DUNDAS, S. R., JAMES, J. L., GUPTA, T., BROWN, R. A., SEXTON, C. J., NAVSARIA, H. A., LEIGH, I. M. & LANE, E. B. 1995. Temperature sensitivity of the keratin cytoskeleton and delayed spreading of keratinocyte lines derived from EBS patients. *J Cell Sci,* 108 (Pt 11)**,** 3463-71.

MORTON, L. F., PEACHEY, A. R. & BARNES, M. J. 1989. Platelet-reactive sites in collagens type I and type III. Evidence for separate adhesion and aggregatory sites. *Biochem J,* 258**,** 157-63.

MOSIOR, M., SIX, D. A. & DENNIS, E. A. 1998. Group IV cytosolic phospholipase A(2) binds with high affinity and specificity to phosphatidylinositol 4,5-bisphosphate resulting in dramatic increases in activity. *Journal of Biological Chemistry,* 273**,** 2184-2191.

MOSS, M. L., JIN, S. L., MILLA, M. E., BICKETT, D. M., BURKHART, W., CARTER, H. L., CHEN, W. J., CLAY, W. C., DIDSBURY, J. R., HASSLER, D., HOFFMAN, C. R., KOST, T. A., LAMBERT, M. H., LEESNITZER, M. A., MCCAULEY, P., MCGEEHAN, G., MITCHELL, J., MOYER, M., PAHEL, G., ROCQUE, W., OVERTON, L. K., SCHOENEN, F., SEATON, T., SU, J. L., BECHERER, J. D. & ~~ET AL~~*ET AL*. 1997. Cloning of a disintegrin metalloproteinase that processes precursor tumour-necrosis factor-alpha. *Nature,* 385**,** 733-6.

MOSS, M. L. & RASMUSSEN, F. H. 2007. Fluorescent substrates for the proteinases ADAM17, ADAM10, ADAM8, and ADAM12 useful for high-throughput inhibitor screening. *Anal Biochem,* 366**,** 144-8.

MULLBERG, J., ALTHOFF, K., JOSTOCK, T. & ROSE-JOHN, S. 2000. The importance of shedding of membrane proteins for cytokine biology. *Eur Cytokine Netw,* 11**,** 27-38.

MUNGER, K., PHELPS, W. C., BUBB, V., HOWLEY, P. M. & SCHLEGEL, R. 1989. The E6 and E7 genes of the human papillomavirus type 16 together are necessary and sufficient for transformation of primary human keratinocytes. *J Virol,* 63**,** 4417-21.

MURAKAMI, M., TAKETOMI, Y., MIKI, Y., SATO, H., HIRABAYASHI, T. & YAMAMOTO, K. 2011. Recent progress in phospholipase A research: from cells to animals to humans. *Prog Lipid Res,* 50**,** 152-92.

MURPHY, G. 2008. The ADAMs: signalling scissors in the tumour microenvironment. *Nat Rev Cancer,* 8**,** 929-41.

MURRAY, D. & HONIG, B. 2002. Electrostatic control of the membrane targeting of C2 domains. *Molecular Cell,* 9**,** 145-154.

NAGANO, O., MURAKAMI, D., HARTMANN, D., DE STROOPER, B., SAFTIG, P., IWATSUBO, T., NAKAJIMA, M., SHINOHARA, M. & SAYA, H. 2004. Cell-matrix interaction via CD44 is independently regulated by different metalloproteinases activated in response to extracellular Ca(2+) influx and PKC activation. *J Cell Biol,* 165**,** 893-902.

NAGANO, O. & SAYA, H. 2004. Mechanism and biological significance of CD44 cleavage. *Cancer Sci,* 95**,** 930-5.
NAGATSU, T. & SAWADA, M. 2005. Inflammatory process in Parkinson's disease: role for cytokines. *Curr Pharm Des,* 11**,** 999-1016.
NAJY, A. J., DAY, K. C. & DAY, M. L. 2008. The ectodomain shedding of E-cadherin by ADAM15 supports ErbB receptor activation. *J Biol Chem,* 283**,** 18393-401.
NALEFSKI, E. A. & FALKE, J. J. 1996. The C2 domain calcium-binding motif: Structural and functional diversity. *Protein Science,* 5**,** 2375-2390.
NANNEY, L. B., STOSCHECK, C. M., MAGID, M. & KING, L. E., JR. 1986. Altered [125I]epidermal growth factor binding and receptor distribution in psoriasis. *J Invest Dermatol,* 86**,** 260-5.
NAVA, P., LAUKOETTER, M. G., HOPKINS, A. M., LAUR, O., GERNER-SMIDT, K., GREEN, K. J., PARKOS, C. A. & NUSRAT, A. 2007. Desmoglein-2: a novel regulator of apoptosis in the intestinal epithelium. *Mol Biol Cell,* 18**,** 4565-78.
NEMES, Z., MAREKOV, L. N., FESUS, L. & STEINERT, P. M. 1999. A novel function for transglutaminase 1: attachment of long-chain omega-hydroxyceramides to involucrin by ester bond formation. *Proc Natl Acad Sci U S A,* 96**,** 8402-7.
NISAR, S. P., LORDKIPANIDZE, M., JONES, M. L., DAWOOD, B., MURDEN, S., CUNNINGHAM, M. R., MUMFORD, A. D., WILDE, J. T., WATSON, S. P., MUNDELL, S. J. & LOWE, G. C. 2014. A novel thromboxane A2 receptor N42S variant results in reduced surface expression and platelet dysfunction. *Thromb Haemost,* 111.
OHGAKI, H., DESSEN, P., JOURDE, B., HORSTMANN, S., NISHIKAWA, T., DI PATRE, P. L., BURKHARD, C., SCHULER, D., PROBST-HENSCH, N. M., MAIORKA, P. C., BAEZA, N., PISANI, P., YONEKAWA, Y., YASARGIL, M. G., LUTOLF, U. M. & KLEIHUES, P. 2004. Genetic pathways to glioblastoma: a population-based study. *Cancer Res,* 64**,** 6892-9.
OJI, V., TADINI, G., AKIYAMA, M., BLANCHET BARDON, C., BODEMER, C., BOURRAT, E., COUDIERE, P., DIGIOVANNA, J. J., ELIAS, P., FISCHER, J., FLECKMAN, P., GINA, M., HARPER, J., HASHIMOTO, T., HAUSSER, I., HENNIES, H. C., HOHL, D., HOVNANIAN, A., ISHIDA-YAMAMOTO, A., JACYK, W. K., LEACHMAN, S., LEIGH, I., MAZEREEUW-HAUTIER, J., MILSTONE, L., MORICE-PICARD, F., PALLER, A. S., RICHARD, G., SCHMUTH, M., SHIMIZU, H., SPRECHER, E., VAN STEENSEL, M., TAIEB, A., TORO, J. R., VABRES, P., VAHLQUIST, A., WILLIAMS, M. & TRAUPE, H. 2010. Revised nomenclature and classification of inherited ichthyoses: results of the First Ichthyosis Consensus Conference in Soreze 2009. *J Am Acad Dermatol,* 63**,** 607-41.
OKINES, A., CUNNINGHAM, D. & CHAU, I. 2011. Targeting the human EGFR family in esophagogastric cancer. *Nat Rev Clin Oncol,* 8**,** 492-503.
ORLANDO, S., SIRONI, M., BIANCHI, G., DRUMMOND, A. H., BORASCHI, D., YABES, D. & MANTOVANI, A. 1997. Role of metalloproteases in the release of the IL-1 type II decoy receptor. *J Biol Chem,* 272**,** 31764-9.
PAI, R., SOREGHAN, B., SZABO, I. L., PAVELKA, M., BAATAR, D. & TARNAWSKI, A. S. 2002. Prostaglandin E2 transactivates EGF receptor: a novel mechanism for promoting colon cancer growth and gastrointestinal hypertrophy. *Nat Med,* 8**,** 289-93.
PAJDO, R., BRZOZOWSKI, T., SZLACHCIC, A., KONTUREK, P. C., PTAK-BELOWSKA, A., DROZDOWICZ, D., TARGOSZ, A., KONTUREK, S. J. & PAWLIK, W. W. 2011. Lipoxins, the novel mediators of gastroprotection and gastric adaptation to ulcerogenic action of aspirin. *Curr Pharm Des,* 17**,** 1541-51.
PALMER, C. N., IRVINE, A. D., TERRON-KWIATKOWSKI, A., ZHAO, Y., LIAO, H., LEE, S. P., GOUDIE, D. R., SANDILANDS, A., CAMPBELL, L. E., SMITH, F. J., O'REGAN, G. M., WATSON, R. M., CECIL, J. E., BALE, S. J., COMPTON, J. G., DIGIOVANNA, J. J., FLECKMAN, P., LEWIS-JONES, S., ARSECULERATNE, G., SERGEANT, A., MUNRO, C. S., EL HOUATE, B., MCELREAVEY, K., HALKJAER, L. B., BISGAARD, H., MUKHOPADHYAY, S. & MCLEAN, W. H. 2006. Common loss-of-function variants of the epidermal barrier protein filaggrin are a major predisposing factor for atopic dermatitis. *Nat Genet,* 38**,** 441-6.

PAN, D. & RUBIN, G. M. 1997. Kuzbanian controls proteolytic processing of Notch and mediates lateral inhibition during Drosophila and vertebrate neurogenesis. *Cell,* 90**,** 271-80.
PARTI, R. P., LOPER, R., BROWN, G. D., GORDON, S., TAYLOR, P. R., BONVENTRE, J. V., MURPHY, R. C., WILLIAMS, D. L. & LESLIE, C. C. 2010. Cytosolic phospholipase a2 activation by Candida albicans in alveolar macrophages: role of dectin-1. *Am J Respir Cell Mol Biol,* 42**,** 415-23.
PASCALL, J. C. & BROWN, K. D. 2004. Intramembrane cleavage of ephrinB3 by the human rhomboid family protease, RHBDL2. *Biochem Biophys Res Commun,* 317**,** 244-52.
PASQUALE, E. B. 2005. EPH receptor signalling casts a wide net on cell behaviour. *Nature Reviews Molecular Cell Biology,* 6**,** 462-475.
PASQUALE, E. B. 2008. Eph-ephrin bidirectional signaling in physiology and disease. *Cell,* 133**,** 38-52.
PASTORE, S., MASCIA, F., MARIANI, V. & GIROLOMONI, G. 2008. The epidermal growth factor receptor system in skin repair and inflammation. *J Invest Dermatol,* 128**,** 1365-74.
PATEL, S., ZIRWAS, M. & ENGLISH, J. C., 3RD 2007. Acquired palmoplantar keratoderma. *Am J Clin Dermatol,* 8**,** 1-11.
PEDUTO, L., REUTER, V. E., SHAFFER, D. R., SCHER, H. I. & BLOBEL, C. P. 2005. Critical function for ADAM9 in mouse prostate cancer. *Cancer Res,* 65**,** 9312-9.
PENNATHUR, A., GIBSON, M. K., JOBE, B. A. & LUKETICH, J. D. 2013. Oesophageal carcinoma. *Lancet,* 381**,** 400-12.
PESCHON, J. J., SLACK, J. L., REDDY, P., STOCKING, K. L., SUNNARBORG, S. W., LEE, D. C., RUSSELL, W. E., CASTNER, B. J., JOHNSON, R. S., FITZNER, J. N., BOYCE, R. W., NELSON, N., KOZLOSKY, C. J., WOLFSON, M. F., RAUCH, C. T., CERRETTI, D. P., PAXTON, R. J., MARCH, C. J. & BLACK, R. A. 1998. An essential role for ectodomain shedding in mammalian development. *Science,* 282**,** 1281-4.
PETTUS, B. J., BIELAWSKA, A., SUBRAMANIAN, P., WIJESINGHE, D. S., MACEYKA, M., LESLIE, C. C., EVANS, J. H., FREIBERG, J., RODDY, P., HANNUN, Y. A. & CHALFANT, C. E. 2004. Ceramide 1-phosphate is a direct activator of cytosolic phospholipase A(2). *Journal of Biological Chemistry,* 279**,** 11320-11326.
PFITZENMAIER, J., VESSELLA, R., HIGANO, C. S., NOTEBOOM, J. L., WALLACE, D., JR. & COREY, E. 2003. Elevation of cytokine levels in cachectic patients with prostate carcinoma. *Cancer,* 97**,** 1211-6.
PIEPKORN, M. 1996. Overexpression of amphiregulin, a major autocrine growth factor for cultured human keratinocytes, in hyperproliferative skin diseases. *Am J Dermatopathol,* 18**,** 165-71.
PIEPKORN, M., LO, C. & PLOWMAN, G. 1994. Amphiregulin-dependent proliferation of cultured human keratinocytes: autocrine growth, the effects of exogenous recombinant cytokine, and apparent requirement for heparin-like glycosaminoglycans. *J Cell Physiol,* 159**,** 114-20.
PIEPKORN, M., PITTELKOW, M. R. & COOK, P. W. 1998. Autocrine regulation of keratinocytes: The emerging role of heparin-binding, epidermal growth factor-related growth factors. *Journal of Investigative Dermatology,* 111**,** 715-721.
PRENZEL, N., ZWICK, E., DAUB, H., LESERER, M., ABRAHAM, R., WALLASCH, C. & ULLRICH, A. 1999. EGF receptor transactivation by G-protein-coupled receptors requires metalloproteinase cleavage of proHB-EGF. *Nature,* 402**,** 884-8.
PROKSCH, E., BRANDNER, J. M. & JENSEN, J. M. 2008. The skin: an indispensable barrier. *Exp Dermatol,* 17**,** 1063-72.
PUENTE, X. S. & LOPEZ-OTIN, C. 2004. A genomic analysis of rat proteases and protease inhibitors. *Genome Res,* 14**,** 609-22.
PUTNAM, E. A., YEN, N., GALLICK, G. E., STECK, P. A., FANG, K., AKPAKIP, B., GAZDAR, A. F. & ROTH, J. A. 1992. Autocrine growth stimulation by transforming growth factor-alpha in human non-small cell lung cancer. *Surg Oncol,* 1**,** 49-60.
RABINOWITZ, M. H., ANDREWS, R. C., BECHERER, J. D., BICKETT, D. M., BUBACZ, D. G., CONWAY, J. G., COWAN, D. J., GAUL, M., GLENNON, K., LAMBERT, M. H., LEESNITZER, M. A.,

MCDOUGALD, D. L., MOSS, M. L., MUSSO, D. L. & RIZZOLIO, M. C. 2001. Design of selective and soluble inhibitors of tumor necrosis factor-alpha converting enzyme (TACE). *J Med Chem,* 44**,** 4252-67.

RAGHUNATH, M., HENNIES, H. C., VELTEN, F., WIEBE, V., STEINERT, P. M., REIS, A. & TRAUPE, H. 1998. A novel ~~in situ~~*in situ* method for the detection of deficient transglutaminase activity in the skin. *Arch Dermatol Res,* 290**,** 621-7.

REDDY, P., SLACK, J. L., DAVIS, R., CERRETTI, D. P., KOZLOSKY, C. J., BLANTON, R. A., SHOWS, D., PESCHON, J. J. & BLACK, R. A. 2000. Functional analysis of the domain structure of tumor necrosis factor-alpha converting enzyme. *J Biol Chem,* 275**,** 14608-14.

REDFERN, J. S. & FELDMAN, M. 1989. Role of endogenous prostaglandins in preventing gastrointestinal ulceration: induction of ulcers by antibodies to prostaglandins. *Gastroenterology,* 96**,** 596-605.

REDFERN, J. S., LEE, E. & FELDMAN, M. 1988. Effect of immunization with prostaglandin metabolites on gastrointestinal ulceration. *Am J Physiol,* 255**,** G723-30.

REHFELD, J. F. 2004. A centenary of gastrointestinal endocrinology. *Horm Metab Res,* 36**,** 735-41.

REISS, K., MARETZKY, T., HAAS, I. G., SCHULTE, M., LUDWIG, A., FRANK, M. & SAFTIG, P. 2006. Regulated ADAM10-dependent ectodomain shedding of gamma-protocadherin C3 modulates cell-cell adhesion. *J Biol Chem,* 281**,** 21735-44.

RENNEKAMPFF, H. O., HANSBROUGH, J. F., KIESSIG, V., DORE, C., STICHERLING, M. & SCHRODER, J. M. 2000. Bioactive interleukin-8 is expressed in wounds and enhances wound healing. *J Surg Res,* 93**,** 41-54.

REPERTINGER, S. K., CAMPAGNARO, E., FUHRMAN, J., EL-ABASERI, T., YUSPA, S. H. & HANSEN, L. A. 2004. EGFR enhances early healing after cutaneous incisional wounding. *J Invest Dermatol,* 123**,** 982-9.

RICHARDSON, R., SLANCHEV, K., KRAUS, C., KNYPHAUSEN, P., EMING, S. & HAMMERSCHMIDT, M. 2013. Adult zebrafish as a model system for cutaneous wound-healing research. *J Invest Dermatol,* 133**,** 1655-65.

RIO, C., BUXBAUM, J. D., PESCHON, J. J. & CORFAS, G. 2000. Tumor necrosis factor-alpha-converting enzyme is required for cleavage of erbB4/HER4. *J Biol Chem,* 275**,** 10379-87.

RISK, J. M., EVANS, K. E., JONES, J., LANGAN, J. E., ROWBOTTOM, L., MCRONALD, F. E., MILLS, H. S., ELLIS, A., SHAW, J. M., LEIGH, I. M., KELSELL, D. P. & FIELD, J. K. 2002. Characterization of a 500 kb region on 17q25 and the exclusion of candidate genes as the familial Tylosis Oesophageal Cancer (TOC) locus. *Oncogene,* 21**,** 6395-402.

RISK, J. M., FIELD, E. A., FIELD, J. K., WHITTAKER, J., FRYER, A., ELLIS, A., SHAW, J. M., FRIEDMANN, P. S., BISHOP, D. T., BODMER, J. & LEIGH, I. M. 1994. Tylosis Esophageal Cancer Mapped. *Nature Genetics,* 8**,** 319-321.

RITTIE, L., KANSRA, S., STOLL, S. W., LI, Y., GUDJONSSON, J. E., SHAO, Y., MICHAEL, L. E., FISHER, G. J., JOHNSON, T. M. & ELDER, J. T. 2007. Differential ErbB1 signaling in squamous cell versus basal cell carcinoma of the skin. *Am J Pathol,* 170**,** 2089-99.

RITTIE, L., VARANI, J., KANG, S., VOORHEES, J. J. & FISHER, G. J. 2006. Retinoid-induced epidermal hyperplasia is mediated by epidermal growth factor receptor activation via specific induction of its ligands heparin-binding EGF and amphiregulin in human skin in vivo. *J Invest Dermatol,* 126**,** 732-9.

ROBERTS, D. E., MCNICOL, A. & BOSE, R. 2004. Mechanism of collagen activation in human platelets. *J Biol Chem,* 279**,** 19421-30.

ROEMER, A., SCHWETTMANN, L., JUNG, M., ROIGAS, J., KRISTIANSEN, G., SCHNORR, D., LOENING, S. A., JUNG, K. & LICHTINGHAGEN, R. 2004. Increased mRNA expression of ADAMs in renal cell carcinoma and their association with clinical outcome. *Oncol Rep,* 11**,** 529-36.

ROGHANI, M., BECHERER, J. D., MOSS, M. L., ATHERTON, R. E., ERDJUMENT-BROMAGE, H., ARRIBAS, J., BLACKBURN, R. K., WESKAMP, G., TEMPST, P. & BLOBEL, C. P. 1999. Metalloprotease-disintegrin MDC9: intracellular maturation and catalytic activity. *J Biol Chem,* 274**,** 3531-40.

ROSE-JOHN, S., SCHELLER, J., ELSON, G. & JONES, S. A. 2006. Interleukin-6 biology is coordinated by membrane-bound and soluble receptors: role in inflammation and cancer. *J Leukoc Biol,* 80**,** 227-36.
ROUZER, C. A. & MARNETT, L. J. 2009. Cyclooxygenases: structural and functional insights. *J Lipid Res,* 50 Suppl**,** S29-34.
ROY, R., WEWER, U. M., ZURAKOWSKI, D., PORIES, S. E. & MOSES, M. A. 2004. ADAM 12 cleaves extracellular matrix proteins and correlates with cancer status and stage. *J Biol Chem,* 279**,** 51323-30.
RUBIN, B. B., DOWNEY, G. P., KOH, A., DEGOUSEE, N., GHOMASHCHI, F., NALLAN, L., STEFANSKI, E., HARKIN, D. W., SUN, C., SMART, B. P., LINDSAY, T. F., CHEREPANOV, V., VACHON, E., KELVIN, D., SADILEK, M., BROWN, G. E., YAFFE, M. B., PLUMB, J., GRINSTEIN, S., GLOGAUER, M. & GELB, M. H. 2005. Cytosolic phospholipase A2-alpha is necessary for platelet-activating factor biosynthesis, efficient neutrophil-mediated bacterial killing, and the innate immune response to pulmonary infection: cPLA2-alpha does not regulate neutrophil NADPH oxidase activity. *J Biol Chem,* 280**,** 7519-29.
RUBIN GRANDIS, J., MELHEM, M. F., GOODING, W. E., DAY, R., HOLST, V. A., WAGENER, M. M., DRENNING, S. D. & TWEARDY, D. J. 1998. Levels of TGF-alpha and EGFR protein in head and neck squamous cell carcinoma and patient survival. *J Natl Cancer Inst,* 90**,** 824-32.
SAARINEN, S., VAHTERISTO, P., LEHTONEN, R., AITTOMAKI, K., LAUNONEN, V., KIVILUOTO, T. & AALTONEN, L. A. 2012. Analysis of a Finnish family confirms RHBDF2 mutations as the underlying factor in tylosis with esophageal cancer. *Fam Cancer*.
SAFTIG, P. & REISS, K. 2011. The "A Disintegrin And Metalloproteases" ADAM10 and ADAM17: novel drug targets with therapeutic potential? *Eur J Cell Biol,* 90**,** 527-35.
SAHIN, U. & BLOBEL, C. P. 2007. Ectodomain shedding of the EGF-receptor ligand epigen is mediated by ADAM17. *FEBS Lett,* 581**,** 41-4.
SAHIN, U., WESKAMP, G., KELLY, K., ZHOU, H. M., HIGASHIYAMA, S., PESCHON, J., HARTMANN, D., SAFTIG, P. & BLOBEL, C. P. 2004. Distinct roles for ADAM10 and ADAM17 in ectodomain shedding of six EGFR ligands. *J Cell Biol,* 164**,** 769-79.
SALOMON, D. S., BRANDT, R., CIARDIELLO, F. & NORMANNO, N. 1995. Epidermal growth factor-related peptides and their receptors in human malignancies. *Crit Rev Oncol Hematol,* 19**,** 183-232.
SANDGREN, E. P., LUETTEKE, N. C., PALMITER, R. D., BRINSTER, R. L. & LEE, D. C. 1990. Overexpression of Tgf-Alpha in Transgenic Mice - Induction of Epithelial Hyperplasia, Pancreatic Metaplasia, and Carcinoma of the Breast. *Cell,* 61**,** 1121-1135.
SCHAFER, B., MARG, B., GSCHWIND, A. & ULLRICH, A. 2004. Distinct ADAM metalloproteinases regulate G protein-coupled receptor-induced cell proliferation and survival. *J Biol Chem,* 279**,** 47929-38.
SCHLONDORFF, J., BECHERER, J. D. & BLOBEL, C. P. 2000. Intracellular maturation and localization of the tumour necrosis factor alpha convertase (TACE). *Biochem J,* 347 Pt 1**,** 131-8.
SCHNEIDER, M. R., WERNER, S., PAUS, R. & WOLF, E. 2008. Beyond wavy hairs - The epidermal growth factor receptor and its ligands in skin biology and pathology. *American Journal of Pathology,* 173**,** 14-24.
SCHULZ, B., PRUESSMEYER, J., MARETZKY, T., LUDWIG, A., BLOBEL, C. P., SAFTIG, P. & REISS, K. 2008. ADAM10 regulates endothelial permeability and T-Cell transmigration by proteolysis of vascular endothelial cadherin. *Circ Res,* 102**,** 1192-201.
SCOTT, C. A., PLAGNOL, V., NITOIU, D., BLAND, P. J., BLAYDON, D. C., CHRONNELL, C. M., POON, D. S., BOURN, D., GARDOS, L., CSASZAR, A., TIHANYI, M., RUSTIN, M., BURROWS, N. P., BENNETT, C., HARPER, J. I., CONRAD, B., VERMA, I. C., TAIBJEE, S. M., MOSS, C., O'TOOLE, E. A. & KELSELL, D. P. 2013. Targeted sequence capture and high-throughput sequencing in the molecular diagnosis of ichthyosis and other skin diseases. *J Invest Dermatol,* 133**,** 573-6.
SCOTT, C. A., TATTERSALL, D., O'TOOLE, E. A. & KELSELL, D. P. 2012. Connexins in epidermal homeostasis and skin disease. *Biochim Biophys Acta,* 1818**,** 1952-61.

SEALS, D. F. & COURTNEIDGE, S. A. 2003. The ADAMs family of metalloproteases: multidomain proteins with multiple functions. *Genes Dev,* 17**,** 7-30.
SERHAN, C. N. 2005. Lipoxins and aspirin-triggered 15-epi-lipoxins are the first lipid mediators of endogenous anti-inflammation and resolution. *Prostaglandins Leukot Essent Fatty Acids,* 73**,** 141-62.
SHARMA, S. V., BELL, D. W., SETTLEMAN, J. & HABER, D. A. 2007. Epidermal growth factor receptor mutations in lung cancer. *Nat Rev Cancer,* 7**,** 169-81.
SHENG, G., BERNABE, K. Q., GUO, J. & WARNER, B. W. 2006. Epidermal growth factor receptor-mediated proliferation of enterocytes requires p21waf1/cip1 expression. *Gastroenterology,* 131**,** 153-64.
SHI, W., CHEN, H., SUN, J., BUCKLEY, S., ZHAO, J., ANDERSON, K. D., WILLIAMS, R. G. & WARBURTON, D. 2003. TACE is required for fetal murine cardiac development and modeling. *Dev Biol,* 261**,** 371-80.
SHIRAKATA, Y., KIMURA, R., NANBA, D., IWAMOTO, R., TOKUMARU, S., MORIMOTO, C., YOKOTA, K., NAKAMURA, M., SAYAMA, K., MEKADA, E., HIGASHIYAMA, S. & HASHIMOTO, K. 2005. Heparin-binding EGF-like growth factor accelerates keratinocyte migration and skin wound healing. *J Cell Sci,* 118**,** 2363-70.
SHMELZER, Z., HADDAD, N., ADMON, E., PESSACH, I., LETO, T. L., EITAN-HAZAN, Z., HERSHFINKEL, M. & LEVY, R. 2003. Unique targeting of cytosolic phospholipase A2 to plasma membranes mediated by the NADPH oxidase in phagocytes. *J Cell Biol,* 162**,** 683-92.
SIBILIA, M. & WAGNER, E. F. 1995. Strain-Dependent Epithelial Defects in Mice Lacking the Egf Receptor (Vol 269, Pg 234, 1995). *Science,* 269**,** 909-909.
SIMPSON, C. L., KOJIMA, S. & GETSIOS, S. 2010. RNA interference in keratinocytes and an organotypic model of human epidermis. *Methods Mol Biol,* 585**,** 127-46.
SIMPSON, M. A., MANSOUR, S., AHNOOD, D., KALIDAS, K., PATTON, M. A., MCKENNA, W. J., BEHR, E. R. & CROSBY, A. H. 2009. Homozygous mutation of desmocollin-2 in arrhythmogenic right ventricular cardiomyopathy with mild palmoplantar keratoderma and woolly hair. *Cardiology,* 113**,** 28-34.
SINGH, R. J., MASON, J. C., LIDINGTON, E. A., EDWARDS, D. R., NUTTALL, R. K., KHOKHA, R., KNAUPER, V., MURPHY, G. & GAVRILOVIC, J. 2005. Cytokine stimulated vascular cell adhesion molecule-1 (VCAM-1) ectodomain release is regulated by TIMP-3. *Cardiovasc Res,* 67**,** 39-49.
SIX, D. A. & DENNIS, E. A. 2000. The expanding superfamily of phospholipase A(2) enzymes: classification and characterization. *Biochim Biophys Acta,* 1488**,** 1-19.
SIX, E., NDIAYE, D., LAABI, Y., BROU, C., GUPTA-ROSSI, N., ISRAEL, A. & LOGEAT, F. 2003. The Notch ligand Delta1 is sequentially cleaved by an ADAM protease and gamma-secretase. *Proc Natl Acad Sci U S A,* 100**,** 7638-43.
SLACK, B. E., MA, L. K. & SEAH, C. C. 2001. Constitutive shedding of the amyloid precursor protein ectodomain is up-regulated by tumour necrosis factor-alpha converting enzyme. *Biochem J,* 357**,** 787-94.
SMYTH, E. M., GROSSER, T., WANG, M., YU, Y. & FITZGERALD, G. A. 2009. Prostanoids in health and disease. *J Lipid Res,* 50 Suppl**,** S423-8.
SOLL, A. H., WEINSTEIN, W. M., KURATA, J. & MCCARTHY, D. 1991. Nonsteroidal anti-inflammatory drugs and peptic ulcer disease. *Ann Intern Med,* 114**,** 307-19.
SOOND, S. M., EVERSON, B., RICHES, D. W. & MURPHY, G. 2005. ERK-mediated phosphorylation of Thr735 in TNFalpha-converting enzyme and its potential role in TACE protein trafficking. *J Cell Sci,* 118**,** 2371-80.
SPRECHER, E., ISHIDA-YAMAMOTO, A., MIZRAHI-KOREN, M., RAPAPORT, D., GOLDSHER, D., INDELMAN, M., TOPAZ, O., CHEFETZ, I., KEREN, H., O'BRIEN T, J., BERCOVICH, D., SHALEV, S., GEIGER, D., BERGMAN, R., HOROWITZ, M. & MANDEL, H. 2005. A mutation in SNAP29, coding for a SNARE protein involved in intracellular trafficking, causes a novel neurocutaneous syndrome characterized by cerebral dysgenesis, neuropathy, ichthyosis, and palmoplantar keratoderma. *Am J Hum Genet,* 77**,** 242-51.

STAEHELIN, L. A. 1974. Structure and function of intercellular junctions. *Int Rev Cytol,* 39**,** 191-283.
STEVENS, H. P., KELSELL, D. P., BRYANT, S. P., BISHOP, D. T., SPURR, N. K., WEISSENBACH, J., MARGER, D., MARGER, R. S. & LEIGH, I. M. 1996. Linkage of an American pedigree with palmoplantar keratoderma and malignancy (palmoplantar ectodermal dysplasia type III) to 17q24. Literature survey and proposed updated classification of the keratodermas. *Arch Dermatol,* 132**,** 640-51.
STOCKER, W. & BODE, W. 1995. Structural features of a superfamily of zinc-endopeptidases: the metzincins. *Curr Opin Struct Biol,* 5**,** 383-90.
STOLL, S., GARNER, W. & ELDER, J. 1997. Heparin-binding ligands mediate autocrine epidermal growth factor receptor activation in skin organ culture. *Journal of Clinical Investigation,* 100**,** 1271-1281.
STOLL, S. W. & ELDER, J. T. 1998. Retinoid regulation of heparin-binding EGF-like growth factor gene expression in human keratinocytes and skin. *Exp Dermatol,* 7**,** 391-7.
STRAUS, D. S., PASCUAL, G., LI, M., WELCH, J. S., RICOTE, M., HSIANG, C. H., SENGCHANTHALANGSY, L. L., GHOSH, G. & GLASS, C. K. 2000. 15-deoxy-delta 12,14-prostaglandin J2 inhibits multiple steps in the NF-kappa B signaling pathway. *Proc Natl Acad Sci U S A,* 97**,** 4844-9.
SUGANUMA, M., OKABE, S., MARINO, M. W., SAKAI, A., SUEOKA, E. & FUJIKI, H. 1999. Essential role of tumor necrosis factor alpha (TNF-alpha) in tumor promotion as revealed by TNF-alpha-deficient mice. *Cancer Res,* 59**,** 4516-8.
SUNPAWERAVONG, P., SUNPAWERAVONG, S., PUTTAWIBUL, P., MITARNUN, W., ZENG, C., BARON, A. E., FRANKLIN, W., SAID, S. & VARELLA-GARCIA, M. 2005. Epidermal growth factor receptor and cyclin D1 are independently amplified and overexpressed in esophageal squamous cell carcinoma. *J Cancer Res Clin Oncol,* 131**,** 111-9.
SWARDFAGER, W., LANCTOT, K., ROTHENBURG, L., WONG, A., CAPPELL, J. & HERRMANN, N. 2010. A meta-analysis of cytokines in Alzheimer's disease. *Biol Psychiatry,* 68**,** 930-41.
SWENDEMAN, S., MENDELSON, K., WESKAMP, G., HORIUCHI, K., DEUTSCH, U., SCHERLE, P., HOOPER, A., RAFII, S. & BLOBEL, C. P. 2008. VEGF-A Stimulates ADAM17-Dependent Shedding of VEGFR2 and Crosstalk Between VEGFR2 and ERK Signaling. *Circulation Research,* 103**,** 916-U42.
SYMONS, J. A., YOUNG, P. R. & DUFF, G. W. 1995. Soluble type II interleukin 1 (IL-1) receptor binds and blocks processing of IL-1 beta precursor and loses affinity for IL-1 receptor antagonist. *Proc Natl Acad Sci U S A,* 92**,** 1714-8.
TAKAKU, K., SONOSHITA, M., SASAKI, N., UOZUMI, N., DOI, Y., SHIMIZU, T. & TAKETO, M. M. 2000. Suppression of intestinal polyposis in Apc(delta 716) knockout mice by an additional mutation in the cytosolic phospholipase A(2) gene. *J Biol Chem,* 275**,** 34013-6.
TAKATA, Y., KANAJI, T., MOROI, M., SEKI, R., SANO, M., NAKAZATO, S., SUEOKA, E., IMAMURA, Y. & OKAMURA, T. 2012. Platelets with a W127X mutation in GPIX express sufficient residual amounts of GPIbalpha to support adhesion to von Willebrand factor and collagen. *Int J Hematol,* 96**,** 733-42.
TANAKA, Y., MIYAMOTO, S., SUZUKI, S. O., OKI, E., YAGI, H., SONODA, K., YAMAZAKI, A., MIZUSHIMA, H., MAEHARA, Y., MEKADA, E. & NAKANO, H. 2005. Clinical significance of heparin-binding epidermal growth factor-like growth factor and a disintegrin and metalloprotease 17 expression in human ovarian cancer. *Clin Cancer Res,* 11**,** 4783-92.
TEUNISSEN, M. B., KOOMEN, C. W., DE WAAL MALEFYT, R., WIERENGA, E. A. & BOS, J. D. 1998. Interleukin-17 and interferon-gamma synergize in the enhancement of proinflammatory cytokine production by human keratinocytes. *J Invest Dermatol,* 111**,** 645-9.
TIAN, W., WIJEWICKRAMA, G. T., KIM, J. H., DAS, S., TUN, M. P., GOKHALE, N., JUNG, J. W., KIM, K. P. & CHO, W. 2008. Mechanism of regulation of group IVA phospholipase A2 activity by Ser727 phosphorylation. *J Biol Chem,* 283**,** 3960-71.
TOKUMARU, S., HIGASHIYAMA, S., ENDO, T., NAKAGAWA, T., MIYAGAWA, J. I., YAMAMORI, K., HANAKAWA, Y., OHMOTO, H., YOSHINO, K., SHIRAKATA, Y., MATSUZAWA, Y.,

HASHIMOTO, K. & TANIGUCHI, N. 2000. Ectodomain shedding of epidermal growth factor receptor ligands is required for keratinocyte migration in cutaneous wound healing. *J Cell Biol,* 151**,** 209-20.
TOLINO, M. A., BLOCK, E. R. & KLARLUND, J. K. 2011. Brief treatment with heparin-binding EGF-like growth factor, but not with EGF, is sufficient to accelerate epithelial wound healing. *Biochim Biophys Acta,* 1810**,** 875-8.
TSAI, S. T., YANG, K. Y., JIN, Y. T., LIN, Y. C., CHANG, M. T. & WU, L. W. 2006. Amphiregulin as a tumor promoter for oral squamous cell carcinoma: involvement of cyclooxygenase 2. *Oral Oncol,* 42**,** 381-90.
UOZUMI, N., KUME, K., NAGASE, T., NAKATANI, N., ISHII, S., TASHIRO, F., KOMAGATA, Y., MAKI, K., IKUTA, K., OUCHI, Y., MIYAZAKI, J. & SHIMIZU, T. 1997. Role of cytosolic phospholipase A2 in allergic response and parturition. *Nature,* 390**,** 618-22.
UOZUMI, N. & SHIMIZU, T. 2002. Roles for cytosolic phospholipase A2alpha as revealed by gene-targeted mice. *Prostaglandins Other Lipid Mediat,* 68-69**,** 59-69.
URBAN, S. & FREEMAN, M. 2003. Substrate specificity of rhomboid intramembrane proteases is governed by helix-breaking residues in the substrate transmembrane domain. *Molecular Cell,* 11**,** 1425-1434.
URBAN, S., LEE, J. R. & FREEMAN, M. 2001. Drosophila rhomboid-1 defines a family of putative intramembrane serine proteases. *Cell,* 107**,** 173-82.
URBAN, S., SCHLIEPER, D. & FREEMAN, M. 2002. Conservation of intramembrane proteolytic activity and substrate specificity in prokaryotic and eukaryotic rhomboids. *Current Biology,* 12**,** 1507-1512.
VAN DER FLIER, L. G. & CLEVERS, H. 2009. Stem cells, self-renewal, and differentiation in the intestinal epithelium. *Annu Rev Physiol,* 71**,** 241-60.
VANDEN EIJNDEN, S., GORIELY, S., DE WIT, D., WILLEMS, F. & GOLDMAN, M. 2005. IL-23 up-regulates IL-10 and induces IL-17 synthesis by polyclonally activated naive T cells in human. *Eur J Immunol,* 35**,** 469-75.
VANE, J. R. 1971. Inhibition of prostaglandin synthesis as a mechanism of action for aspirin-like drugs. *Nat New Biol,* 231**,** 232-5.
VANE, J. R., BAKHLE, Y. S. & BOTTING, R. M. 1998. Cyclooxygenases 1 and 2. *Annu Rev Pharmacol Toxicol,* 38**,** 97-120.
VARELA, A. B., BLANCO RODRIGUEZ, M. M., BOULLOSA, P. E. & SILVA, J. G. 2011. Tylosis A with squamous cell carcinoma of the oesophagus in a Spanish family. *Eur J Gastroenterol Hepatol,* 23**,** 286-8.
VIGNOLA, M. J., KASHATUS, D. F., TAYLOR, G. A., COUNTER, C. M. & VALDIVIA, R. H. 2010. cPLA2 regulates the expression of type I interferons and intracellular immunity to Chlamydia trachomatis. *J Biol Chem,* 285**,** 21625-35.
VINAY, D. S. & KWON, B. S. 2011. The tumour necrosis factor/TNF receptor superfamily: therapeutic targets in autoimmune diseases. *Clin Exp Immunol,* 164**,** 145-57.
VONG, L., FERRAZ, J. G., PANACCIONE, R., BECK, P. L. & WALLACE, J. L. 2010. A pro-resolution mediator, prostaglandin D(2), is specifically up-regulated in individuals in long-term remission from ulcerative colitis. *Proc Natl Acad Sci U S A,* 107**,** 12023-7.
WADA, H., SAITO, K., KANDA, T., KOBAYASHI, I., FUJII, H., FUJIGAKI, S., MAEKAWA, N., TAKATSU, H., FUJIWARA, H., SEKIKAWA, K. & SEISHIMA, M. 2001. Tumor necrosis factor-alpha (TNF-alpha) plays a protective role in acute viralmyocarditis in mice: A study using mice lacking TNF-alpha. *Circulation,* 103**,** 743-9.
WANG, K., LI, M. & HAKONARSON, H. 2010. ANNOVAR: functional annotation of genetic variants from high-throughput sequencing data. *Nucleic Acids Res,* 38**,** e164.
WANG, Y., GEER, L. Y., CHAPPEY, C., KANS, J. A. & BRYANT, S. H. 2000. Cn3D: sequence and structure views for Entrez. *Trends Biochem Sci,* 25**,** 300-2.
WANG, Y. C., ZHANG, Y. J. & HA, Y. 2006. Crystal structure of a rhomboid family intramembrane protease. *Nature,* 444**,** 179-183.

WEBB, N. R. 2005. Secretory phospholipase A(2) enzymes in atherogenesis. *Current Opinion in Lipidology,* 16**,** 341-344.
WERNER, S. & GROSE, R. 2003. Regulation of wound healing by growth factors and cytokines. *Physiol Rev,* 83**,** 835-70.
WILD-BODE, C., FELLERER, K., KUGLER, J., HAASS, C. & CAPELL, A. 2006. A basolateral sorting signal directs ADAM10 to adherens junctions and is required for its function in cell migration. *J Biol Chem,* 281**,** 23824-9.
WOLFORD, J. K., KONHEIM, Y. L., COLLIGAN, P. B. & BOGARDUS, C. 2003. Association of a F479L variant in the cytosolic phospholipase A2 gene (PLA2G4A) with decreased glucose turnover and oxidation rates in Pima Indians. *Mol Genet Metab,* 79**,** 61-6.
YAMABUKI, T., DAIGO, Y., KATO, T., HAYAMA, S., TSUNODA, T., MIYAMOTO, M., ITO, T., FUJITA, M., HOSOKAWA, M., KONDO, S. & NAKAMURA, Y. 2006. Genome-wide gene expression profile analysis of esophageal squamous cell carcinomas. *Int J Oncol,* 28**,** 1375-84.
YAMADA, T., DEITCH, E., SPECIAN, R. D., PERRY, M. A., SARTOR, R. B. & GRISHAM, M. B. 1993. Mechanisms of acute and chronic intestinal inflammation induced by indomethacin. *Inflammation,* 17**,** 641-62.
YAMAZAKI, S., IWAMOTO, R., SAEKI, K., ASAKURA, M., TAKASHIMA, S., YAMAZAKI, A., KIMURA, R., MIZUSHIMA, H., MORIBE, H., HIGASHIYAMA, S., ENDOH, M., KANEDA, Y., TAKAGI, S., ITAMI, S., TAKEDA, N., YAMADA, G. & MEKADA, E. 2003. Mice with defects in HB-EGF ectodomain shedding show severe developmental abnormalities. *J Cell Biol,* 163**,** 469-75.
YARDEN, Y. & SLIWKOWSKI, M. X. 2001. Untangling the ErbB signalling network. *Nat Rev Mol Cell Biol,* 2**,** 127-37.
YOKOZEKI, T., WAKATSUKI, S., HATSUZAWA, K., BLACK, R. A., WADA, I. & SEHARA-FUJISAWA, A. 2007. Meltrin beta (ADAM19) mediates ectodomain shedding of Neuregulin beta1 in the Golgi apparatus: fluorescence correlation spectroscopic observation of the dynamics of ectodomain shedding in living cells. *Genes Cells,* 12**,** 329-43.
YU, Y. & FUNK, C. D. 2007. A novel genetic model of selective COX-2 inhibition: comparison with COX-2 null mice. *Prostaglandins Other Lipid Mediat,* 82**,** 77-84.
ZANDI, R., LARSEN, A. B., ANDERSEN, P., STOCKHAUSEN, M. T. & POULSEN, H. S. 2007. Mechanisms for oncogenic activation of the epidermal growth factor. *Cellular Signalling,* 19**,** 2013-2023.
ZETTL, M., ADRAIN, C., STRISOVSKY, K., LASTUN, V. & FREEMAN, M. 2011. Rhomboid family pseudoproteases use the ER quality control machinery to regulate intercellular signaling. *Cell,* 145**,** 79-91.
ZHANG, D. X., SLIWKOWSKI, M. X., MARK, M., FRANTZ, G., AKITA, R., SUN, Y., HILLAN, K., CROWLEY, C., BRUSH, J. & GODOWSKI, P. J. 1997. Neuregulin-3 (NRG3): A novel neural tissue-enriched protein that binds and activates ErbB4. *Proceedings of the National Academy of Sciences of the United States of America,* 94**,** 9562-9567.
ZHAO, J., CHEN, H., PESCHON, J. J., SHI, W., ZHANG, Y., FRANK, S. J. & WARBURTON, D. 2001. Pulmonary hypoplasia in mice lacking tumor necrosis factor-alpha converting enzyme indicates an indispensable role for cell surface protein shedding during embryonic lung branching morphogenesis. *Dev Biol,* 232**,** 204-18.
ZHENG, Y., PENG, Z., WANG, Y., TAN, S., XI, Y. & WANG, G. 2003. Alteration and significance of heparin-binding epidermal-growth-factor-like growth factor in psoriatic epidermis. *Dermatology,* 207**,** 22-7.
ZHOU, X. P., WAITE, K. A., PILARSKI, R., HAMPEL, H., FERNANDEZ, M. J., BOS, C., DASOUKI, M., FELDMAN, G. L., GREENBERG, L. A., IVANOVICH, J., MATLOFF, E., PATTERSON, A., PIERPONT, M. E., RUSSO, D., NASSIF, N. T. & ENG, C. 2003. Germline PTEN promoter mutations and deletions in Cowden/Bannayan-Riley-Ruvalcaba syndrome result in aberrant PTEN protein and dysregulation of the phosphoinositol-3-kinase/Akt pathway. *Am J Hum Genet,* 73**,** 404-11.